frontiers | Research Topics

Cellular and molecular communication networks within the cutaneous immune system

Edited by
Tina Sumpter, Sherrie Divito
and Alicia R. Mathers

Published in
Frontiers in Immunology

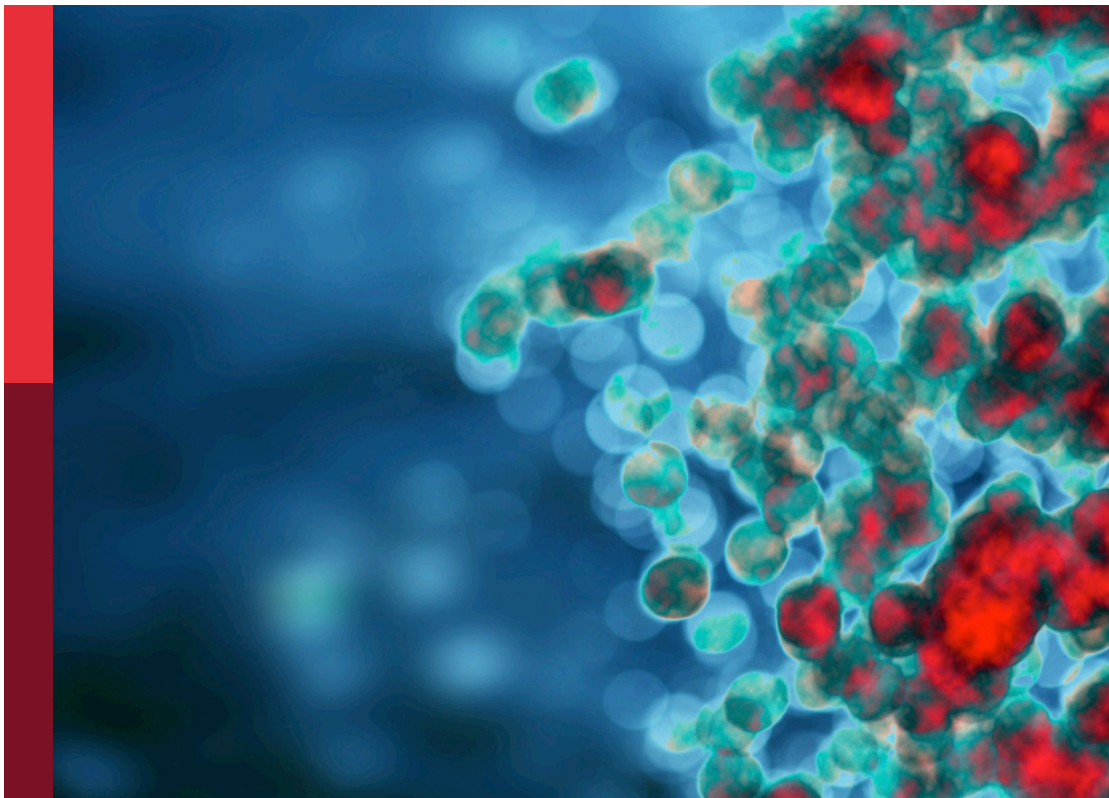

ISSN 1664-8714
ISBN 978-2-8325-3293-5
DOI 10.3389/978-2-8325-3293-5

About Frontiers

Frontiers is more than just an open access publisher of scholarly articles: it is a pioneering approach to the world of academia, radically improving the way scholarly research is managed. The grand vision of Frontiers is a world where all people have an equal opportunity to seek, share and generate knowledge. Frontiers provides immediate and permanent online open access to all its publications, but this alone is not enough to realize our grand goals.

Frontiers journal series

The Frontiers journal series is a multi-tier and interdisciplinary set of open-access, online journals, promising a paradigm shift from the current review, selection and dissemination processes in academic publishing. All Frontiers journals are driven by researchers for researchers; therefore, they constitute a service to the scholarly community. At the same time, the *Frontiers journal series* operates on a revolutionary invention, the tiered publishing system, initially addressing specific communities of scholars, and gradually climbing up to broader public understanding, thus serving the interests of the lay society, too.

Dedication to quality

Each Frontiers article is a landmark of the highest quality, thanks to genuinely collaborative interactions between authors and review editors, who include some of the world's best academicians. Research must be certified by peers before entering a stream of knowledge that may eventually reach the public - and shape society; therefore, Frontiers only applies the most rigorous and unbiased reviews. Frontiers revolutionizes research publishing by freely delivering the most outstanding research, evaluated with no bias from both the academic and social point of view. By applying the most advanced information technologies, Frontiers is catapulting scholarly publishing into a new generation.

What are Frontiers Research Topics?

Frontiers Research Topics are very popular trademarks of the *Frontiers journals series*: they are collections of at least ten articles, all centered on a particular subject. With their unique mix of varied contributions from Original Research to Review Articles, Frontiers Research Topics unify the most influential researchers, the latest key findings and historical advances in a hot research area.

Find out more on how to host your own Frontiers Research Topic or contribute to one as an author by contacting the Frontiers editorial office: frontiersin.org/about/contact

Cellular and molecular communication networks within the cutaneous immune system

Topic editors

Tina Sumpter — University of Pittsburgh, United States

Sherrie Divito — Brigham and Women's Hospital, Harvard Medical School, United States

Alicia R. Mathers — University of Pittsburgh, United States

Citation

Sumpter, T., Divito, S., Mathers, A. R., eds. (2023). *Cellular and molecular communication networks within the cutaneous immune system*. Lausanne: Frontiers Media SA. doi: 10.3389/978-2-8325-3293-5

Table of contents

frontiers in Immunology

MINI REVIEW
published: 30 March 2022
doi: 10.3389/fimmu.2022.876515

Alarmin Cytokines as Central Regulators of Cutaneous Immunity

Tatsuya Hasegawa[1], *Tomonori Oka*[2] *and Shadmehr Demehri*[2]*

[1] Shiseido Global Innovation Center, Yokohama, Japan, [2] Center for Cancer Immunology and Cutaneous Biology Research Center, Department of Dermatology and Center for Cancer Research, Massachusetts General Hospital and Harvard Medical School, Boston, MA, United States

Skin acts as the primary interface between the body and the environment. The skin immune system is composed of a complex network of immune cells and factors that provide the first line of defense against microbial pathogens and environmental insults. Alarmin cytokines mediate an intricate intercellular communication between keratinocytes and immune cells to regulate cutaneous immune responses. Proper functions of the type 2 alarmin cytokines, thymic stromal lymphopoietin (TSLP), interleukin (IL)-25, and IL-33, are paramount to the maintenance of skin homeostasis, and their dysregulation is commonly associated with allergic inflammation. In this review, we discuss recent findings on the complex regulatory network of type 2 alarmin cytokines that control skin immunity and highlight the mechanisms by which these cytokines regulate skin immune responses in host defense, chronic inflammation, and cancer.

Keywords: TSLP, IL-33, IL-25, skin immunlogy, allergic inflammation, cancer, host defense, skin homeostasis

OPEN ACCESS

Edited by:
Alicia R. Mathers,
University of Pittsburgh, United States

Reviewed by:
Yongyao Fu,
Indiana University, United States

***Correspondence:**
Shadmehr Demehri
sdemehri1@mgh.harvard.edu

Specialty section:
This article was submitted to Molecular Innate Immunity, a section of the journal Frontiers in Immunology

Received: *15 February 2022*
Accepted: *08 March 2022*
Published: *30 March 2022*

Citation:
Hasegawa T, Oka T and Demehri S (2022) Alarmin Cytokines as Central Regulators of Cutaneous Immunity. Front. Immunol. 13:876515. doi: 10.3389/fimmu.2022.876515

INTRODUCTION

Skin is the largest organ and acts as a protective barrier separating the body from the outside environment (1). Epidermis, dermis, and subcutaneous fat together with skin appendages, sweat glands, sebaceous glands, and hair follicles, form an integrated structure that enables proper skin function (2). The foremost physical barrier of the skin consists of the epidermis, which in its outermost layer is composed of brick and mortar-like stratum corneum and tight junctions that regulate the inward and outward passage of fluid and electrolytes in and out of the skin (1, 3). The skin has developed complex protective functions against constant exposure to various environmental insults, such as solar radiation, pollutants, a broad range of microbial pathogens, and allergens (4, 5). The immune system contributes to this first line of defense against microbial pathogens and chemical insults (2).

In the epidermis, Langerhans cells (LCs) are epidermal-resident antigen-presenting cells (APCs), which play a sentinel role as the first professional immune cells confronting the environmental insults (6, 7). Activated LCs capture foreign antigens by extending their dendrites through epidermal tight junctions. Next, they migrate to the lymph nodes to initiate cutaneous adaptive immunity (8, 9). In addition, tissue-resident memory T cells (T_{RM} cells), which are noncirculating lymphocytes in peripheral tissues, persist in the epidermis to provide long-lasting protective defense against future immunological challenges at the most probable sites of invasion (10–12). The dermis is the stromal layer below the epidermis that encompasses an active immunological microenvironment (2). The superficial papillary dermis is composed of a relatively loose

connective tissue and contains vessels and sensory nerves (13). A diverse range of immune cell types, including several T cell subsets, macrophages, dendritic cells (DCs), innate lymphoid cells (ILCs), and mast cells, is localized around vasculature and extracellular matrix proteins in the dermis (14–16). This complex network of dermal immune cells helps in many aspects of host physiology, including protection against pathogens, wound healing (17), sebum production (18), and hair follicle homeostasis (19).

Cytokine-mediated communication allows immune cells to achieve a context-appropriate response, as the homeostasis of a multi-cellular organism is made possible by the proper cell-cell communication across different cell types (20). The cytokine superfamily consists of many ligands and receptors that mediate key interactions between immune cells and non-immune cells, including keratinocytes, fibroblasts, and endothelial cells, in the skin microenvironment (21–23). As the primary barrier, which is constantly exposed to environmental insults, the epidermis functions as a key sensor and integrator of environmental cues to regulate immunity in the skin (24, 25). As such, epidermis-derived alarmin cytokines mediate an intricate intercellular communication between epidermal keratinocytes and immune cells to regulate cutaneous immune surveillance. Alarmins are endogenous molecules that function as danger signals and are rapidly released to the extracellular milieu in response to tissue damage to trigger defensive immune responses (26). Among them, the proper functions of type 2 alarmin cytokines, thymic stromal lymphopoietin (TSLP), interleukin (IL)-25 and IL-33, as central orchestrators of T helper 2 (Th2) immunity, are paramount to the skin homeostasis and their dysregulation is commonly associated with chronic allergic inflammation (27–29).

In this review, we discuss recent findings on the complex functions of type 2 alarmin cytokines in regulating epithelium-immune cell communication that governs host defense, chronic inflammation, and cancer.

TSLP

TSLP is a member of the IL-2 family of cytokines, and its receptor is a heterodimer that consists of the IL-7 receptor α chain (IL-7Rα), which is shared with IL-7, and the TSLP receptor (TSLPR) (30–32). TSLP is mainly expressed by the epithelial cells of the gut, lung, and skin. Other cell types including DCs, basophils, and mast cells can express TSLP (33, 34). At the organ level, TSLP is widely distributed in several organs including the heart, liver, testis, spleen, prostate, skin, lung, kidney, ovary, small intestine, and colon (35). A variety of endogenous and environmental factors, such as pro-inflammatory cytokines, tryptase, invading pathogens, allergens, irritants, pollutants, and cigarette smoke, stimulate epithelial cells to release TSLP at barrier surfaces (36–45). Activation of protease-activated receptor 2 (PAR2), Toll-like receptor 4 (TLR4), and a member of transient receptor potential vanilloid (TRPV) channel family, including TRPV1, on the cell membrane mediate the production of TSLP through transcription factors, nuclear factor of activated T cells (NFAT), nuclear factor-kappa B (NF-κB), and interferon regulatory factor 3 (IRF-3) (46–48). TSLP is post-translationally modified by endogenous proteases, and cleaved TSLP has an increased biological activity (49). Despite poor sequence homology of TSLP (43% amino acid identity) and TSLPR (39% amino acid identity) between humans and mice, TSLP has been shown to exhibit similar biological functions in humans and mice (50).

Hematopoietic cell populations and sensory neurons express TSLPR. TSLP first interacts with the cognate TSLPR, then IL-7Rα can be recruited to the TSLP/TSLPR assembly to form the extracellular ternary complex. This leads to the activation of an intricate network of signaling pathways, including Janus kinase/signal transducer activator of transcription (JAK/STAT) and phosphatidylinositol-3 kinase (PI3K) pathways (51). Similar to IL-7, this signaling plays a critical role in the activation and differentiation of immune cells, such as B cells and T cells (52). In contrast, TSLP also mediates Th2 immunity associated with protection from helminth parasites and the pathogenesis of allergic inflammation at barrier surfaces. TSLP strongly induces the expression of major histocompatibility complex (MHC) class I and II molecules and costimulatory molecules on DCs. TSLP-activated DCs produce Th2-attracting chemokines, such as CCL17 and CCL22 (53), and induce Th2 differentiation through OX40 ligand upregulation on these cells (54, 55). Furthermore, TSLP can directly activate naïve $CD4^+$ T cells to differentiate and promote Th2 effector function in a TCR-dependent manner (56–58), indicating that TSLP is a key driver of Th2 immunity. In addition, TSLP acts on $CD4^+$ T cells to promote T helper 9 (Th9) differentiation and function through STAT5 activation in airway inflammation (59). Th9 cells, IL-9 producing $CD4^+$ T cells, are closely related to Th2 cells and contribute to allergic inflammation and anti-tumor immunity (60, 61). It remains unclear whether these cells represent a truly unique Th cell subset. TSLP also acts on basophils and group 2 ILCs (ILC2s) to induce Th2 responses (62, 63). Thus, TSLP orchestrates type 2 immune responses by innate and adaptive immune cells at barrier sites.

TSLP in Skin

Keratinocytes are a powerful source of TSLP in the skin under chronic and severe barrier disruption (64, 65). TSLP is released from keratinocytes in response to cutaneous pathogens, such as *Staphylococcus aureus* (66) and *Malassezia* yeasts (67), and environmental stimuli, such as ultraviolet radiation (68), mechanical injury (41), and air pollutants (69). The thermosensitive transient receptor potential channels TRPV3 and TRPV4 (70, 71), pattern recognition receptor TLR3 (72, 73), and PAR2 (38, 74) are among the receptors that can sense the external stimuli and induce the production of TSLP in keratinocytes. Vitamin D3 also induces the expression of TSLP in keratinocytes, which leads to the development of an atopic dermatitis-like phenotype (75). In contrast, TSLP is negatively regulated by retinoid X receptor αβ (RXRαβ) (76), aryl hydrocarbon receptor (AhR) (77), and Notch signaling (64), which function as a gatekeeper in keratinocytes. Chronic TSLP release by keratinocytes responding to cellular and tissue damage instigates type 2 immune response that leads to atopic dermatitis.

High TSLP expression is observed in a broad spectrum of skin lesions of atopic dermatitis (53), psoriasis (78), Netherton syndrome (79), and keloid (80). Continuous skin barrier disruption, characterized by atopic dermatitis, facilitates epicutaneous sensitization, which accelerates TSLP expression in keratinocytes. Furthermore, *TSLP* promoter demethylation is detected in skin lesions from patients with atopic dermatitis (81).

TSLPR is broadly expressed by immune cells and sensory neurons in the skin. In particular, DCs are important TSLP-responsive immune cell populations (27, 53–55, 82). Several DC subsets, including epidermal LCs and dermal type 1 and 2 conventional DCs, respond to keratinocytes-derived TSLP signals to initiate cutaneous adaptive immunity and provide multiple soluble and surface-bound signals that help to guide T cell differentiation, in particular Th2 cells (83–86). In atopic dermatitis lesions, TSLP may contribute to the activation of LCs, which then migrate to the draining lymph nodes and prime allergen-specific Th2 responses (53). In addition, TSLP-mediated LC activation can promote the differentiation of $CD4^+$ T cells into Th2 and follicular helper T cells (Tfh cells), which are important regulators of humoral responses (87). Moreover, TSLP and transforming growth factor-β1 (TGF-β1) synergistically contribute to the pool of LCs during inflammation *via* the promotion of LC differentiation from human blood BDCA-1^+ DCs (88). Dermal DCs act as critical responders in TSLP-mediated type 2 allergic inflammatory responses. TSLP activates CCL17-producing $CD11b^+$ dermal DCs to migrate to draining lymph nodes and attract naïve $CD4^+$ T cells to differentiate into Th2 cells during contact hypersensitivity in mice (89). Furthermore, TSLP-stimulated DCs act not only on the priming of Th2 cells but also on the maintenance and further polarization of Th2 central memory cells in allergic inflammation (90). Besides Th2 priming, TSLP-mediated DC activation conducts multiple $CD4^+$ T cell fate specifications in the skin, depending on the surrounding inflammatory microenvironment. TSLP drives the differentiation of IL-21-producing human Tfh cells through OX40 ligand in $CD1c^+$ DCs and helps memory B cells to produce immunoglobulin G (IgG) and IgE in a Th2 cell-dominated environment (91). Furthermore, TSLP is highly produced by keratinocytes in patients with psoriasis, where it synergizes with CD40 ligand in skin DCs to promote the expression of the Th17-polarizing cytokine IL-23 (78).

TSLP can directly activate $CD4^+$ T cells and induce the differentiation of a distinct population of effector Th2 cells in lymph nodes (58). TSLP/TSLPR signaling amplifies IL-4 production from $CD4^+$ T cells, which results in driving a positive feedback loop between TSLP and IL-4 to exacerbate Th2 cell-mediated allergic inflammation (92). In fact, atopic dermatitis patients possess circulating $CD4^+$ T cells expressing high TSLPR levels, and the frequency of this subset correlates with the severity of atopic dermatitis (93). In addition, Th2 cells express more TSLPR than Th1 or Th17 cells (94). ILC2s are also important targets of TSLP in allergic inflammation (95). TSLP-elicited ILC2 promotes allergic inflammation, whereas IL-25 and IL-33 are dispensable for this ILC2 response in an atopic dermatitis-like mouse model (95). Although IL-25 and IL-33 are critical mediators to elicit ILC2s in the gut and lung for anti-helminth immunity and allergic inflammation (96), skin-specific ILCs may have distinct properties. Accordingly, transcriptomic heterogeneity of ILC2s is apparent across tissues, and skin-resident ILC2s express relatively low levels of receptors of type 2 cytokines, such as TSLP, IL-25, and IL-33, and instead dominantly express IL-18 receptor (IL-18R1), compared with other tissues (97, 98). Indeed, IL-18 can activate skin ILC2s and synergize with type 2 cytokines in the development of atopic dermatitis-like disease (98). Furthermore, two distinct populations of ILC2s, consisting of skin-resident and circulating ILC2s, exist in the murine skin, and they exhibit distinctive phenotypes and functions (99). The response of ILC2s may ultimately depend on the nature of the inflammatory stimulus in the microenvironment.

Keratinocytes-released TSLP signals directly reach out to sensory neurons in the skin. PAR2-triggered release of TSLP can stimulate sensory neurons to evoke the itch response in allergic diseases such as atopic dermatitis, in a TSLPR- and TRPA1-dependent manner (38). In addition, TRPV4 triggers TSLP release, which activates sensory neurons through TSLPR and TRPV4 in a dry skin-induced pruritus model (71). TSLP is found to be involved in the later phase of itch progression in allergic inflammation while neutrophil-derived CXCL10 drives itch in the acute phase, which is mediated through CXCR3 on sensory neurons (100). TSLP widely impacts a broad array of dermal immune cells in the skin. TSLP elicits skin basophils, and TSLP-dependent basophil-derived IL-4 promotes ILC2 responses during atopic dermatitis-like inflammation (101). Furthermore, TSLP induces mast cell development through the activation of mouse double minute 2 (MDM2) and STAT6, which results in skin allergic inflammation (45, 102).

Excessive TSLP that is secreted by barrier-defective skin into the systemic circulation leads to sensitization of the lung airways to inhaled allergens characterized by allergic asthma-like phenotype in mice (103, 104). Thus, high systemic levels of skin-derived TSLP instigate the atopic march whereas IL-25 does not (105). Meanwhile, regulatory T cell (Treg)-mediated immunosuppression directly by TSLP from keratinocytes protects against progression from a local skin inflammatory response to a lethal systemic condition (106). TSLP has a dual function as a pro-inflammatory and pro-homeostatic modulator, and this may depend at least in part on the nature of surrounding immune signals and the type of cells responding to TSLP in the tissue microenvironment.

IL-25

IL-25 (also known as IL-17E) belongs to the IL-17 cytokine family, which consists of six members, and shares relatively low sequence similarity to the prototype member, IL-17 (alternative name IL-17A) (107–109). IL-25 receptor (IL-25R) is a heterodimer of the IL-17RA chain, which is shared with other IL-17 family members, and the IL-25-specific IL-17RB chain (108). Therefore, IL-25 exhibits a distinct function from other

members of the IL-17 cytokine family and has been implicated as a type 2 cytokine that induces the production of IL-4, IL-5, and IL-13, which in turn inhibit the IL-17-dependent autoimmune diseases (110). Furthermore, IL-25 enhances Th9 cell response to prevent parasitic helminths infection (111, 112). IL-25 is produced by epithelial and immune cells including Th2 cells, macrophages, ILC2s, mast cells, basophils, and eosinophils (109, 113). In the extracellular space, IL-25 has been reported to be a substrate for proteolytic cleavage by matrix metalloproteinase-7 (MMP-7) from airway epithelial cells during inflammation, and cleaved IL-25 increases its activity to induce type 2 cytokines (114). Expression of IL-25R has been reported on non-immune cells, including fibroblasts and endothelial cells, and immune cells, such as Th2 cells, natural killer T cells (NKT cells), DCs, macrophages, ILC2s, mast cells, basophils, and eosinophils in the inflammatory state (115, 116).

IL-25 in Skin

IL-25 has been reported to be highly expressed in several skin inflammatory diseases, including atopic dermatitis (117), psoriasis (118), pyoderma gangrenosum (119), acute generalized exanthematous pustulosis (119), and cutaneous T-cell lymphoma (CTCL) (120). IL-4, IL-13, IL-22, endothelin-1, and periostin enhance the production of IL-25 from keratinocytes (120–122). IL-25 induces allergic skin inflammation, characterized by elevated expression of IL-4 and IL-5, dermal infiltration of immune cells, epidermal hyperplasia, and impairment of skin barrier function in mice (118). Epidermal keratinocytes-derived IL-25 is a central regulator of a broad array of allergic inflammatory responses, and the major targets of IL-25 are dermal ILC2s and macrophages in the skin (123). IL-25 activates ILC2s to promote IL-13 production, which in turn helps keratinocytes proliferate and produce immune cell-attracting chemokines (124, 125). IL-25 also promotes the recruitment of neutrophils *via* activation of macrophages in a p38-dependent manner (119). On the other hand, IL-25 responds to tissue injury and participates in cutaneous would healing through an amelioration of angiogenesis and collagen deposition in diabetic mice model (126).

The autocrine function of IL-25 in keratinocytes promotes proliferation and inflammatory responses *via* STAT3 transcriptional factor, which results in amplification of psoriatic skin inflammation (118). Unlike IL-17, IL-25 is not capable of inducing antimicrobial peptides, β-defensin 2 and LL-37, in keratinocytes (121). IL-25 acts synergistically with Th2 cytokines, IL-4 and IL-13, to down-regulate filaggrin expression in keratinocytes exacerbating skin barrier defects (127). Down-regulation of filaggrin expression by IL-25 is mediated at least in part through the activation of NF-κB (107), whereas Th2 cytokines activate STAT6 (128, 129). In the fluorescein isothiocyanate-induced contact hypersensitivity model, IL-25 induces hapten-specific Th17 immunity, rather than Th2 immunity, in the elicitation phase of contact hypersensitivity (130). Following the hapten challenge, dermal DCs release IL-1β in response to IL-25, and IL-1β directly activates Th17 cells. This contrasts with the observed role of TSLP in DC activation and hapten-specific Th2 cell differentiation in the sensitization phase of contact hypersensitivity (131). These findings indicate that type 2 alarmin cytokines have distinct mechanisms for the regulation of T cell responses during inflammation.

IL-33

IL-33 is the most recently discovered member of type 2 alarmin cytokines (132). IL-33 was first described in 2005. It belongs to the IL-1 family of cytokines, which includes IL-1α, IL-1β, IL-18, IL-36α, IL-36β, IL-36γ, and IL-37, and the receptor antagonists IL-1Ra, IL-36Ra, and IL-38 (133). In contrast to its other family members, IL-1 and IL-18, IL-33 has been shown to promote Th2 cytokine responses in helminth infection and allergic inflammation (132). IL-33 is mainly expressed by non-immune cells, including epithelial cells, endothelial cells, and fibroblasts. It can also be expressed by immune cells, including macrophages and mast cells, at the barrier sites, where it functions as an alarmin following tissue damage (134, 135). IL-33 is localized in the cell nucleus, and its N-terminal domain, which includes a chromatin-binding motif, is required for its nuclear localization (136). Unlike IL-1β and IL-18, the N-terminal portion of IL-33 does not require inflammasome-mediated cleavage by caspase-1 for extracellular release of the active form. Apoptosis-associated caspase-3 and caspase-7 cleave and inactivate IL-33 at a conserved residue, Asp^{178} (Asp^{175} in mouse), within the IL-1-like cytokine domain (137). On the other hand, N-terminal processing of extracellular full-length IL-33 can occur in the central domain between the nuclear domain and the IL-1-like cytokine domain. These residues are targeted by extracellular proteases in the inflammatory microenvironment, including neutrophil cathepsin G, neutrophil elastase, and mast cell serine proteases, and the resulting 18-21 kDa cytokine forms of IL-33 exhibit higher biological activity (138, 139). Full-length IL-33 can be rapidly cleaved in its central sensor domain by extracellular environmental allergens-derived proteases within 10-20 minutes (140). In contrast, cysteine oxidation of extracellular IL-33 diminishes its biological activity (141). Thus, following IL-33 release, the impact of IL-33 is tightly regulated by post-translational modifications in the extracellular milieu. Although IL-33 lacks a secretion sequence and is sequestered in the nucleus *via* chromatin binding, IL-33 seems to be released into extracellular space through an unconventional secretion pathway following various stimuli. Environmental allergens, including fungi and mites, and mechanical stress trigger the release of IL-33 (142–145). Two primary scenarios for IL-33 release have been proposed: passive release as alarmin from necrotic cells during tissue damage and unconventional secretion from living cells. A recent study suggests that IL-33 is secreted through the extracellular vesicles pathway, commonly referred to as exosomes, as surface-bound cargo, from living airway epithelial cells (146). However, the molecular mechanisms and pathways of IL-33 secretion in living cells remain unclear.

IL-33 binds to its receptor, suppressor of tumorigenesis 2 (ST2), on target cells (147, 148). ST2 is classified as a member of the IL-1 receptor superfamily, which has a common intracellular domain, known as the Toll/Interleukin-1 receptor (TIR) domain

(147, 148). IL-33 signals *via* its cognate receptor ST2, which is highly expressed on Th2 cells, ILC2s, and mast cells, and induces Th2-skewed immunity to help with the removal of invading pathogens and helminths (29, 149). However, the detrimental effects of its chronic expression in response to environmental insults cause allergic inflammation. In addition, inappropriate activation of the IL-33/ST2 axis after tissue injury can lead to impaired wound healing and tissue remodeling (150–152). In contrast, IL-33 can also support tissue homeostasis and repair mediated by Tregs, which express ST2 predominantly in nonlymphoid tissue (153, 154).

IL-33 in Skin

Epidermal keratinocytes are the predominant producer of IL-33 while also expressing ST2 on their surface (132, 155). Dermal fibroblasts and macrophages can also produce IL-33 (104). IL-33 has been reported to be highly expressed in several skin diseases, including atopic dermatitis (155), psoriasis (156), and vitiligo (157). Serum IL-33 levels are higher in atopic dermatitis patients compared with healthy individuals and it correlates with excoriation and xerosis scores in atopic dermatitis (158). On the other hand, an increase in IL-33 is observed in skin lesions of psoriasis while no increase is observed in the serum (158). ST2 is distributed widely on dermal immune cells, including Th2 cells, Tregs, ILC2s, and mast cells. IL-33 is released from keratinocytes exposed to the invading pathogens, such as *Staphylococcus aureus* and house dust mite allergens, to instigate cutaneous immunity (159, 160). Environmental insults, such as ultraviolet B radiation and hypo-osmotic stress, and mechanical injury, also trigger the induction of IL-33 in keratinocytes (161–163). Interferon (IFN)-γ and tumor necrosis factor (TNF)-α are other known inducers of IL-33 in keratinocytes (164, 165). Nuclear IL-33 is elevated in human keratinocytes stimulated by TSLP and is required for TSLP-mediated suppression of epidermal barrier integrity components, indicating that nuclear IL-33 is a key mediator for chronic TSLP-induced skin barrier dysfunction (166).

IL-33 is implicated in type 2 immune response and the pathogenesis of allergic inflammatory diseases, such as atopic dermatitis (167). Excess IL-33 release from keratinocytes activates ILC2s to produce IL-5 and IL-13, which induce the accumulation of eosinophils in the dermis (168). Basophils induced by IL-33 also boost the ILC2 function *via* IL-4 signaling (169). IL-33 increases histamine generation in mast cells through p38 activation (170). Furthermore, IL-33 is involved in the induction of systemic allergic inflammation as keratinocyte-derived IL-33 can mediate skin-gut crosstalk culminating in the expansion of intestinal mast cells through ILC2 activation and food anaphylaxis (163, 171).

IL-33/ST2 signaling activates sensory neurons to mediate itch and pain responses (172–174). Excessive release of IL-33 from keratinocytes irradiated with poison ivy-derived allergen urushiol enhances the calcium influx in dermal peripheral dorsal root ganglia neurons through its receptor, ST2, to evoke itch and inflammatory responses (172). Neuronal ST2 signaling is a critical regulator of the development of the dry skin itch, but not an itch associated with atopic dermatitis (173). On the other hand, pathogen-derived lipopeptides, such as fibroblast-stimulating lipopeptide-1, can activate TLR2 in dorsal root ganglia, which, in turn, leads to infiltration of macrophages and release of IL-33 from keratinocytes. IL-33 activates the nociceptive sensory neurons at the superficial layers of the skin to instigate and prime the inflammatory pain responses (174). IL-33-mediated molecular mechanisms responsible for itch and pain are an active area of investigation.

IL-33 also plays a regulatory role in the inflamed tissue to restrain inflammation and promote remodeling in the skin, at least in part through the regulation of Tregs and M2 macrophages (175, 176). IL-33/ST2 signaling induces the expansion of Tregs, which have potent anti-inflammatory activity (177). IL-33 release from keratinocytes following skin barrier disruption induces antigen-specific Tregs to suppress excessive skin inflammation in a model of contact hypersensitivity (175). The diabetic mice model shows that IL-33 enhances extracellular matrix deposition and angiogenesis through the polarization of M2 macrophages to promote wound healing (176). Dysregulation of IL-33-mediated Treg induction causes aberrant chronic inflammation and fibrosis in the skin (151, 178). Furthermore, skin-resident Tregs from patients with systemic sclerosis are differentiated into Th2-like Tregs, which produce a higher amount of IL-4 and IL-13, by high expression of skin-localized IL-33, suggesting that IL-33 might be an important factor that contributes to fibrosis due to loss of normal skin-localized Tregs function (98). Single-cell RNA sequencing analysis of skin murine Tregs reveals a predominance of Th2-like Tregs, which preferentially express high levels of the master Th2 transcription factor, GATA3, and are more differentiated into cells, which have tissue reparative capacity (179). $GATA3^+$ Tregs in skin express ST2, which enables them to enact reparative functions in response to alarmin IL-33 (180). Thus, IL-33/ST2 signaling has diverse impacts on skin-resident Tregs and their function in the steady-state and fibrosis development.

BEYOND THE ROLE OF TYPE 2 CYTOKINES AS ALARMINS IN SKIN HEALTH

TSLP, IL-25, and IL-33 alert the immune system in the skin to respond to environmental insults, and their chronic overexpression triggers allergic inflammation at barrier sites (**Figure 1**). Importantly, the function of type 2 alarmin cytokines extends beyond their physiological function in host defense and pathological function in allergic inflammation and involves other critical roles including skin cancer regulation and sebum secretion (**Figure 2**). Keratinocyte-derived TSLP protects the skin from carcinogenesis (181, 182). TSLP exerts its dominant anti-tumor effects through the induction of $CD4^+$ Th2 cell immunity in the early stages of keratinocyte cancer development (181). In contrast, TSLP induces proliferation of the malignant $CD4^+$ T cells in CTCL lesions, which are marked by a Th2 cell-dominant phenotype in advanced stages (183). It has also been shown that TSLP can recruit IgE-bearing basophils into inflamed skin, and IgE promotes inflammation-driven

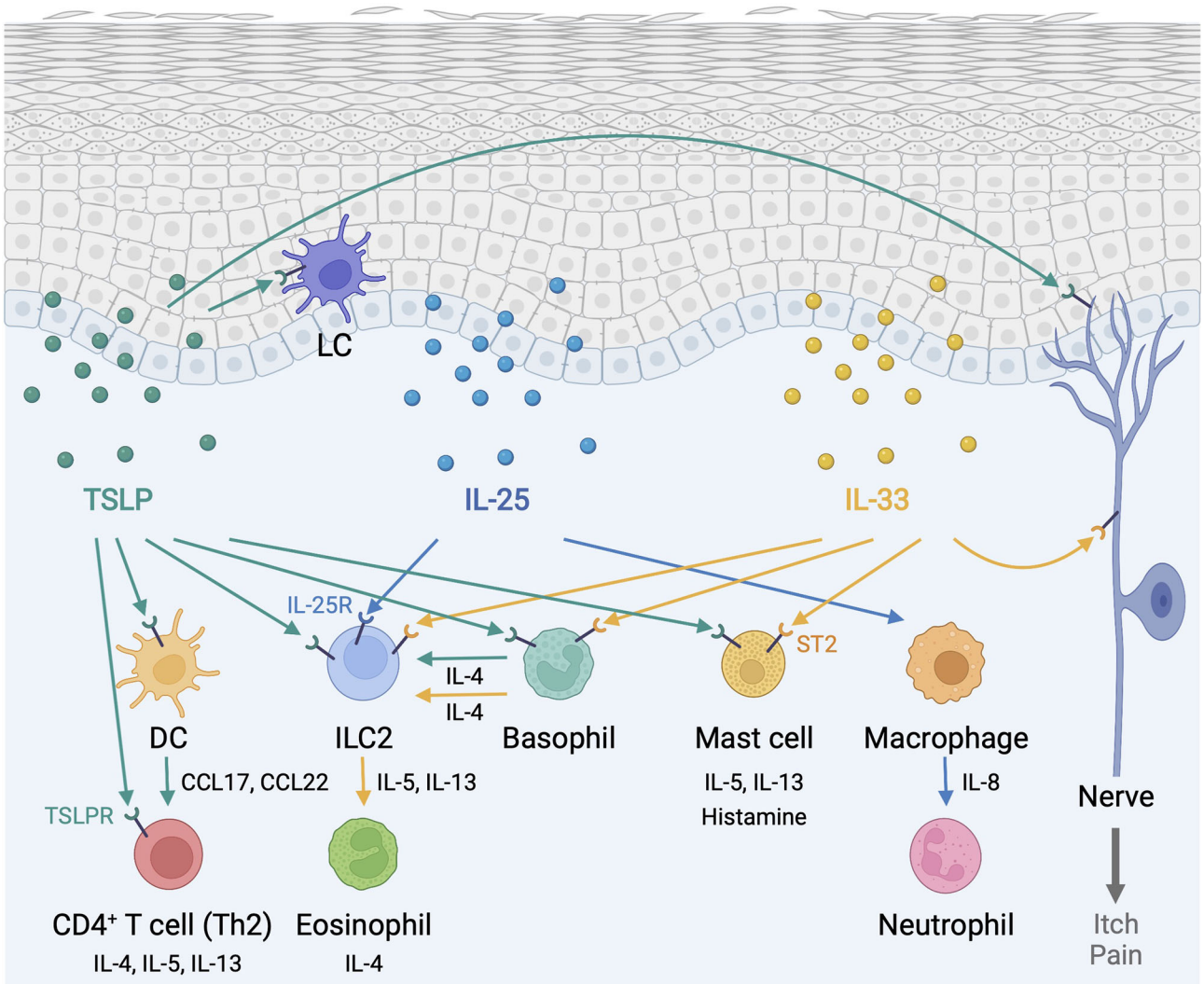

FIGURE 1 | Type 2 alarmin cytokines orchestrate immune responses in the skin. Epidermis-derived TSLP, IL-25, and IL-33 act as alarmins to instigate cutaneous type 2 immunity through a complex and pleiotropic network of innate and adaptive immune cells. In addition, TSLP and IL-33 provoke sensory neurons to mediate itch and pain responses. DC, dendritic cell; ILC2, group2 innate lymphoid cell; LC, Langerhans cell; TSLP, thymic stromal lymphopoietin; TSLPR, thymic stromal lymphopoietin receptor. Created with BioRender.com.

tumor growth during chronic tissue inflammation in a cutaneous squamous cell carcinoma model (184). Baseline TSLP expression in breast and pancreatic cancer has been linked to a pro-tumorigenic function (185–188). A tumor-myeloid cell axis independent of T cell response may mediate this tumor-promoting function of TSLP (189). However, systemic TSLP induction from the skin causes an effective $CD4^+$ T cell-mediated anti-tumor immune response at the site of developing cancer in the breast (185). Topical treatment of calcipotriol, a TSLP inducer (75), blocks skin cancer development in mice in a TSLP-dependent manner, and synergistically with 5-fluorouracil (5-FU) induces an effective $CD4^+$ T cell-mediated immunity against actinic keratosis, which is a precursor to cutaneous squamous cell carcinoma in humans (190). IL-25 also has potent anti-tumor effects against several tumor types, including melanoma, through an increase in eosinophils recruitment into the tumor (191, 192). In other models, IL-25 itself exhibits anti-tumor activity through the induction of apoptosis in cancer cells without affecting nonmalignant cells (193). In contrast, epidermal IL-33 contributes to a microenvironment that supports tumor growth and progression in murine skin. Nuclear IL-33 mediates focal adhesion kinase (FAK)-dependent secretion of soluble ST2, a decoy receptor, and CCL5 from squamous cell carcinoma cells, which stimulates immunosuppressive Tregs leading to cancer immune evasion (194). Continuous IL-33-driven stimulation of Tregs shapes a tumor-promoting immune environment associated with chronic inflammation in the murine skin, and

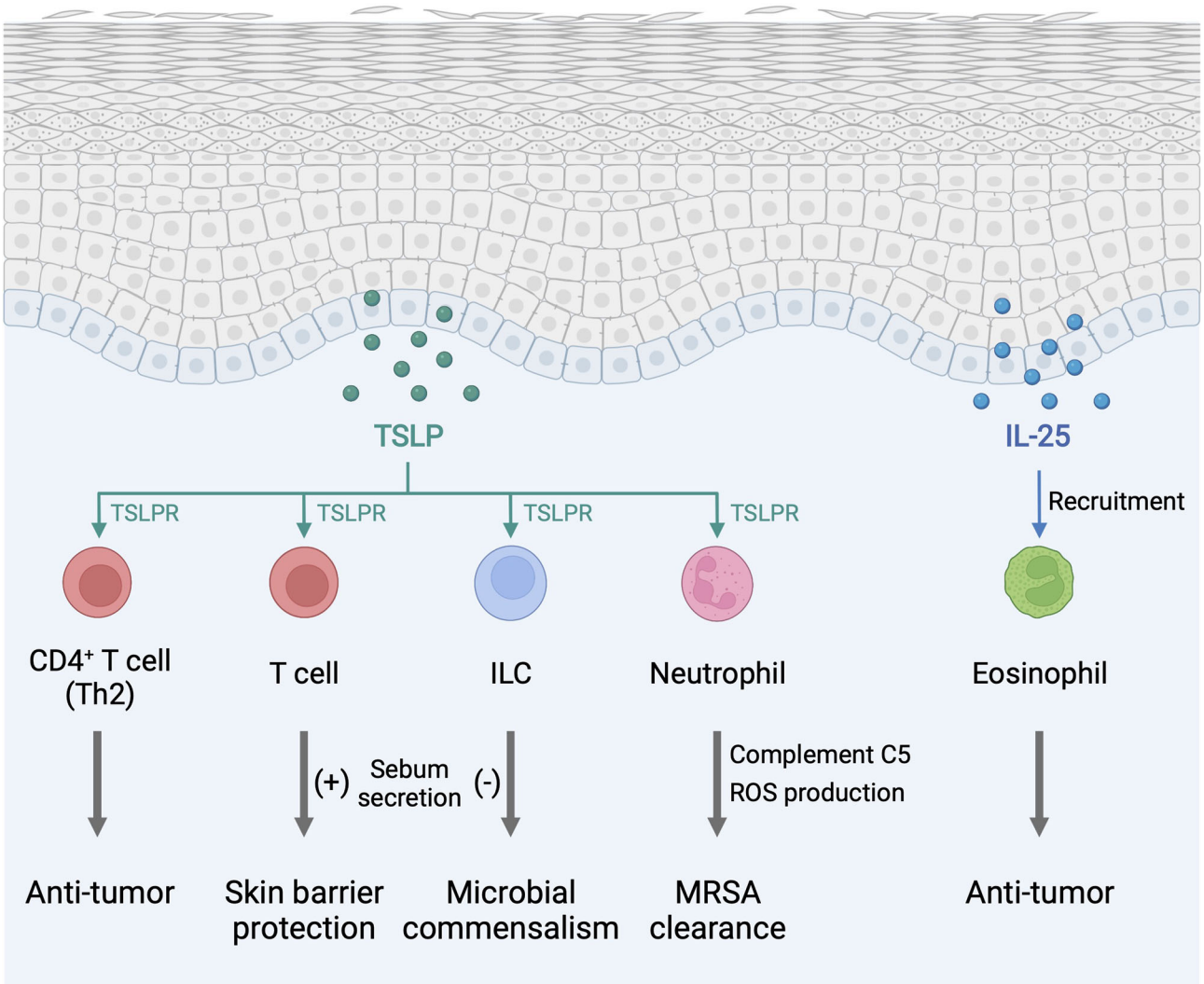

FIGURE 2 | Type 2 alarmin cytokines exhibit pro-homeostatic properties in the skin. The function of type 2 alarmin cytokines extends beyond their conventional Th2-associated function in host defense and allergy. In the skin, these cytokines play critical roles in cancer regulation and sebum secretion. ILC, innate lymphoid cell; MRSA, methicillin-resistant *Staphylococcus aureus*; ROS, reactive oxygen species; TSLP, thymic stromal lymphopoietin; TSLPR, thymic stromal lymphopoietin receptor. Created with BioRender.com.

an increase in IL-33 expression and Treg accumulation are observed in the perilesional skin of patients with cancer-prone chronic inflammation (178). Furthermore, IL-33 induces the recruitment of a subset of tumor-associated macrophages, which express ST2 and high-affinity IgE receptor, FcεRIα, and produce TGF-β, in the tumor microenvironment, which results in tumor progression in a mouse model of squamous cell carcinoma (195). Nuclear IL-33 in keratinocytes also promotes intrinsic TGF-β signaling through the SMAD signaling pathway, which constitutes a cell-autonomous tumor promotion mechanism in chronic inflammation (196). IL-33-stimulated macrophages highly produce MMP-9, which proteolytically trims activating receptor natural killer group 2, member D (NKG2D) and its ligands MHC class I polypeptide-related sequence A/B (MICA/B) on the surface of tumor-infiltrating lymphocytes and melanoma cells, and thus impedes the immune surveillance of tumor-infiltrating lymphocytes (197). These findings indicate that type 2 alarmin cytokines have distinct mechanisms for the regulation of cutaneous malignancies.

Endogenous TSLP controls the steady-state level of sebum secretion and sebum-associated antimicrobial peptide expression through the activation of T cells in murine skin. TSLP overexpression results in loss of white adipose tissue in conjunction with sebum hypersecretion (18). TSLP helps to maintain skin-resident RORγt$^+$ ILCs within hair follicles, and, by the virtue of their location, ILCs negatively regulate surrounding sebaceous gland size and lipid content to regulate commensal bacteria equilibrium and fine-tune the skin barrier

surface in mice (198). These findings suggest that TSLP-elicited ILCs and T cells play opposing functions in sebum secretion. Finally, TSLP is found to activate neutrophils to protect the skin from infection by methicillin-resistant *Staphylococcus aureus* (MRSA) (199).

CONCLUSION

Epidermis-derived TSLP, IL-25, and IL-33 act as alarmins to instigate cutaneous type 2 immunity through a complex and pleiotropic network of innate and adaptive immune cells. Accumulating evidence indicates that these type 2 alarmin cytokines not only function in concert but also have distinct physiological functions. Thus, the panoramic view of the communications between keratinocytes and immune cells through type 2 alarmin cytokines is required to fully understand how these cytokines regulate cutaneous immunity. The function of type 2 alarmin cytokines partly depends on the nature of the inflammatory stimulus, the presence of supporting cytokines and chemokines, and the surrounding microenvironment. Recent studies indicate that type 2 alarmin cytokines exhibit not only conventional type 2 inflammatory properties but also pro-homeostatic properties in the skin. Therefore, further understanding of the spectrum of biologic processes regulated by type 2 alarmin cytokines will provide new insights for the development of effective therapeutic approaches to combat allergic inflammation while utilizing the beneficial effects of these cytokines in the skin.

AUTHOR CONTRIBUTIONS

All authors contributed to the writing of the manuscript and approved the submitted version.

ACKNOWLEDGMENTS

Shadmehr Demehri, M.D., Ph.D., holds a Career Award for Medical Scientists award from the Burroughs Wellcome Fund.

REFERENCES

1. Elias PM. Stratum Corneum Defensive Functions: An Integrated View. *J Invest Dermatol* (2005) 125(2):183–200. doi: 10.1111/j.0022-202X.2005.23668.x
2. Kabashima K, Honda T, Ginhoux F, Egawa G. The Immunological Anatomy of the Skin. *Nat Rev Immunol* (2019) 19(1):19–30. doi: 10.1038/s41577-018-0084-5
3. Simpson CL, Patel DM, Green KJ. Deconstructing the Skin: Cytoarchitectural Determinants of Epidermal Morphogenesis. *Nat Rev Mol Cell Biol* (2011) 12(9):565–80. doi: 10.1038/nrm3175
4. Suwanpradid J, Holcomb ZE, MacLeod AS. Emerging Skin T-Cell Functions in Response to Environmental Insults. *J Invest Dermatol* (2017) 137(2):288–94. doi: 10.1016/j.jid.2016.08.013
5. Suzuki T, Hidaka T, Kumagai Y, Yamamoto M. Environmental Pollutants and the Immune Response. *Nat Immunol* (2020) 21(12):1486–95. doi: 10.1038/s41590-020-0802-6
6. Doebel T, Voisin B, Nagao K. Langerhans Cells - The Macrophage in Dendritic Cell Clothing. *Trends Immunol* (2017) 38(11):817–28. doi: 10.1016/j.it.2017.06.008
7. Deckers J, Hammad H, Hoste E. Langerhans Cells: Sensing the Environment in Health and Disease. *Front Immunol* (2018) 9:93. doi: 10.3389/fimmu.2018.00093
8. Kubo A, Nagao K, Yokouchi M, Sasaki H, Amagai M. External Antigen Uptake by Langerhans Cells With Reorganization of Epidermal Tight Junction Barriers. *J Exp Med* (2009) 206(13):2937–46. doi: 10.1084/jem.20091527
9. Ouchi T, Kubo A, Yokouchi M, Adachi T, Kobayashi T, Kitashima DY, et al. Langerhans Cell Antigen Capture Through Tight Junctions Confers Preemptive Immunity in Experimental Staphylococcal Scalded Skin Syndrome. *J Exp Med* (2011) 208(13):2607–13. doi: 10.1084/jem.20111718
10. Mueller SN, Zaid A, Carbone FR. Tissue-Resident T Cells: Dynamic Players in Skin Immunity. *Front Immunol* (2014) 5:332. doi: 10.3389/fimmu.2014.00332
11. Watanabe R, Gehad A, Yang C, Scott LL, Teague JE, Schlapbach C, et al. Human Skin is Protected by Four Functionally and Phenotypically Discrete Populations of Resident and Recirculating Memory T Cells. *Sci Transl Med* (2015) 7(279):279ra39. doi: 10.1126/scitranslmed.3010302
12. Szabo PA, Miron M, Farber DL. Location, Location, Location: Tissue Resident Memory T Cells in Mice and Humans. *Sci Immunol* (2019) 4(34). doi: 10.1126/sciimmunol.aas9673
13. Watt FM, Fujiwara H. Cell-Extracellular Matrix Interactions in Normal and Diseased Skin. *Cold Spring Harb Perspect Biol* (2011) 3(4). doi: 10.1101/cshperspect.a005124
14. Nestle FO, Di Meglio P, Qin JZ, Nickoloff BJ. Skin Immune Sentinels in Health and Disease. *Nat Rev Immunol* (2009) 9(10):679–91. doi: 10.1038/nri2622
15. Eyerich S, Eyerich K, Traidl-Hoffmann C, Biedermann T. Cutaneous Barriers and Skin Immunity: Differentiating A Connected Network. *Trends Immunol* (2018) 39(4):315–27. doi: 10.1016/j.it.2018.02.004
16. Bhattacharjee O, Ayyangar U, Kurbet AS, Ashok D, Raghavan S. Unraveling the ECM-Immune Cell Crosstalk in Skin Diseases. *Front Cell Dev Biol* (2019) 7:68. doi: 10.3389/fcell.2019.00068
17. Brazil JC, Quiros M, Nusrat A, Parkos CA. Innate Immune Cell-Epithelial Crosstalk During Wound Repair. *J Clin Invest* (2019) 129(8):2983–93. doi: 10.1172/JCI124618
18. Choa R, Tohyama J, Wada S, Meng H, Hu J, Okumura M, et al. Thymic Stromal Lymphopoietin Induces Adipose Loss Through Sebum Hypersecretion. *Science* (2021) 373(6554). doi: 10.1126/science.abd2893
19. Rahmani W, Sinha S, Biernaskie J. Immune Modulation of Hair Follicle Regeneration. *NPJ Regener Med* (2020) 5:9. doi: 10.1038/s41536-020-0095-2
20. Altan-Bonnet G, Mukherjee R. Cytokine-Mediated Communication: A Quantitative Appraisal of Immune Complexity. *Nat Rev Immunol* (2019) 19(4):205–17. doi: 10.1038/s41577-019-0131-x
21. Jiang Y, Tsoi LC, Billi AC, Ward NL, Harms PW, Zeng C, et al. Cytokinocytes: The Diverse Contribution of Keratinocytes to Immune Responses in Skin. *JCI Insight* (2020) 5(20). doi: 10.1172/jci.insight.142067
22. Davidson S, Coles M, Thomas T, Kollias G, Ludewig B, Turley S, et al. Fibroblasts as Immune Regulators in Infection, Inflammation and Cancer. *Nat Rev Immunol* (2021) 21(11):704–17. doi: 10.1038/s41577-021-00540-z
23. Pober JS, Sessa WC. Evolving Functions of Endothelial Cells in Inflammation. *Nat Rev Immunol* (2007) 7(10):803–15. doi: 10.1038/nri2171
24. Kupper TS, Fuhlbrigge RC. Immune Surveillance in the Skin: Mechanisms and Clinical Consequences. *Nat Rev Immunol* (2004) 4(3):211–22. doi: 10.1038/nri1310
25. Denda M, Nakanishi S. Do Epidermal Keratinocytes Have Sensory and Information Processing Systems? *Exp Dermatol* (2021). doi: 10.1111/exd.14494
26. Rider P, Voronov E, Dinarello CA, Apte RN, Cohen I. Alarmins: Feel the Stress. *J Immunol* (2017) 198(4):1395–402. doi: 10.4049/jimmunol.1601342
27. Wang SH, Zuo YG. Thymic Stromal Lymphopoietin in Cutaneous Immune-Mediated Diseases. *Front Immunol* (2021) 12:698522. doi: 10.3389/fimmu.2021.698522

28. Borowczyk J, Shutova M, Brembilla NC, Boehncke WH. IL-25 (IL-17E) in Epithelial Immunology and Pathophysiology. *J Allergy Clin Immunol* (2021) 148(1):40–52. doi: 10.1016/j.jaci.2020.12.628
29. Martin NT, Martin MU. Interleukin 33 is a Guardian of Barriers and a Local Alarmin. *Nat Immunol* (2016) 17(2):122–31. doi: 10.1038/ni.3370
30. Pandey A, Ozaki K, Baumann H, Levin SD, Puel A, Farr AG, et al. Cloning of a Receptor Subunit Required for Signaling by Thymic Stromal Lymphopoietin. *Nat Immunol* (2000) 1(1):59–64. doi: 10.1038/76923
31. Park LS, Martin U, Garka K, Gliniak B, Di Santo JP, Muller W, et al. Cloning of the Murine Thymic Stromal Lymphopoietin (TSLP) Receptor: Formation of a Functional Heteromeric Complex Requires Interleukin 7 Receptor. *J Exp Med* (2000) 192(5):659–70. doi: 10.1084/jem.192.5.659
32. Tonozuka Y, Fujio K, Sugiyama T, Nosaka T, Hirai M, Kitamura T. Molecular Cloning of a Human Novel Type I Cytokine Receptor Related to Delta1/TSLPR. *Cytogenet Cell Genet* (2001) 93(1-2):23–5. doi: 10.1159/000056941
33. He R, Geha RS. Thymic Stromal Lymphopoietin. *Ann N Y Acad Sci* (2010) 1183:13–24. doi: 10.1111/j.1749-6632.2009.05128.x
34. Takai T. TSLP Expression: Cellular Sources, Triggers, and Regulatory Mechanisms. *Allergol Int* (2012) 61(1):3–17. doi: 10.2332/allergolint.11-RAI-0395
35. Quentmeier H, Drexler HG, Fleckenstein D, Zaborski M, Armstrong A, Sims JE, et al. Cloning of Human Thymic Stromal Lymphopoietin (TSLP) and Signaling Mechanisms Leading to Proliferation. *Leukemia* (2001) 15 (8):1286–92. doi: 10.1038/sj.leu.2402175
36. Bernard M, Carrasco C, Laoubi L, Guiraud B, Rozieres A, Goujon C, et al. IL-1beta Induces Thymic Stromal Lymphopoietin and an Atopic Dermatitis-Like Phenotype in Reconstructed Healthy Human Epidermis. *J Pathol* (2017) 242(2):234–45. doi: 10.1002/path.4887
37. Segawa R, Shigeeda K, Hatayama T, Dong J, Mizuno N, Moriya T, et al. EGFR Transactivation is Involved in TNF-Alpha-Induced Expression of Thymic Stromal Lymphopoietin in Human Keratinocyte Cell Line. *J Dermatol Sci* (2018) 89(3):290–8. doi: 10.1016/j.jdermsci.2017.12.008
38. Wilson SR, The L, Batia LM, Beattie K, Katibah GE, McClain SP, et al. The Epithelial Cell-Derived Atopic Dermatitis Cytokine TSLP Activates Neurons to Induce Itch. *Cell* (2013) 155(2):285–95. doi: 10.1016/j.cell.2013.08.057
39. Wells JM, Rossi O, Meijerink M, van Baarlen P. Epithelial Crosstalk at the Microbiota-Mucosal Interface. *Proc Natl Acad Sci USA* (2011) 108 Suppl 1:4607–14. doi: 10.1073/pnas.1000092107
40. Cui X, Gao N, Me R, Xu J, Yu FX. TSLP Protects Corneas From Pseudomonas Aeruginosa Infection by Regulating Dendritic Cells and IL-23-IL-17 Pathway. *Invest Ophthalmol Vis Sci* (2018) 59(10):4228–37. doi: 10.1167/iovs.18-24672
41. Leyva-Castillo JM, Hener P, Jiang H, Li M. TSLP Produced by Keratinocytes Promotes Allergen Sensitization Through Skin and Thereby Triggers Atopic March in Mice. *J Invest Dermatol* (2013) 133(1):154–63. doi: 10.1038/jid.2012.239
42. Kumari V, Babina M, Hazzan T, Worm M. Thymic Stromal Lymphopoietin Induction by Skin Irritation is Independent of Tumour Necrosis Factor-Alpha, But Supported by Interleukin-1. *Br J Dermatol* (2015) 172(4):951–60. doi: 10.1111/bjd.13465
43. Bleck B, Grunig G, Chiu A, Liu M, Gordon T, Kazeros A, et al. MicroRNA-375 Regulation of Thymic Stromal Lymphopoietin by Diesel Exhaust Particles and Ambient Particulate Matter in Human Bronchial Epithelial Cells. *J Immunol* (2013) 190(7):3757–63. doi: 10.4049/jimmunol.1201165
44. Smelter DF, Sathish V, Thompson MA, Pabelick CM, Vassallo R, Prakash YS. Thymic Stromal Lymphopoietin in Cigarette Smoke-Exposed Human Airway Smooth Muscle. *J Immunol* (2010) 185(5):3035–40. doi: 10.4049/jimmunol.1000252
45. Allakhverdi Z, Comeau MR, Jessup HK, Yoon BR, Brewer A, Chartier S, et al. Thymic Stromal Lymphopoietin is Released by Human Epithelial Cells in Response to Microbes, Trauma, or Inflammation and Potently Activates Mast Cells. *J Exp Med* (2007) 204(2):253–8. doi: 10.1084/jem.20062211
46. Kouzaki H, O'Grady SM, Lawrence CB, Kita H. Proteases Induce Production of Thymic Stromal Lymphopoietin by Airway Epithelial Cells Through Protease-Activated Receptor-2. *J Immunol* (2009) 183(2):1427–34. doi: 10.4049/jimmunol.0900904
47. Jia X, Zhang H, Cao X, Yin Y, Zhang B. Activation of TRPV1 Mediates Thymic Stromal Lymphopoietin Release *via* the Ca2+/NFAT Pathway in Airway Epithelial Cells. *FEBS Lett* (2014) 588(17):3047–54. doi: 10.1016/j.febslet.2014.06.018
48. Kang JH, Yang HW, Park JH, Shin JM, Kim TH, Lee SH, et al. Lipopolysaccharide Regulates Thymic Stromal Lymphopoietin Expression *via* TLR4/MAPK/Akt/NF-kappaB-Signaling Pathways in Nasal Fibroblasts: Differential Inhibitory Effects of Macrolide and Corticosteroid. *Int Forum Allergy Rhinol* (2021) 11(2):144–52. doi: 10.1002/alr.22641
49. Poposki JA, Klingler AI, Stevens WW, Peters AT, Hulse KE, Grammer LC, et al. Proprotein Convertases Generate a Highly Functional Heterodimeric Form of Thymic Stromal Lymphopoietin in Humans. *J Allergy Clin Immunol* (2017) 139(5):1559–67 e8. doi: 10.1016/j.jaci.2016.08.040
50. Liu YJ, Soumelis V, Watanabe N, Ito T, Wang YH, Malefyt Rde W, et al. TSLP: An Epithelial Cell Cytokine That Regulates T Cell Differentiation by Conditioning Dendritic Cell Maturation. *Annu Rev Immunol* (2007) 25:193–219. doi: 10.1146/annurev.immunol.25.022106.141718
51. Verstraete K, van Schie L, Vyncke L, Bloch Y, Tavernier J, Pauwels E, et al. Structural Basis of the Proinflammatory Signaling Complex Mediated by TSLP. *Nat Struct Mol Biol* (2014) 21(4):375–82. doi: 10.1038/nsmb.2794
52. Ziegler SF, Artis D. Sensing the Outside World: TSLP Regulates Barrier Immunity. *Nat Immunol* (2010) 11(4):289–93. doi: 10.1038/ni.1852
53. Soumelis V, Reche PA, Kanzler H, Yuan W, Edward G, Homey B, et al. Human Epithelial Cells Trigger Dendritic Cell Mediated Allergic Inflammation by Producing TSLP. *Nat Immunol* (2002) 3(7):673–80. doi: 10.1038/ni805
54. Gilliet M, Soumelis V, Watanabe N, Hanabuchi S, Antonenko S, de Waal-Malefyt R, et al. Human Dendritic Cells Activated by TSLP and CD40L Induce Proallergic Cytotoxic T Cells. *J Exp Med* (2003) 197(8):1059–63. doi: 10.1084/jem.20030240
55. Ito T, Wang YH, Duramad O, Hori T, Delespesse GJ, Watanabe N, et al. TSLP-Activated Dendritic Cells Induce an Inflammatory T Helper Type 2 Cell Response Through OX40 Ligand. *J Exp Med* (2005) 202(9):1213–23. doi: 10.1084/jem.20051135
56. Omori M, Ziegler S. Induction of IL-4 Expression in CD4(+) T Cells by Thymic Stromal Lymphopoietin. *J Immunol* (2007) 178(3):1396–404. doi: 10.4049/jimmunol.178.3.1396
57. Rochman I, Watanabe N, Arima K, Liu YJ, Leonard WJ. Cutting Edge: Direct Action of Thymic Stromal Lymphopoietin on Activated Human CD4+ T Cells. *J Immunol* (2007) 178(11):6720–4. doi: 10.4049/jimmunol.178.11.6720
58. Ochiai S, Jagot F, Kyle RL, Hyde E, White RF, Prout M, et al. Thymic Stromal Lymphopoietin Drives the Development of IL-13(+) Th2 Cells. *Proc Natl Acad Sci USA* (2018) 115(5):1033–8. doi: 10.1073/pnas.1714348115
59. Yao W, Zhang Y, Jabeen R, Nguyen ET, Wilkes DS, Tepper RS, et al. Interleukin-9 is Required for Allergic Airway Inflammation Mediated by the Cytokine TSLP. *Immunity* (2013) 38(2):360–72. doi: 10.1016/j.immuni.2013.01.007
60. Angkasekwinai P, Dong C. IL-9-Producing T Cells: Potential Players in Allergy and Cancer. *Nat Rev Immunol* (2021) 21(1):37–48. doi: 10.1038/s41577-020-0396-0
61. Rivera Vargas T, Humblin E, Vegran F, Ghiringhelli F, Apetoh L. TH9 Cells in Anti-Tumor Immunity. *Semin Immunopathol* (2017) 39(1):39–46. doi: 10.1007/s00281-016-0599-4
62. Siracusa MC, Saenz SA, Hill DA, Kim BS, Headley MB, Doering TA, et al. TSLP Promotes Interleukin-3-Independent Basophil Haematopoiesis and Type 2 Inflammation. *Nature* (2011) 477(7363):229–33. doi: 10.1038/nature10329
63. Stier MT, Bloodworth MH, Toki S, Newcomb DC, Goleniewska K, Boyd KL, et al. Respiratory Syncytial Virus Infection Activates IL-13-Producing Group 2 Innate Lymphoid Cells Through Thymic Stromal Lymphopoietin. *J Allergy Clin Immunol* (2016) 138(3):814–24 e11. doi: 10.1016/j.jaci.2016.01.050
64. Demehri S, Liu Z, Lee J, Lin MH, Crosby SD, Roberts CJ, et al. Notch-Deficient Skin Induces a Lethal Systemic B-Lymphoproliferative Disorder by Secreting TSLP, a Sentinel for Epidermal Integrity. *PloS Biol* (2008) 6(5): e123. doi: 10.1371/journal.pbio.0060123
65. Zhang Z, Hener P, Frossard N, Kato S, Metzger D, Li M, et al. Thymic Stromal Lymphopoietin Overproduced by Keratinocytes in Mouse Skin

Aggravates Experimental Asthma. *Proc Natl Acad Sci USA* (2009) 106 (5):1536–41. doi: 10.1073/pnas.0812668106
66. Vu AT, Baba T, Chen X, Le TA, Kinoshita H, Xie Y, et al. Staphylococcus Aureus Membrane and Diacylated Lipopeptide Induce Thymic Stromal Lymphopoietin in Keratinocytes Through the Toll-Like Receptor 2-Toll-Like Receptor 6 Pathway. *J Allergy Clin Immunol* (2010) 126(5):985–93. doi: 10.1016/j.jaci.2010.09.002
67. Ishibashi Y, Sugawara K, Sugita T, Nishikawa A. Secretion of Thymic Stromal Lymphopoietin From Human Keratinocytes in Response to Malassezia Yeasts. *J Dermatol Sci* (2011) 62(2):134–8. doi: 10.1016/j.jdermsci.2011.02.012
68. Jang Y, Jeong SH, Park YH, Bae HC, Lee H, Ryu WI, et al. UVB Induces HIF-1alpha-Dependent TSLP Expression *via* the JNK and ERK Pathways. *J Invest Dermatol* (2013) 133(11):2601–8. doi: 10.1038/jid.2013.203
69. Hidaka T, Ogawa E, Kobayashi EH, Suzuki T, Funayama R, Nagashima T, et al. The Aryl Hydrocarbon Receptor AhR Links Atopic Dermatitis and Air Pollution *via* Induction of the Neurotrophic Factor Artemin. *Nat Immunol* (2017) 18(1):64–73. doi: 10.1038/ni.3614
70. Seo SH, Kim S, Kim SE, Chung S, Lee SE. Enhanced Thermal Sensitivity of TRPV3 in Keratinocytes Underlies Heat-Induced Pruritogen Release and Pruritus in Atopic Dermatitis. *J Invest Dermatol* (2020) 140(11):2199–209 e6. doi: 10.1016/j.jid.2020.02.028
71. Lee WJ, Shim WS. Cutaneous Neuroimmune Interactions of TSLP and TRPV4 Play Pivotal Roles in Dry Skin-Induced Pruritus. *Front Immunol* (2021) 12:772941. doi: 10.3389/fimmu.2021.772941
72. Vu AT, Chen X, Xie Y, Kamijo S, Ushio H, Kawasaki J, et al. Extracellular Double-Stranded RNA Induces TSLP *via* an Endosomal Acidification- and NF-kappaB-Dependent Pathway in Human Keratinocytes. *J Invest Dermatol* (2011) 131(11):2205–12. doi: 10.1038/jid.2011.185
73. Lee KH, Cho KA, Kim JY, Kim JY, Baek JH, Woo SY, et al. Filaggrin Knockdown and Toll-Like Receptor 3 (TLR3) Stimulation Enhanced the Production of Thymic Stromal Lymphopoietin (TSLP) From Epidermal Layers. *Exp Dermatol* (2011) 20(2):149–51. doi: 10.1111/j.1600-0625.2010.01203.x
74. Moniaga CS, Jeong SK, Egawa G, Nakajima S, Hara-Chikuma M, Jeon JE, et al. Protease Activity Enhances Production of Thymic Stromal Lymphopoietin and Basophil Accumulation in Flaky Tail Mice. *Am J Pathol* (2013) 182(3):841–51. doi: 10.1016/j.ajpath.2012.11.039
75. Li M, Hener P, Zhang Z, Kato S, Metzger D, Chambon P. Topical Vitamin D3 and Low-Calcemic Analogs Induce Thymic Stromal Lymphopoietin in Mouse Keratinocytes and Trigger an Atopic Dermatitis. *Proc Natl Acad Sci USA* (2006) 103(31):11736–41. doi: 10.1073/pnas.0604575103
76. Li M, Messaddeq N, Teletin M, Pasquali JL, Metzger D, Chambon P. Retinoid X Receptor Ablation in Adult Mouse Keratinocytes Generates an Atopic Dermatitis Triggered by Thymic Stromal Lymphopoietin. *Proc Natl Acad Sci USA* (2005) 102(41):14795–800. doi: 10.1073/pnas.0507385102
77. Jeong H, Shin JY, Kim MJ, Na J, Ju BG. Activation of Aryl Hydrocarbon Receptor Negatively Regulates Thymic Stromal Lymphopoietin Gene Expression *via* Protein Kinase Cdelta-P300-NF-kappaB Pathway in Keratinocytes Under Inflammatory Conditions. *J Invest Dermatol* (2019) 139(5):1098–109. doi: 10.1016/j.jid.2018.11.012
78. Volpe E, Pattarini L, Martinez-Cingolani C, Meller S, Donnadieu MH, Bogiatzi SI, et al. Thymic Stromal Lymphopoietin Links Keratinocytes and Dendritic Cell-Derived IL-23 in Patients With Psoriasis. *J Allergy Clin Immunol* (2014) 134(2):373–81. doi: 10.1016/j.jaci.2014.04.022
79. Hovnanian A. Netherton Syndrome: Skin Inflammation and Allergy by Loss of Protease Inhibition. *Cell Tissue Res* (2013) 351(2):289–300. doi: 10.1007/s00441-013-1558-1
80. Shin JU, Kim SH, Kim H, Noh JY, Jin S, Park CO, et al. TSLP Is a Potential Initiator of Collagen Synthesis and an Activator of CXCR4/SDF-1 Axis in Keloid Pathogenesis. *J Invest Dermatol* (2016) 136(2):507–15. doi: 10.1016/j.jid.2015.11.008
81. Luo Y, Zhou B, Zhao M, Tang J, Lu Q. Promoter Demethylation Contributes to TSLP Overexpression in Skin Lesions of Patients With Atopic Dermatitis. *Clin Exp Dermatol* (2014) 39(1):48–53. doi: 10.1111/ced.12206
82. Nakajima S, Igyarto BZ, Honda T, Egawa G, Otsuka A, Hara-Chikuma M, et al. Langerhans Cells Are Critical in Epicutaneous Sensitization With Protein Antigen *via* Thymic Stromal Lymphopoietin Receptor Signaling. *J Allergy Clin Immunol* (2012) 129(4):1048–55 e6. doi: 10.1016/j.jaci.2012.01.063
83. Malissen B, Tamoutounour S, Henri S. The Origins and Functions of Dendritic Cells and Macrophages in the Skin. *Nat Rev Immunol* (2014) 14 (6):417–28. doi: 10.1038/nri3683
84. Boltjes A, van Wijk F. Human Dendritic Cell Functional Specialization in Steady-State and Inflammation. *Front Immunol* (2014) 5:131. doi: 10.3389/fimmu.2014.00131
85. Eisenbarth SC. Dendritic Cell Subsets in T Cell Programming: Location Dictates Function. *Nat Rev Immunol* (2019) 19(2):89–103. doi: 10.1038/s41577-018-0088-1
86. Oyoshi MK, Larson RP, Ziegler SF, Geha RS. Mechanical Injury Polarizes Skin Dendritic Cells to Elicit a T(H)2 Response by Inducing Cutaneous Thymic Stromal Lymphopoietin Expression. *J Allergy Clin Immunol* (2010) 126(5):976–84. doi: 10.1016/j.jaci.2010.08.041
87. Marschall P, Wei R, Segaud J, Yao W, Hener P, German BF, et al. Dual Function of Langerhans Cells in Skin TSLP-Promoted TFH Differentiation in Mouse Atopic Dermatitis. *J Allergy Clin Immunol* (2021) 147(5):1778–94. doi: 10.1016/j.jaci.2020.10.006
88. Martinez-Cingolani C, Grandclaudon M, Jeanmougin M, Jouve M, Zollinger R, Soumelis V. Human Blood BDCA-1 Dendritic Cells Differentiate Into Langerhans-Like Cells With Thymic Stromal Lymphopoietin and TGF-Beta. *Blood* (2014) 124(15):2411–20. doi: 10.1182/blood-2014-04-568311
89. Kitajima M, Ziegler SF. Cutting Edge: Identification of the Thymic Stromal Lymphopoietin-Responsive Dendritic Cell Subset Critical for Initiation of Type 2 Contact Hypersensitivity. *J Immunol* (2013) 191(10):4903–7. doi: 10.4049/jimmunol.1302175
90. Wang YH, Ito T, Wang YH, Homey B, Watanabe N, Martin R, et al. Maintenance and Polarization of Human TH2 Central Memory T Cells by Thymic Stromal Lymphopoietin-Activated Dendritic Cells. *Immunity* (2006) 24(6):827–38. doi: 10.1016/j.immuni.2006.03.019
91. Pattarini L, Trichot C, Bogiatzi S, Grandclaudon M, Meller S, Keuylian Z, et al. TSLP-Activated Dendritic Cells Induce Human T Follicular Helper Cell Differentiation Through OX40-Ligand. *J Exp Med* (2017) 214(5):1529–46. doi: 10.1084/jem.20150402
92. Kitajima M, Kubo M, Ziegler SF, Suzuki H. Critical Role of TSLP Receptor on CD4 T Cells for Exacerbation of Skin Inflammation. *J Immunol* (2020) 205(1):27–35. doi: 10.4049/jimmunol.1900758
93. Tatsuno K, Fujiyama T, Yamaguchi H, Waki M, Tokura Y. TSLP Directly Interacts With Skin-Homing Th2 Cells Highly Expressing Its Receptor to Enhance IL-4 Production in Atopic Dermatitis. *J Invest Dermatol* (2015) 135 (12):3017–24. doi: 10.1038/jid.2015.318
94. Kitajima M, Lee HC, Nakayama T, Ziegler SF. TSLP Enhances the Function of Helper Type 2 Cells. *Eur J Immunol* (2011) 41(7):1862–71. doi: 10.1002/eji.201041195
95. Kim BS, Siracusa MC, Saenz SA, Noti M, Monticelli LA, Sonnenberg GF, et al. TSLP Elicits IL-33-Independent Innate Lymphoid Cell Responses to Promote Skin Inflammation. *Sci Transl Med* (2013) 5(170):170ra16. doi: 10.1126/scitranslmed.3005374
96. Halim TY. Group 2 Innate Lymphoid Cells in Disease. *Int Immunol* (2016) 28(1):13–22. doi: 10.1093/intimm/dxv050
97. Simoni Y, Fehlings M, Kloverpris HN, McGovern N, Koo SL, Loh CY, et al. Human Innate Lymphoid Cell Subsets Possess Tissue-Type Based Heterogeneity in Phenotype and Frequency. *Immunity* (2017) 46(1):148–61. doi: 10.1016/j.immuni.2016.11.005
98. Ricardo-Gonzalez RR, Van Dyken SJ, Schneider C, Lee J, Nussbaum JC, Liang HE, et al. Tissue Signals Imprint ILC2 Identity With Anticipatory Function. *Nat Immunol* (2018) 19(10):1093–9. doi: 10.1038/s41590-018-0201-4
99. Nakatani-Kusakabe M, Yasuda K, Tomura M, Nagai M, Yamanishi K, Kuroda E, et al. Monitoring Cellular Movement With Photoconvertible Fluorescent Protein and Single-Cell RNA Sequencing Reveals Cutaneous Group 2 Innate Lymphoid Cell Subtypes, Circulating ILC2 and Skin-Resident Ilc2. *JID Innov* (2021) 1(3):100035. doi: 10.1016/j.xjidi.2021.100035
100. Walsh CM, Hill RZ, Schwendinger-Schreck J, Deguine J, Brock EC, Kucirek N, et al. Neutrophils Promote CXCR3-Dependent Itch in the Development of Atopic Dermatitis. *Elife* (2019) 8. doi: 10.7554/eLife.48448
101. Kim BS, Wang K, Siracusa MC, Saenz SA, Brestoff JR, Monticelli LA, et al. Basophils Promote Innate Lymphoid Cell Responses in Inflamed Skin. *J Immunol* (2014) 193(7):3717–25. doi: 10.4049/jimmunol.1401307

102. Han NR, Oh HA, Nam SY, Moon PD, Kim DW, Kim HM, et al. TSLP Induces Mast Cell Development and Aggravates Allergic Reactions Through the Activation of MDM2 and STAT6. *J Invest Dermatol* (2014) 134 (10):2521–30. doi: 10.1038/jid.2014.198
103. Demehri S, Morimoto M, Holtzman MJ, Kopan R. Skin-Derived TSLP Triggers Progression From Epidermal-Barrier Defects to Asthma. *PloS Biol* (2009) 7(5):e1000067. doi: 10.1371/journal.pbio.1000067
104. Li C, Li H, Jiang Z, Zhang T, Wang Y, Li Z, et al. Interleukin-33 Increases Antibacterial Defense by Activation of Inducible Nitric Oxide Synthase in Skin. *PloS Pathog* (2014) 10(2):e1003918. doi: 10.1371/journal.ppat.1003918
105. Han H, Xu W, Headley MB, Jessup HK, Lee KS, Omori M, et al. Thymic Stromal Lymphopoietin (TSLP)-Mediated Dermal Inflammation Aggravates Experimental Asthma. *Mucosal Immunol* (2012) 5(3):342–51. doi: 10.1038/mi.2012.14
106. Kashiwagi M, Hosoi J, Lai JF, Brissette J, Ziegler SF, Morgan BA, et al. Direct Control of Regulatory T Cells by Keratinocytes. *Nat Immunol* (2017) 18 (3):334–43. doi: 10.1038/ni.3661
107. Lee J, Ho WH, Maruoka M, Corpuz RT, Baldwin DT, Foster JS, et al. IL-17E, a Novel Proinflammatory Ligand for the IL-17 Receptor Homolog IL-17rh1. *J Biol Chem* (2001) 276(2):1660–4. doi: 10.1074/jbc.M008289200
108. Moseley TA, Haudenschild DR, Rose L, Reddi AH. Interleukin-17 Family and IL-17 Receptors. *Cytokine Growth Factor Rev* (2003) 14(2):155–74. doi: 10.1016/s1359-6101(03)00002-9
109. Deng C, Peng N, Tang Y, Yu N, Wang C, Cai X, et al. Roles of IL-25 in Type 2 Inflammation and Autoimmune Pathogenesis. *Front Immunol* (2021) 12:691559. doi: 10.3389/fimmu.2021.691559
110. Kleinschek MA, Owyang AM, Joyce-Shaikh B, Langrish CL, Chen Y, Gorman DM, et al. IL-25 Regulates Th17 Function in Autoimmune Inflammation. *J Exp Med* (2007) 204(1):161–70. doi: 10.1084/jem.20061738
111. Angkasekwinai P, Chang SH, Thapa M, Watarai H, Dong C. Regulation of IL-9 Expression by IL-25 Signaling. *Nat Immunol* (2010) 11(3):250–6. doi: 10.1038/ni.1846
112. Angkasekwinai P, Srimanote P, Wang YH, Pootong A, Sakolvaree Y, Pattanapanyasat K, et al. Interleukin-25 (IL-25) Promotes Efficient Protective Immunity Against Trichinella Spiralis Infection by Enhancing the Antigen-Specific IL-9 Response. *Infect Immun* (2013) 81(10):3731–41. doi: 10.1128/IAI.00646-13
113. Paul WE, Zhu J. How Are T(H)2-Type Immune Responses Initiated and Amplified? *Nat Rev Immunol* (2010) 10(4):225–35. doi: 10.1038/nri2735
114. Goswami S, Angkasekwinai P, Shan M, Greenlee KJ, Barranco WT, Polikepahad S, et al. Divergent Functions for Airway Epithelial Matrix Metalloproteinase 7 and Retinoic Acid in Experimental Asthma. *Nat Immunol* (2009) 10(5):496–503. doi: 10.1038/ni.1719
115. Gaffen SL. Structure and Signalling in the IL-17 Receptor Family. *Nat Rev Immunol* (2009) 9(8):556–67. doi: 10.1038/nri2586
116. Yao X, Sun Y, Wang W, Sun Y. Interleukin (IL)-25: Pleiotropic Roles in Asthma. *Respirology* (2016) 21(4):638–47. doi: 10.1111/resp.12707
117. Hvid M, Vestergaard C, Kemp K, Christensen GB, Deleuran B, Deleuran M. IL-25 in Atopic Dermatitis: A Possible Link Between Inflammation and Skin Barrier Dysfunction? *J Invest Dermatol* (2011) 131(1):150–7. doi: 10.1038/jid.2010.277
118. Xu M, Lu H, Lee YH, Wu Y, Liu K, Shi Y, et al. An Interleukin-25-Mediated Autoregulatory Circuit in Keratinocytes Plays a Pivotal Role in Psoriatic Skin Inflammation. *Immunity* (2018) 48(4):787–98.e4. doi: 10.1016/j.immuni.2018.03.019
119. Senra L, Mylonas A, Kavanagh RD, Fallon PG, Conrad C, Borowczyk-Michalowska J, et al. IL-17e (IL-25) Enhances Innate Immune Responses During Skin Inflammation. *J Invest Dermatol* (2019) 139(8):1732–42 e17. doi: 10.1016/j.jid.2019.01.021
120. Nakajima R, Miyagaki T, Hirakawa M, Oka T, Takahashi N, Suga H, et al. Interleukin-25 is Involved in Cutaneous T-Cell Lymphoma Progression by Establishing a T Helper 2-Dominant Microenvironment. *Br J Dermatol* (2018) 178(6):1373–82. doi: 10.1111/bjd.16237
121. Borowczyk J, Buerger C, Tadjrischi N, Drukala J, Wolnicki M, Wnuk D, et al. IL-17e (IL-25) and IL-17a Differentially Affect the Functions of Human Keratinocytes. *J Invest Dermatol* (2020) 140(7):1379–89.e2. doi: 10.1016/j.jid.2019.12.013
122. Aktar MK, Kido-Nakahara M, Furue M, Nakahara T. Mutual Upregulation of Endothelin-1 and IL-25 in Atopic Dermatitis. *Allergy* (2015) 70(7):846–54. doi: 10.1111/all.12633
123. Roan F, Obata-Ninomiya K, Ziegler SF. Epithelial Cell-Derived Cytokines: More Than Just Signaling the Alarm. *J Clin Invest* (2019) 129(4):1441–51. doi: 10.1172/JCI124606
124. Salimi M, Barlow JL, Saunders SP, Xue L, Gutowska-Owsiak D, Wang X, et al. A Role for IL-25 and IL-33-Driven Type-2 Innate Lymphoid Cells in Atopic Dermatitis. *J Exp Med* (2013) 210(13):2939–50. doi: 10.1084/jem.20130351
125. Leyva-Castillo JM, Galand C, Mashiko S, Bissonnette R, McGurk A, Ziegler SF, et al. ILC2 Activation by Keratinocyte-Derived IL-25 Drives IL-13 Production at Sites of Allergic Skin Inflammation. *J Allergy Clin Immunol* (2020) 145(6):1606–14 e4. doi: 10.1016/j.jaci.2020.02.026
126. Zhang F, Liu Y, Wang S, Yan X, Lin Y, Chen D, et al. Interleukin-25-Mediated-IL-17rb Upregulation Promotes Cutaneous Wound Healing in Diabetic Mice by Improving Endothelial Cell Functions. *Front Immunol* (2022) 13:809755. doi: 10.3389/fimmu.2022.809755
127. Kim BE, Bin L, Ye YM, Ramamoorthy P, Leung DYM. IL-25 Enhances HSV-1 Replication by Inhibiting Filaggrin Expression, and Acts Synergistically With Th2 Cytokines to Enhance HSV-1 Replication. *J Invest Dermatol* (2013) 133(12):2678–85. doi: 10.1038/jid.2013.223
128. Howell MD, Kim BE, Gao P, Grant AV, Boguniewicz M, Debenedetto A, et al. Cytokine Modulation of Atopic Dermatitis Filaggrin Skin Expression. *J Allergy Clin Immunol* (2007) 120(1):150–5. doi: 10.1016/j.jaci.2007.04.031
129. Sehra S, Yao Y, Howell MD, Nguyen ET, Kansas GS, Leung DY, et al. IL-4 Regulates Skin Homeostasis and the Predisposition Toward Allergic Skin Inflammation. *J Immunol* (2010) 184(6):3186–90. doi: 10.4049/jimmunol.0901860
130. Suto H, Nambu A, Morita H, Yamaguchi S, Numata T, Yoshizaki T, et al. IL-25 Enhances TH17 Cell-Mediated Contact Dermatitis by Promoting IL-1beta Production by Dermal Dendritic Cells. *J Allergy Clin Immunol* (2018) 142(5):1500–9.e10. doi: 10.1016/j.jaci.2017.12.1007
131. Larson RP, Zimmerli SC, Comeau MR, Itano A, Omori M, Iseki M, et al. Dibutyl Phthalate-Induced Thymic Stromal Lymphopoietin is Required for Th2 Contact Hypersensitivity Responses. *J Immunol* (2010) 184(6):2974–84. doi: 10.4049/jimmunol.0803478
132. Schmitz J, Owyang A, Oldham E, Song Y, Murphy E, McClanahan TK, et al. IL-33, an Interleukin-1-Like Cytokine That Signals *via* the IL-1 Receptor-Related Protein ST2 and Induces T Helper Type 2-Associated Cytokines. *Immunity* (2005) 23(5):479–90. doi: 10.1016/j.immuni.2005.09.015
133. Garlanda C, Dinarello CA, Mantovani A. The Interleukin-1 Family: Back to the Future. *Immunity* (2013) 39(6):1003–18. doi: 10.1016/j.immuni.2013.11.010
134. Moussion C, Ortega N, Girard JP. The IL-1-Like Cytokine IL-33 is Constitutively Expressed in the Nucleus of Endothelial Cells and Epithelial Cells *In Vivo*: A Novel A'larmin'? *PloS One* (2008) 3(10):e3331. doi: 10.1371/journal.pone.0003331
135. Pichery M, Mirey E, Mercier P, Lefrancais E, Dujardin A, Ortega N, et al. Endogenous IL-33 is Highly Expressed in Mouse Epithelial Barrier Tissues, Lymphoid Organs, Brain, Embryos, and Inflamed Tissues: In *Situ* Analysis Using a Novel Il-33-LacZ Gene Trap Reporter Strain. *J Immunol* (2012) 188 (7):3488–95. doi: 10.4049/jimmunol.1101977
136. Carriere V, Roussel L, Ortega N, Lacorre DA, Americh L, Aguilar L, et al. IL-33, the IL-1-Like Cytokine Ligand for ST2 Receptor, is a Chromatin-Associated Nuclear Factor *In Vivo*. *Proc Natl Acad Sci USA* (2007) 104 (1):282–7. doi: 10.1073/pnas.0606854104
137. Luthi AU, Cullen SP, McNeela EA, Duriez PJ, Afonina IS, Sheridan C, et al. Suppression of Interleukin-33 Bioactivity Through Proteolysis by Apoptotic Caspases. *Immunity* (2009) 31(1):84–98. doi: 10.1016/j.immuni.2009.05.007
138. Lefrancais E, Roga S, Gautier V, Gonzalez-de-Peredo A, Monsarrat B, Girard JP, et al. IL-33 is Processed Into Mature Bioactive Forms by Neutrophil Elastase and Cathepsin G. *Proc Natl Acad Sci USA* (2012) 109(5):1673–8. doi: 10.1073/pnas.1115884109
139. Lefrancais E, Duval A, Mirey E, Roga S, Espinosa E, Cayrol C, et al. Central Domain of IL-33 is Cleaved by Mast Cell Proteases for Potent Activation of Group-2 Innate Lymphoid Cells. *Proc Natl Acad Sci USA* (2014) 111 (43):15502–7. doi: 10.1073/pnas.1410700111
140. Cayrol C, Duval A, Schmitt P, Roga S, Camus M, Stella A, et al. Environmental Allergens Induce Allergic Inflammation Through Proteolytic Maturation of IL-33. *Nat Immunol* (2018) 19(4):375–85. doi: 10.1038/s41590-018-0067-5

141. Cohen ES, Scott IC, Majithiya JB, Rapley L, Kemp BP, England E, et al. Oxidation of the Alarmin IL-33 Regulates ST2-Dependent Inflammation. *Nat Commun* (2015) 6:8327. doi: 10.1038/ncomms9327
142. Kouzaki H, Iijima K, Kobayashi T, O'Grady SM, Kita H. The Danger Signal, Extracellular ATP, is a Sensor for an Airborne Allergen and Triggers IL-33 Release and Innate Th2-Type Responses. *J Immunol* (2011) 186(7):4375–87. doi: 10.4049/jimmunol.1003020
143. Hiraishi Y, Yamaguchi S, Yoshizaki T, Nambu A, Shimura E, Takamori A, et al. IL-33, IL-25 and TSLP Contribute to Development of Fungal-Associated Protease-Induced Innate-Type Airway Inflammation. *Sci Rep* (2018) 8(1):18052. doi: 10.1038/s41598-018-36440-x
144. de Kleer IM, Kool M, de Bruijn MJ, Willart M, van Moorleghem J, Schuijs MJ, et al. Perinatal Activation of the Interleukin-33 Pathway Promotes Type 2 Immunity in the Developing Lung. *Immunity* (2016) 45(6):1285–98. doi: 10.1016/j.immuni.2016.10.031
145. Sanada S, Hakuno D, Higgins LJ, Schreiter ER, McKenzie AN, Lee RT. IL-33 and ST2 Comprise a Critical Biomechanically Induced and Cardioprotective Signaling System. *J Clin Invest* (2007) 117(6):1538–49. doi: 10.1172/JCI30634
146. Katz-Kiriakos E, Steinberg DF, Kluender CE, Osorio OA, Newsom-Stewart C, Baronia A, et al. Epithelial IL-33 Appropriates Exosome Trafficking for Secretion in Chronic Airway Disease. *JCI Insight* (2021) 6(4). doi: 10.1172/jci.insight.136166
147. Yanagisawa K, Takagi T, Tsukamoto T, Tetsuka T, Tominaga S. Presence of a Novel Primary Response Gene ST2L, Encoding a Product Highly Similar to the Interleukin 1 Receptor Type 1. *FEBS Lett* (1993) 318(1):83–7. doi: 10.1016/0014-5793(93)81333-u
148. Xu Y, Tao X, Shen B, Horng T, Medzhitov R, Manley JL, et al. Structural Basis for Signal Transduction by the Toll/interleukin-1 Receptor Domains. *Nature* (2000) 408(6808):111–5. doi: 10.1038/35040600
149. Griesenauer B, Paczesny S. The ST2/IL-33 Axis in Immune Cells During Inflammatory Diseases. *Front Immunol* (2017) 8:475. doi: 10.3389/fimmu.2017.00475
150. Rankin AL, Mumm JB, Murphy E, Turner S, Yu N, McClanahan TK, et al. IL-33 Induces IL-13-Dependent Cutaneous Fibrosis. *J Immunol* (2010) 184 (3):1526–35. doi: 10.4049/jimmunol.0903306
151. MacDonald KG, Dawson NAJ, Huang Q, Dunne JV, Levings MK, Broady R. Regulatory T Cells Produce Profibrotic Cytokines in the Skin of Patients With Systemic Sclerosis. *J Allergy Clin Immunol* (2015) 135(4):946–55.e9. doi: 10.1016/j.jaci.2014.12.1932
152. Molofsky AB, Savage AK, Locksley RM. Interleukin-33 in Tissue Homeostasis, Injury, and Inflammation. *Immunity* (2015) 42(6):1005–19. doi: 10.1016/j.immuni.2015.06.006
153. Schiering C, Krausgruber T, Chomka A, Frohlich A, Adelmann K, Wohlfert EA, et al. The Alarmin IL-33 Promotes Regulatory T-Cell Function in the Intestine. *Nature* (2014) 513(7519):564–8. doi: 10.1038/nature13577
154. Faustino LD, Griffith JW, Rahimi RA, Nepal K, Hamilos DL, Cho JL, et al. Interleukin-33 Activates Regulatory T Cells to Suppress Innate Gammadelta T Cell Responses in the Lung. *Nat Immunol* (2020) 21(11):1371–83. doi: 10.1038/s41590-020-0785-3
155. Savinko T, Matikainen S, Saarialho-Kere U, Lehto M, Wang G, Lehtimaki S, et al. IL-33 and ST2 in Atopic Dermatitis: Expression Profiles and Modulation by Triggering Factors. *J Invest Dermatol* (2012) 132(5):1392–400. doi: 10.1038/jid.2011.446
156. Theoharides TC, Zhang B, Kempuraj D, Tagen M, Vasiadi M, Angelidou A, et al. IL-33 Augments Substance P-Induced VEGF Secretion From Human Mast Cells and is Increased in Psoriatic Skin. *Proc Natl Acad Sci USA* (2010) 107(9):4448–53. doi: 10.1073/pnas.1000803107
157. Li P, Ma H, Han D, Mou K. Interleukin-33 Affects Cytokine Production by Keratinocytes in Vitiligo. *Clin Exp Dermatol* (2015) 40(2):163–70. doi: 10.1111/ced.12464
158. Tamagawa-Mineoka R, Okuzawa Y, Masuda K, Katoh N. Increased Serum Levels of Interleukin 33 in Patients With Atopic Dermatitis. *J Am Acad Dermatol* (2014) 70(5):882–8. doi: 10.1016/j.jaad.2014.01.867
159. Al Kindi A, Williams H, Matsuda K, Alkahtani AM, Saville C, Bennett H, et al. Staphylococcus Aureus Second Immunoglobulin-Binding Protein Drives Atopic Dermatitis *via* IL-33. *J Allergy Clin Immunol* (2021) 147 (4):1354–68 e3. doi: 10.1016/j.jaci.2020.09.023
160. Dai X, Tohyama M, Murakami M, Shiraishi K, Liu S, Mori H, et al. House Dust Mite Allergens Induce Interleukin 33 (IL-33) Synthesis and Release From Keratinocytes *via* ATP-Mediated Extracellular Signaling. *Biochim Biophys Acta Mol Basis Dis* (2020) 1866(5):165719. doi: 10.1016/j.bbadis.2020.165719
161. Meephansan J, Komine M, Tsuda H, Tominaga S, Ohtsuki M. Ultraviolet B Irradiation Induces the Expression of IL-33 mRNA and Protein in Normal Human Epidermal Keratinocytes. *J Dermatol Sci* (2012) 65(1):72–4. doi: 10.1016/j.jdermsci.2011.10.004
162. Pietka W, Khnykin D, Bertelsen V, Lossius AH, Stav-Noraas TE, Hol Fosse J, et al. Hypo-Osmotic Stress Drives IL-33 Production in Human Keratinocytes-An Epidermal Homeostatic Response. *J Invest Dermatol* (2019) 139(1):81–90. doi: 10.1016/j.jid.2018.07.023
163. Leyva-Castillo JM, Galand C, Kam C, Burton O, Gurish M, Musser MA, et al. Mechanical Skin Injury Promotes Food Anaphylaxis by Driving Intestinal Mast Cell Expansion. *Immunity* (2019) 50(5):1262–75.e4. doi: 10.1016/j.immuni.2019.03.023
164. Meephansan J, Tsuda H, Komine M, Tominaga S, Ohtsuki M. Regulation of IL-33 Expression by IFN-Gamma and Tumor Necrosis Factor-Alpha in Normal Human Epidermal Keratinocytes. *J Invest Dermatol* (2012) 132 (11):2593–600. doi: 10.1038/jid.2012.185
165. Sundnes O, Pietka W, Loos T, Sponheim J, Rankin AL, Pflanz S, et al. Epidermal Expression and Regulation of Interleukin-33 During Homeostasis and Inflammation: Strong Species Differences. *J Invest Dermatol* (2015) 135 (7):1771–80. doi: 10.1038/jid.2015.85
166. Dai X, Muto J, Shiraishi K, Utsunomiya R, Mori H, Murakami M, et al. TSLP Impairs Epidermal Barrier Integrity by Stimulating the Formation of Nuclear IL-33/Phosphorylated STAT3 Complex in Human Keratinocytes. *J Invest Dermatol* (2022). doi: 10.1016/j.jid.2022.01.005
167. Imai Y. Interleukin-33 in Atopic Dermatitis. *J Dermatol Sci* (2019) 96(1):2–7. doi: 10.1016/j.jdermsci.2019.08.006
168. Imai Y, Yasuda K, Sakaguchi Y, Haneda T, Mizutani H, Yoshimoto T, et al. Skin-Specific Expression of IL-33 Activates Group 2 Innate Lymphoid Cells and Elicits Atopic Dermatitis-Like Inflammation in Mice. *Proc Natl Acad Sci USA* (2013) 110(34):13921–6. doi: 10.1073/pnas.1307321110
169. Imai Y, Yasuda K, Nagai M, Kusakabe M, Kubo M, Nakanishi K, et al. IL-33-Induced Atopic Dermatitis-Like Inflammation in Mice Is Mediated by Group 2 Innate Lymphoid Cells in Concert With Basophils. *J Invest Dermatol* (2019) 139(10):2185–94.e3. doi: 10.1016/j.jid.2019.04.016
170. Babina M, Wang Z, Franke K, Guhl S, Artuc M, Zuberbier T. Yin-Yang of IL-33 in Human Skin Mast Cells: Reduced Degranulation, But Augmented Histamine Synthesis Through P38 Activation. *J Invest Dermatol* (2019) 139 (7):1516–25.e3. doi: 10.1016/j.jid.2019.01.013
171. Galand C, Leyva-Castillo JM, Yoon J, Han A, Lee MS, McKenzie ANJ, et al. IL-33 Promotes Food Anaphylaxis in Epicutaneously Sensitized Mice by Targeting Mast Cells. *J Allergy Clin Immunol* (2016) 138(5):1356–66. doi: 10.1016/j.jaci.2016.03.056
172. Liu B, Tai Y, Achanta S, Kaelberer MM, Caceres AI, Shao X, et al. IL-33/ST2 Signaling Excites Sensory Neurons and Mediates Itch Response in a Mouse Model of Poison Ivy Contact Allergy. *Proc Natl Acad Sci USA* (2016) 113(47): E7572–E9. doi: 10.1073/pnas.1606608113
173. Trier AM, Mack MR, Fredman A, Tamari M, Ver Heul AM, Zhao Y, et al. IL-33 Signaling in Sensory Neurons Promotes Dry Skin Itch. *J Allergy Clin Immunol* (2021). doi: 10.1016/j.jaci.2021.09.014
174. Huang J, Gandini MA, Chen L, M'Dahoma S, Stemkowski PL, Chung H, et al. Hyperactivity of Innate Immunity Triggers Pain *via* TLR2-IL-33-Mediated Neuroimmune Crosstalk. *Cell Rep* (2020) 33(1):108233. doi: 10.1016/j.celrep.2020.108233
175. Bruhs A, Proksch E, Schwarz T, Schwarz A. Disruption of the Epidermal Barrier Induces Regulatory T Cells *via* IL-33 in Mice. *J Invest Dermatol* (2018) 138(3):570–9. doi: 10.1016/j.jid.2017.09.032
176. He R, Yin H, Yuan B, Liu T, Luo L, Huang P, et al. IL-33 Improves Wound Healing Through Enhanced M2 Macrophage Polarization in Diabetic Mice. *Mol Immunol* (2017) 90:42–9. doi: 10.1016/j.molimm.2017.06.249
177. Kawai K, Uchiyama M, Hester J, Issa F. IL-33 Drives the Production of Mouse Regulatory T Cells With Enhanced *In Vivo* Suppressive Activity in Skin Transplantation. *Am J Transplant* (2021) 21(3):978–92. doi: 10.1111/ajt.16266

178. Ameri AH, Moradi Tuchayi S, Zaalberg A, Park JH, Ngo KH, Li T, et al. IL-33/Regulatory T Cell Axis Triggers the Development of a Tumor-Promoting Immune Environment in Chronic Inflammation. *Proc Natl Acad Sci USA* (2019) 116(7):2646–51. doi: 10.1073/pnas.1815016116
179. Kalekar LA, Cohen JN, Prevel N, Sandoval PM, Mathur AN, Moreau JM, et al. Regulatory T Cells in Skin Are Uniquely Poised to Suppress Profibrotic Immune Responses. *Sci Immunol* (2019) 4(39). doi: 10.1126/sciimmunol.aaw2910
180. Delacher M, Imbusch CD, Weichenhan D, Breiling A, Hotz-Wagenblatt A, Trager U, et al. Genome-Wide DNA-Methylation Landscape Defines Specialization of Regulatory T Cells in Tissues. *Nat Immunol* (2017) 18 (10):1160–72. doi: 10.1038/ni.3799
181. Demehri S, Turkoz A, Manivasagam S, Yockey LJ, Turkoz M, Kopan R. Elevated Epidermal Thymic Stromal Lymphopoietin Levels Establish an Antitumor Environment in the Skin. *Cancer Cell* (2012) 22(4):494–505. doi: 10.1016/j.ccr.2012.08.017
182. Di Piazza M, Nowell CS, Koch U, Durham AD, Radtke F. Loss of Cutaneous TSLP-Dependent Immune Responses Skews the Balance of Inflammation From Tumor Protective to Tumor Promoting. *Cancer Cell* (2012) 22(4):479–93. doi: 10.1016/j.ccr.2012.08.016
183. Takahashi N, Sugaya M, Suga H, Oka T, Kawaguchi M, Miyagaki T, et al. Thymic Stromal Chemokine TSLP Acts Through Th2 Cytokine Production to Induce Cutaneous T-Cell Lymphoma. *Cancer Res* (2016) 76(21):6241–52. doi: 10.1158/0008-5472.CAN-16-0992
184. Hayes MD, Ward S, Crawford G, Seoane RC, Jackson WD, Kipling D, et al. Inflammation-Induced IgE Promotes Epithelial Hyperplasia and Tumour Growth. *Elife* (2020) 9. doi: 10.7554/eLife.51862
185. Demehri S, Cunningham TJ, Manivasagam S, Ngo KH, Moradi Tuchayi S, Reddy R, et al. Thymic Stromal Lymphopoietin Blocks Early Stages of Breast Carcinogenesis. *J Clin Invest* (2016) 126(4):1458–70. doi: 10.1172/JCI83724
186. Pedroza-Gonzalez A, Xu K, Wu TC, Aspord C, Tindle S, Marches F, et al. Thymic Stromal Lymphopoietin Fosters Human Breast Tumor Growth by Promoting Type 2 Inflammation. *J Exp Med* (2011). doi: 10.1084/jem.20102131
187. Olkhanud PB, Rochman Y, Bodogai M, Malchinkhuu E, Wejksza K, Xu M, et al. Thymic Stromal Lymphopoietin Is a Key Mediator of Breast Cancer Progression. *J Immunol* (2011). doi: 10.4049/jimmunol.1100463
188. De Monte L, Reni M, Tassi E, Clavenna D, Papa I, Recalde H, et al. Intratumor T Helper Type 2 Cell Infiltrate Correlates With Cancer-Associated Fibroblast Thymic Stromal Lymphopoietin Production and Reduced Survival in Pancreatic Cancer. *J Exp Med* (2011) 208(3):469–78. doi: 10.1084/jem.20101876
189. Kuan EL, Ziegler SF. A Tumor-Myeloid Cell Axis, Mediated *via* the Cytokines IL-1alpha and TSLP, Promotes the Progression of Breast Cancer. *Nat Immunol* (2018) 19(4):366–74. doi: 10.1038/s41590-018-0066-6
190. Cunningham TJ, Tabacchi M, Eliane JP, Tuchayi SM, Manivasagam S, Mirzaalian H, et al. Randomized Trial of Calcipotriol Combined With 5-Fluorouracil for Skin Cancer Precursor Immunotherapy. *J Clin Invest* (2017) 127(1):106–16. doi: 10.1172/JCI89820
191. Benatar T, Cao MY, Lee Y, Li H, Feng N, Gu X, et al. Virulizin Induces Production of IL-17E to Enhance Antitumor Activity by Recruitment of Eosinophils Into Tumors. *Cancer Immunol Immunother* (2008) 57 (12):1757–69. doi: 10.1007/s00262-008-0502-9
192. Benatar T, Cao MY, Lee Y, Lightfoot J, Feng N, Gu X, et al. IL-17E, a Proinflammatory Cytokine, has Antitumor Efficacy Against Several Tumor Types *In Vivo*. *Cancer Immunol Immunother* (2010) 59(6):805–17. doi: 10.1007/s00262-009-0802-8
193. Furuta S, Jeng YM, Zhou L, Huang L, Kuhn I, Bissell MJ, et al. IL-25 Causes Apoptosis of IL-25R-Expressing Breast Cancer Cells Without Toxicity to Nonmalignant Cells. *Sci Transl Med* (2011) 3(78):78ra31. doi: 10.1126/scitranslmed.3001374
194. Serrels B, McGivern N, Canel M, Byron A, Johnson SC, McSorley HJ, et al. IL-33 and ST2 Mediate FAK-Dependent Antitumor Immune Evasion Through Transcriptional Networks. *Sci Signal* (2017) 10(508). doi: 10.1126/scisignal.aan8355
195. Taniguchi S, Elhance A, Van Duzer A, Kumar S, Leitenberger JJ, Oshimori N. Tumor-Initiating Cells Establish an IL-33-TGF-Beta Niche Signaling Loop to Promote Cancer Progression. *Science* (2020) 369(6501). doi: 10.1126/science.aay1813
196. Park JH, Ameri AH, Dempsey KE, Conrad DN, Kem M, Mino-Kenudson M, et al. Nuclear IL-33/SMAD Signaling Axis Promotes Cancer Development in Chronic Inflammation. *EMBO J* (2021) 40(7):e106151. doi: 10.15252/embj.2020106151
197. Wu J, Chen Z, Wickstrom SL, Gao J, He X, Jing X, et al. Interleukin-33 is a Novel Immunosuppressor That Protects Cancer Cells From TIL Killing by a Macrophage-Mediated Shedding Mechanism. *Adv Sci (Weinh)* (2021) 8(21): e2101029. doi: 10.1002/advs.202101029
198. Kobayashi T, Voisin B, Kim DY, Kennedy EA, Jo JH, Shih HY, et al. Homeostatic Control of Sebaceous Glands by Innate Lymphoid Cells Regulates Commensal Bacteria Equilibrium. *Cell* (2019) 176(5):982–97 e16. doi: 10.1016/j.cell.2018.12.031
199. West EE, Spolski R, Kazemian M, Yu ZX, Kemper C, Leonard WJ. A TSLP-Complement Axis Mediates Neutrophil Killing of Methicillin-Resistant Staphylococcus Aureus. *Sci Immunol* (2016) 1(5). doi: 10.1126/sciimmunol.aaf8471

Conflict of Interest: TH is an employee of Shiseido Co. Ltd.

The remaining author declares that the research was conducted in the absence of any commercial or financial relationships that could be construed as a potential conflict of interest.

Publisher's Note: All claims expressed in this article are solely those of the authors and do not necessarily represent those of their affiliated organizations, or those of the publisher, the editors and the reviewers. Any product that may be evaluated in this article, or claim that may be made by its manufacturer, is not guaranteed or endorsed by the publisher.

frontiers | Frontiers in Immunology

REVIEW
published: 06 May 2022
doi: 10.3389/fimmu.2022.880850

UVB-Induced Microvesicle Particle Release and Its Effects on the Cutaneous Microenvironment

Timothy C. Frommeyer[1†], Michael M. Gilbert[1†], Garrett V. Brittain[1†], Tongfan Wu[1†], Trang Q. Nguyen[1†], Craig A. Rohan[1,2,3] and Jeffrey B. Travers[1,2,3]*

[1] Department of Pharmacology and Toxicology, Boonshoft School of Medicine at Wright State University, Dayton, OH, United States, [2] Department of Dermatology, Boonshoft School of Medicine at Wright State University, Dayton, OH, United States, [3] Department of Medicine, Dayton Veterans Administration Medical Center, Dayton, OH, United States

OPEN ACCESS

Edited by:
Alicia R. Mathers, University of Pittsburgh, United States

Reviewed by:
Andrzej T. Slominski, University of Alabama at Birmingham, United States
Stephen Balmert, University of Pittsburgh, United States
Nabiha Yusuf, University of Alabama at Birmingham, United States

***Correspondence:**
Jeffrey B. Travers
jeffrey.travers@wright.edu

[†]These authors have contributed equally to this work and share first authorship

Specialty section:
This article was submitted to Molecular Innate Immunity, a section of the journal Frontiers in Immunology

Received: *21 February 2022*
Accepted: *04 April 2022*
Published: *06 May 2022*

Citation:
Frommeyer TC, Gilbert MM, Brittain GV, Wu T, Nguyen TQ, Rohan CA and Travers JB (2022) UVB-Induced Microvesicle Particle Release and Its Effects on the Cutaneous Microenvironment. Front. Immunol. 13:880850. doi: 10.3389/fimmu.2022.880850

Ultraviolet B radiation (UVB) has profound effects on human skin that results in a broad spectrum of immunological local and systemic responses and is the major cause of skin carcinogenesis. One important area of study in photobiology is how UVB is translated into effector signals. As the skin is exposed to UVB light, subcellular microvesicle particles (MVP), a subtype of bioactive extracellular vesicles, are released causing a variety of local and systemic immunological effects. In this review, we highlight keratinocyte MVP release in keratinocytes in response to UVB. Specifically, Platelet-activating factor receptor agonists generated by UVB result in MVP released from keratinocytes. The downstream effects of MVP release include the ability of these subcellular particles to transport agents including the glycerophosphocholine-derived lipid mediator Platelet-activating factor (PAF). Moreover, even though UVB is only absorbed in the epidermis, it appears that PAF release from MVPs also mediates systemic immunosuppression and enhances tumor growth and metastasis. Tumor cells expressing PAF receptors can use this mechanism to evade chemotherapy responses, leading to treatment resistance for advanced cancers such as melanoma. Furthermore, novel pharmacological agents provide greater insight into the UVB-induced immune response pathway and a potential target for pharmacological intervention. This review outlines the need to more clearly elucidate the mechanism linking UVB-irradiation with the cutaneous immune response and its pathological manifestations. An improved understanding of this process can result in new insights and treatment strategies for UVB-related disorders from carcinogenesis to photosensitivity.

Keywords: microvesicle particles, platelet-activating factor, ultraviolet light, UVB, platelet-activating factor receptor, immunosuppression, local inflammation, aSMase inhibitors

INTRODUCTION

Ultraviolet B (UVB; 290-320nm) radiation found in sunlight is essential for the production of vitamin D in humans (1). However, prolonged exposure can lead to a myriad of pathologic effects including erythema, photoaging, inflammatory responses, and skin cancer (2–4). Within the epidermis, UVB is able to damage DNA in various cell types in the skin, especially the keratinocyte (5–7). The UVB rays

induce formation of cyclobutane pyrimidine dimers which have the potential to be propagated to subsequent cellular populations, which may result in pro-carcinogenic changes (8, 9). UVB also has the ability to act as a pro-oxidative stressor, generating various immunoregulatory mediators including prostaglandin E_2, serotonin, histamines, interleukin (IL)-6, IL-10, tumor necrosis factor-alpha (TNFα) and the lipid mediator Platelet-activating factor (PAF) (10–12). UVB-induced production of these bioactive molecules results in acute inflammation, erythema, cancer, and degenerative aging (13, 14). Moreover, at high doses, UVB-irradiation and subsequent release of PAF and other agents such as TNFα can lead to systemic effects including fever, malaise, and immunosuppression (15, 16). PAF exerts a variety of effects through the G-protein coupled transmembrane Platelet-activating factor receptor (PAFR), which is expressed on multiple cell types including keratinocytes (17, 18). Cutaneous UVB exposure and activation of keratinocytic PAFR results in similar signaling pathways, which suggests that many UVB-induced effects are mediated *via* PAFR or modified by associated PAFR activation (19, 20). Since UVB absorption is limited to the epidermis, bioactive agents that leave the skin are thought to act as effectors for UVB responses.

Platelet-activating factor (PAF) is the term denoting a family of glycerophosphocholine (GPC)-derived lipid mediators implicated in a number of pathologic processes including skin carcinogenesis, liver disease, and allergic rhinitis (16, 21, 22). Although PAF application results in pro-inflammatory processes similar to the acute effects of UVB radiation, it can also produce immunosuppressive effects *via* upregulation of regulatory T cells (10, 16, 17, 23). The synthesis of PAF is associated with several different pathways including the remodeling and *de novo* pathways (24, 25). Of particular interest is the formation of PAFR agonists in response to increased reactive oxygen species (ROS) resulting in non-enzymatic formation of oxidized GPC (ox-GPC) with PAFR agonistic activities (26–28). This has prompted the notion that UVB-irradiation results in activation of the PAF system. The link between UVB, PAFR signaling, and photobiology is further implicated by PAFR activation in the early acute response of UVB as well as UVB-mediated systemic immunosuppression (10, 16, 17, 23, 29, 30). Thus, the PAF system plays an integral role in dermal pathophysiology and skin response to environmental stressors (31). After generation, PAF resides in cellular membranes where it can act upon itself or neighboring cells through juxtacrine signaling (32, 33). It should be noted that once generated, PAF/ox-GPCs are rapidly metabolized by removal of the *sn-2* short-chained fatty acid by acetyl hydrolases. However, certain cell types such as keratinocytes have demonstrated the ability of PAF to exert its effects some distance away from the host cell (34). Previous studies by our group have shown that UVB-irradiated keratinocytes can induce the production of subcellular microvesicle particles (MVP), which contains PAFR agonist activity (34, 35).

Abbreviations: UVB, Ultraviolet B; MVP, microvesicle particles; PAF, platelet-activating factor; PAFR, Platelet-activating factor receptor; GPC, glycerophosphocholine; PAF-AH, PAF acetylhydrolase; aSMase, acid sphingomyelinase.

Microvesicle particles are small membrane-bound particles that are shed from the plasma membrane of various cell types including keratinocytes (36). Their release is largely dependent on the action of the lipid enzyme acid sphingomyelinase (aSMase) (37, 38). Also named microvesicles and microparticles, MVPs are thought to provide a cellular mechanism to transport a variety of bioactive substances including proteins, lipids, cytokines, and nucleic acids (39, 40). Furthermore, their integral role within cell-to-cell signaling has suggested their mediation of pathogenic processes (41). Emerging literature suggests that UVB-generated ox-GPC PAFR agonists activate keratinocytic PAFR, which translocates aSMase to trigger MVP release from the plasma membrane (42). However, the exact mechanism linking UVB-irradiation with the cutaneous immune response and its pathological manifestations needs to be further elucidated. In this review, we highlight the potential role of UVB-generated MVPs and subsequent release of PAF in cutaneous immune responses.

BACKGROUND

Cutaneous Microenvironment

Skin with subcutaneous fat (called the hypodermis) is the largest and most exposed organ of the human body. As such, it acts as a physical barrier, which leaves it vulnerable to a myriad of potentially harmful agents including bacteria, viruses and other environmental contaminants. In addition, the skin has important functions in regulating body temperature, preventing dehydration, and protecting against ultraviolet (UV) radiation (43). Cutaneous anatomy consists of an outer epidermal layer and an inner dermal layer that are joined by a basement membrane as well as an underlying layer of subcutaneous fat and connective tissue (44, 45). The epidermal layer is made up of five distinct layers that consist primarily of keratinocytes, which are bioactive cells that are highly proliferative and secrete a variety of cytokines (46). As keratinocytes detach from the basal layer of the epidermis, they stop dividing and undergo a final differentiation process known as cornification (44, 47). Melanocytes, Langerhans cells (LC), and Merkel cells are other cell types in the epidermis that are involved in melanin synthesis, immunoregulation and sensory functions respectively (46). The underlying dermis supplies nutrients to the epidermis and consists of two layers: the upper papillary layer and the lower reticular layer. The papillary dermis consists of densely packed fibroblasts whereas the reticular layer has lesser numbers of cells such as fibroblasts but contains more densely packed collagen and sits just above the subcutaneous fat (44). Various immune cells reside in the dermis which provide routine immune surveillance; these include macrophages, dendritic cells, T cells, mast cells, neutrophils and eosinophils. Inflammation and immune responses lead to significant proliferation of dermal immune cell populations (48, 49). The underlying hypodermis is a layer of subcutaneous tissue, composed of blood vessels and adipocytes that provide storage of lipids and fatty acids. Adipocytes help generate a number of bioactive lipid mediators and peptide hormones that partake in a number of dermal

biological processes including cell signaling, inflammation, and regulation of local and systemic effects (50, 51). The connection between the local and systemic pathways are based on both internal and external variables including serotonergic, melatoninergic, and cholinergic pathways (52). The skin responds distinctly depending on the type of stressor and amount of exposure, which results in specific physiologic responses and subsequent signaling pathways. Of particular interest is the effect of UVB radiation on the skin and its effects on keratinocytes.

Ultraviolet radiation is implicated in a number of cutaneous pathologies and is divided into three distinct wavelengths: UVA (320-400 nm), UVB (290-320 nm) and UVC (100 -290 nm). Accounting for only 0.3% of the total light, UVB is absorbed by the epidermis, and can directly damage DNA by forming photoproducts including cyclobutane pyrimidine dimers and 6-4 photoproducts (53). In addition, UVB exposure results in the upregulation and release of various factors from keratinocytes including growth factors, antimicrobial peptides (human β-defensin-2, -3, ribonuclease-7 and psoriasin (SA100A7)) and cytokines (IL-1α, IL-1β, IL-6, IL-8, granulocyte colony stimulating factor [G-CSF], macrophage-CSF, interferon gamma [INF-γ], platelet-derived growth factor (PDGF) as well as the increased accumulation of reactive oxygen species (ROS) (54, 55). UVB also has additional roles in immune function by upregulating toll-like receptors and can disrupt the delicate skin microbiome (56, 57). One such consequence of prolonged UV-exposure is immune suppression, which includes inhibition of antigen presentation, induction of leukocyte apoptosis, and generation of immunosuppressive cytokines and (16). Additionally, UV-induced immunosuppression has been implicated to act through several molecular including DNA and membrane lipids, tryptophan in skin cells, and trans-urocanic acid (UCA) as well as through the depletion of other molecules including nicotinamide adenine dinucleotide (NAD) levels in keratinocytes (58). Moreover, UVB appears to inhibit immune reactions in an antigen-specific fashion, suppressing primary immune reactions. This is evidenced by suppressed contact hypersensitivity and delayed type hypersensitivity (DTH) reactions after UVB-irradiation, which show a diminished T-cell mediated immune response and generation of antigen-specific tolerance and desensitization (59–61). Extensive UVB damage alters vitamin D uptake, induces wrinkling of the skin, promotes photoaging, and can result in skin carcinogenesis as well as immunosuppression (14, 58, 62, 63). Simultaneously, vitamin D has been shown to have photoprotective effects against UV damage, which include diminishing the production of free radicals and attenuating DNA repair (64). As a result, the mechanisms by which UVB-mediated damage has a wide spectrum of effects in the epidermis and beyond are becoming increasingly important. Interestingly, UV radiation is able to upregulate local neuroendocrine axes through locally induced cytokines, corticotropin-releasing hormones, urocortin's, proopiomelanocortin-peptides, and enkephalins. These local compounds can induce systemic effects such as the activation of central hypothalamic-pituitary-adrenal axis as well as immunosuppression (65). Of note, UVB enhances the production of a variety of bioactive lipids including PAF and eicosanoids such as PGE_2, which appear to play an important role in UV-induced immunosuppression, inflammation, and carcinogenesis (26, 66).

The Platelet-Activating Factor Family

In 1972, the term Platelet-activating Factor was first utilized in reference to a released product of IgE-induced basophil activation which results in subsequent platelet aggregation in rabbit models (67). Since its initial discovery, further investigations have indicated that PAF asserts a multitude of physiological and pathophysiological effects through binding with a specific G-protein-coupled receptor, PAF-R, extensively expressed by many immune and epithelial cell types (68). Despite new understandings of the functional significance, Benveniste and colleague's cognomination persisted. The PAF family has been implicated in a variety of conditions ranging from malignancies to neurological conditions. PAF-related mechanisms have also been described in asthma and of interest to our group, UVB-mediated responses (42). Interestingly, PAF's proposed acute and chronic impacts appear contradictory, the former pro-inflammatory and the latter immunosuppressive as will be discussed further (31).

Throughout the body, PAF production can be stimulated by a variety of cell types. Through a variety of mechanisms, eosinophils, neutrophils, macrophages, monocytes, basophils, and mast cells all play a role in PAF synthesis (69). The biosynthesis of PAF has two separate pathways: a remodeling pathway and a *de novo* pathway (**Figure 1**). An interesting facet of the remodeling pathway of PAF production includes its influences from cell-specific inflammatory tracks. Upon cellular stimulation, increased intracellular calcium levels activate Ca-dependent MAPK kinase which phosphorylates phospholipase A_2 (PLA_2). PLA_2 then deacylates alkylacyl-glycerophosphocholine to produce lyso-PAF and the unsaturated *sn-2* fatty acid, often arachidonate. Lyso-PAF (1-alkyl-sn-glycero-3-phosphocholine) is further acetylated by CoA lyso PAF acetyltransferase (LPCAT2) forming PAF (1-*O*-alkyl-2-acetyl-sn-glycero-3-phosphocholine) and Coenzyme A. The terminal enzyme in PAF biosynthesis, LPCAT2, is also highly expressed in inflammatory cells (16, 42, 70). One example of this includes its role in macrophages. Following lipopolysaccharides (LPS) binding to TLR4 on macrophages, protein kinase 2 activates MAPK which phosphorylates LPCAT2 resulting in a rapid surge in PAF. In addition, the PAFR, once activated, results in the activation of protein kinase Cα which phosphorylates LPCAT2, modeling a positive feed forward loop for PAF formation (16, 31, 69). Moreover, the *de novo* model of PAF production, unlike its counterpart, is not influenced by inflammatory pathways but plays an important role in baseline PAF levels due to constitutive activation. This pathway has three primary steps. Initially, 1-alkyl-2-lyso-*sn*-glycero-3-P is acetylated by CoA-alkyl-lysoglycero-P acetyltransferase forming 1-alkyl-2-acetyl-sn-glycero-3-P. Next, this intermediate undergoes dephosphorylation *via* an alkylacylglycerol-P phosphohydrolase forming 1-alkyl-2-lyso-sn-glycerol. Lastly, this glycerol molecule receives a phosphate

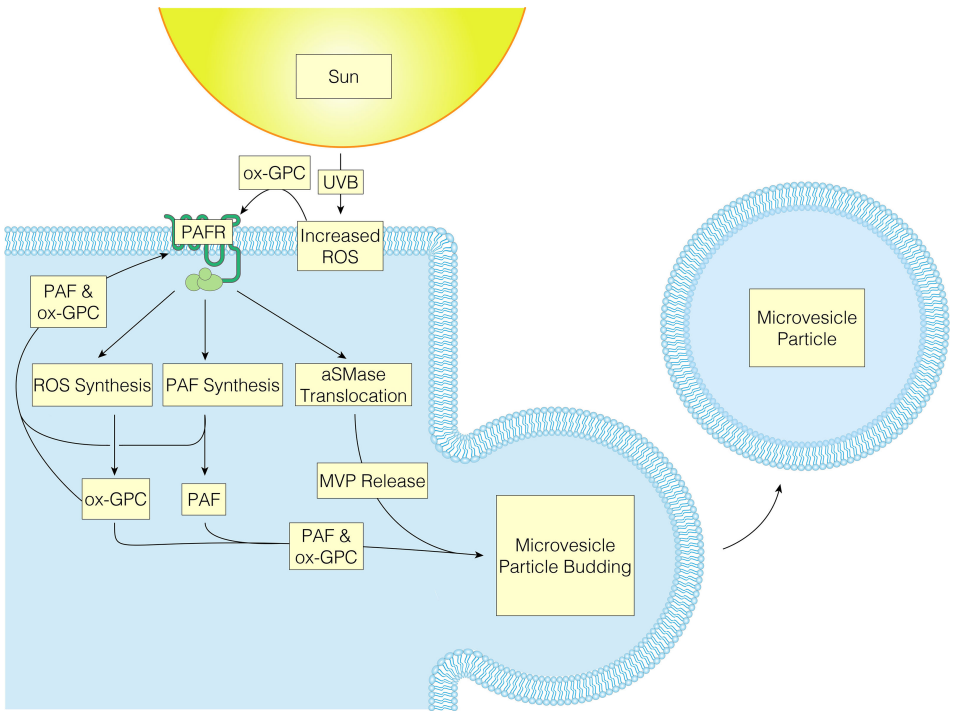

FIGURE 1 | PAF biosynthesis pathways.

group and choline by CDP-choline alkylacetylglycerol cholinephosphotransferase (25, 71, 72).

The metabolism of PAF is highly regulated by the PAF acetylhydrolase (PAF-AH) subclass of phospholipase A2 enzymes (73). By hydrolyzing the short-chained fatty acid moiety (e.g., acetyl group) at the *sn-2* position of PAF and related GPC, these signaling molecules form the biologically inactive lyso-PAF. The PAF-AH family members PAF-AH type I, PAF-AH type II, and plasma PAF-AH are pertinent to PAF degradation (31, 74). While these enzymes were originally named due to their role in PAF metabolism, they play a multitude of physiological and pathophysiological roles which are further discussed in the literature (73). The intracellular PAH-AH type II heterotetrameric has also been found in both sebaceous glands and epidermal keratinocytes (73, 75). Due to the rapid degradation and tight regulation of PAF and its implication in a vast number of processes, there is a need to better understand the mechanisms which allow for the systemic effects of PAF. Keratinocyte-derived MVPs are a major point of interest for this role.

Microvesicle Particles

UVB-mediated bioactive product release can take place in a variety of ways, including through the release of MVPs. MVPs are extracellular vesicles that are formed from outward protrusion of the plasma membrane when there is an increase in intracellular calcium (76). Ranging from 100 – 1,000 nm, MVPs are important for cellular signaling due to them carrying a variety of different proteins, lipids, and mRNA. MVPs can be shed during physiological conditions including cell growth but also are increased in a variety of pathological processes ranging from hypoxia to oxidative stress (40, 77). Many cytokines including TNFα and cell damage can release MVP (38). They are present in a range of physiologic and pathologic processes throughout the body (77–79). Of particular interest are MVPs generated by a keratinocyte cell line through budding from the plasma membrane which contains PAFR agonist activity (80, 81). Both MVPs and PAF are released due to activation of PAFR. In fact, MVP production and activation can be triggered by a great variety of mechanisms, including acute alcohol poisoning (35, 82).

Throughout the human body, extracellular vesicles like MVPs and smaller exosomes frequent matrices of the system. UVB has been demonstrated to induce the release of both of these particles (34, 83). While MVPs are often parceled with exosomes, each are separate entities expressing different characteristics. Exosome formation occurs *via* reverse budding of multivesicular bodies prior to cellular release (84, 85). This process allows for delivery of exosome contents with plasma membrane fusion (85). On the other hand, MVPs are contrived from external budding and fission of cellular plasma membrane which allows for an additional function in MVPs of cargo delivery into the extracellular environments (86). The variance in formation of each of these extracellular vesicles results in discrepancy in sizes as well. Exosomes typically range from 30nm – 150nm with less deviance from mean values (84–86). This range is smaller than

the previously mentioned range for MVPs and has a lower peak value. Due to the external plasma membrane invagination formation mechanisms of MVPs, cytosolic elements are accrued secondary to proximity to the plasma membrane. In exosomes, contiguity with intraluminal vesicles play a greater significance in free exosome content (85, 87).

While the exact mechanisms of keratinocyte-derived MVP generation and release are unclear, much research has been done on the biogenesis of MVPs (34). The production of MVPs has three elemental steps. To begin, membrane and lipid proteins are reorganized into distinct groups within the plasma membrane. Next, these microdomains aid in various pathways attracting cargo. Lastly, in conjunction with other machinery, membrane budding and fission is promoted (88). The initiation of these processes is highly unlikely to be secondary to spontaneous intrinsic property changes of the phospholipid bilayer but rather unclear emerging external mechanisms (86). In particular, MVP generation from diverse stimuli involve the enzyme acid sphingomyelinase (aSMase) appears to play an important role in this process (42). Furthermore, MVP cargo, which is dependent upon parent cell archetype, is preferentially gathered through a variety of possible mechanisms- most notably ARF6 of the GTPase family (89). Downstream effects of MVPs are secondary to their respective cargo, highlighting the importance of these pathways. Of interest, keratinocyte-formed MVPs contain a myriad of bioactive agents and molecules including PAF and ox-GPC, which have implications in systemic immune responses (34). Of interest, protein cytokines found in UVB-generated MVP contain lesser numbers of classic pro-inflammatory cytokines (e.g., TNF-alpha), but increased numbers of anti-inflammatory cytokines such as IL-1 receptor antagonist, in comparison to baseline (unstimulated) MVP (37).

As previously discussed, MVPs functions are dependent upon the appropriate intercellular messaging and respective cargo. As more research is needed on keratinocyte-derived MVPs uptake at their respective target cells, we will only briefly cover this topic. Parent cells of MVP, by nature of their biosynthesis pathway, additionally impact the plasma membrane content of this extracellular vesicle. The adoption of plasma membrane from origin cells is believed to play a role in MVP intercellular communication (88). With this in mind, certain MVPs transmit signals by direct physical contact between membrane-associated ligands and cell surface receptors. One such example is the production of chemokine (C-C motif) ligand 3 (CCL3), chemokine (C-C motif) ligand 7 (CCL7) and IL-24 in T-cell-derived MVPs co-cultured with *in-vitro* keratinocytes (90, 91). Indirect mechanisms of MVP function have also been observed. For instance, MVP release of cargo into extracellular milieu near the vicinity of target cells has been shown to stimulate cell surface receptors (92). Furthermore, MVPs can merge with beneficiary cells' plasma membranes, sending internal cargo into the recipient cells' cytoplasm with the additional potential of membrane property transference (93). Finally, select MVPs are absorbed into their destination cells through non-selective macropinocytosis or endocytosis (94).

UVB ACTIVATION OF MVPS

UVB radiation (290-320 nm) results in a pro-oxidative stress that exerts significant effects within the skin. One of which is the generation of ROS, which modify biologically active agents, such as lipids (28). GPC is an integral structural lipid found in all cellular membranes and functions as a precursor of bioactive PAF. Due to the presence of bisallylic double bonds, esterified polyunsaturated fatty acids are vulnerable to oxidation from ROS attack of the hydrogen donors. This results in the introduction of oxy functions to the chain of carbon atoms, rearranges bonds, fragments carbon-carbon bonds by β-scission, which can all give rise to a multitude of lipid reaction products (27, 28). In particular are a series of phospholipids with oxidatively fragmented *sn-2* acyl residues with a terminal methyl group or ω-oxy function. Potent PAF agonists (ox-GPC) are generated if the oxidatively modified *sn-2* acyl residue is a 1-alkyl GPC (26–28). There are multiple literature reports that link UVB generation of ROS with subsequent activation of the PAF system (10, 16, 17, 23, 29, 30). Early research into these findings was based on a knowledge of how UV response affects the cell membrane rather than the nucleus (95). Additional evidence found overexpressing the PAFR enhances PAF synthesis by keratinocytes in response to UVB radiation, while administering a PAFR antagonist inhibits PAF synthesis in UVB radiated keratinocytes (96). Furthermore, Yao and colleagues discovered that a PAFR antagonist inhibited UVB-mediated skin inflammation and TNF-alpha synthesis in the photosensitive *Xpa-/-* mice (29). Interestingly, it has also been found that PAFR expression is necessary for UVB-induced activation and subsequent migration of mast cells (97). Thus, UVB acts as a pro-oxidative stressor that generates ox-GPC and subsequent activation of PAFR through its PAFR agonist activity. Of importance, ox-GPC activation of the PAFR can generate enzymatic PAF synthesis, thus forming a positive feedback loop (31).

UVB radiation and PAFR activation of keratinocytes have been noted to result in multiple similar signaling pathways, implying that some UVB-induced effects are mediated *via* PAFR or modified by associated PAFR activation (19, 20). There are several cutaneous cell types that express PAFR including keratinocytes, mast cells, monocytes, granulocytes, and B cells (30, 97–102). The actions of PAF and its agonists are mediated through the PAFR, a unique G-protein-coupled seven transmembrane receptor (GPCR), which when activated results in several intracellular signaling pathways (68). These include mitogen kinase (both ERK and P38), JNK, and can also indirectly activate the EGFR (80). While coupled to G proteins Gi, Gq, and G12/13, PAFR also controls the production of inositol 1,4,5-triphosphate (IP_3) and calcium mobilization in GPCRs, while suppressing forskolin-stimulated cAMP synthesis (103). Emerging literature supports the theory that UVB produces ox-GPC PAFR agonists, which then act upon PAFR-positive keratinocytes, resulting in PAFR activation. As a result of PAFR activation, more PAF is produced enzymatically as well

as more ROS and subsequent ox-GPC. Finally, PAFR activation induces aSMase to translocate to the plasma membrane causing MVP to be generated and released from the keratinocyte plasma membrane. As the PAF/ox-GPC will be retained in the plasma membranes this allows PAFR agonist to be transported in the MVP to additional locations (**Figure 2**) (42). Of interest, studies of the crystal structure of the PAFR have revealed one of the protein loops appears draped over the central area of this GPCR (100). This novel putative conformational change suggests that PAFR agonists interact with the receptor optimally from the plasma membrane rather from the exterior of the cell. Hence, it is possible that the PAFR agonists in the MVP when are incorporated into the target cell could be in a pharmacologically active form. In sum, a feed-forward loop is created because PAFR activation results in continual release of PAF from MVPs and subsequent activation of PAFR.

As mentioned previously, a common lipid pathway causing MVP release is the stimulus-mediated translocation of the enzyme aSMase from lysosomes to plasma membranes (38, 42, 104). Importantly, activation of PAFR has been shown to generate membrane translocation of aSMase as well as boost its enzymatic activity (105, 106). Multiple lines of evidence support aSMase serving as the effector for PAFR-mediated MVP release. For instance, our group found that both application of the metabolically stable PAFR agonist carbamyl-PAF (CPAF) as well as UVB exposure led to increased aSMase enzymatic activity in HaCaT keratinocytes (37). In addition, after UVB irradiation, application of the aSMase inhibitor imipramine inhibited MVP generation in HaCaT keratinocyte cells, human skin explants, and murine skin. Of note, multiple agents including many tricyclic anti-depressants act as functional inhibitors of aSMase (FIASM) (107).These findings were further substantiated by the use of PAFR-KO (*Ptafr-/-*) and aSMase-KO (*Smpd1-/-*) mice, which corroborated functions of PAFR and aSMase in UVB-mediated MVP release in skin (37). Of note, application of the phorbol ester phorbol-12-myristate -13-acetate (TPA) results in MVP generation in PAFR-deficient but not in aSMase-deficient hosts. Finally, topical treatment with the aSMase product C2 ceramide also resulted in amplified MVP levels in mice, including aSMase-deficient animals. Ultimately, UVB-induced production of MVPs relies on a process that involves both PAFR signaling and aSMase.

There are many stressors and pathways that can generate MVP. However, our group was the first to demonstrate the ability of UVB to induce PAF-mediated MVP formation and release (35). Using a keratinocyte-derived cell line (HaCaT), UVB irradiation resulted in increased levels of MVP generation. Furthermore, application of the non-metabolizable PAFR agonist CPAF resulted in MVP formation in a dose-dependent manner. In addition, to test if the PAF system was involved in UVB-mediated MVP generation, we exposed UVB to PAFR-positive and PAFR-negative cell lines (KBP and KBM, respectively). UVB-irradiation generated MVP formation in only the PAFR-positive cell line, while no differences in MVP levels were seen in the PAFR-negative cells. Similar findings were noted using PAFR-deficient mice. These findings demonstrate PAF's involvement in UVB-induced MVP formation, which adds to the extensive literature supporting the role of the PAF system in mediated UVB-induced acute inflammation and delayed immunosuppression (19, 27, 66). It is also known that UVB-induced PAF agonists involve ROS that can be blocked by antioxidants (18, 27, 66). Our group found that UVB-mediated MVP generation involves ROS-induced PAF agonists, as evidenced by the ability of antioxidants to block MVP

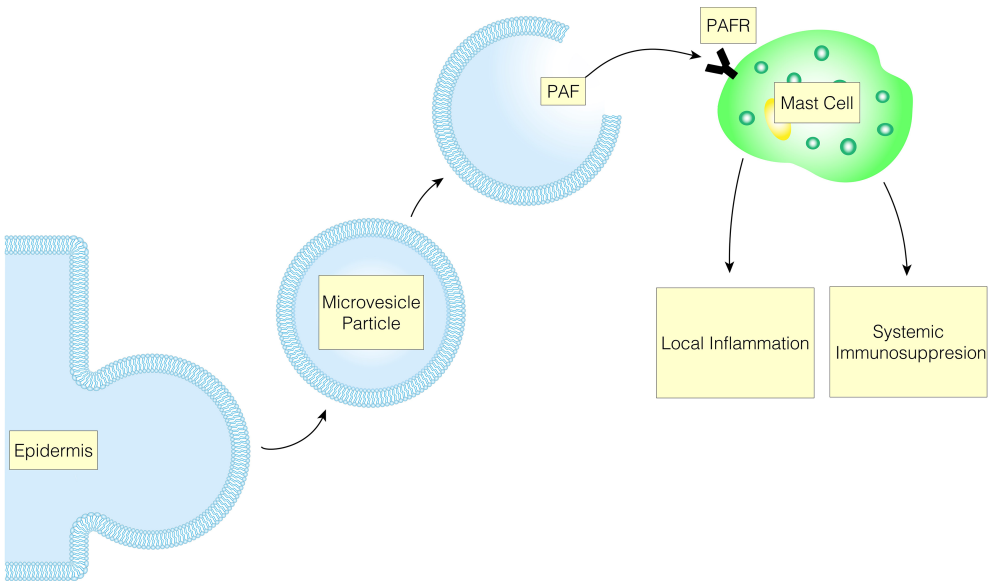

FIGURE 2 | UVB oxidized-GPC results in PAFR activation, causing MVP to be released from the keratinocyte plasma membrane, allowing PAFR agonist to be transported to additional locations.

production (35). More specifically, pretreatment of HaCaT cells with N-acetylcysteine and vitamin C resulted in hampered UVB-induced MVP release while CPAF-mediated MVP release was unaffected. Furthermore, the UVB fluences required to produce MVP in keratinocytes are quite high, with a two- to three-fold increase in the minimum erythema dosage required to detect quantifiable MVP within the skin (108). While addressing this phenomenon, our group demonstrated that pretreatment of epithelial skin cells with PAFR agonist can synergize with low fluences of UVB to produce high levels of MVP. This suggests that MVP could play a role in combinatorial pathologic processes involving UVB, which is important since synergistic responses from multiple agents are likely more common than presently recognized (108).

PAF persists in the cellular membrane after production where it can operate on itself or nearby cells *via* juxtacrine signaling (32, 33). Additionally, studies have shown that in certain cell types, such as keratinocytes, PAF can exert its effects some distance away from the host cell (34). This phenomenon is likely the result of MVPs, which are thought to provide PAF protection from degradation by PAF-AH as opposed to being free or protein-bound within tissue fluids (42). By extension, the advantage of this arrangement is the protection of metabolically unstable compounds from enzymatic degradation. Thus, UVB-induced systemic effects may be mediated in part by MVPs produced by epithelial cells.

MVP-MEDIATED LOCAL INFLAMMATION

UVB damage causes both local and systemic inflammation and immunosuppression. While considering the cutaneous response to environmental stressors, there are a number of cytokines and cells signaling pathways that are mediated through T-cells, antigen-presenting cells (APCs), mast cells, fibroblasts, and keratinocytes. Consequently, the release of many cytokines including TNF-alpha, IL-6, IL-8, IL-10, and others leading to a range of pathological processes (11, 109). The aforementioned effector cells and cytokines create a complex interaction that initially generates an acute and local reaction that may eventually progress to a systemic response. It appears that this UVB-induced systemic response is in part mediated by MVPs, which act on these effector cells and amplify the UVB-damage. The end result is an MVP-mediated inflammation and immunosuppression that may give rise to a number of pathological processes.

As aforementioned, UVB produces ox-GPC PAFR agonists, which then activate PAFR in PAFR-positive keratinocytes. More PAF is created enzymatically as a result of PAFR activation along with more ROS and hence more ox-GPC. Moreover, its activation also causes aSMase to translocate, leading to MVP release. The epidermis then releases MVP, which contains PAF and ox-GPC (42). Locally, a variety of downstream effects are then generated as previously mentioned (11, 109). Recently, MVP release has been found to be associated with the production of the pro-inflammatory cytokine IL-8. Studies done by Bhadri and colleagues explored the possible link between the pro-inflammatory cytokine IL-8 and MVP. The authors demonstrated that pretreatment of HaCaT keratinocytes with PAFR agonists synergizes with low fluences of UBV to produce increased levels of IL-8 and MVPs (110). Further illustrating this linkage, application of the FIASM imipramine blocked both MVP and IL-8 release following UVB treatment (110). Furthermore, the ability of IL-8 to activate and attract neutrophils suggests that it may play a role in the acute UVB response. This is highlighted by the report that treatment with an IL-8 neutralizing antibody, which reduced UVB-induced synthesis of fibroblast neprilysin and matrix metalloproteinase 1 (MMP-1) in keratinocyte-fibroblast cocultures (94). Interestingly, the role of PAF in local immunosuppression is still under debate due to Sahu and colleagues showing that UVB-mediated LC depletion is not mediated though PAFR (111). Rather, UVB-exposed mouse skin treated with the contact allergen DNFB (2,4-dinitro-1-fluorobenzene) resulted in a significant inhibition of contact hypersensitive response in both WT and PAFR knockout mice. Additionally, the presence of LC was reduced in both types of mice compared to their sham irradiated controls (111). Thus, it appears that MVP-mediated PAF release caused by UVB needs further research to establish a causal role in the local immune response.

The immunological responses to UVB are characterized by both local and systemic inflammation and immunosuppression. These phenomena are not mutually exclusive as many acute mediators serve to bridge the local and systemic responses. The connection between these two systems is illustrated by the effect of PAF on keratinocytes with the mast cell playing an effector role (**Figure 3**). UVB-induced damage mediated through PAF on keratinocytes decreases DNA repair mechanisms by decreasing the expression of response elements such as ataxia telangiectasia and rad3 related protein (ATR) (112). Additionally, the secretion of PAF by keratinocytes increases IL-10, activates COX-2 and decreases delayed type hypersensitivity reactions (102, 113). Furthermore, PAF release from keratinocytes promotes mast cell migration into the lymph nodes and subsequent systemic effects. Moreover, PAF stimulation of mast cells upregulates the epigenome to increase the expression of DNMT1/3b and p300, and decreases the expression of HDAC2. Ultimately, this increases the responsiveness of mast cells to CXCR4 agonist, in which mast cells will release IL-10 and histamine (112, 114, 115). Further, this relationship is supported by UV radiation not suppressing the contact hypersensitivity (CHS) response in mast-cell deficient mice, but when these mice are reconstituted with normal bone marrow-derived mast cells, UV-induced suppression of CHS is restored (115).

The role of LC UV-induced PAF-mediated local inflammation is still being established, but there appears to be a relationship between PAF-induced LC migration, consequently leading to immunosuppression (116). In particular, UV irradiation induces expression of RANK-L in keratinocytes which stimulates the migration of LC to the lymph nodes where they activate immunological Treg cells, decreasing the DTH, CHS, and tumor immunity (117–120). PAF-induced

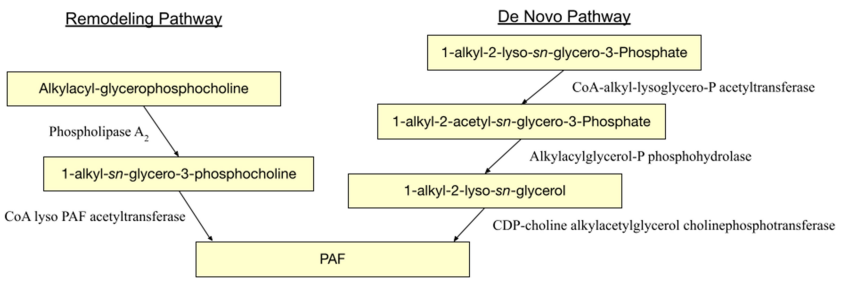

FIGURE 3 | UVB-induced MVP release leads to mast cell PAFR activation, which results in immunological responses characterized by both local and systemic inflammation and immunosuppression.

PGE2 may be implicated in the process by upregulation of RANK-L on keratinocytes since inhibiting PGE2 binding to its receptor EP4 with specific receptor antagonists inhibits RANK-L upregulation, impairs UV-induced Treg activation, and inhibits UV-induced CHS suppression (121). PAF is also known to induce regulatory dendritic cells through several cytokines including PGE2 and IL-10 (122). These examples help illustrate the growing picture linking UV exposure, MVP-mediated PAF release, and subsequent local and systemic immunosuppression.

The relationship between UVB-mediated MVP release in systemic cutaneous disease is still evolving, but current literature has shown the PAF system induces inflammation in a variety of skin pathologies. For example, PAF can be found to be increased in inflammatory lesions of psoriasis favoring Th17 development. More specifically, this appears to occur through PAF-mediated increase in the expression of IL-1ß, IL-5, and IL-23 in LC and keratinocyte, subsequently leading to Th17 development (123–125). Other illustrations of the detection of the PAF in cutaneous disease states are in bullous pemphigoid, sunburn, cold urticaria and in burn injuries (66, 126–128). However, it is unclear in these pathogenic states if the PAF measured is truly contributory or serves as a "bystander effect" of the concomitant inflammation. In sum, there is a need to use specific pharmacologic and genetic tools to expand on this body of knowledge, particularly MVP's role in UVB-induced cutaneous inflammation, immunosuppression, and systemic cutaneous disease.

DELAYED IMMUNOSUPPRESSION AND BLOCKING OF TUMOR IMMUNITY

Tumorigenesis/Metastasis in Melanoma

Exposure to UVB radiation is a major risk factor in developing skin cancer, especially melanoma. UVB induces oxidative stress and generates lipid mediators such as PAF and Ox-GPC (129). These factors signal inflammatory cytokines that lead to systemic immunosuppression, which leads to tumor augmentation in experimental murine models by two-fold (130). Not only are MVPs released by UVB-induced PAFs, Lima et al. demonstrated that malignant melanoma cells (B16F10) produce a large quantity of microvesicles *in vitro* that mediate immunosuppression and tumor progression (131). TGF-beta is an important immunoregulatory factor produced by phagocytes; B16F10-produced MVP upregulates this production, leading to changes in the tumor microenvironment promoting tumor dissemination (131). Moreover, it is noteworthy that antioxidants attenuate the effect of UVB-irradiation induced melanoma growth, suggesting that reactive oxygen species (ROS) leading to PAF release could play an important role in tumor growth. Likewise, UVB radiation activates tumorigenesis through the PAF-PAFR pathway. While PAFR are not found in melanocytes, the release of PAFR agonist due to environmental stressors, such as UVB, activates a cascade of downstream effects that leads to tumorigenesis and metastasis. Overexpression of PAFR has been shown to lead to acanthosis and increased numbers of dermal melanocytes, fibroblasts, mast cells, filaggrin and endothelial cells (132, 133). Interestingly, PAFR transgenic mice spontaneously developed hyperpigmentation on the ears, tails, and external genital area and melanocytic tumors in the dermis with age (132). It is likely that keratinocyte hyperplasia stimulated this growth of dermal melanocytes directly or indirectly. Of note, topical use of PAFR antagonist, WEB 2086, inhibited keratinocyte proliferation in both transgenic mice and control mice, suggesting that PAFR inhibition may mediate cellular hyperplasia and tumor growth (132). However, the phenotype of the PAFR transgenic mouse could likely be due to inappropriate expression of the PAFR using a widespread actin promoter. Sahu and colleagues found the mechanism which leads to melanoma tumor progression is due to the systemic expression and activation of PAFR; and that whether the tumor cells themselves expressed PAFR or not does not impact the tumor development, suggesting that PAFR-mediated anti-tumoral immunity effects are involved (130). Support for this finding relies on several mechanisms. One, PAF-induced release of inflammatory cytokines, such as IL-10, Treg, IL-1, and TNF-alpha lead to systemic immunosuppression and tumor metastasis (130, 134). Two, UVB-induced immunosuppression can be blocked by PAFR-antagonists, therefore attenuating the effect on tumorigenesis (135). Three, administration of a systemic PAFR agonist, carbamoyl PAF (CPAF), will increase tumor growth in wildtype mice or mice injected with PAFR onto host cells. However, CPAF failed to augment the tumor size in *PAFR* -/- mice (130). Lastly, PAFR acetylhydrolase (PAFR-AH), an enzyme that breaks down PAF, will decrease tumor vascularization and growth (133).

These observations suggest that systemic PAF/PAFR expression and activation contribute to carcinogenesis, and inhibition of these reactions may provide insight to cancer treatment.

Melanoma is the most lethal skin cancer due to its high likelihood to metastasize and ability to evade therapy (136). The PAF-PAFR pathway has been implicated for the promotion of metastasis in melanoma (134, 137, 138). An inflammatory tumor microenvironment leads to proliferation, invasion, and angiogenesis of tumors which may metastasize. Matrix metalloproteinase-2 (MMP-2) is a main contributor to cancer cell migration, which can be stimulated by PAFR (139). Melnikova and their group studied melanoma metastasis to the lung and found that these cell lines all expressed PAFR to a varying degree, although the extent of metastasis does not correspond to the level of PAFR expressed (5). PAF upregulates multiple pathways that lead to cell migration and metastasis (137, 138). Importantly, PAF-induced expression of pro-MMP-2 was related to PAF-induced cAMP response element (CREB) and activating transcription factor (ATF-1) phosphorylation, and addition of a PAFR antagonist prevented this stimulation (137). It is thought that PAFR-induced CREB phosphorylation in more aggressive melanoma is through two intermediate signaling proteins, PKA and p38 MAPK. In addition, incubation of melanoma cell lines with the PAF analog, CPAF, increased phosphorylation of CREB (138). Another study looking at lung metastasis relating to melanoma also found that PAF enhances metastasis (134). In Im and colleagues' experiments, pulmonary metastasis from B16F10 melanoma were significantly increased with addition of dose- and time-dependent PAF. Furthermore, administration of PAF-R antagonists reduced the pulmonary tumor colonization (134). Additionally, IL-1 and TNF-alpha were thought to be at least partially mediated by PAF generation, which can cause metastasis (134). Another important mechanism for metastasis is the cooperation between PAR-1 and PAFR to regulate the expression of MCAM/MUC18 (melanoma cellular adhesion molecules) (138). Taken together, metastatic melanoma carries higher expression of PAF/PAFR and increases migration through mechanisms modulated by the inflammatory tumor microenvironment.

Angiogenesis is an important step in tumor metastasis. Platelets and factors in the coagulation cascade, especially thrombin, are stimulated by PAFR and play crucial roles in vascularization that leads to tumor growth and metastasis (137, 138). Notably, PAF/PAFR modulate tumor cell adhesion to endothelial cells, angiogenesis, tumor growth, and metastasis (137). Inhibition of neoangiogenesis by inhibiting PAF could play a part in mediating metastasis. Indeed, mice bearing B16F10/PAF-AH tumors survived significantly longer than those bearing B16F10/neo tumors (133). Thus, it is clear that the PAF/PAFR systemic activation is implicated in tumorigenesis, which further highlights the need to understand how UVB-induced MVPs mediate this process. Finally, metastatic melanoma has especially poor prognosis due to failure of response to chemotherapeutics and radiation therapy. Therefore, understanding mechanisms for metastasis and tumor survival will provide insight to better treatment in melanoma.

Chemotherapeutics

Environmental stressors, such as UVB radiation and cigarette smoke, could help tumors such as melanomas escape antitumor immunity. Similarly, chemotherapy and radiation therapy increase PAFR expression in tumors as a protective response through generating reactive oxygen species (ROS). ROS activates host-immunity and increases glycerophosphocholine (GPC) species that can act as PAFR agonists (129, 130, 140). The release of PAF subsequently augments cytokine production through the NF-kB pathway, assisting the evasion of chemotherapy. The NF-κB pathway leads to the loss of E-cadherin, contributing to melanoma invasion and resistance to apoptosis (136). Another study showed that cancer therapy activated PAF-R systems augment the cytokine production, specifically IL-8 and TNF-alpha through the NF-κB pathway (141). Cyclooxygenase-2 (COX-2) is a major promoter in immune suppression in melanoma, through its ability to stimulate angiogenesis, inhibit apoptosis, increase cellular proliferation and increase cellular invasiveness, enhance immunosuppression, and produce mutagens (136). PAF is deducted to be a component of oxidative stress and these downstream pathways, and manipulation of PAF/PAFR gene expression, provides an understanding of tumor cell reactions to ROS and chemotherapy.

Cell repopulation is the phenomenon where tumor cells that survive chemotherapy or radiation therapy will undergo accelerated proliferation (142). Thus, finding the mediator that allows tumor cell survival will improve cancer treatment outcomes. Treatment with cisplatin increased PAFR gene expression and accumulation of its products in SKmel37 (melanoma cells) *in vitro* that express PAFR (143). Blocking the release of PAF induced by chemotherapy or the PAF systemic effect may enhance cancer treatment. Indeed, Onuchic et al. found a combination therapy with cisplatin and WEB2086, a PAFR-antagonist, in melanoma-bearing mice showed slowing tumor progression and increasing tumor regression (143). It is conceivable that PAF release protects tumor cells. Another example in the literature was done by Sahu et al. with the focus on ROS and COX-2 inhibition. Both chemotherapy and radiation therapy induce the release of PAF and PAF-like ox-GPC due to oxidative stress and generation of ROS. In a murine model of melanoma, addition of antioxidant regimen reduced the formation of PAFR agonist activity, therefore preventing the augmentation of tumor growth (130). Moreover, COX-2 inhibitors contribute to antitumor immunity by downregulating IL-10 and Tregs that modulate the systemic effect of PAFR-mediated tumor growth (130). Inhibiting effects of PAFR will block immunosuppression and photocarcinogenesis as well as accelerating DNA repair. Therefore, PAF induced immunosuppression may promote survival response in tumor cells (144). Finally, PAF antagonists may work synergistically with other agents that reduce immune suppression, such as 5-HT_{2A} receptor antagonists. Evidence shows that combination of PAF and 5-HT_{2A} receptor antagonists blocks skin cancer induction in UV-irradiated mice (145). These antagonists first prevent UV-induced damage in the

skin from apoptosis after a single exposure to UV radiation, then prevent cytokine release and immune suppression (145). In conclusion, these results provide compelling evidence that potentially future chemotherapeutics could be created by manipulating the PAF/PAFR-mediated responses.

Prosurvival Response in Tumor Cells - Anti-Apoptosis

Most chemotherapeutic agents exert their therapeutic effects through programmed cell death. It is understood that some cancer treatment failures can be attributed to tumor cells' prosurvival response mechanisms that escape the apoptotic activities induced by chemotherapy. Chemotherapy and radiation therapy cause oxidative stress and induce PAF/PAF-like molecules release. PAFR-activated modification of cell microenvironment and upregulation of anti-apoptotic molecules favor tumor growth (146, 147). Specifically, PAF increases the expression of mRNA and protein synthesis of anti-apoptotic factors and inhibits caspase activities (147). Tumor-derived microvesicle particles are another source of anti-apoptosis endorsed by cancer cells to evade cell death (148). Chemotherapeutic agents induce cell death by increasing mitochondrial enzyme caspases. De Olivera and colleagues found that combination of dacarbazine (DTIC) and WEB 2170 (PAFR antagonist) significantly improves survival of B16F10 melanoma-bearing mice compared to either agent used alone (146). Using a PAFR antagonist alone, however, did substantially delay tumor growth (146). PAF molecules are found to inhibit the activities of caspase-3, caspase-8, and caspase-9, as well as cell death induced by etoposide, a common chemotherapy agent (147). These findings suggest that tumor cells release PAF/PAF-like molecules to prolong tumor survival and escape treatment desired cell death.

While abundant reports provide evidence that PAF leads to anti-apoptotic activities, some have found that the opposite could also happen. PAF may produce pro-apoptotic response to chemotherapy as well as anti-apoptotic response depending on which agent is being used (149). This finding complicates our understanding of the effects PAF has on chemotherapeutics and survival of tumor cells. The differences in PAF effect on chemotherapy may be due to varying pathways that PAF can induce. Depending on how the cancer medication works and what it targets, PAF may augment or attenuate the efficacy of chemotherapeutics. PAFR, for example, can enhance apoptosis induced by etoposide and mitomycin C, but not by other agents such as C2 ceramide or tumor necrosis factor related apoptosis-induced ligand (TRAIL) (149).. In sum, further research is needed to study the specifics of how PAF/PAFR affects cancer treatment and tumor cell survival response.

MECHANISTIC INSIGHT THROUGH PHARMACOLOGICAL INTERVENTIONS

The downstream effects mediated by UVB-induced MVP release have been implicated in both local and systemic pathological processes, including inflammatory responses, immunosuppression, and blocking of tumor immunity. As outlined, the mechanism involves UVB-generated ox-PAFR agonists and subsequent MVP generation, which then transports several bioactive molecules such as PAF both locally and systemically. There are a number of pharmacological agents that may modulate this pathway including aSMase inhibitors, antioxidants, COX-2 inhibitors, and PAFR modulators (agonists and antagonists). These agents may serve as potential pharmaceutical strategies to mitigate the pathological consequences seen from UVB exposure.

aSMase Inhibitors

MVP and ceramide release are dependent upon the lipid enzyme aSMase (38, 150). Thus, as evidenced by multiple lines of evidence, aSMase inhibitors pharmacologically inhibit the effects of MVPs and PAF. The literature demonstrating the utility of aSMase inhibitors within the skin is limited. However, there are many models supporting their value in other tissues and organ systems. For example, the mechanisms driving formation of hepatic steatosis are due in part to the activation of aSMase and the production of ceramide in response to ethanol consumption. Liangpunsakul and colleagues found that aSMase inhibitors, such as imipramine, may serve as a therapeutic target for alcohol-induced hepatic steatosis by inhibiting the release of ceramides by aSMase (151). In addition, transfusion-related acute lung injury (TRALI) is mediated by ceramide-mediated endothelial barrier dysfunction, in which extracellular vesicles (EVs) may be required for transport from platelets to endothelial cells. McVey and colleagues reported that blockage of aSMase reduced the formation of EVs and may present as a promising strategy for TRALI prevention (150). By increasing vascular permeability, PAF is a known mediator of pulmonary edema in acute lung injury. This is due in part through the activation of aSMase (152). Yang and collaborators found that pharmacological inhibition of the aSMase pathway blocked the PAF-induced increase in caveolin-1 and endothelial nitric oxide synthase, suggesting aSMase inhibitors as a novel mechanism to regulate vascular permeability (152). Importantly, Chauhan and colleagues explored the role of PAFR signaling in MVP release and the underlying mechanisms using non-small cell lung cancer cell lines. They found that aSMase inhibition significantly blocked MVP release, highlighting the utility of modulating the aSMase and PAFR pathways for targeted therapies in lung cancer cells (153). Lastly, the Sahu research group determined the significance of PAFR in chemotherapy-mediated MVP generation in human pancreatic cancer cells and found the inhibition of aSMase blocked the generation of MVP (154). The aforementioned studies demonstrate the utility of aSMase inhibition in prevention of various pathologies within targeted tissues.

While sparse, there is some literature highlighting the usefulness of aSMase inhibitors within the dermis. Nakatsuji and collaborators found that *C.acnes* Christie, Atkins, Munch-Peterson (CAMP) factor may hijack host aSMase to increase bacterial virulence in order to impair and invade host cells (155). Similarly, Ma and colleagues demonstrated how *S.aureus* α-toxin activates aSMase in macrophages and precipitates the release of

ceramides, which activate the inflammasome and mediate the generation and release of cytokines (156). Of note, a-toxin has been reported to be a potent stimulus for enzymatic PAF production (151). These findings suggest that inhibition of aSMase may block cutaneous microbial-driven pathogenesis. Furthermore, UV irradiation is known to impart a variety of negative pathological consequences within the skin. Appelqvist and colleagues explored the initial signaling during UV-induced damage in human keratinocytes by investigating apoptosis induction and lysosomal exocytosis. The authors found that the addition of anti-aSMase reduced the activation of caspase-8, which plays a central role in the execution-phase of cellular apoptosis (157). Likewise, UV irradiation stimulates the generation of ceramide through the *de novo* synthesis and hydrolysis of sphingomyelin. Kim and collaborators found that UV-induced intracellular ceramide may activate matrix metalloproteinase-1 (MMP-1) expression in dermal fibroblasts *via* JAK1/STAT-1 pathway (158). The findings from these two reports suggest that the targeted modulation of ceramide signaling and aSMase may offer a novel therapeutic approach to allay the risk of UV-mediated cutaneous pathology. Similarly to aSMase inhibitors, antioxidants have shown utility in the prevention of MVP release.

Antioxidants and PAFR Antagonists

The PAF/PAFR signaling pathway has been shown to be exploited by UVB-induced oxidation and PAFR-agonists. This allows for the therapeutic potential of pharmacological agents including antioxidants and PAFR antagonists. Antioxidants may diminish the effects of UVB-induced ROS, which generate PAF agonists and trigger MVP release (34). There are multiple lines of evidence exhibiting the ability of antioxidants to block UVB-mediated PAFR agonist formation and UVB-MVP release (27, 34, 35, 66, 130). Moreover, the antioxidants N-acetyl cysteine, 1,1,3,3-tetramethyl-2-thiourea, and vitamins C and E completely suppressed PAF synthesis in cultured keratinocytes and human skin (159, 160). Furthermore, Sahu and colleagues demonstrated that pretreatment with antioxidants could block PAFR-dependent tumor growth (129). Antioxidants also restricted gefitinib and erlotinib ROS generation and subsequent PAFR activation, which highlights how modulation of PAFR signaling can modify the cellular responses of targeted cancer therapies (153). Lastly, pretreatment with PAFR antagonists and the antioxidant vitamin E resulted in inhibition of UVB-induced TNF-alpha production, suggesting that epidermal PAF-R may be a pharmacological target for UVB in skin (19).

As aforementioned, PAF-R antagonist intervention has the potential to reduce the negative effects of PAFR agonist signaling. Early *in vitro* literature showed pretreatment of PAFR positive keratinocytes with PAFR antagonists Web 2086 and A-85783 reduced UVB-induced TNF-alpha production. Zhang and collaborators provided additional support of the role of PAFR antagonist in the skin, demonstrating that sebaceous glands express PAFRs and PAFR antagonism can suppress COX-2 production in sebaceous glands (161). Interestingly, PAFR activity has been inhibited by pharmacological inhibitors of protein kinase C (PKC), implying that PKC mediates some PAFR actions (162). Inasmuch the subsequent release of MVP particles leads to immunomodulatory effects, the role of PAFR antagonists have also been shown to alter systemic immune effects (163). Additionally, PAFR antagonists have reduced experimental tumor repopulation both *in vitro* and *in vivo* (142, 164). These studies further illustrate the utility of PAFR antagonists as a pharmacological agent aimed at modulating the PAF/PAFR system and subsequent MVP release. Unfortunately, selective PAFR antagonists are not commercially available for clinical application for the targeting of MVP's.

Selective COX-2 Inhibitors

Nonsteroidal anti-inflammatory drugs (NSAIDs) are commercially accessible drugs utilized across the globe for anti-inflammatory, antipyretic, and analgesic use. Through inhibition of cyclooxygenase (COX) enzymes in the arachidonic acid metabolism pathway, these pharmaceutical agents decrease prostaglandin and thromboxane levels. Within this group of medications, COX-1 and COX-2 isoforms are inhibited to various degrees of selection by pharmaceutical agents. Of interest, our lab has shown the activation of epidermal PAFR leads to increased PAF, eicosanoids, COX-2, its product PGE2, arachidonic acid, IL-6, and IL-8. Furthermore, our lab's findings with HaCaT and KB keratinocytes demonstrate that PAFR is sufficient to induce epidermal COX-2 production (165) Additionally, ultraviolet radiation, along with CPAF induced COX-2 activation, and subsequent PGE2 and IL-10 production, has been found to be inhibited by PAFR and COX-2 antagonists, further highlighting the linkage between PAF and its downstream effects with COX-2 (10, 17).

Due to the increased levels of COX-2 and prostaglandins in cutaneous malignancies, pharmacological intervention with COX-2 inhibitors for skin cancer has been examined in clinical trials and systematic reviews. In 2010, a double-blinded placebo-controlled trial on patients with pre-existing actinic keratoses found fewer incidences of squamous cell carcinomas and basal cell carcinomas in patients taking 200 mg of celecoxib twice daily (161). It has been hypothesized that these changes are linked in part to the impact of COX-2 inhibitors on UVB-based systemic immune suppression (42, 166). In particular with melanomas, COX-2 has been implicated as an important pro-immunosuppressive agent. COX-2 also enhances tumor-induced melanoma angiogenesis by increasing vascular endothelial growth factor (VEGF) through phosphoinositide 3-kinase (PI3K)/protein kinase C (PKC) mechanisms. Furthermore, there is emerging evidence correlating COX-2 with Breslow thickness and metastasis, indicating COX-2 roles in prognostic outcomes (136). One mechanism of interest is the role of COX-2 inhibitors on Treg cell depletion in PAFR pathways thus inhibiting tumor growth (42, 129). The woven nature of COX-2 and melanoma implicates roles for COX-2 inhibitors possibly impacting downstream effects of MVPs. Nonetheless, selective COX-2 inhibitors have associated cardiovascular risks which must be taken into account when considering a broad application in skin cancer (167, 168). In conclusion, targeted therapy of COX-2 offers a prospective mechanism to inhibit PAFR activation and MVP release.

CONCLUSION

In conclusion, accumulating evidence has implicated the PAF family of mediators in UV cutaneous responses. Recent studies have suggested that their ability to generate and travel in MVP could provide a mechanism by which a highly potent yet metabolically labile family of lipids may leave the epidermis and thus impact the host. Moreover, it is likely that other agents can utilize subcellular particles such as MVP or exosomes to travel from the skin. These new areas of study have tremendous therapeutic implications, especially given the ability of aSMase inhibitors including FIASM agents such as imipramine and other FIASMs to potently block this pathway. The use of these pharmacologic tools can provide important insights into the roles of this pathway in UV as well as other environmental cutaneous insults.

AUTHOR CONTRIBUTIONS

TF, MG, GB, TW, and TN contributed equally to this work and wrote the first draft; JT and CR helped conceptualize the work and edited and provided further input. All authors contributed to the article and approved the submitted version.

FUNDING

This research was supported in part by grants from the National Institutes of Health R01 HL062996 (JT), R01 ES031087 (JT and CR) and Veteran's Administration Merit Award 5I01BX000853 (JT).

REFERENCES

1. Leitenberger J, Jacobe HT, Cruz PD Jr. Photoimmunology–illuminating the Immune System Through Photobiology. *Semin Immunopathol* (2007) 29 (1):65–70. doi: 10.1007/s00281-007-0063-6
2. Murphy GM. Ultraviolet Radiation and Immunosuppression. *Br J Dermatol* (2009) 161(Suppl 3):90–5. doi: 10.1111/j.1365-2133.2009.09455.x
3. Soehnge H, Ouhtit A, Ananthaswamy ON. Mechanisms of Induction of Skin Cancer by UV Radiation. *Front Biosci* (1997) 2:d538–51. doi: 10.2741/a211
4. Narayanan DL, Saladi RN, Fox JL. Ultraviolet Radiation and Skin Cancer. *Int J Dermatol* (2010) 49(9):978–86. doi: 10.1111/j.1365-4632.2010.04474.x
5. Melnikova VO, Ananthaswamy HN. Cellular and Molecular Events Leading to the Development of Skin Cancer. *Mutat Res* (2005) 571(1-2):91–106. doi: 10.1016/j.mrfmmm.2004.11.015
6. Ichihashi M, Ueda M, Budiyanto A, Bito T, Oka M, Fukunaga M, et al. UV-Induced Skin Damage. *Toxicology* (2003) 189(1-2):21–39. doi: 10.1016/S0300-483X(03)00150-1
7. Nishigori C. Cellular Aspects of Photocarcinogenesis. *Photochem Photobiol Sci* (2006) 5(2):208–14. doi: 10.1039/B507471A
8. Krtolica A, Campisi J. Cancer and Aging: A Model for the Cancer Promoting Effects of the Aging Stroma. *Int J Biochem Cell Biol* (2002) 34 (11):1401–14. doi: 10.1016/S1357-2725(02)00053-5
9. Campisi J. Cancer and Ageing: Rival Demons? *Nat Rev Cancer* (2003) 3 (5):339–49. doi: 10.1038/nrc1073
10. Walterscheid JP, Ullrich SE, Nghiem DX. Platelet-Activating Factor, a Molecular Sensor for Cellular Damage, Activates Systemic Immune Suppression. *J Exp Med* (2002) 195(2):171–9. doi: 10.1084/jem.20011450
11. Ullrich SE. Mechanisms Underlying UV-Induced Immune Suppression. *Mutat Res* (2005) 571(1-2):185–205. doi: 10.1016/j.mrfmmm.2004.06.059
12. Shreedhar V, Giese T, Sung VW, Ullrich SE. A Cytokine Cascade Including Prostaglandin E2, IL-4, and IL-10 is Responsible for UV-Induced Systemic Immune Suppression. *J Immunol* (1998) 160(8):3783–9.
13. Kochevar IE, Taylor CR, Krutmann J. Chapter 90. In: LA Goldsmith, editor. *Fundamentals of Cutaneous Photobiology and Photoimmunology, in Fitzpatrick's Dermatology in General Medicine, 8e*. New York, NY: The McGraw-Hill Companies (2012).
14. D'Orazio J, Jarrett S, Amaro-Orti A, Scott T. UV Radiation and the Skin. *Int J Mol Sci* (2013) 14(6):12222–48. doi: 10.3390/ijms140612222
15. Ansel JC, Luger TA, Green I. Fever and Increased Serum IL-1 Activity as a Systemic Manifestation of Acute Phototoxicity in New Zealand White Rabbits. *J Invest Dermatol* (1987) 89(1):32–7. doi: 10.1111/1523-1747.ep12580362
16. Damiani E, Ullrich SE. Understanding the Connection Between Platelet-Activating Factor, a UV-Induced Lipid Mediator of Inflammation, Immune Suppression and Skin Cancer. *Prog Lipid Res* (2016) 63:14–27. doi: 10.1016/j.plipres.2016.03.004
17. Zhang Q, Yao Y, Konger RL, Sinn AL, Cai S, Pollok KE, et al. UVB Radiation-Mediated Inhibition of Contact Hypersensitivity Reactions is Dependent on the Platelet-Activating Factor System. *J Invest Dermatol* (2008) 128(7):1780–7. doi: 10.1038/sj.jid.5701251
18. Yao Y, Wolverton JE, Zhang Q, Marathe GK, Al-Hassani M, Konger RL, et al. Ultraviolet B Radiation Generated Platelet-Activating Factor Receptor Agonist Formation Involves EGF-R-Mediated Reactive Oxygen Species. *J Immunol* (2009) 182(5):2842–8. doi: 10.4049/jimmunol.0802689
19. Dy LC, Pei Y, Travers JB. Augmentation of Ultraviolet B Radiation-Induced Tumor Necrosis Factor Production by the Epidermal Platelet-Activating Factor Receptor. *J Biol Chem* (1999) 274(38):26917–21. doi: 10.1074/jbc.274.38.26917
20. Travers JB, Edenberg HJ, Zhang Q, Al-Hassani M, Yi Q, Baskaran S, et al. Augmentation of UVB Radiation-Mediated Early Gene Expression by the Epidermal Platelet-Activating Factor Receptor. *J Invest Dermatol* (2008) 128 (2):455–60. doi: 10.1038/sj.jid.5701083
21. Detopoulou P, Nomikos T, Fragopoulou E, Antonopoulou S. Association of PAF and its Metabolic Enzymes With GGT and the Fatty Liver Index in Healthy Volunteers. *Curr Vasc Pharmacol* (2021) 19(6):663–72. doi: 10.2174/1570161119666210628125239
22. Muñoz-Cano RM, Casas-Saucedo R, Valero Santiago A, Bobolea I, Ribó P, Mullol J. Platelet-Activating Factor (PAF) in Allergic Rhinitis: Clinical and Therapeutic Implications. *J Clin Med* (2019) 8(9):1338. doi: 10.3390/jcm8091338
23. Bernard JJ, Gallo RL, Krutmann J. Photoimmunology: How Ultraviolet Radiation Affects the Immune System. *Nat Rev Immunol* (2019) 19(11):688–701. doi: 10.1038/s41577-019-0185-9
24. Shimizu T. Lipid Mediators in Health and Disease: Enzymes and Receptors as Therapeutic Targets for the Regulation of Immunity and Inflammation. *Annu Rev Pharmacol Toxicol* (2009) 49:123–50. doi: 10.1146/annurev.pharmtox.011008.145616
25. Kita Y, Shindou H, Shimizu T. Cytosolic Phospholipase A(2) and Lysophospholipid Acyltransferases. *Biochim Biophys Acta Mol Cell Biol Lipids* (2019) 1864(6):838–45. doi: 10.1016/j.bbalip.2018.08.006
26. Marathe GK, Prescott SM, Zimmerman GA, McIntyre TM. Oxidized LDL Contains Inflammatory PAF-Like Phospholipids. *Trends Cardiovasc Med* (2001) 11(3-4):139–42. doi: 10.1016/S1050-1738(01)00100-1
27. Marathe GK, Johnson C, Billings SD, Southall MD, Pei Y, Spandau D, et al. Ultraviolet B Radiation Generates Platelet-Activating Factor-Like Phospholipids Underlying Cutaneous Damage. *J Biol Chem* (2005) 280 (42):35448–57. doi: 10.1074/jbc.M503811200
28. Konger RL, Marathe GK, Yao Y, Zhang Q, Travers JB. Oxidized Glycerophosphocholines as Biologically Active Mediators for Ultraviolet Radiation-Mediated Effects. *Prostaglandins Other Lipid Mediat* (2008) 87(1-4):1–8. doi: 10.1016/j.prostaglandins.2008.04.002

29. Yao Y, Harrison KA, Al-Hassani M, Murphy RC, Rezania S, Konger RL, et al. Platelet-Activating Factor Receptor Agonists Mediate Xeroderma Pigmentosum A Photosensitivity. *J Biol Chem* (2012) 287(12):9311–21. doi: 10.1074/jbc.M111.332395
30. Ocana JA, Romer E, Sahu R, Pawelzik SC, FitzGerald GA, Kaplan MH, et al. Platelet-Activating Factor-Induced Reduction in Contact Hypersensitivity Responses Is Mediated by Mast Cells via Cyclooxygenase-2-Dependent Mechanisms. *J Immunol* (2018) 200(12):4004–11. doi: 10.4049/jimmunol.1701145
31. Travers JB. Platelet-Activating Factor as an Effector for Environmental Stressors. *Handb Exp Pharmacol* (2020) 259:185–203. doi: 10.1007/164_2019_218
32. Silva AR, de Assis EF, Caiado LF, Marathe GK, Bozza MT, McIntyre TM, et al. Monocyte Chemoattractant Protein-1 and 5-Lipoxygenase Products Recruit Leukocytes in Response to Platelet-Activating Factor-Like Lipids in Oxidized Low-Density Lipoprotein. *J Immunol* (2002) 168(8):4112–20. doi: 10.4049/jimmunol.168.8.4112
33. Zimmerman GA, McIntyre TM, Prescott SM, Stafforini DM. The Platelet-Activating Factor Signaling System and its Regulators in Syndromes of Inflammation and Thrombosis. *Crit Care Med* (2002) 30(5 Suppl):S294–301. doi: 10.1097/00003246-200205001-00020
34. Fahy K, Liu L, Rapp CM, Borchers C, Bihl JC, Chen Y, et al. UVB-Generated Microvesicle Particles: A Novel Pathway by Which a Skin-Specific Stimulus Could Exert Systemic Effects. *Photochem Photobiol* (2017) 93(4):937–42. doi: 10.1111/php.12703
35. Bihl JC, Rapp CM, Chen Y, Travers JB. UVB Generates Microvesicle Particle Release in Part Due to Platelet-Activating Factor Signaling. *Photochem Photobiol* (2016) 92(3):503–6. doi: 10.1111/php.12577
36. Mause SF, Weber C. Microparticles: Protagonists of a Novel Communication Network for Intercellular Information Exchange. *Circ Res* (2010) 107(9):1047–57. doi: 10.1161/CIRCRESAHA.110.226456
37. Liu L, Awoyemi AA, Fahy KE, Thapa P, Borchers C, Wu BY, et al. Keratinocyte-Derived Microvesicle Particles Mediate Ultraviolet B Radiation-Induced Systemic Immunosuppression. *J Clin Invest* (2021) 131 (10):e144963. doi: 10.1172/JCI144963
38. Bianco F, Perrotta C, Novellino L, Francolini M, Riganti L, Menna E, et al. Acid Sphingomyelinase Activity Triggers Microparticle Release From Glial Cells. *EMBO J* (2009) 28(8):1043–54. doi: 10.1038/emboj.2009.45
39. Camussi G, Deregibus MC, Bruno S, Cantaluppi V, Biancone L. Exosomes/Microvesicles as a Mechanism of Cell-to-Cell Communication. *Kidney Int* (2010) 78(9):838–48. doi: 10.1038/ki.2010.278
40. Ratajczak J, Wysoczynski M, Hayek F, Janowska-Wieczorek A, Ratajczak MZ. Membrane-Derived Microvesicles: Important and Underappreciated Mediators of Cell-to-Cell Communication. *Leukemia* (2006) 20(9):1487–95. doi: 10.1038/sj.leu.2404296
41. Xiao X, Ma X, Liu L, Wang J, Bi K, Liu Y, et al. Cellular Membrane Microparticles: Potential Targets of Combinational Therapy for Vascular Disease. *Curr Vasc Pharmacol* (2015) 13(4):449–58. doi: 10.2174/1570161112666141014145440
42. Travers JB, Rohan JG, Sahu RP. New Insights Into the Pathologic Roles of the Platelet-Activating Factor System. *Front Endocrinol (Lausanne)* (2021) 12:624132. doi: 10.3389/fendo.2021.624132
43. Jensen JM, Proksch E. The Skin's Barrier. *G Ital Dermatol Venereol* (2009) 144(6):689–700.
44. Gruber F, Kremslehner C, Eckhart L, Tschachler E. Cell Aging and Cellular Senescence in Skin Aging - Recent Advances in Fibroblast and Keratinocyte Biology. *Exp Gerontol* (2020) 130:110780. doi: 10.1016/j.exger.2019.110780
45. Gordon R. Skin Cancer: An Overview of Epidemiology and Risk Factors. *Semin Oncol Nurs* (2013) 29(3):160–9. doi: 10.1016/j.soncn.2013.06.002
46. Nguyen AV, Soulika AM. The Dynamics of the Skin's Immune System. *Int J Mol Sci* (2019) 20(8):1811. doi: 10.3390/ijms20081811
47. Eckhart L, Zeeuwen P. The Skin Barrier: Epidermis vs Environment. *Exp Dermatol* (2018) 27(8):805–6. doi: 10.1111/exd.13731
48. Kish DD, Li X, Fairchild RL. CD8 T Cells Producing IL-17 and IFN-Gamma Initiate the Innate Immune Response Required for Responses to Antigen Skin Challenge. *J Immunol* (2009) 182(10):5949–59. doi: 10.4049/jimmunol.0802830
49. Friedmann PS, Strickland I, Memon AA, Johnson PM. Early Time Course of Recruitment of Immune Surveillance in Human Skin After Chemical Provocation. *Clin Exp Immunol* (1993) 91(3):351–6. doi:10.1111/j.1365-2249.1993.tb05908.x
50. Falcão-Pires I, Castro-Chaves P, Miranda-Silva D, Lourenço AP, Leite-Moreira AF. Physiological, Pathological and Potential Therapeutic Roles of Adipokines. *Drug Discov Today* (2012) 17(15-16):880–9. doi: 10.1016/j.drudis.2012.04.007
51. Iyer A, Fairlie DP, Prins JB, Hammock BD, Brown L. Inflammatory Lipid Mediators in Adipocyte Function and Obesity. *Nat Rev Endocrinol* (2010) 6 (2):71–82. doi: 10.1038/nrendo.2009.264
52. Zmijewski M, Skobowiat C, Zbytek B, Slominski R, Steketee J. Sensing the Environment: Regulation of Local and Global Homeostasis by the Skin Neuroendocrine System. *Adv Anatomy Embryol Cell Biol* (2012) 212:1–115. doi: 10.1007/978-3-642-19683-6_1
53. Berneburg M, Plettenberg H, Krutmann J. Photoaging of Human Skin. *Photodermatol Photoimmunol Photomed* (2000) 16(6):239–44. doi: 10.1034/j.1600-0781.2000.160601.x
54. Gläser R, Navid F, Schuller W, Jantschitsch C, Harder J, Schröder JM, et al. UV-B Radiation Induces the Expression of Antimicrobial Peptides in Human Keratinocytes In Vitro and In Vivo. *J Allergy Clin Immunol* (2009) 123(5):1117–23. doi: 10.1016/j.jaci.2009.01.043
55. Heck DE, Vetrano AM, Mariano TM, Laskin JD. UVB Light Stimulates Production of Reactive Oxygen Species: Unexpected Role for Catalase. *J Biol Chem* (2003) 278(25):22432–6. doi: 10.1074/jbc.C300048200
56. Johnson KE, Wulff BC, Oberyszyn TM, Wilgus TA. Ultraviolet Light Exposure Stimulates HMGB1 Release by Keratinocytes. *Arch Dermatol Res* (2013) 305(9):805–15. doi: 10.1007/s00403-013-1401-2
57. Burns EM, Ahmed H, Isedeh PN, Kohli I, Van DerPol W, Shaheen A, et al. Ultraviolet Radiation, Both UVA and UVB, Influences the Composition of the Skin Microbiome. *Exp Dermatol* (2019) 28(2):136–41. doi: 10.1111/exd.13854
58. Hart PH, Gorman S, Finlay-Jones JJ. Modulation of the Immune System by UV Radiation: More Than Just the Effects of Vitamin D? *Nat Rev Immunol* (2011) 11(9):584–96. doi: 10.1038/nri3045
59. Schwarz T. Mechanisms of UV-Induced Immunosuppression. *Keio J Med* (2005) 54(4):165–71. doi: 10.2302/kjm.54.165
60. Nghiem DX, Kazimi N, Clydesdale G, Ananthaswamy HN, Kripke ML, Ullrich SE. Ultraviolet a Radiation Suppresses an Established Immune Response: Implications for Sunscreen Design. *J Invest Dermatol* (2001) 117(5):1193–9. doi: 10.1046/j.0022-202x.2001.01503.x
61. Moyal DD, Fourtanier AM. Broad-Spectrum Sunscreens Provide Better Protection From the Suppression of the Elicitation Phase of Delayed-Type Hypersensitivity Response in Humans. *J Invest Dermatol* (2001) 117 (5):1186–92. doi: 10.1046/j.0022-202x.2001.01545.x
62. Bikle DD. Protective Actions of Vitamin D in UVB Induced Skin Cancer. *Photochem Photobiol Sci* (2012) 11(12):1808–16. doi: 10.1039/c2pp25251a
63. Imokawa G. Mechanism of UVB-Induced Wrinkling of the Skin: Paracrine Cytokine Linkage Between Keratinocytes and Fibroblasts Leading to the Stimulation of Elastase. *J Investig Dermatol Symp Proc* (2009) 14(1):36–43. doi: 10.1038/jidsymp.2009.11
64. Slominski AT, Chaiprasongsuk A, Janjetovic Z, Kim T-K, Stefan J, Slominski RM, et al. Photoprotective Properties of Vitamin D and Lumisterol Hydroxyderivatives. *Cell Biochem Biophysics* (2020) 78(2):165–80. doi: 10.1007/s12013-020-00913-6
65. Slominski AT, Zmijewski MA, Plonka PM, Szaflarski JP, Paus R. How UV Light Touches the Brain and Endocrine System Through Skin, and Why. *Endocrinology* (2018) 159(5):1992–2007. doi: 10.1210/en.2017-03230
66. Travers JB, Berry D, Yao Y, Yi Q, Konger RL, Travers JB. Ultraviolet B Radiation of Human Skin Generates Platelet-Activating Factor Receptor Agonists. *Photochem Photobiol* (2010) 86(4):949–54. doi: 10.1111/j.1751-1097.2010.00743.x
67. Benveniste J, Henson PM, Cochrane CG. Leukocyte-Dependent Histamine Release From Rabbit Platelets. The Role of IgE, Basophils, and a Platelet-Activating Factor. *J Exp Med* (1972) 136(6):1356–77. doi: 10.1084/jem.136.6.1356

68. Ishii S, Nagase T, Shimizu T. Platelet-Activating Factor Receptor. *Prostaglandins Other Lipid Mediators* (2002) 68-69:599–609. doi: 10.1016/S0090-6980(02)00058-8
69. Gill P, Jindal NL, Jagdis A, Vadas P. Platelets in the Immune Response: Revisiting Platelet-Activating Factor in Anaphylaxis. *J Allergy Clin Immunol* (2015) 135(6):1424–32. doi: 10.1016/j.jaci.2015.04.019
70. Abate W, Alrammah H, Kiernan M, Tonks AJ, Jackson SK. Lysophosphatidylcholine Acyltransferase 2 (LPCAT2) Co-Localises With TLR4 and Regulates Macrophage Inflammatory Gene Expression in Response to LPS. *Sci Rep* (2020) 10(1):10355. doi: 10.1038/s41598-020-67000-x
71. Prescott SM, Zimmerman GA, Stafforini DM, McIntyre TM. Platelet-Activating Factor and Related Lipid Mediators. *Annu Rev Biochem* (2000) 69:419–45. doi: 10.1146/annurev.biochem.69.1.419
72. Snyder F. Platelet-Activating Factor: The Biosynthetic and Catabolic Enzymes. *Biochem J* (1995) 305(Pt 3):689–705. doi: 10.1042/bj3050689
73. Kono N, Arai H. Platelet-Activating Factor Acetylhydrolases: An Overview and Update. *Biochim Biophys Acta (BBA) Mol Cell Biol Lipids* (2019) 1864 (6):922–31. doi: 10.1016/j.bbalip.2018.07.006
74. Karasawa K, Inoue K. *Chapter One - Overview of PAF-Degrading Enzymes, in The Enzymes*. K Inoue, DM Stafforini and F Tamanoi, editors. Cambridge, MA: Academic Press (2015) p. 1–22.
75. Marques M, Pei Y, Southall MD, Johnston JM, Arai H, Aoki J, et al. Identification of Platelet-Activating Factor Acetylhydrolase II in Human Skin. *J Invest Dermatol* (2002) 119(4):913–9. doi: 10.1046/j.1523-1747.2002.01859.x
76. Pasquet JM, Dachary-Prigent J, Nurden AT. Calcium Influx is a Determining Factor of Calpain Activation and Microparticle Formation in Platelets. *Eur J Biochem* (1996) 239(3):647–54. doi: 10.1111/j.1432-1033.1996.0647u.x
77. Ståhl AL, Arvidsson I, Johansson KE, Chromek M, Rebetz J, Loos S, et al. A Novel Mechanism of Bacterial Toxin Transfer Within Host Blood Cell-Derived Microvesicles. *PloS Pathog* (2015) 11(2):e1004619. doi:10.1371/journal.ppat.1004619
78. Kahn R, Mossberg M, Ståhl AL, Johansson K, Lopatko Lindman I, Heijl C, et al. Microvesicle Transfer of Kinin B1-Receptors is a Novel Inflammatory Mechanism in Vasculitis. *Kidney Int* (2017) 91(1):96–105. doi: 10.1016/j.kint.2016.09.023
79. Abid Hussein MN, Böing AN, Sturk A, Hau CM, Nieuwland R. Inhibition of Microparticle Release Triggers Endothelial Cell Apoptosis and Detachment. *Thromb Haemost* (2007) 98(5):1096–107. doi:10.1160/th05-04-0231
80. Liu L, Fahy KE, Awoyemi AA, Thapa P, Kelly LE, Chen J, et al. Thermal Burn Injury Generates Bioactive Microvesicles: Evidence for a Novel Transport Mechanism for the Lipid Mediator Platelet-Activating Factor (PAF) That Involves Subcellular Particles and the PAF Receptor. *J Immunol* (2020) 205(1):193–201. doi: 10.4049/jimmunol.1901393
81. Liu L, Rapp CM, Zheng S, Travers JB. 627 UVB-Generated Microvesicle Particles Mediate Systemic Immunosuppression. *J Invest Dermatol* (2020) 140(7):S85. doi: 10.1016/j.jid.2020.03.638
82. Awoyemi AA, Borchers C, Liu L, Chen Y, Rapp CM, Brewer CA, et al. Acute Ethanol Exposure Stimulates Microvesicle Particle Generation in Keratinocytes. *Toxicol Lett* (2022) 355:100–5. doi: 10.1016/j.toxlet.2021.11.008
83. Wang J, Pothana K, Chen S, Sawant H, Travers JB, Bihl J, et al. Ultraviolet B Irradiation Alters the Level and miR Contents of Exosomes Released by Keratinocytes in Diabetic Condition. *Photochem Photobiol* (2021). doi: 10.1111/php.13583
84. Pitt JM, Kroemer G, Zitvogel L. Extracellular Vesicles: Masters of Intercellular Communication and Potential Clinical Interventions. *J Clin Invest* (2016) 126(4):1139–43. doi: 10.1172/JCI87316
85. McBride JD, Rodriguez-Menocal L, Badiavas EV. Extracellular Vesicles as Biomarkers and Therapeutics in Dermatology: A Focus on Exosomes. *J Invest Dermatol* (2017) 137(8):1622–9. doi: 10.1016/j.jid.2017.04.021
86. Muralidharan-Chari V, Clancy JW, Sedgwick A, D'Souza-Schorey C. Microvesicles: Mediators of Extracellular Communication During Cancer Progression. *J Cell Sci* (2010) 123(Pt 10):1603–11. doi: 10.1242/jcs.064386
87. Riazifar M, Pone EJ, Lötvall J, Zhao W. Stem Cell Extracellular Vesicles: Extended Messages of Regeneration. *Annu Rev Pharmacol Toxicol* (2017) 57:125–54. doi: 10.1146/annurev-pharmtox-061616-030146
88. van Niel G, D'Angelo G, Raposo G. Shedding Light on the Cell Biology of Extracellular Vesicles. *Nat Rev Mol Cell Biol* (2018) 19(4):213–28. doi: 10.1038/nrm.2017.125
89. Tricarico C, Clancy J, D'Souza-Schorey C. Biology and Biogenesis of Shed Microvesicles. *Small GTPases* (2017) 8(4):220–32. doi: 10.1080/21541248.2016.1215283
90. Leroyer AS, Rautou P-E, Silvestre J-S, Castier Y, Lesèche G, Devue C, et al. CD40 Ligand+ Microparticles From Human Atherosclerotic Plaques Stimulate Endothelial Proliferation and Angiogenesis: A Potential Mechanism for Intraplaque Neovascularization. *J Am Coll Cardiol* (2008) 52(16):1302–11. doi: 10.1016/j.jacc.2008.07.032
91. Shefler I, Pasmanik-Chor M, Kidron D, Mekori YA, Hershko AY. T Cell-Derived Microvesicles Induce Mast Cell Production of IL-24: Relevance to Inflammatory Skin Diseases. *J Allergy Clin Immunol* (2014) 133(1):217–24.e1-3. doi: 10.1016/j.jaci.2013.04.035
92. Taverna S, Ghersi G, Ginestra A, Rigogliuso S, Pecorella S, Alaimo G, et al. Shedding of Membrane Vesicles Mediates Fibroblast Growth Factor-2 Release From Cells *. *J Biol Chem* (2003) 278(51):51911–9. doi: 10.1074/jbc.M304192200
93. Obregon C, Rothen-Rutishauser B, Gitahi SK, Gehr P, Nicod LP. Exovesicles From Human Activated Dendritic Cells Fuse With Resting Dendritic Cells, Allowing Them to Present Alloantigens. *Am J Pathol* (2006) 169(6):2127–36. doi: 10.2353/ajpath.2006.060453
94. Faille D, El-Assaad F, Mitchell AJ, Alessi M-C, Chimini G, Fusai T, et al. Endocytosis and Intracellular Processing of Platelet Microparticles by Brain Endothelial Cells. *J Cell Mol Med* (2012) 16(8):1731–8. doi: 10.1111/j.1582-4934.2011.01434.x
95. Simon MM, Aragane Y, Schwarz A, Luger TA, Schwarz T. UVB Light Induces Nuclear Factor Kappa B (NF Kappa B) Activity Independently From Chromosomal DNA Damage in Cell-Free Cytosolic Extracts. *J Invest Dermatol* (1994) 102(4):422–7. doi: 10.1111/1523-1747.ep12372194
96. Barber LA, Spandau DF, Rathman SC, Murphy RC, Johnson CA, Kelley SW, et al. Expression of the Platelet-Activating Factor Receptor Results in Enhanced Ultraviolet B Radiation-Induced Apoptosis in a Human Epidermal Cell Line. *J Biol Chem* (1998) 273(30):18891–7. doi: 10.1074/jbc.273.30.18891
97. Chacón-Salinas R, Chen L, Chávez-Blanco AD, Limón-Flores AY, Ma Y, Ullrich SE. An Essential Role for Platelet-Activating Factor in Activating Mast Cell Migration Following Ultraviolet Irradiation. *J Leukoc Biol* (2014) 95(1):139–48. doi: 10.1189/jlb.0811409
98. Wardlaw AJ, Moqbel R, Cromwell O, Kay AB. Platelet-Activating Factor. A Potent Chemotactic and Chemokinetic Factor for Human Eosinophils. *J Clin Invest* (1986) 78(6):1701–6. doi: 10.1172/JCI112765
99. Håkansson L, Venge P. Inhibition of Neutrophil and Eosinophil Chemotactic Responses to PAF by the PAF-Antagonists WEB-2086, L-652,731, and SRI-63441. *J Leukoc Biol* (1990) 47(5):449–56. doi: 10.1002/jlb.47.5.449
100. Travers JB, Li Q, Kniss DA, Fertel RH. Identification of Functional Platelet-Activating Factor Receptors in Raji Lymphoblasts. *J Immunol* (1989) 143 (11):3708–13.
101. Travers JB, Shaw JE, Li Q, Kniss DA, Fertel RH. Evidence for Platelet-Activating Factor Receptors in Several B Lymphoblastoid Cell Lines. *Life Sci* (1991) 49(23):1755–60. doi: 10.1016/0024-3205(91)90318-6
102. Travers JB, et al. Identification of Functional Platelet-Activating Factor Receptors on Human Keratinocytes. *J Invest Dermatol* (1995) 105(6):816–23. doi: 10.1111/1523-1747.ep12326581
103. Honda Z, Ishii S, Shimizu T. Platelet-Activating Factor Receptor. *J Biochem* (2002) 131(6):773–9. doi: 10.1093/oxfordjournals.jbchem.a003164
104. Record M, Silvente-Poirot S, Poirot M, Wakelam MJO. Extracellular Vesicles: Lipids as Key Components of Their Biogenesis and Functions. *J Lipid Res* (2018) 59(8):1316–24. doi: 10.1194/jlr.E086173
105. Göggel R, Winoto-Morbach S, Vielhaber G, Imai Y, Lindner K, Brade L, et al. PAF-Mediated Pulmonary Edema: A New Role for Acid Sphingomyelinase and Ceramide. *Nat Med* (2004) 10(2):155–60. doi: 10.1038/nm977

106. Lang PA, Kempe DS, Tanneur V, Eisele K, Klarl BA, Myssina S, et al. Stimulation of Erythrocyte Ceramide Formation by Platelet-Activating Factor. *J Cell Sci* (2005) 118(Pt 6):1233–43. doi: 10.1242/jcs.01730
107. Kornhuber J, Muehlbacher M, Trapp S, Pechmann S, Friedl A, Reichel M, et al. Identification of Novel Functional Inhibitors of Acid Sphingomyelinase. *PloS One* (2011) 6(8):e23852. doi: 10.1371/journal.pone.0023852
108. Thapa P, Bhadri S, Borchers C, Liu L, Chen Y, Rapp CM, et al. Low UVB Fluences Augment Microvesicle Particle Generation in Keratinocytes. *Photochem Photobiol* (2021) 98(1):248–53. doi: 10.1111/php.13495
109. Ullrich SE, Byrne SN. The Immunologic Revolution: Photoimmunology. *J Invest Dermatol* (2012) 132(3 Pt 2):896–905. doi: 10.1038/jid.2011.405
110. Bhadri S, Thapa P, Chen Y, Rapp CM, Travers JB. Evidence for Microvesicle Particles in UVB-Mediated IL-8 Generation in Keratinocytes. *J Clin Invest Dermatol* (2021) 9(2):10.13188/2373-1044.1000076. doi: 10.13188/2373-1044.1000076
111. Sahu RP, Yao Y, Konger RL, Travers JB. Platelet-Activating Factor Does Not Mediate UVB-Induced Local Immune Suppression. *Photochem Photobiol* (2012) 88(2):490–3. doi: 10.1111/j.1751-1097.2011.01071.x
112. Puebla-Osorio N, Damiani E, Bover L, Ullrich SE. Platelet-Activating Factor Induces Cell Cycle Arrest and Disrupts the DNA Damage Response in Mast Cells. *Cell Death Dis* (2015) 6(5):e1745. doi: 10.1038/cddis.2015.115
113. Vieyra-Garcia PA, Wolf P. From Early Immunomodulatory Triggers to Immunosuppressive Outcome: Therapeutic Implications of the Complex Interplay Between the Wavebands of Sunlight and the Skin. *Front Med* (2018) 5:232–2. doi: 10.3389/fmed.2018.00232
114. Damiani E, Puebla-Osorio N, Gorbea E, Ullrich SE. Platelet-Activating Factor Induces Epigenetic Modifications in Human Mast Cells. *J Invest Dermatol* (2015) 135(12):3034–40. doi: 10.1038/jid.2015.336
115. Hart PH, Grimbaldeston MA, Swift GJ, Jaksic A, Noonan FP, Finlay-Jones JJ. Dermal Mast Cells Determine Susceptibility to Ultraviolet B-Induced Systemic Suppression of Contact Hypersensitivity Responses in Mice. *J Exp Med* (1998) 187(12):2045–53. doi: 10.1084/jem.187.12.2045
116. Schwarz A, Noordegraaf M, Maeda A, Torii K, Clausen BE, Schwarz T. Langerhans Cells are Required for UVR-Induced Immunosuppression. *J Invest Dermatol* (2010) 130(5):1419–27. doi: 10.1038/jid.2009.429
117. Fukunaga A, Khaskhely NM, Ma Y, Sreevidya CS, Taguchi K, Nishigori C, et al. Langerhans Cells Serve as Immunoregulatory Cells by Activating NKT Cells. *J Immunol* (2010) 185(8):4633–40. doi: 10.4049/jimmunol.1000246
118. Moodycliffe AM, Nghiem D, Clydesdale G, Ullrich SE. Immune Suppression and Skin Cancer Development: Regulation by NKT Cells. *Nat Immunol* (2000) 1(6):521–5. doi: 10.1038/82782
119. Schwarz T. 25 Years of UV-Induced Immunosuppression Mediated by T Cells-From Disregarded T Suppressor Cells to Highly Respected Regulatory T Cells. *Photochem Photobiol* (2008) 84(1):10–8. doi: 10.1111/j.1751-1097.2007.00223.x
120. Loser K, Mehling A, Loeser S, Apelt J, Kuhn A, Grabbe S, et al. Epidermal RANKL Controls Regulatory T-Cell Numbers via Activation of Dendritic Cells. *Nat Med* (2006) 12(12):1372–9. doi: 10.1038/nm1518
121. Soontrapa K, Honda T, Sakata D, Yao C, Hirata T, Hori S, et al. Prostaglandin E_2–Prostoglandin E Receptor Subtype 4 (EP4) Signaling Mediates UV Irradiation-Induced Systemic Immunosuppression. *Proc Natl Acad Sci* (2011) 108(16):6668–73. doi: 10.1073/pnas.1018625108
122. Koga MM, Bizzarro B, Sá-Nunes A, Rios FJ, Jancar S, et al. Activation of PAF-Receptor Induces Regulatory Dendritic Cells Through PGE2 and IL-10. *Prostaglandins Leukot Essent Fatty Acids* (2013) 89(5): 319–26. doi: 10.1016/j.plefa.2013.09.003
123. Acosta-Rodriguez EV, Napolitani G, Lanzavecchia A, Sallusto F. Interleukins 1beta and 6 but Not Transforming Growth Factor-Beta Are Essential for the Differentiation of Interleukin 17-Producing Human T Helper Cells. *Nat Immunol* (2007) 8(9):9427–9. doi: 10.1038/ni1496
124. Wilson NJ, Boniface K, Chan JR, McKenzie BS, Blumenschein WM, Mattson JD, et al. Development, Cytokine Profile and Function of Human Interleukin 17-Producing Helper T Cells. *Nat Immunol* (2007) 8(9):950–7. doi: 10.1038/ni1497
125. Drolet A-M, Thivierge M, Turcotte S, Hanna D, Maynard B, Stankovà J, et al. Platelet-Activating Factor Induces Th17 Cell Differentiation. *Mediators Inflammation* (2011) 913802. doi: 10.1155/2011/913802
126. Travers JB, Murphy RC, Johnson CA, Pei Y, Morin SM, Clay KL, et al Identification and Pharmacological Characterization of Platelet-Activating Factor and Related 1-Palmitoyl Species in Human Inflammatory Blistering Diseases. *Prostaglandins Other Lipid Mediat* (1998) 56(5–6):305–24. doi: 10.1016/S0090-6980(98)00060-4
127. Grandel KE, Farr RS, Wanderer AA, Eisenstadt TC, Wasserman SI. Association of Platelet-Activating Factor With Primary Acquired Cold Urticaria. *N Engl J Med* (1985) 313(7):405–9. doi: 10.1056/NEJM198508153130702
128. Harrison KA, Romer E, Weyerbacher J, Ocana JA, Sahu RP, Murphy RC, et al. Enhanced Platelet-Activating Factor Synthesis Facilitates Acute and Delayed Effects of Ethanol-Intoxicated Thermal Burn Injury. *J Invest Dermatol* (2018) 138(11):2461–9. doi: 10.1016/j.jid.2018.04.039
129. Sahu RP, Ocana JA, Harrison KA, Ferracini M, Touloukian CE, Al-Hassani M, et al. Chemotherapeutic Agents Subvert Tumor Immunity by Generating Agonists of Platelet-Activating Factor. *Cancer Res* (2014) 74(23):7069–78. doi: 10.1158/0008-5472.CAN-14-2043
130. Sahu RP, Turner MJ, DaSilva SC, Rashid BM, Ocana JA, Perkins SM, et al. The Environmental Stressor Ultraviolet B Radiation Inhibits Murine Antitumor Immunity Through Its Ability to Generate Platelet-Activating Factor Agonists. *Carcinogenesis* (2012) 33(7):1360–7. doi: 10.1093/carcin/bgs152
131. Lima LG, Chammas R, Monteiro RQ, Moreira ME, Barcinski MA. Tumor-Derived Microvesicles Modulate the Establishment of Metastatic Melanoma in a Phosphatidylserine-Dependent Manner. *Cancer Lett* (2009) 283(2):168–75. doi: 10.1016/j.canlet.2009.03.041
132. Sato S, Kume K, Ito C, Ishii S, Shimizu T. Accelerated Proliferation of Epidermal Keratinocytes by the Transgenic Expression of the Platelet-Activating Factor Receptor. *Arch Dermatol Res* (1999) 291(11):614–21. doi: 10.1007/s004030050463
133. Biancone L, Cantaluppi V, Del Sorbo L, Russo S, Tjoelker LW, Camussi G, et al. Platelet-activating Factor Inactivation by Local Expression of Platelet-activating Factor Acetyl-Hydrolase Modifies Tumor Vascularization and Growth. *Clin Cancer Res* (2003) 9(11):4214–20.
134. Im SY, Ko HM, Kim JW, Lee HK, Ha TY, Lee HB, et al. Augmentation of Tumor Metastasis by Platelet-Activating Factor. *Cancer Res* (1996) 56 (11):2662–5.
135. Shimada A, Ota Y, Sugiyama Y, Inoue S, Sato S, Kume K, et al. In Situ Expression of Platelet-Activating Factor (PAF)-Receptor Gene in Rat Skin and Effects of PAF on Proliferation and Differentiation of Cultured Human Keratinocytes. *J Invest Dermatol* (1998) 110(6):889–93. doi: 10.1046/j.1523-1747.1998.00202.x
136. Tudor DV, Bâldea I, Lupu M, Kacso T, Kutasi E, Hopârtean A, et al. COX-2 as a Potential Biomarker and Therapeutic Target in Melanoma. *Cancer Biol Med* (2020) 17(1):20–31. doi: 10.20892/j.issn.2095-3941.2019.0339
137. Melnikova VO, Villares GJ, Bar-Eli M. Emerging Roles of PAR-1 and PAFR in Melanoma Metastasis. *Cancer Microenviron* (2008) 1(1):103–11. doi: 10.1007/s12307-008-0002-7
138. Braeuer RR, Zigler M, Villares GJ, Dobroff AS, Bar-Eli M. Transcriptional Control of Melanoma Metastasis: The Importance of the Tumor Microenvironment. *Semin Cancer Biol* (2011) 21(2):83–8. doi: 10.1016/j.semcancer.2010.12.007
139. Xu X, Wang Y, Chen Z, Sternlicht MD, Hidalgo M, Steffensen B. Matrix Metalloproteinase-2 Contributes to Cancer Cell Migration on Collagen. *Cancer Res* (2005) 65(1):130–6.
140. Sahu RP, Harrison KA, Weyerbacher J, Murphy RC, Konger RL, Garrett JE, et al. Radiation Therapy Generates Platelet-Activating Factor Agonists. *Oncotarget* (2016) 7(15):20788–800. doi: 10.18632/oncotarget.7878
141. Darst M, Al-Hassani M, Li T, Yi Q, Travers JM, Lewis DA, et al. Augmentation of Chemotherapy-Induced Cytokine Production by Expression of the Platelet-Activating Factor Receptor in a Human Epithelial Carcinoma Cell Line. *J Immunol* (2004) 172(10):6330–5. doi: 10.4049/jimmunol.172.10.6330
142. da Silva Junior IA, de SousaAndrade LN, Jancar S, Chammas R, et al. Platelet Activating Factor Receptor Antagonists Improve the Efficacy of Experimental Chemo- and Radiotherapy. *Clinics (Sao Paulo Brazil)* (2018) 73(suppl 1):e792s. doi: 10.6061/clinics/2018/e792s

143. Onuchic AC, Machado CML, Saito RF, Rios FJ, Jancar S, Chammas R. Expression of PAFR as Part of a Prosurvival Response to Chemotherapy: A Novel Target for Combination Therapy in Melanoma. *Mediators Inflamm* (2012) 2012:175408. doi: 10.1155/2012/175408
144. Sreevidya CS, Fukunaga A, Khaskhely NM, Masaki T, Ono R, Nishigori C, et al. Agents That Reverse UV-Induced Immune Suppression and Photocarcinogenesis Affect DNA Repair. *J Invest Dermatol* (2010) 130 (5):1428–37. doi: 10.1038/jid.2009.329
145. Sreevidya CS, Khaskhely NM, Fukunaga A, Khaskina P, Ullrich SE. Inhibition of Photocarcinogenesis by Platelet-Activating Factor or Serotonin Receptor Antagonists. *Cancer Res* (2008) 68(10):3978–84. doi: 10.1158/0008-5472.CAN-07-6132
146. de Oliveira SI, Andrade LNS, Onuchic AC, Nonogaki S, Fernandes PD, Pinheiro MC, et al. Platelet-Activating Factor Receptor (PAF-R)-Dependent Pathways Control Tumour Growth and Tumour Response to Chemotherapy. *BMC Cancer* (2010) 10(1):200. doi: 10.1186/1471-2407-10-200
147. Heon Seo K, Ko H-M, Kim H-A, Choi J-H, Jun Park S, Kim K-J, et al. Platelet-Activating Factor Induces Up-Regulation of Antiapoptotic Factors in a Melanoma Cell Line Through Nuclear Factor-κb Activation. *Cancer Res* (2006) 66(9):4681–6. doi: 10.1158/0008-5472.CAN-05-3186
148. Baj-Krzyworzeka M, Szatanek R, Węglarczyk K, Baran J, Urbanowicz B, Brański P, et al. Tumour-Derived Microvesicles Carry Several Surface Determinants and mRNA of Tumour Cells and Transfer Some of These Determinants to Monocytes. *Cancer Immunol Immunother* (2006) 55 (7):808–18. doi: 10.1007/s00262-005-0075-9
149. Li T, Southall MD, Yi Q, Pei Y, Lewis D, Al-Hassani M, et al. The Epidermal Platelet-Activating Factor Receptor Augments Chemotherapy-Induced Apoptosis in Human Carcinoma Cell Lines*. *J Biol Chem* (2003) 278 (19):16614–21. doi: 10.1074/jbc.M211287200
150. McVey MJ, Weidenfeld S, Maishan M, Spring C, Kim M, Tabuchi A, et al. Platelet Extracellular Vesicles Mediate Transfusion-Related Acute Lung Injury by Imbalancing the Sphingolipid Rheostat. *Blood* (2021) 137 (5):690–701. doi: 10.1182/blood.2020005985
151. Liangpunsakul S, Rahmini Y, Ross RA, Zhao Z, Xu Y, Crabb DW. Imipramine Blocks Ethanol-Induced ASMase Activation, Ceramide Generation, and PP2A Activation, and Ameliorates Hepatic Steatosis in Ethanol-Fed Mice. *Am J Physiol Gastrointest Liver Physiol* (2012) 302(5): G515–23. doi: 10.1152/ajpgi.00455.2011
152. Yang Y, Yin J, Baumgartner W, Samapati R, Solymosi EA, Reppien E, et al. Platelet-Activating Factor Reduces Endothelial Nitric Oxide Production: Role of Acid Sphingomyelinase. *Eur Respir J* (2010) 36(2):417–27. doi: 10.1183/09031936.00095609
153. Chauhan SJ, Thyagarajan A, Chen Y, Travers JB, Sahu RP. Platelet-Activating Factor-Receptor Signaling Mediates Targeted Therapies-Induced Microvesicle Particles Release in Lung Cancer Cells. *Int J Mol Sci* (2020) 21(22):8517. doi: 10.3390/ijms21228517
154. Thyagarajan A, Kadam SM, Liu L, Kelly LE, Rapp CM, Chen Y, et al. Gemcitabine Induces Microvesicle Particle Release in a Platelet-Activating Factor-Receptor-Dependent Manner via Modulation of the MAPK Pathway in Pancreatic Cancer Cells. *Int J Mol Sci* (2018) 20(1):32. doi: 10.3390/ijms20010032
155. Nakatsuji T, Tang DC, Zhang L, Gallo RL, Huang CM. Propionibacterium Acnes CAMP Factor and Host Acid Sphingomyelinase Contribute to Bacterial Virulence: Potential Targets for Inflammatory Acne Treatment. *PloS One* (2011) 6(4):e14797. doi: 10.1371/journal.pone.0014797
156. Ma J, Gulbins E, Edwards MJ, Caldwell CC, Fraunholz M, Becker KA, et al. Staphylococcus Aureus α-Toxin Induces Inflammatory Cytokines via Lysosomal Acid Sphingomyelinase and Ceramides. *Cell Physiol Biochem* (2017) 43(6):2170–84. doi: 10.1159/000484296
157. Appelqvist H, Wäster P, Eriksson I, Rosdahl I, Ollinger K. Lysosomal Exocytosis and Caspase-8-Mediated Apoptosis in UVA-Irradiated Keratinocytes. *J Cell Sci* (2013) 126(Pt 24):5578–84. doi: 10.1242/jcs.130633
158. Kim S, Kim Y, Lee Y, Chung JH. Ceramide Accelerates Ultraviolet-Induced MMP-1 Expression Through JAK1/STAT-1 Pathway in Cultured Human Dermal Fibroblasts. *J Lipid Res* (2008) 49(12):2571–81. doi: 10.1194/jlr.M800112-JLR200
159. Calignano A, Cirino G, Meli R, Persico P. Isolation and Identification of Platelet-Activating Factor in UV-Irradiated Guinea Pig Skin. *J Pharmacol Methods* (1988) 19(1):89–91. doi: 10.1016/0160-5402(88)90049-6
160. Sheng Y, Birkle DL. Release of Platelet Activating Factor (PAF) and Eicosanoids in UVC-Irradiated Corneal Stromal Cells. *Curr Eye Res* (1995) 14(5):341–7. doi: 10.3109/02713689508999931
161. Zhang Q, Seltmann H, Zouboulis CC, Travers JB. Activation of Platelet-Activating Factor Receptor in SZ95 Sebocytes Results in Inflammatory Cytokine and Prostaglandin E2 Production. *Exp Dermatol* (2006) 15 (10):769–74. doi: 10.1111/j.1600-0625.2006.00458.x
162. Wolverton JE, Al-Hassani M, Yao Y, Zhang Q, Travers JB. Epidermal Platelet-Activating Factor Receptor Activation and Ultraviolet B Radiation Result in Synergistic Tumor Necrosis Factor-Alpha Production. *Photochem Photobiol* (2010) 86(1):231–5. doi: 10.1111/j.1751-1097.2009.00618.x
163. Koga MM, Bizzarro B, Sá-Nunes A, Rios FJ, Jancar S. Boosting Adaptive Immunity: A New Role for PAFR Antagonists. *Sci Rep* (2016) 6(1):39146. doi: 10.1038/srep39146
164. Sahu RP. Expression of the Platelet-Activating Factor Receptor Enhances Benzyl Isothiocyanate-Induced Apoptosis in Murine and Human Melanoma Cells. *Mol Med Rep* (2015) 12(1):394–400. doi: 10.3892/mmr.2015.3371
165. Pei Y, Barber LA, Murphy RC, Johnson CA, Kelley SW, Dy LC, et al. Activation of the Epidermal Platelet-Activating Factor Receptor Results in Cytokine and Cyclooxygenase-2 Biosynthesis. *J Immunol* (1998) 161(4):1954–61.
166. Elmets CA, Viner JL, Pentland AP, Cantrell W, Lin H-Y, Bailey H, et al. Chemoprevention of Nonmelanoma Skin Cancer With Celecoxib: A Randomized, Double-Blind, Placebo-Controlled Trial. *J Natl Cancer Institute* (2010) 102(24):1835–44. doi: 10.1093/jnci/djq442
167. Tang JY, Aszterbaum M, Athar M, Barsanti F, Cappola C, Estevez N. Basal Cell Carcinoma Chemoprevention With Nonsteroidal Anti-Inflammatory Drugs in Genetically Predisposed PTCH1+/- Humans and Mice. *Cancer Prev Res (Philadelphia Pa)* (2010) 3(1):25–34. doi: 10.1158/1940-6207.CAPR-09-0200
168. Funk CD, FitzGerald GA. COX-2 Inhibitors and Cardiovascular Risk. *J Cardiovasc Pharmacol* (2007) 50(5):470–9. doi: 10.1097/FJC.0b013e318157f72d

Conflict of Interest: The authors declare that the research was conducted in the absence of any commercial or financial relationships that could be construed as a potential conflict of interest.

Publisher's Note: All claims expressed in this article are solely those of the authors and do not necessarily represent those of their affiliated organizations, or those of the publisher, the editors and the reviewers. Any product that may be evaluated in this article, or claim that may be made by its manufacturer, is not guaranteed or endorsed by the publisher.

frontiers | Frontiers in Immunology

REVIEW
published: 26 May 2022
doi: 10.3389/fimmu.2022.868386

Cold Atmospheric Plasma Ameliorates Skin Diseases Involving Reactive Oxygen/Nitrogen Species-Mediated Functions

Si-yue Zhai[1,2], *Michael G. Kong*[2,3]* *and Yu-min Xia*[1]*

[1] Department of Dermatology, The Second Affiliated Hospital of Xi'an Jiaotong University, Xi'an, China, [2] Center of Plasma Biomedicine, State Key Laboratory of Electrical Insulation and Power Equipment, Xi'an Jiaotong University, Xi'an, China, [3] School of Electrical Engineering, Xi'an Jiaotong University, Xi'an, China

OPEN ACCESS

Edited by:
Kai Fang,
University of California, Los Angeles, United States

Reviewed by:
Chih-Yao Hou,
National Kaohsiung University of Science and Technology, Taiwan
Lia-Mara Ditu,
University of Bucharest, Romania
Xiaofeng Dai,
Jiangnan University, China

***Correspondence:**
Michael G. Kong
mglin5g@gmail.com
Yu-min Xia
xiayumin1202@163.com

Specialty section:
This article was submitted to Inflammation, a section of the journal Frontiers in Immunology

Received: 02 February 2022
Accepted: 09 May 2022
Published: 26 May 2022

Citation:
Zhai S-y, Kong MG and Xia Y-m (2022) Cold Atmospheric Plasma Ameliorates Skin Diseases Involving Reactive Oxygen/Nitrogen Species-Mediated Functions. Front. Immunol. 13:868386. doi: 10.3389/fimmu.2022.868386

Skin diseases are mainly divided into infectious diseases, non-infectious inflammatory diseases, cancers, and wounds. The pathogenesis might include microbial infections, autoimmune responses, aberrant cellular proliferation or differentiation, and the overproduction of inflammatory factors. The traditional therapies for skin diseases, such as oral or topical drugs, have still been unsatisfactory, partly due to systematic side effects and reappearance. Cold atmospheric plasma (CAP), as an innovative and non-invasive therapeutic approach, has demonstrated its safe and effective functions in dermatology. With its generation of reactive oxygen species and reactive nitrogen species, CAP exhibits significant efficacies in inhibiting bacterial, viral, and fungal infections, facilitating wound healing, restraining the proliferation of cancers, and ameliorating psoriatic or vitiligous lesions. This review summarizes recent advances in CAP therapies for various skin diseases and implicates future strategies for increasing effectiveness or broadening clinical indications.

Keywords: cold atmospheric plasma, reactive oxygen species, reactive nitrogen species, skin disease, therapy

INTRODUCTION

It is widely accepted that there are various kinds of skin diseases, including infectious diseases, cancers, wounds, and non-communicable inflammatory skin diseases (ncISDs). The pathogenic factors of these skin disorders include microbial infections, excessive cytokines release, inflammatory cell infiltration, and aberrant cell proliferation or differentiation (1–3). Currently, the comprehensive treatments include systemic or topical medications or in combination with different phototherapies. However, these applications have still been challenged due to systemic side effects, the high recurrence rate of the disease, or the serious impact on daily life or working (4). As an innovative non-invasive application, cold atmospheric plasma (CAP) has exhibited significant efficacy in treating skin diseases such as microbial infections, cutaneous wounds, cancers, and ncISDs (5, 6). It is well clarified that the biological functions of CAP involve ultra-violet radiation, reactive oxygen species, and reactive nitrogen species while exhibiting little damage to the normal cells or tissues (7). CAP may destroy biofilms or even the integrity of cells, degrade cellular proteins and DNA, generate DNA and protein crosslinking, and dysregulate pH value- or calcium-related

microenvironments (7–11). In this review, we summarize recent advances in the applications of CAP in treating skin diseases and possible therapeutic mechanisms.

THE CHARACTERISTICS OF CAP

Containing with the positive and negative changed species, plasma is the fourth state of matter, which is different from the common three substances (solid, liquid, and gas) (12). According to the gas temperature of plasma, the plasma generated by different methods can be divided into hot plasm, warm plasma, and cold plasma. Because high temperature can cause thermal damage to organisms, the plasma applied to medical treatment should be considered a kind of plasma at atmospheric pressure with its temperature close to room temperature (13). CAP has been used in medical treatments widely (6). As **Figure 1** described, there are two common devices for CAP generators, dielectric barrier discharges (DBD) and atmospheric pressure plasma jet (APPJ). Surface DBD is consisted of two parallel electrodes sandwiching a ceramic slab to strike a surface discharge plasma at a high voltage in a narrow discharge gap (7). The other is the APPJ, consisting of a quartz capillary equipped with a pin-type electrode at a high voltage generated in an open space (12). In order to improve the efficiency of CAP, helium (He), argon (Ar), nitrogen (N_2), oxygen (O_2), artificial air, and two or more mixtures of these gases can be utilized to generate CAP (14). It is documented that reactive oxygen species (ROS) (15) or reactive nitrogen species (RNS) (16), play an essential role in CAP application in dermatology. **Figure 2** has shown the interconverting ROS and RNS that could be classified into short-lived and long-lived species, such as singlet oxygen ($^1O_2$), superoxide anions (O_2^-), hydroxyl radicals ($^{\bullet}OH$), hydrogen peroxide (H_2O_2), nitric oxide (NO), peroxynitrite ($ONOO^-$), nitrite (HNO_2/NO_2^-) and nitrate (HNO_3/NO_3^-). $^1O_2$ is a highly reactive molecule that participates in apoptosis processes and produces some oxidants and cytotoxic molecules. O_2^- has relatively high reactivity and results in oxidative stress in cells to generate hydroxyl radicals. It is displayed that $^{\bullet}OH$ belongs to extremely reactive oxidizing

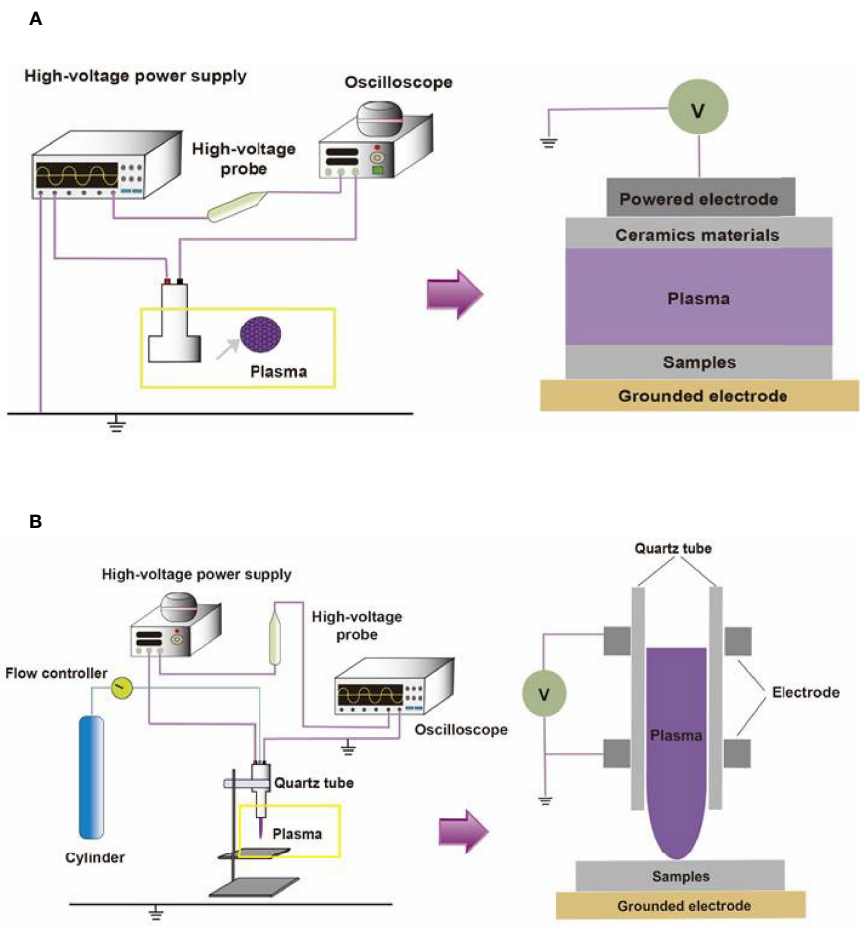

FIGURE 1 | The compositions of two different CAP platforms. **(A)** The surface barrier discharges or **(B)** the atmospheric pressure plasma jet consists of a high-voltage source, high-voltage probe, oscilloscope, quartz tube, cylinder, and flow controller.

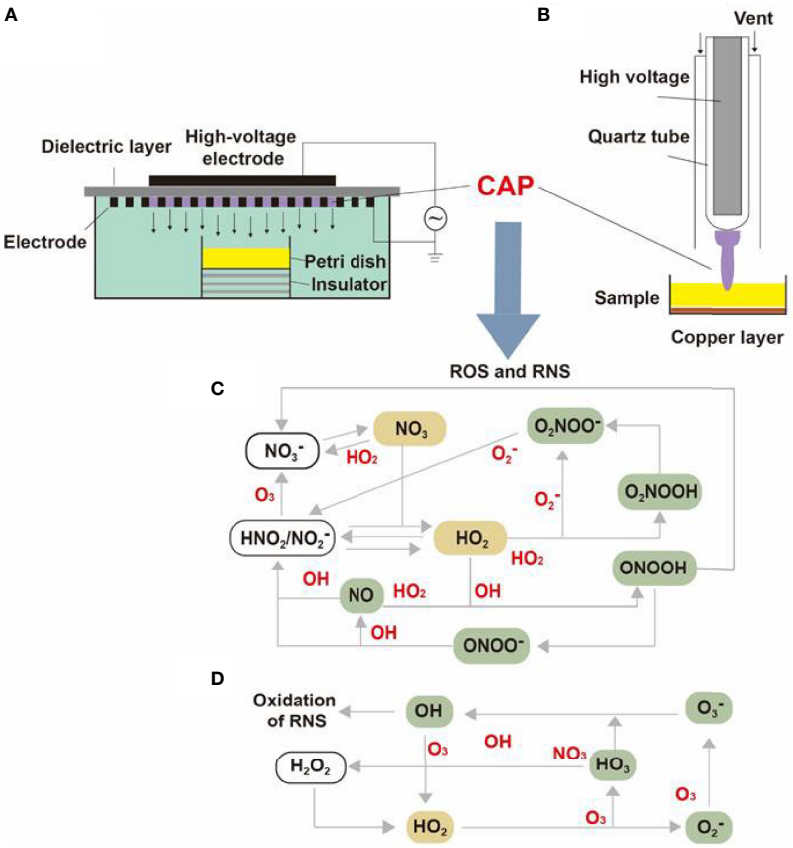

FIGURE 2 | The internal structure of surface DBD and APPJ and the transformation of CAP particles. The internal structures of **(A)** surface DBD and **(B)** APPJ were consisted of electrodes, high-voltage probes, quartz tubes, and a dielectric layer. The **(C)** RNS and **(D)** RNS generated under high voltage could be converted into different molecules or ions and finally synthesized into effective particles like $^1O_2$, $ONOO^-$, NO_2^-, NO_3^-, and H_2O_2.

species, which can damage the lipid peroxidation, protein, membrane and result in cell death. As for $ONOO^-$, it reacted with H_2O_2 to generate $^1O_2$, which inhibited the catalase activity of tumor cells, resulting in the accumulation of H_2O_2 in the part of the peripheral environment. Then H_2O_2 entered tumor cells through aquaporin on the cell surface and consumed internal glutathione, which could promote the apoptosis of tumor cells *via* lipid peroxidation (17, 18). Besides, as a long-lived species and second messenger for signaling cascades, H_2O_2 can inhibit the activity of microbes and kill them directly (19). It has been documented that CAP-induced changes in target cells are often closely related to intervention time, voltage, and other factors. For example, CAP could induce cell cycle arrest, senescence, and autophagy at low doses, but high doses of CAP could lead to irreversible cell necrosis (20). Moreover, RNS has been confirmed to regulate cell differentiation, self-renewal, and the balance between quiescence and proliferation (21). The occurrence and development of tumors can be influenced by NO concentration, which can accelerate tumor growth in the low-level concentration but inhibit it at high levels (22). The typical functions of ROS and RNS have been presented in **Figure 3**.

ROS AND RNS INACTIVATED MICROORGANISMS BY DESTROYING CELL BIOFILMS AND COMPONENTS

It is well displayed that CAP has shown promising effects in inactivating microorganisms (**Figure 4**). CAP can inhibit the proliferation of microorganisms on the surface of medical devices but prohibit the infection of various microorganisms, including *Staphylococcus aureus*, *Streptococcus pyogenes*, *Pseudomonas aeruginosa*, *Yersinia enterocolitica*, MRSA, and MRGN (8, 23, 24). In addition, related studies have reported that CAP has satisfactory efficacy in treating the pathogens of infectious skin diseases, such as *Trichophyton rubrum*, *Mycobacterium canis*, and *Candida albicans* (**Table 1**) (8, 25). In this section, we will explore the inactivation mechanisms of CAP against bacteria, fungi, and viruses, respectively.

Bacteria

Generally speaking, bacterial biofilms have widely existed on the surfaces of various foods, medical devices, and human tissues or organs under pathological conditions. Due to the widespread use

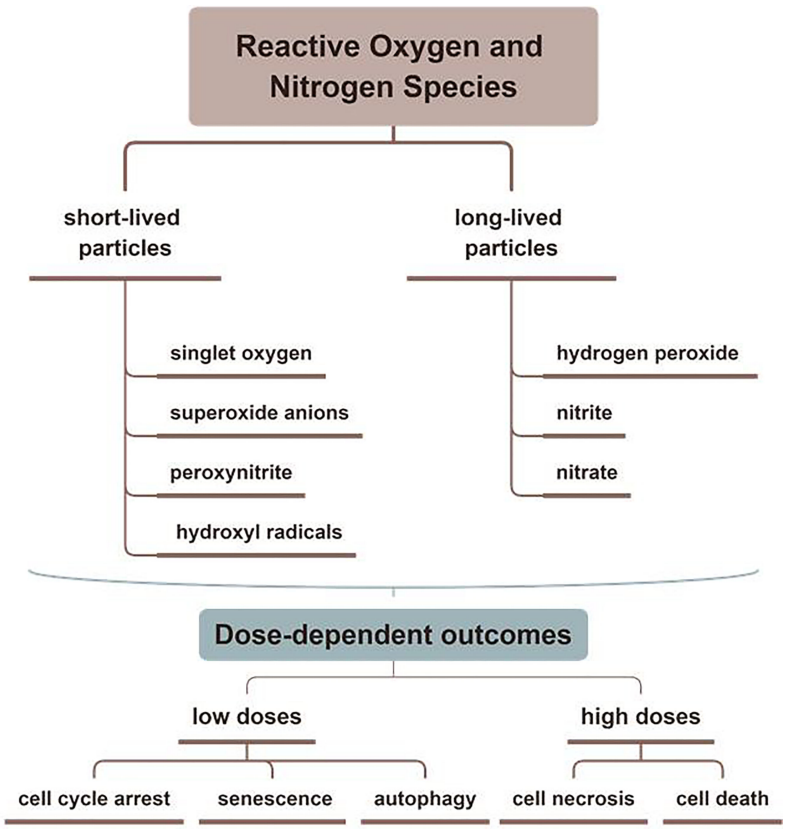

FIGURE 3 | The typical functions of ROS and RNS in CAP. Various kinds of effective particles, including ROS and RNS, are divided into short-lived or long-lived substances, which display different mechanisms in treating skin diseases by CAP.

of antibiotics, opportunistic pathogen infections caused by bacterial biofilms have gradually increased. Once a biofilm is formed, the organism will resist the action of antibiotics, making it difficult for antibiotics to remove bacterial biofilms or kill isolated bacteria on the organism's surface. Due to its anti-biofilm properties, CAP has been widely used in sterilization (26, 27). First, CAP can accelerate the death of bacteria *via* wrecking bacterial biofilms. Theinkom used SMD to treat Enterococcus faecalis to investigate the potential effects of CAP on microbial biofilms with 3.5 kV, 4.0 kHz, and 0.5-1 W/cm^2. And the results showed that CAP treatment for 1 minute could inactivate bacterial biofilms and cause bacterial death directly. Moreover, a 10-min CAP intervention showed higher inactivating efficiency than a 5-min intervention (28). Utilizing a DBD with helium gas, Govaert treated the biofilms of *L. monochromous* and *S. typhimurium* for different minutes to explore the sterilization effects and mechanisms of CAP application by detecting the density of remaining cells (29). Scientists have confirmed the inactivating effects of CAP on bacterial biofilms formed by bacteria, such as *S. bacteria*, *P. aeruginosa*, *K. pneumoniae*, *E. faecalis*, *S. aureus*, *L. monochromous*, and *P. fluorescens* (30–33). Guo and her teams utilized a 6-min CAP intervention to treat *S. aureus* to explore the mechanisms of CAP inactivating microbial biofilms. Their results showed that ROS or RNS from CAP could result in biofilm lysis and bacterial death by promoting the oxidative modification of bacterial nucleoproteins, accelerating the filamentous temperature-sensitive Z of *S. aureus* (SaFtsZ) to lose its assembly ability, and disrupting the activity of ATP-dependent caseinolytic protease P subunit of *S. aureus* (SaClpP) (34). In conclusion, CAP can expand the ROS/RNS binding area, enhance the oxidative modification of cellular proteins and promote the fusion of microbial biofilms with extracellular matrix components, which triggers the degradation of microbial biofilms and inhibits the proliferation of microorganisms.

Second, the changes in cell composition and microenvironment also affect bacterial inactivation. After DBD treatment, Helmke confirmed that the extracellular environment of bacteria was significantly acidified, and the cell membrane of bacteria gradually collapsed. After a while, the cell membrane of bacteria was destroyed, and its DNA was rapidly broken down (11). The destruction of bacterial DNA is the cause of bacterial inactivation, but the modification of bacterial proteins is considered a significant cause of bacterial inactivation. After DBD treatment, Helmke confirmed that the extracellular environment of bacteria was significantly acidified, and the cell membrane of bacteria gradually collapsed. After a while, the cell membrane of bacteria was

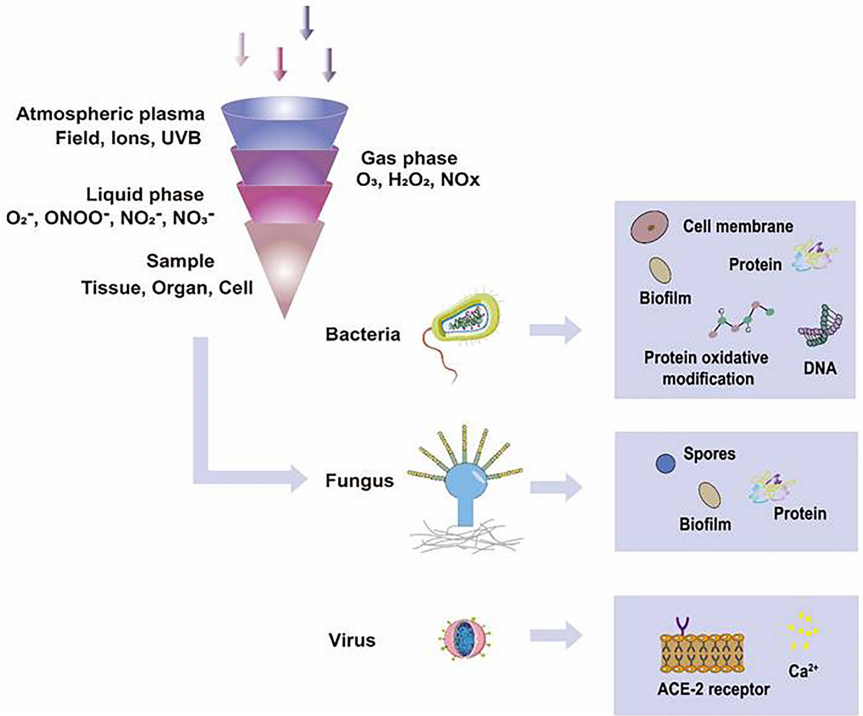

FIGURE 4 | The functions of CAP on microorganisms. In different gas or liquid media, CAP could produce different ROS and RNS, such as $^1O_2$, $ONOO^-$, NO_2^-, NO_3^-, and H_2O_2, which inactivated microorganisms effectively. The possible mechanisms that CAP applied in inactivating organic samples included destroying biofilms, damaging cell membranes, degrading DNA, RNA, and proteins, changing the chemical modification of proteins, and directly leading to the death of microorganisms.

destroyed, and its DNA was rapidly broken down (11). Although the exact type of DNA damage has not been identified, it is well documented that ROS and RNS from CAP can destroy bacterial DNA directly (35, 36). The destruction of bacterial DNA is the cause of bacterial inactivation, but the modification of bacterial proteins is also considered a significant cause of bacterial inactivation. Dezest's study aimed to explore the interactions between active substances from CAP and the activity and proliferation of E. coli. Their results demonstrated that CAP could produce bacterial inactivation through selective carbonylation of proteins (37). Of course, CAP can also produce the interaction of DNA and proteins to inactivate bacteria. Guo, with her faculties, indicated that the CAP could generate DNA and protein crosslinking (DPC) *in vitro*. They used a DBD device to intervene in E. coli with the gas mixture of helium and artificial air. By analysis of mass spectrometry and hydroperoxide, the results indicated that the formation of DPC caused by $^1O_2$ from CAP was the principal mechanism of DNA damage (7). In addition, other studies also documented that the shape of bacteria and the thickness of the bacterial cell wall might also be relevant to the CAP inactivation of bacteria (38–40). Taken together, CAP could inhibit bacterial infection by attacking the bacterial biofilms, destroying the integrity of the cell membrane, and inducing the selective carbonylation protein, DNA degradation, and protein crosslinking. The phenomenon could be explained by the mutual transformation and synergy of the ROS/RNS by CAP. The inactivation of CAP for the main pathogenic bacteria in the skin has been shown in **Table 2**.

Fungus and Virus

A series of chemical processes based on ROS and RNS have been considered the main reason for the destruction of fungal biofilm (40). Fricke, with his faculties, confirmed that the biofilm of C. albicans could be wrecked by CAP (41). Heinlin et al. used CAP application to assess its efficacy against the dermatophytes such as *T. rubrum* and *M. canis in vitro*. The fungal growth was then measured after CAP treatment. The results proved that CAP exhibited efficient effects on the decontamination of *T. rubrum* and *M. canis* (42). Ouf et al. used CAP to treat five types of skin fungus- *E. floccosum*, *M. canis*, *M. gypseum*, and *T. rubrum*. They found that the fungal cell wall had been damaged under the scanning electron microscope, which indicated that CAP exhibited therapeutic effects in inhibiting fungal growth. Furthermore, they also indicated that the CAP could ameliorate symptoms of fungal skin diseases by the generation of NO, which could inhibit the activity of fungal spores *via* reducing the activity of keratinase and increasing the mycelium permeability (43). Generally speaking, ROS and RNS from CAP could destroy fungal spores and the integrity of cell membrane to inhibit the growth of fungus.

TABLE 1 | The mechanisms of CAP for inactivating pathogens.

Bacteria	**Time**	**Device**	**Gas**	**Target**
E. faecalis	2019	DBD	O_2	Biofilm
L. monochromous	2019	DBD	He	Biofilm
S. typhimurium	2019	DBD	He	Biofilm
S. bacteria	2014	APPJ	Air	Biofilm
P. aeruginosa	2014	APPJ	Air	Biofilm
K. pneumonia	2014	APPJ	Air	Biofilm
S. aureus	2014	APPJ	He	Biofilm
	2012	DBD	Air	Membrane
P. fluorescens	2014	APPJ	He	Biofilm Membrane
	2012	DBD	Air	
S. epidermidis	2011	DBD	Air	Biofilm
				DNA
E. coli	2018	DBD	He + air	Protein
	2017	APPJ	He + O_2	DNA
				DPC
Fungus	**Time**	**Device**	**Gas**	**Target**
C. albicans	2012	APPJ	Argon	Biofilm
			Argon + O_2	
T. rubrum	2013	DBD	Air	Biofilm
M. canis	2015	APPJ	Air	Biofilm
	2013	DBD	Air	Protein
				Spores
E. floccosum	2015	APPJ	Air	Protein
				Spores
M. gypseum	2015	APPJ	Air	Protein
				Spores
Visus	**Time**	**Device**	**Gas**	**Target**
hAV	2018	DBD	Argon	Protein
				DNA
COVID-19	2021	APPJ	He	Ca^{2+}
	2022	APPJ	Argon	ACE2

E. faecalis, Enterococcus faecalis; L. monochromous, Listeria monochromous; S. typhimurium, Salmonella typhimurium; S. bacteria, Salmonella bacteria; P. aeruginosa, Pseudomonas aeruginosa; K. pneumonia, Klebsiella pneumonia; S. aureus, Staphylococcus aureus; P. fluorescens, Pseudomonas fluorescens; S.epidermidis, Staphylococcus epidermidis; E. coli, Escherichia coli; DPC, DNA and protein crosslinking; C. albicans, Candida albicans; T. rubrum, Trichophyton rubrum; M. canis, Microsporum canis; E. floccosum, Epidermophyton floccosum; M. gypseum, Microsporum gypseum; hAV, Human adenovirus; COVID-19, coronavirus disease-19; ACE2, angiotensin-converting enzyme 2; DBD, dielectric barrier discharge; APPJ, atmospheric pressure plasma jet.

TABLE 2 | The inactivation of CAP for the main skin pathogenic microorganisms.

Microorganism	**Skin disease**	**Skin lesion**	**Device**	**Target**
S. aureus	Impetigo	VesiclesBullousBlisters	APPJDBD	Biofilm
C. albicans	Tinea	ItchyWhite PlaquesErythema	APPJ	Biofilm
T. rubrum	Tinea capitis, Tinea corporis, Tinea manus	ErythemaScalyItchy	DBD	Biofilm
M. canis	Tinea capitis, Tinea corporis, Tinea manus	ErythemaScalyItchy	APPJDBD	Biofilm Protein Spores
M. gypseum	Tinea capitis, Tinea manus	ErythemaScalyItchy	APPJ	Protein Spores

Staphylococcus aureus, S. aureus; Candida albicans, C. albicans; Trichophyton rubrum, T. rubrum; Microsporum canis, M. canis; Microsporum gypseum, M. gypseum; DBD, dielectric barrier discharge; APPJ, atmospheric pressure plasma jet.

Initially, research on whether CAP could effectively inactivate human pathogenic virus was mainly based on the studies conducted in different phage models (8). Yasuda et al. studied the effects of CAP treatment on λ phage. They utilized the DBD device to treat λ phage for 20 seconds. Then they found that due to the rapid denaturation of its protein, the virus was inactivated totally. Their study noted that CAP inactivated viral proteins through denaturation or chemical/physical modification (44). Aboubakr et al. supported that the degradation of viral capsid protein might be the primary mechanism by which CAP caused viral inactivation. Their study showed that CAP treatment for 2 min could wreck the capsid protein (45). From the studies mentioned above, the degradation of viral protein could be the responsible mechanism for CAP-dependent virus inactivation. Compared with protein degradation, was the mechanism by which CAP inactivated viruses included the destruction of viral DNA or RNA by CAP? Guo utilized CAP to treat water-containing bacteriophages T4, Φ174, and MS2. According to the analysis of the genetic materials of bacteriophages, CAP could destroy both their nucleic acids and proteins *via* $^1O_2$ (46). Besides the viral protein and DNA/RNA, the unique structure "envelope" should also be considered as the third potential mechanism. CAP is more conducive to suppressing non-

enveloped viruses (47). HAV is a kind of non-enveloped dsDNA virus. Zimmermann et al. studied the inactivating effect of CAP on HAV. After CAP treatment for 240 seconds, they found that the virus was inactivated efficiently. Moreover, before infecting CMS-5 cells, HAV, eGFP, and firefly luciferase, were treated by CAP. The results showed that the infectivity and replication of HAV were inhibited directly. They believed that the effect of inactivating HAV was mainly due to the RNS from CAP, which could destroy viral proteins and DNA (48). Virus infection of eukaryotic cells was complicated, including multiple signaling mechanisms inside and outside (49). The COVID-19 virus has spread worldwide in the past two years, and people's health is facing a considerable threat (50). To explore the interaction between CAP and COVID-19 virus, we selected surface discharge plasma to inactivate the COVID-19 pseudovirus. We utilized CAP with 8.36 kV, 23 kHz, and 0.25 W/cm^2 to treat deionized water to generate solutions including ROS and RNS. Then a COVID-19 pseudovirus incorporated with SARS-CoV-2S protein was recognized as the virus model. The results showed that the short-lived species from CAP-activated deionized water, such as $ONOO^-$ and O_2^-, could modify the amino acids in proteins, inactivate S protein and prevent the binding between receptor-binding domain and angiotensin-converting enzyme 2 (ACE2) to achieve the disinfection of COVID-19 virus (25). As we all know, developing a new coronavirus vaccine is crucial in helping humans defend against the inflammatory outbreak caused by kinds of viruses. A recent article demonstrated that CAP could promote ROS accumulation in host cells, leading to the lipid peroxidation of the cell membrane, increasing the influx of Ca^{2+}, and activating selective autophagy. The phenomenon caused by CAP would accelerate the entry of host cells into G1 and stop at the G2/M stage to increase the nutrients for viral multiplication, which was conducive to the development of new vaccines and clinical treatments (51). Furthermore, although vaccines that treat SARS-CoV-2 have been produced, the continuous mutation of SARS-CoV-2 may reduce the specificity of the vaccines. Dai, with his faculties, explored the effect of CAP on mutant SARS-CoV-2 viruses. Their results confirmed that the interaction of $^{\bullet}OH$ and other substances produced by CAP or CAP-activated medium (PAM) could trigger the nuclear translocation of the viral receptor ACE2 and inhibit the SARS-CoV-2 virus to invasive host cells (52). Due to the different complexity of virus particles, viruses infect host cells through a series of strategies, resulting in physical interactions between host cells and viruses. The ROS and RNS produced by CAP can promote the inactivation of the viruses by destroying the virus envelope, degrading their DNA or protein, and modifying the protein binding site.

ROS AND RNS ACCELERATED WOUND HEALING *VIA* CELLS' PROLIFERATION, GROWTH FACTORS' SECRETION, AND VESSELS' GENERATION

Recent studies have demonstrated that CAP can promote wound healing by regulating cell viability, proliferation, migration, and inflammatory reaction (53–55). As a secondary messenger, H_2O_2 could drive redox signaling pathways and participate in the steady-state, inflammation, proliferation, and remodeling stages of wound healing (56). In addition, ROS and RNS also acted as the mediator of various cellular reactions, affecting cell differentiation, cell apoptosis, cell structure, and the structural integrity of connective tissue (57–60). Shome used a co-culture model to study the effect of CAP on wound healing and paracrine crosstalk between keratinocytes and fibroblasts *in vitro*. They observed that CAP treatment resulted in the up-regulation of the HIPPO transcription factor YAP in HaCaT and fibroblasts. As downstream effectors of the HIPPO signaling pathway, CTGF and Cyr61 were also up-regulated in their studies (56). In conclusion, their results confirmed that at the beginning of wound healing, CAP activated regeneration signaling pathways and stimulated communication between skin fibroblasts and keratinocytes, which promoted the healing of keratinocyte wounds co-culture model *in vitro*.

Schmidt et al. utilized the APPJ with Ar working gas to treat female mouse wound models for 20 seconds daily. Over 14 days, compared with the control group, the CAP group significantly accelerated the wound's epithelial regeneration from day three to nine by quantitative analysis. They demonstrated that CAP could stimulate the migration of keratinocytes and fibroblasts *in vitro*, which resulted in the accelerated closure of gaps in scratch assays. The cause of this effect was related to the down-regulation of the gap junctional protein Cx43 mentioned above. Due to the down-regulation of E- cadherin, several integrins, and actin reorganization after CAP application, they confirmed that CAP could induce changes in adhesion junctions and cytoskeleton dynamics to accelerate wound healing (61). Lin utilized a DBD device with helium gas to treat the wound on the mice's skin at 66 kHz and 6.0 kV. They found that galectin-1, as a β-galactose-binding lectin, was involved in many physiological functions to induce myofibroblast activation, which wound secret growth factors and chemoattractants to create new substrates and proteins in the extracellular matrix in wound healing. It was reported that galectin-1 accelerated wound healing by regulating the theneuropilin-1/Smad3/NOX4 pathway and ROS production in myofibroblasts (62). They examined the efficacy of low-temperature plasma on galectin expression in the skin using immunoelectron microscopy and found that the galectins increased quickly after the low-temperature plasma treatment and accelerated wound healing through the Smad pathway (6). Besides, CAP could increase the generation of fibroblasts and inner wall cells of blood vessels in wounds. The effect resulted from the link to the activity of some proteins, such as the vascular-associated migration cell protein (AAMP). CAP could strongly up-regulate the expression of the gene encoding AAMP, which could drive the RhoA–ROCK and Nod2–NF-κB signaling pathway to accelerate cell movement and promote wound healing (63). In summary, as **Figure 5** displayed, CAP promoted wound healing by enhancing the proliferation of keratinocytes, up-regulating the expression of cell growth-related genes, strengthening the release of cytokines, inhibiting wound microbial infection, and inducing the formation of blood vessels.

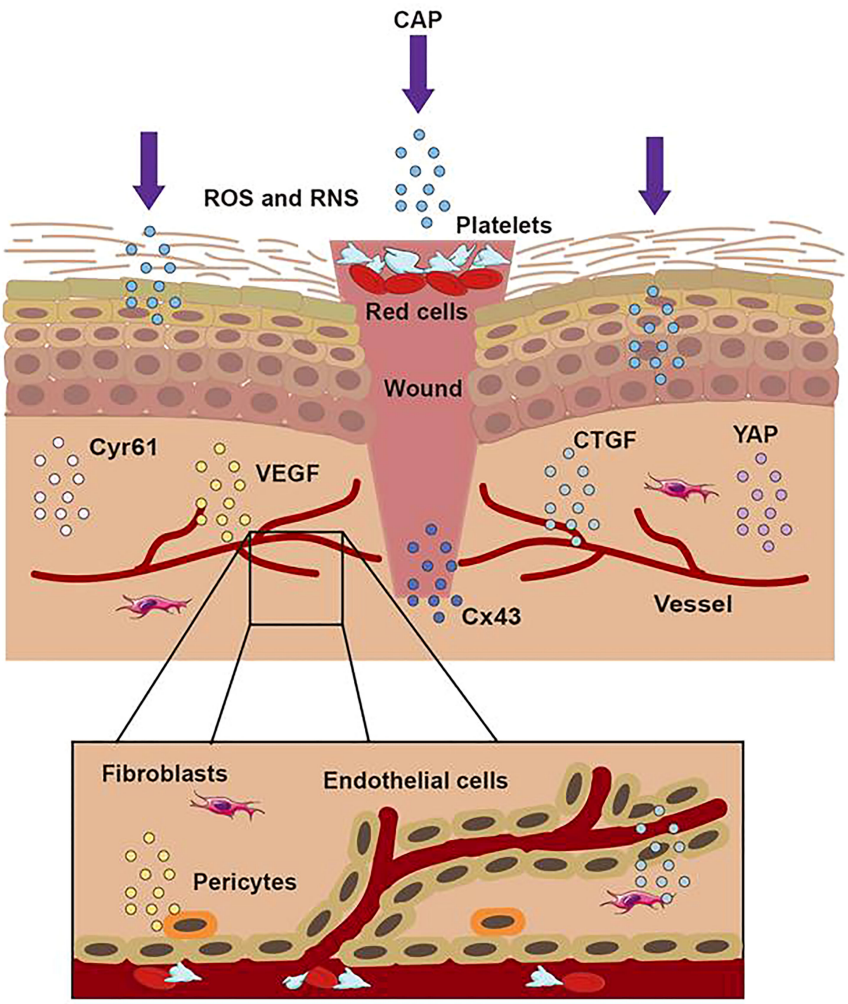

FIGURE 5 | The treatment of CAP on wound. When the skin was hurt, the first step was to form a blood scab to protect the wound. CAP could accomplish wound healing through short-lived and long-lived ROS and RNS. CAP could promote the formation of new blood vessels, strengthen the release of CTGF and VEGF, activate the activation of the YAP pathway, and upregulate the expression of Cx43 and Cyr61.

ROS AND RNS ATTENUATED NCISDS *VIA* KERATINOCYTES' APOPTOSIS, IMMUNE REGULATION, AND ANTIOXIDANT SYSTEMS' ACCELERATING

According to the lesions and pathological changes of skin diseases, ncISDs include nearly 100 different immune diseases caused by immune cells. For example, Th17 and ILC3 cells can lead to psoriasis characterized by neutrophil infiltration. Th2 cell can lead to eczema characterized by the abnormal infiltration of eosinophils. As for vitiligo, the CD8+T cell is critical, resulting in the high secretion of CXCL10, IFN-γ, and IL-17. These diseases have seriously affected the quality of patients' lives and caused enormous socio-economic costs. Due to the genetic susceptibility of the body and the influence of the peripheral environments, ncISDs often lead to impaired epithelial function and pathological changes, including immune cell infiltration (64).

As a kind of complex hyperproliferative skin disease, psoriasis is an autoimmune disease. The typical clinical features are characterized by erythema, plaques, and scaly (65). In addition, excessive proliferation of keratinocytes, inflammation, infiltration, and pathological angiogenesis has been regarded as the typical pathological changes of psoriasis (66, 67). Our team used a DBD device with 0.06 W/cm^2 to treat keratinocytes and evaluated the initial treatment effect of CAP on psoriasis by observing the death of keratinocytes and the release of related cytokines. We placed a petri dish containing HaCaT cells 10 mm below the surface DBD device. Then we explored the therapeutic effects of CAP on psoriasis by detecting the concentrations of

ROS and RNS, observing the morphology, the viability, the apoptosis of keratinocytes, and the secretion of different cytokines, which played an essential role in the pathogenesis in psoriasis. From the results, we confirmed that CAP could suppress psoriasis. The main mechanisms of the results were exhibited: producing keratinocyte apoptosis, inhibiting excessive proliferation of keratinocyte and T lymphocytes, up-regulating the expression of IFN-γ and the mRNA of VEGF, increasing IL-6, IL-8, TNF-α, and VEGF release and decreasing the content of IL-12 (68). Lu et al. used cell and animal experiments to confirm CAP's therapeutic function in psoriasis. They chose an APPJ device that flushed into helium and oxygen working gas with 15 kV and 1 kHz. Firstly, the cell model of psoriasis-like inflammation was simulated by adding LPS or TNF-α into HaCaT keratinocytes and then using a CAP-treated medium to cultivate HaCaT cells. Secondly, APPJ was directly applied to imiquimod-induced psoriasis-like dermatitis in mice. They observed that CAP increased ROS in HaCaT keratinocytes and caused keratinocyte apoptosis. Moreover, it was interesting that the IMQ-induced psoriasiform dermatitis gradually ameliorated lesions that displayed weakened epidermal proliferation and performed a thinner epidermal layer after APPJ treatment (69). Lee et al. indicated that CAP treatment might suppress psoriasis-like lesions in mice. Compared with the mice without CAP treatment, increasing epithelial thickness and the expression of pro-inflammatory molecules were inhibited in the skin of psoriasis-like mice treated with CAP. It has been well accepted that the expression of PD-L1 was relevant to the excessive activation of T cells. To their surprise, CAP could inhibit excessive activation of T cells *via* increasing PD-L1 expression in HaCaT cells (70). ROS and RNS from CAP could inhibit the excessive proliferation of keratinocytes and promote their apoptosis but restrain the proliferation of T lymphocytes and enhance the expression of PD-L1 protein, which was negatively correlated with the T lymphocytes' proliferation. Moreover, ROS and RNS could also directly regulate the release of inflammatory factors such as IL-6, IL-12, and VEGF in lesions to achieve the effects of alleviating psoriasis.

Vitiligo is the most frequent cause of depigmentation globally (71). Its standard treatment methods make vitiligo treatment challenging, owing to side effects, low cure, and high recurrence rates (72). Our team recently conducted experiments on CAP to treat vitiligo *in vitro* and *in vivo*. We used APPJ and DBD generating devices to treat vitiligo-like mice and patients with active focal vitiligo up to one month. With 8 kV and 9 kHz, CAP showed satisfactory efficiency in attenuating vitiligo. We used CAP-activated hydrogel and APPJ device to observe the interaction between CAP and vitiligo. From the vitiligo-like mouse, we documented that CAP could ameliorate vitiligo lesions and accelerate the distribution of follicular melanin. Furthermore, we confirmed that CAP could inhibit the infiltration of immune cells such as $CD8^+$T cells, $CD3^+$ cells, and $CD11c^+$ cells, decrease the secretion of immune cytokines, and strengthen the responsibility of anti-oxidative systems. Moreover, we also observed the same changes in active focal vitiligo patients in the clinical trial without any side effects. In conclusion, we thought that CAP could inhibit the excessive activation of immune cells, restrain the release of inflammatory chemokines, induce the expression of Nrf2 and weaken the inducible nitric oxide synthase activity to attenuate vitiligo (73). From these studies, we considered that CAP ameliorated vitiligo by producing the generation of follicular melanocytes, inhibiting the excessive infiltration of immune cells, restraining the release of inflammatory cytokines, and regulating the activity of oxidative or anti-oxidative systems (**Figure 6**). As we all know, ncISDs are chronic and T-cell-associated inflammatory skin diseases. For psoriasis, with the characteristics of thickening and scaling, its pathogenesis was considered the proliferation of keratinocytes, infiltration of inflammatory or immune cells, and form of vessels. As for vitiligo, it involved oxidative stress pathways, immune inflammation, and the destruction of melanocytes. It could be known from the above documents that CAP attenuated ncISDs by promoting the apoptosis of keratinocytes, inhibiting the proliferation of keratinocytes, restraining excessive immune responses, regulating inflammatory cytokines, and reinforcing antioxidant systems.

ROS AND RNS INHIBITED CANCER *VIA* PRODUCING CELL APOPTOSIS, INCREASING CYTOKINES RELEASE, AND ACTIVATING THE DIFFERENT PATHWAYS

Recent studies have suggested that researchers have concluded that the primary mechanism of CAP's anti-cancer treatment might be related to the generation of ROS and RNS (74, 75). Free radicals, especially ROS and RNS, had been reported as the common mediator of apoptosis. ROS, RNS, and charged particles have been determined to be significant contributors to plasma-induced cell death (76). The excessive generation of ROS and RNS might damage cellular components, including DNA, proteins, and lipid membranes. However, most apoptosis pathways observed in CAP-treated cancer cells mainly depend on the injury of significant protein and DNA or the damage to the cell microenvironment.

Melanoma is considered as a highly invasive cancer that is highly resistant to most traditional chemotherapy and radiation therapies (77). Previous studies had provided several possible mechanisms by which CAP inactivated cancer cells, including ROS and RNS, charged particles, heat, pressure gradients, and changes in electrostatic and electromagnetic fields. In Keidar's study, CAP had been translated into *in vivo* models of tumor treatment. From the results, they found that the mid-sized tumors in nude mice ameliorated after 2-min CAP treatment without any thermal damage (78). Chernets et al. utilized CAP application to treat melanoma in a mouse model, and the results confirmed that CAP could prohibit the activity and proliferation of melanoma. Their study showed that ROS, RNS, and its radicals from CAP created a chemistry response for eliminating subdermal B16 melanoma. They also indicated that the heat from CAP was insufficient to prohibit melanoma

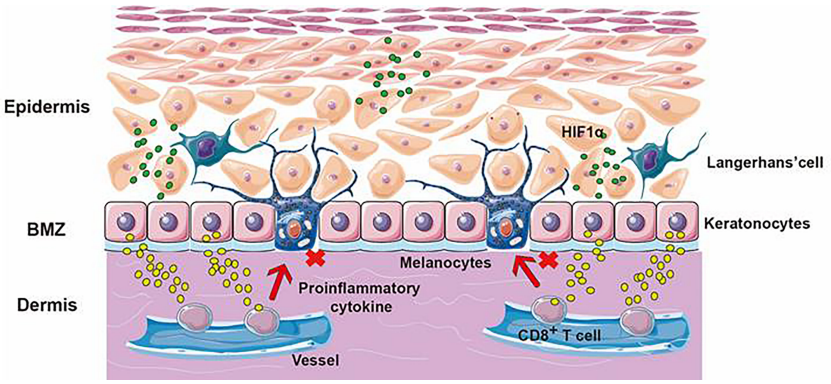

FIGURE 6 | The application of CAP application on vitiligo. The skin is divided into the epidermis, dermis, and subcutaneous tissue layers. Vitiligo results from the targeted destruction of melanocytes. ROS and RNS from CAP could promote the release of HIF-1α, cause keratinocytes to release cytokines, inhibit the cytotoxicity of $CD8^+$T cells and avoid the targeted destruction of melanocytes.

proliferation without the presence of reactive species (79). Ishaq et al. showed that CAP caused melanoma cells to over-expression TP73, which will lead to growth arrest and apoptosis (80). Ardnt et al. discovered that CAP treatment for 2 seconds could lead to irreversible cell cycle arrest, induction of phosphor-H2AX, and DNA damage (81, 82). In addition, Schneider et al. analyzed intracellular Ca^{2+} indicator fura-2 AM to analyze changes in cytoplasmic Ca^{2+} levels after CAP treatment of malignant melanoma cells. The results showed that CAP caused the acidification of water and solution, and the influx of Ca^{2+} in melanoma cells induced by CAP was enhanced in an acidic environment. Besides, NO induced by CAP was dose- and pH-dependent, and CAP-treated solutions could cause protein nitrification in cells under acidic conditions. Therefore, they believed that the decrease in pH caused by CAP treatment inhibited tumor cells' proliferation and growth. The possible mechanism was that the synergistic effect of ROS, RNS, and acidic conditions produced by CAP affected the intracellular Ca^{2+} level of melanoma cells. Since the microenvironment of tumors was usually acidic, further acidification may be one reason for the specific anti-cancer effect of CAP (10). These results might indicate that CAP shared some similarities in their mechanism of action, possibly by causing ROS-dependent DNA or protein damage in melanoma. Of course, acidifying the microenvironment of tumor cells and enhancing the influx of Ca^{2+} to tumor cells could also cause the death of tumors.

Non-melanoma skin tumor primarily includes basal cell and squamous cell carcinoma. Basal cell carcinoma (BCC), most common in the head and neck region, is the most common form of skin tumor and 3 to 5 times more common than squamous cell carcinoma. Squamous cell carcinoma mainly occurs in the head and neck region and is more common in older men (83). Recently, Wang studied the effects and the related mechanisms of CAP-activated medium on cutaneous squamous carcinoma cells (SCC). They selected A431 epidermoid carcinoma cell lines and a CAP-activated PBS medium to incubate the A431 cells for 2 hours. Their results showed that the CAP-activated PBS medium could increase the intracellular ROS levels and inhibit the proliferation of A431 cells in a dose/time-dependent manner. At the same time, the CAP-activated PBS medium could lead to the apoptosis of A431 cells (84). Yang's study aimed to explore the effects and related mechanisms of two CAP-activated solutions on TE354T cell and HaCaT keratinocyte cell lines. PAS was prepared by CAP irradiation of DMEM and PBS. Then they treated TE354T cells with PAS *in vitro* and evaluated the viability and apoptosis rate of TE354T cells and HaCaT cells. Western blotting and RNA sequencing were also detected. The results showed that CAP-activated PAS solution strengthened the apoptosis signaling in BCC, and the mechanisms were related to the activation of the different signaling pathways (85).

Besides the skin tumors mentioned above, CAP has shown remarkable effects on other kinds of tumors, such as the triple-negative breast cancers through hsa_circRNA_0040462 (86–88), glioblastoma multiforme (89), lung cancers (90), and pancreatic ductal adenocarcinoma (91). Recent studies confirmed that invivopen, a new source of CAP for cancer therapy, could ameliorate triple-negative breast cancer successfully. They found that CAP or PAM could inhibit the proliferation of triple-negative breast cancer, which showed a more significant inactivation on mesenchymal breast cancer than epithelial-derived breast cancer. Surprisingly, the above results also applied to the CAP inactivation of mesenchymal-derived bladder cancers (92, 93). In addition, tumor recurrence is often related to the rapid proliferation of remaining tumor cells in the body. In order to solve the threat of residual tumor cells, our team developed a new type of therapeutic plasma-activated biogel that could be implanted into mice to inhibit the proliferation of residual tumor cells. With 10 kHz and 7.5 kV, CAP could transform the solution into the plasma-activated biogel containing ROS with its temperature rising to 35°C. Then the plasma-activated biogel was placed in the tissue where the tumor cells were removed, and the tumor growth on the skin of the

right-back of the mouse was monitored three times a week. The results showed that compared with other groups, the mouse in the plasma-activated biogel group was ameliorated entirely within two weeks. Moreover, the survival rate was more than six weeks, and no tumor recurrence had been seen. Through experiments, it could be known that the effect substances, such as H_2O_2, NO_2^-, NO_3^-, $ONOO^-$ and O_2^-, could be released by plasma-activated biogel would inhibit the growth and recurrence of residual tumor tissues without any side effects (94). All in all, CAP could promote tumor cell apoptosis by activating the cell culture medium, acting on tumor cells, and directly inhibiting the proliferation of tumors. It could be seen from the above findings that the increase in the concentration of ROS and RNS in tumor cells was the key to the treatment of tumors by CAP. On the one hand, ROS and RNS could damage the DNA of tumor cells and the proteins such as tumor protein 73. On the other hand, the acidification of the tumor's microenvironment and the increased concentration of Ca^{2+} in the microenvironment were also crucial in prohibiting tumor cells by CAP. In addition, the MAPK/JNK or NF-κB signaling pathway was also the main mechanism for CAP to inhibit the proliferation of tumors.

CONCLUSION

CAP has shown its apparent effects on different skin diseases such as infectious diseases, skin tumors, psoriasis, vitiligo, and wound healing. **Figure 7** has described the main mechanisms of CAP application on skin diseases. In terms of inhibiting microbial infections, with ROS and RNS, CAP destroyed biofilms or the cell membranes of microorganisms and damaged the DNA, RNA, or protein of microbes in a time or dose-dependent manner directly or indirectly; In wound healing, CAP could promote the proliferation of keratinocytes, enhance the expression of genes related to cell growth, and enhance the release of inflammatory factors. As for the ncISDs, CAP could promote the apoptosis of keratinocytes, inhibit the proliferation of keratinocytes, and suppress the excessive activation of T lymphocytes, which played a crucial role in psoriasis. CAP could also ameliorate the occurrence of vitiligo by reducing the excessive activation of the immune response and enhancing the ability of the antioxidant system. Finally, CAP could activate the apoptosis of cells, restrain the acidification of the cells' microenvironment, increase intracellular Ca^{2+}, and damage DNA to ameliorate melanoma. Last but not least, for the other tumor such as glioblastoma multiforme,

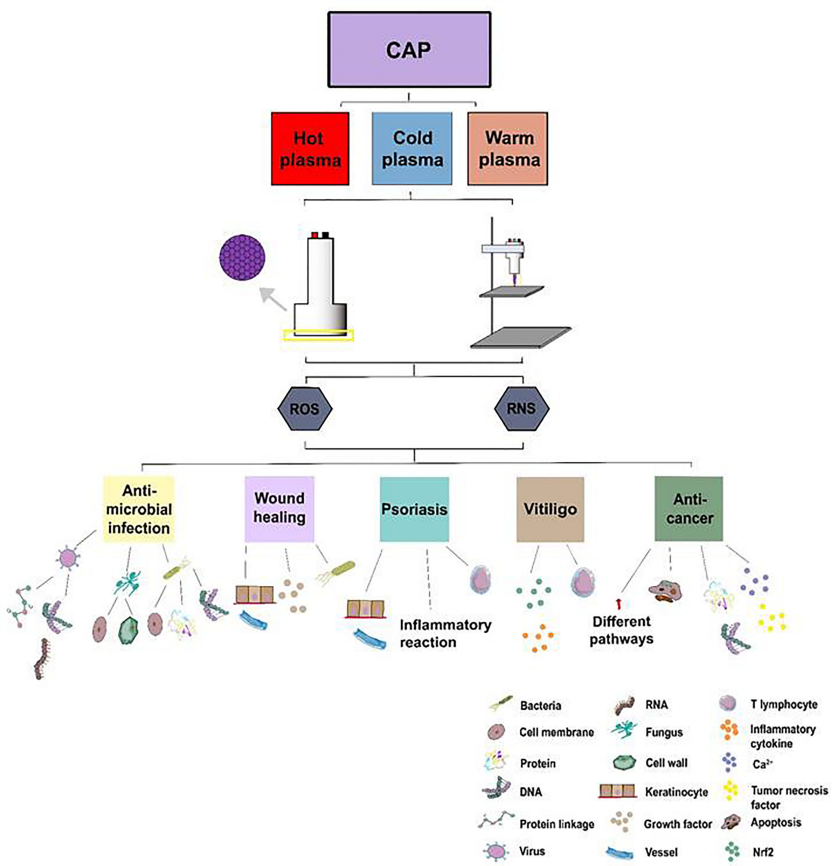

FIGURE 7 | The treatment of CAP application on skin diseases. Atmospheric plasma has been divided into hot, warm, and cold atmospheric plasma. Two main kinds of CAP generators, DBD and APPJ, have been utilized to treat skin diseases such as inactivating microorganisms, accelerating wound healing, ameliorating ncISDs, and inhibiting tumors *via* ROS and RNS from CAP.

lung cancers, and pancreatic ductal adenocarcinoma, ROS, and RNS could activate the apoptosis of the tumor and accelerate the release of the necrosis factors related to MAPK or NF-κB signaling pathways to inhibit tumors. As a new type of non-invasive physical tool, CAP has shown satisfactory results in medicine. It is believed that CAP will be applied to treat more skin diseases in the future and apply more therapeutic options for the treatment of skin diseases.

AUTHOR CONTRIBUTIONS

Y-mX and MK designed the manuscript. S-yZ wrote the manuscript. S-yZ and Y-mX created the figures. Y-mX and MK revised the manuscript. All authors contributed to the article and approved the submitted version.

ACKNOWLEDGMENTS

We thank helpful discussions with Dr. Ding-xin Liu (State Key Laboratory of Electrical Insulation and Power Equipment, Xi'an Jiaotong University). And we also thank the financial support by the National Natural Science Foundation of China (No. 82173445) and the Innovation Capability Support Plan of Shaanxi Province (No.2019TD-034).

REFERENCES

1. Lugović-Mihić L, Ćesić D, Vuković P, Novak Bilić G, Šitum M, Špoljar S. Melanoma Development: Current Knowledge on Melanoma Pathogenesis. *Acta Dermatovenerol Croat* (2019) 27:163–8.
2. Rendon A, Schäkel K. Psoriasis Pathogenesis and Treatment. *Int J Mol Sci* (2019) 23:1475. doi: 10.3390/ijms20061475
3. Wang P, Huang B, Horng H, Yeh C, Chen Y. Wound Healing. *J Chin Med Assoc* (2018) 81:94–101. doi: 10.1016/j.jcma.2017.11.002
4. Mruwat R, Cohen Y, Yedgar S. Phospholipase A_2 Inhibition as Potential Therapy for Inflammatory Skin Diseases. *Immunotherapy* (2013) 5:315–7. doi: 10.2217/imt.13.18
5. Wang B, Liu D, Zhang Z, Li Q, Wang X, Kong MG. A New Surface Discharge Source: Plasma Characteristic and Delivery of Reactive Species. *IEEE Trans Plasma Sci* (2016) 44:1–7. doi: 10.1109/TPS.2016.0620565
6. Akimoto Y, Ikehara S, Yamaguchi T, Kim J, Kawakami H, Shimizu N, et al. Galectin Expression in Healing Wounded Skin Treated With Low-Temperature Plasma: Comparison With Treatment by Electronical Coagulation. *Arch Biochem Biophys* (2016) 1:86–94. doi: 10.1016/j.abb.2016.01.012
7. Guo L, Zhao Y, Liu D, Liu Z, Chen C, Xu R, et al. Cold Atmospheric-Pressure Plasma Induces DNA-Protein Crosslinks Through Protein Oxidation. *Free Radic Res* (2018) 52:783–98. doi: 10.1080/10715762
8. Weiss M, Daeschlein G, Kramer A, Burchardt M, Brucker S, Wallwiener D, et al. Virucide Properties of Cold Atmospheric Plasma for Future Clinical Applications. *J Med Virol* (2017) 89:952–9. doi: 10.1002/jmv.24701
9. Brun P, Pathak S, Castagliuolo I, Palù G, Zuin M, Cavazzana R, et al. Helium Generated Cold Plasma Finely Regulates Activation of Human Fibroblast-Like Primary Cells. *PloS One* (2014) 9:e104397. doi: 10.1371/journal.pone.0104397
10. Schneider C, Gebhardt L, Arndt S, Karrer S, Zimmermann JL, Fischer MJM, et al. Acidification is an Essential Process of Cold Atmospheric Plasma and Promotes the Anti-Cancer Effect on Malignant Melanoma Cells. *Cancers (Basel)* (2019) 11:671. doi: 10.3390/cancers11050671
11. Helmke A, Hoffmeister D, Berge F, Emmert S, Laspe P, Mertens N, et al. Physical and Microbiological Characterisation of *Staphylococcus Epidermidis* Inactivation by Dielectric Barrier Discharge Plasma. *Plasma Process Polym* (2011) 8:278–86. doi: 10.1002/ppap201000168
12. Friedman PC. Cold Atmospheric Pressure (Physical) Plasma in Dermatology: Where are We Today? *Int J Dermatol* (2020) 59:1171–84. doi: 10.1111/ijd.15110
13. von Woedtke T, Metelmann HR, Weltmann KD. Clinical Plasma Medicine: State and Perspectives of *In Vivo* Application of Cold Atmospheric Plasma. *Contrib Plasma Physics* (2014) 54:104–17. doi: 10.1002/ctpp201300168
14. Nguyen DB, Lee WG. Effects of Ambient Gas on Cold Atmospheric Plasma Discharge in the Decomposition of Trifluoromethane. *RSC Advances* (2016) 32:26505–13. doi: 10.1039/C6RA01485B
15. Bernhardt T, Semmler ML, Schäfer M, Bekeschus S, Emmert S, Boeckmann L. Plasma Medicine: Applications of Cold Atmospheric Pressure Plasma in Dermatology. *Oxid Med Cell Longev* (2019) 3:3873928. doi: 10.1155/2019/3873928
16. Schmidt A, Wende K, Bekeschus S, Bundscherer L, Barton A, Ottmüller K, et al. Non-Thermal Plasma Treatment is Associated With Changes in Transcriptome of Human Epithelial Skin Cells. *Free Radic Res* (2013) 47:577–92. doi: 10.3109/10715762.2013.804623
17. Lukes P, Dolezalova E, Sisrova I, Clupek M. Aqueous-Phase Chemistry and Bactericidal Effects From an Air Discharge Plasma in Contact With Water: Evidence for the Formation of Peroxynitrite Through a Pseudo-Second-Order Post-Discharge Reaction of H_2O_2 and HNO_2. *Plasma Sourc Sci Technol* (2014) 23:015019. doi: 10.1088/0963-0252/23/1/015019
18. Bauer G, Sersenová D, Graves DB, Machala Z. Cold Atmospheric Plasma and Plasma-Activated Medium Trigger RONS-Based Tumor Cell Apoptosis. *Sci Rep* (2019) 9:14210. doi: 10.1038/s41598-019-50291-0
19. Mitra S, Nguyen LN, Akter M, Park G, Choi EH, Kaushik NK. Impact of ROS Generated by Chemical, Physical, and Plasma Techniques on Cancer Attenuation. *Cancers (Basel)* (2019) 11:1030. doi: 10.3390/cancers11071030
20. Dai X, Zhang Z, Zhang J, Ostrikov K. Dosing: The Key to Precision Plasma Oncology. *Processes Polymers* (2020) 10:e1900178. doi: 10.1002/ppap.201900178
21. Vlaski-Lafarge M, Ivanovic Z. Reliability of ROS and RNS Detection in Hematopoietic Stem Cells–Potential Issues With Probes and Target Cell Population. *J Cell Sci* (2015) 128:3849–60. doi: 10.1242/jcs.171496
22. Xia J, Zeng W, Xia Y, Wang B, Xu D, Liu D, et al. Cold Atmospheric Plasma Induces Apoptosis of Melanoma Cells *via* Sestrin2-Mediated Nitric Oxide Synthase Signaling. *J Biophotonics* (2019) 12:e201800046. doi: 10.1002/jbio.201800046
23. Daeschlein G, Scholz S, von Woedtke T, Niggemeier M, Kindel E, Brandenburg R, et al. *In Vitro* Killing of Clinical Fungal Strains by Low-Temperature Atmospheric Pressure Plasma Jet. *IEEE Trans Plasma Sci* (2011) 39:815–21. doi: 10.1109/tps.2010.2063441
24. Daeschlein G, Napp M, von Podewils S, Scholz S, Arnold A, Emmert S, et al. Antimicrobial Efficacy of a Historical High-Frequency Plasma Apparatus in Comparison With 2 Modern, Cold Atmospheric Pressure Plasma Devices. *Surg Innov* (2015) 22:394–400. doi: 10.1177/1553350615573584
25. Guo L, Yao Z, Yang L, Zhang H, Qi Y, Gou L, et al. Plasma-Activated Water: An Alternative Disinfectant for S Protein Inactivation to Prevent SARS-CoV-2 Infection. *Chem Eng J* (2012) 421:127742. doi: 10.1016/j.cej.2020.127742
26. Ali A, Kim YH, Lee JY, Lee SH, Uhm HS, Cho G, et al. Inactivation of Propionibacterium Acnes and its Biofilm by non-Thermal Plasma. *Curr Appl Physics* (2014) 14:S142–8. doi: 10.1016/j.cap.2013.12.034
27. Del Pozo JL. Biofilm-Related Disease. *Expert Rev Anti Infect Ther* (2018) 16:51–65. doi: 10.1080/14787210.2018.1417036
28. Theinkom F, Singer L, Cieplik F, Cantzler S, Weilemann H, Cantzler M, et al. Antibacterial Efficacy of Cold Atmospheric Plasma Against Enterococcus Faecalis Planktonic Cultures and Biofilms *In Vitro*. *PloS One* (2019) . 14: e0223925. doi: 10.1371/journal.pone.0223925
29. Govaert M, Smet C, Walsh JL, van Impe JFM. Dual-Species Model Biofilm Consisting of Listeria Monocytogenes and *Salmonella Typhimurium*: Development and Inactivation With Cold Atmospheric Plasma (CAP). *Front Microbiol* (2019) 7:2524. doi: 10.3389/fmicb.2019.02524
30. Niemira BA, Boyd G, Sites J. Cold Plasma Rapid Decontamination of Food Contact Surfaces Contaminated With Salmonella Biofilms. *J Food Sci* (2014) 79:M917–922. doi: 10.1111/1750-3841.12379

31. Modic M, McLeod NP, Sutton JM, Walsh JL. Cold Atmospheric Pressure Plasma Elimination of Clinically Important Single- and Mixed-Species Biofilms. *Int J Antimicrob Agents* (2017) 49:375–8. doi: 10.1016/j.ijantimicag.2016.11.022
32. Patange A, Boehm D, Ziuzina D, Cullen PJ, Gilmore B, Bourke P. High Voltage Atmospheric Cold Air Plasma Control of Bacterial Biofilms on Fresh Produce. *Int J Food Microbiol* (2019) 16:137–45. doi: 10.1016/j.ijfoodmicro.2019.01.005
33. Fahmide F, Ehsani P, Atyabi SM. Time-Dependent Behavior of the *Staphylococcus Aureus* Biofilm Following Exposure to Cold Atmospheric Pressure Plasma. *Iran J Basic Med Sci* (2021) 24:744–51. doi: 10.22038/Ijbms.2021.52541.11866
34. Guo L, Yang L, Qi Y, Niyazi G, Huang L, Gou L, et al. Cold Atmospheric-Pressure Plasma Caused Protein Damage in Methicillin-Resistant Cells in Biofilms. *Microorganisms* (2021) 9:1072. doi: 10.3390/microorganisms9051072
35. Colagar AH, Memariani H, Sohbatzadeh F, Omran AV. Nonthermal Atmospheric Argon Plasma Jet Effects on Escherichia Coli Biomacromolecules. *Appl Biochem Biotechnol* (2013) 171:1617–29. doi: 10.1007/s12010-013-0430-9
36. Han X, Cantrell WA, Escobara EE, Ptasinskab S. Plasmid DNA Damage Induced by Helium Atmospheric Pressure Plasma Jet. *Eur Phys J D* (2014) 68:7. doi: 10.1140/epjd/e2014-40753-y
37. Dezest M, Bulteau AL, Quinton D, Chavatte L, Bechec ML, Cambus JP, et al. Oxidative Modification and Electrochemical Inactivation of Upon Cold Atmospheric Pressure Plasma Exposure. *PloS One* (2017) 12:e0173618. doi: 10.1371/journal.pone.0173618
38. Hähnel M, von Woedtke T, Weltmann KD. Influence of the Air Humidity on the Reduction of Bacillus Spores in a Defined Environment at Atmospheric Pressure Using a Dielectric Barrier Surface Discharge. *Plasma Process Polym* (2010) 7:244–9. doi: 10.1002/ppap.200900076
39. Cahill OJ, Claro T, O'Connor N, Cafolla AA, Stevens NT, Daniels S, et al. Cold Air Plasma to Decontaminate Inanimate Surfaces of the Hospital Environment. *Appl Environ Microbiol* (2014) 80:2004–10. doi: 10.1128/AEM.03480-13
40. Joshi SG, Cooper M, Yost A, Paff M, Ercan UK, Fridman G, et al. Nonthermal Dielectric-Barrier Discharge Plasma-Induced Inactivation Involves Oxidative DNA Damage and Membrane Lipid Peroxidation in Escherichia Coli. *Antimicrob Agents Chemother* (2011) 55:1053–62. doi: 10.1128/AAC.01002-10
41. Fricke K, Koban I, Tresp H, Jablonowski L, Schroder K, Kramer A, et al. Atmospheric Pressure Plasma: A High- Performance Tool for the Efficient Removal of Biofilms. *PloS One* (2012) 7:e42539. doi: 10.1371/journal.pone.0042539
42. Heinlin J, Maisch T, Zimmermann JL, Shimizu T, Holzmann T, Simon M, et al. Contact-Free Inactivation of Trichophyton Rubrum and Microsporum Canis by Cold Atmospheric Plasma Treatment. *Future Microbiol* (2013) 8:1097–106. doi: 10.2217/fmb.13.86
43. Ouf SA, El-Adly AA, Mohamed AH. Inhibitory Effect of Silver Nanoparticles Mediated by Atmospheric Pressure Air Cold Plasma Jet Against Dermatophyte Fungi. *J Med Microbiol* (2015) 64:1151–61. doi: 10.1099/jmm.0.000133
44. Yasuda H, Miura T, Kurita H, Takashima K, Mizuno A. Biological Evaluation of DNA Damage in Bacteriophages Inactivated by Atmospheric Pressure Cold Plasma. *Plasma Process Polym* (2010) 7:301–8. doi: 10.1002/ppap.200900088
45. Aboubakr HA, Mor SK, Higgins LA, Armien A, Youssef MM, Bruggenman PJ, et al. Cold Argon-Oxygen Plasma Species Oxidize and Disintegrate Capsid Protein of Feline Calicivirus. *PloS One* (2018) 13:e0194618. doi: 10.1371/journal.pone.0194618
46. Guo L, Xu R, Gou L, Liu Z, Zhao Y, Liu D, et al. Mechanism of Virus Inactivation by Cold Atmospheric-Pressure Plasma and Plasma-Activated Water. *Appl Environ Microbiol* (2018) 84:e00726–18. doi: 10.1128/AEM.00726-18
47. Brun P, Vono M, Venier P, Tarricone E, Deligianni V, Martines E, et al. Disinfection of Ocular Cells and Tissues by Atmospheric-Pressure Cold Plasma. *PloS One* (2012) 7:e33245. doi: 10.1371/journal.pone.0033245
48. Zimmermann JL, Dumler K, Shimizu T, Morfill GE, Wolf A, Boxhammer V, et al. Effects of Cold Atmospheric Plasmas on Adenoviruses in Solution. *J Phys D Appl Phys* (2011) 44:505201. doi: 10.1088/0022-3727/44/50/505201
49. Galdiero S, Falanga A, Vitiello M, Grieco P, Caraglia M, Morelli G, et al. Exploitation of Viral Properties for Intracellular Delivery. *J Pept Sci* (2014) 20:468–78. doi: 10.1002/psc.2649
50. Xiang Y, Li W, Zhang Q, Jin Y, Rao W, Zeng L, et al. Timely Research Papers About COVID-19 in China. *Lancet* (2020) 395:684–5. doi: 10.1016/S0140-6736(20)30375-5
51. Miao Y, Han P, Hua D, Zhou R, Guan Z, Lv Q, et al. Cold Atmospheric Plasma Increases IBRV Titer in MDBK Cells by Orchestrating the Host Cell Network. *Virulence* (2021) 1:679–89. doi: 10.1080/21505594.2021.1883933
52. Wang P, Zhou R, Zhou R, Li W, Weerasinghe J, Chen S, et al. Cold Atmospheric Plasma for Preventing Infection of Viruses That Use ACE2 for Entry. *Theranostics* (2022) 6:2811–32. doi: 10.7150/thno.70098
53. Wende K, Strassenburg S, Haertel B, Harms M, Holtz S, Barton A, et al. Atmospheric Pressure Plasma Jet Treatment Evokes Transient Oxidative Stress in HaCaT Keratinocytes and Influences Cell Physiology. *Cell Biol Int* (2014) 38:412–25. doi: 10.1002/cbin.10200
54. Bekeschus S, Schmidt A, Bethge L, Masur K, von Woedtke T, Hasse S, et al. Stimulation of Human THP-1 Monocytes in Response to Cold Physical Plasma. *Oxid Med Cell Longev* (2016) 2016:5910695. doi: 10.1155/2016/5910695
55. Arndt S, Landthaler M, Zimmermann JL, Unger P, Wacker E, Shimizu T. Effects of Cold Atmospheric Plasma (CAP) on ß-Defensins, Inflammatory Cytokines, and Apoptosis-Related Molecules in Keratinocytes *In Vitro* and *In Vivo*. *PloS One* (2015) 10:e0120041. doi: 10.1371/journal.pone.0120041
56. Shome D, von Woedtke T, Riedel K, Masur K. The HIPPO Transducer YAP and its Targets CTGF and Cyr61 Drive a Paracrine Signalling in Cold Atmospheric Plasma-Mediated Wound Healing. *Oxid Med Cell Longev* (2020) 13:4910280. doi: 10.1155/2020/4910280
57. Balzer J, Heuer K, Demir E, Hoffmanns MA, Baldus S, Fuchs PC, et al. Non-Thermal Dielectric Barrier Discharge (DBD) Effects on Proliferation and Differentiation of Human Fibroblasts are Primary Mediated by Hydrogen Peroxide. *PloS One* (2015) 10:e0144968. doi: 10.1371/journal.pone.0144968
58. Bekeschus S, von Woedtke T, Kramer A, Weltmann KD, Masur K. Cold Physical Plasma Treatment Alters Redox Balance in Human Immune Cells. *Plasma Med* (2013) 3:267–78. doi: 10.1615/plasmamed.2014011972
59. Schmidt A, Bekeschus S, von Woedtke T, Hasse S. Cell Migration and Adhesion of a Human Melanoma Cell Line is Decreased by Cold Plasma Treatment. *Clin Plasma Med* (2015) 3:24–31. doi: 10.1016/j.cpme.2015.05.003
60. Arndt S, Unger P, Wacker E, Shimizu T, Heinlin J, Li Y, et al. Cold Atmospheric Plasma (CAP) Changes Gene Expression of Key Molecules of the Wound Healing Machinery and Improves Wound Healing *In Vitro* and *In Vivo*. *PloS One* (2013) 8:e79325. doi: 10.1371/journal.pone.0079325
61. Schmidt A, Bekeschus S, Wende K, Vollmar B, Woedtkevon T. A Cold Plasma Jet Accelerates Wound Healing in a Murine Model of Full-Thickness Skin Wounds. *Exp Dermatol* (2017) 26:156–62. doi: 10.1111/exd.13156
62. Lin Y, Chen J, Wu M, Hsieh I, Liang C, Hsu C, et al. Galectin-1 Accelerates Wound Healing by Regulating the Neuropilin-1/Smad3/NOX4 Pathway and ROS Production in Myofibroblasts. *J Invest Dermatol* (2015) 135:258–68. doi: 10.1038/jid.2014.288
63. Daeschlein G, von Woedtke T, Kindel E, Brandenburg R, Weltmann KD, Jünger M. Antibacterial Activity of an Atmospheric Pressure Plasma Jet Against Relevant Wound Pathogens *In Vitro* on a Simulated Wound Environment. *Plasma Processes Polymers* (2010) 7:224–30. doi: 10.1002/ppap.200900059
64. Eyerich K, Eyerich S. Immune Response Patterns in non-Communicable Inflammatory Skin Diseases. *J Eur Acad Dermatol Venereol* (2018) 32:692–703. doi: 10.1111/jdv.14673
65. Michalek IM, Loring B, John SM. A Systematic Review of Worldwide Epidemiology of Psoriasis. *J Eur Acad Dermatol Venereol* (2017) 31:205–12. doi: 10.1111/jdv.13854
66. Ogawa E, Sato Y, Minagawa A, Okuyama R. Pathogenesis of Psoriasis and Development of Treatment. *J Dermatol* (2018) 45:264–72. doi: 10.3390/ijms20061475
67. Nussbaum L, Chen YL, Ogg GS. Role of Regulatory T Cells in Psoriasis Pathogenesis and Treatment. *Br J Dermatol* (2021) 184:14–24. doi: 10.1111/bjd.19380
68. Zhong S, Dong Y, Liu D, Xu D, Xiao S, Chen H, et al. Surface Air Plasma-Induced Cell Death and Cytokine Release of Human Keratinocytes in the Context of Psoriasis. *Br J Dermatol* (2016) 174:542–52. doi: 10.1111/bjd.14236
69. Lu G, Duan J, Zhang S, Liu X, Poorun D, Liu X. Cold Atmospheric Plasma Ameliorates Imiquimod-Induced Psoriasiform Dermatitis in Mice by

Mediating Ntiproliferative Effects. *Free Radic Res* (2019) 53:269–80. doi: 10.1080/10715762.2018.1564920
70. Lee YS, Lee MH, Kim HJ, Won HR, Kim CH. Non-Thermal Atmospheric Plasma Ameliorates Imiquimod-Induced Psoriasis-Like Skin Inflammation in Mice Through Inhibition of Immune Responses and Up-Regulation of PD-L1 Expression. *Sci Rep* (2017) 7:15564. doi: 10.1038/s41598-017-15725-7
71. Ezzedine K, Eleftheriadou V, Whitton M, van Geel N. Vitiligo. *Lancet* (2015) 386:74–84. doi: 10.1016/S0140-6736(14)60763-7
72. Speeckaert R, van Geel N. Vitiligo: An Update on Pathophysiology and Treatment Options. *Am J Clin Dermatol* (2017) 6:733–44. doi: 10.1007/s40257-017-0298-5
73. Zhai S, Xu M, Li Q, Guo K, Chen H, Kong MG, et al. Successful Treatment of Vitiligo With Cold Atmospheric Plasma–Activated Hydrogel. *J Invest Dermatol* (2021) 11:2710–9. doi: 10.1016/j.jid.2021.04.019
74. Dai X, Bazaka K, Thompson EW, Ostrikov KK. Cold Atmospheric Plasma: A Promising Controller of Cancer Cell States. *Cancers (Basel)* (2020) 11:3360. doi: 10.3390/cancers12113360
75. Dai X, Bazaka K, Richard DJ, Thompson ERW, Ostrikov KK. The Emerging Role of Gas Plasma in Oncotherapy. *Trends Biotechnol* (2018) 11:1183–98. doi: 10.1016/j.tibtech.2018.06.010
76. Lin A, Chernets N, Han J, Alicea Y, Dobrynin D, Fridman G, et al. Non-Equilibrium Dielectric Barrier Discharge Treatment of Mesenchymal Stem Cells: Charges and Reactive Oxygen Species Play the Major Role in Cell Death. *Plasma Processes Polymers* (2015) 12:1117–27. doi: 10.1002/ppap.201400232
77. Hoek KS, Goding CR. Cancer Stem Cells Versus Phenotype-Switching in Melanoma. *Pigment Cell Melanoma Res* (2010) 23:746. doi: 10.1111/j.1755-148X.2010.00757
78. Keidar M, Walk R, Shashurin A, Srinivasan P, Sandler A, Dasgupta S, et al. Cold Plasma Selectivity and the Possibility of a Paradigm Shift in Cancer Therapy. *Br J Cancer* (2011) 105:1295–301. doi: 10.1038/bjc.2011.386
79. Chernets N, Kurpad DS, Alexeev V, Rodrigues DB, Freeman TA. Reaction Chemistry Generated by Nanosecond Pulsed Dielectric Barrier Discharge Treatment is Responsible for the Tumor Eradication in the B16 Melanoma Mouse Model. *Plasma Process Polym* (2015) 12:1400–9. doi: 10.1002/ppap.201500140
80. Ishaq M, Bazaka K, Ostrikov K. Intracellular Effects of Atmospheric-Pressure Plasmas on Melanoma Cancer Cells. *Phys Plasmas* (2015) 22:122003. doi: 10.1021/acsami.0c06500
81. Arndt S, Wacker E, Li Y, Shimizu T, Thomas HM, Morfill GE, et al. Cold Atmospheric Plasma, a New Strategy to Induce Senescence in Melanoma Cells. *Exp Dermatol* (2013) 22:284–9. doi: 10.1111/exd.12127
82. Kalghatgi S, Kelly CM, Cerchar E, Torabi B, Alekseev O, Fridman A, et al. Effects of non-Thermal Plasma on Mammalian Cells. *PloS One* (2011) 6: e16270. doi: 10.1371/journal.pone.0016270
83. Losquadro WD. Anatomy of the Skin and the Pathogenesis of Nonmelanoma Skin Cancer. *Facial Plast Surg Clin North Am* (2017) 25:283–9. doi: 10.1016/j.fsc.2017.03.001
84. Wang L, Yang X, Yang C, Gao J, Zhao Y, Cheng C, et al. The Inhibition Effect of Cold Atmospheric Plasma-Activated Media in Cutaneous Squamous Carcinoma Cells. *Future Oncol* (2019) 15:495–505. doi: 10.2217/fon-2018-0419
85. Yang X, Yang C, Wang L, Cao Z, Wang Y, Cheng C, et al. Inhibition of Basal Cell Carcinoma Cells by Cold Atmospheric Plasma-Activated Solution and Differential Gene Expression Analysis. *Int J Oncol* (2020) 56:1262–73. doi: 10.3892/ijo.2020.5009
86. Xiang L, Xu X, Zhang S, Cai D, Dai X. Cold Atmospheric Plasma Conveys Selectivity on Triple Negative Breast Cancer Cells Both *In Vitro* and *In Vivo*. *Free Radic Biol Med* (2018) 124:205–13. doi: 10.1016/j.freeradbiomed.2018.06.001
87. Xu X, Dai X, Xiang L, Cai D, Xiao S, Ostrikov K. Quantitative Assessment of Cold Atmospheric Plasma Anti-Cancer Efficacy in Triple-Negative Breast Cancers. *Processes Polymers* (2018) 8:e1800052. doi: 10.1002/ppap.201800052
88. Tian Y, Zhang Z, Zhang Z, Dai X. Hsa_circRNA_0040462: A Sensor of Cells' Response to CAP Treatment With Double-Edged Roles on Breast Cancer Malignancy. *Int J Med Sci* (2022) 4:640–50. doi: 10.7150/ijms.66940
89. Almeida ND, Klein AL, Hogan EA, Terhaar SJ, Kedda J, Uppal P, et al. Cold Atmospheric Plasma as an Adjunct to Immunotherapy for Glioblastoma Multiforme. *World Neurosurg* (2019) 130:369–76. doi: 10.1016/j.wneu.2019.06.209
90. Li W, Yu H, Ding D, Chen Z, Wang Y, Wang S, et al. Cold Atmospheric Plasma and Iron Oxide-Based Magnetic Nanoparticles for Synergetic Lung Cancer Therapy. *Free Radic Biol Med* (2019) 130:71–81. doi: 10.1016/j.freeradbiomed.2018.10.429
91. van Loenhout J, Flieswasser T, Boullosa LF, Waele JD, van Audenaerde J, Marcq E, et al. Cold Atmospheric Plasma-Treated Pbs Eliminates Immunosuppressive Pancreatic Stellate Cells and Induces Immunogenic Cell Death of Pancreatic Cancer Cells. *Cancers (Basel)* (2019) 11:1597. doi: 10.3390/cancers11101597
92. Zhou X, Cai D, Xiao S, Ning M, Zhou R, Zhang S, et al. pen: A Novel Plasma Source for Cancer Treatment. *J Cancer* (2020) 8:2273–82. doi: 10.7150/jca.38613
93. Wang P, Zhou R, Thomas P, Zhao L, Zhou R, Mandal S, et al. Epithelial-To-Mesenchymal Transition Enhances Cancer Cell Sensitivity to Cytotoxic Effects of Cold Atmospheric Plasmas in Breast and Bladder Cancer Systems. *Cancers (Basel)* (2021) 12:2889. doi: 10.3390/cancers13122889
94. Zhang H, Xu S, Zhang J, Wang Z, Liu D, Guo L, et al. Plasma-Activated Thermosensitive Biogel as an Exogenous ROS Carrier for Post-Surgical Treatment of Cancer. *Biomaterials* (2021) 276:121057. doi: 10.1016/j.biomaterials.2021.121057

Conflict of Interest: The authors declare that the research was conducted in the absence of any commercial or financial relationships that could be construed as a potential conflict of interest.

Publisher's Note: All claims expressed in this article are solely those of the authors and do not necessarily represent those of their affiliated organizations, or those of the publisher, the editors and the reviewers. Any product that may be evaluated in this article, or claim that may be made by its manufacturer, is not guaranteed or endorsed by the publisher.

frontiers | Frontiers in Immunology

PERSPECTIVE
published: 27 May 2022
doi: 10.3389/fimmu.2022.883239

Controlling Inflammation Pre-Emptively or at the Time of Cutaneous Injury Optimises Outcome of Skin Scarring

Sara Ud-Din [1] *and Ardeshir Bayat* [1,2*]

[1] Plastic and Reconstructive Surgery Research, National Institute for Health Research (NIHR) Manchester Biomedical Research Centre, University of Manchester, Manchester, United Kingdom, [2] Medical Research Council - South Africa (MRC-SA) Wound Healing Unit, Division of Dermatology, University of Cape Town, Cape Town, South Africa

OPEN ACCESS

Edited by:
Perenlei Enkhbaatar, University of Texas Medical Branch at Galveston, United States

Reviewed by:
Julia K. Bohannon, Vanderbilt University Medical Center, United States
Amina El Ayadi, University of Texas Medical Branch at Galveston, United States

***Correspondence:**
Ardeshir Bayat
ardeshir.bayat@uct.ac.za
orcid.org/0000-0002-4116-6491

Specialty section:
This article was submitted to Inflammation, a section of the journal Frontiers in Immunology

Received: *24 February 2022*
Accepted: *21 April 2022*
Published: *27 May 2022*

Citation:
Ud-Din S and Bayat A (2022) Controlling Inflammation Pre-Emptively or at the Time of Cutaneous Injury Optimises Outcome of Skin Scarring. Front. Immunol. 13:883239. doi: 10.3389/fimmu.2022.883239

Inflammation plays an active role during the wound healing process. There is a direct association between the extent of injury as well as inflammation and the amount of subsequent cutaneous scarring. Evidence to date demonstrates that high levels of inflammation are associated with excessive dermal scarring and formation of abnormal pathological scars such as keloids and hypertrophic scars. In view of the multiple important cell types being involved in the inflammatory process and their influence on the extent of scar formation, many scar therapies should aim to target these cells in order to control inflammation and by association help improve scar outcome. However, most current treatment strategies for the management of a newly formed skin scar often adopt a watch-and-wait approach prior to commencing targeted anti-inflammatory therapy. Moreover, most of these therapies have been evaluated in the remodelling phase of wound healing and the evaluation of anti-inflammatory treatments at earlier stages of healing have not been fully explored and remain limited. Taken together, in order to minimise the risk of developing a poor scar outcome, it is clear that adopting an early intervention prior to skin injury would be optimal, however, the concept of pre-emptively priming the skin prior to injury has not yet been thoroughly evaluated. Therefore, the aim of this review was to evaluate the available literature regarding scar therapies that aim to target inflammation which are commenced prior to when a scar is formed or immediately after injury, with a particular focus on the role of pre-emptive priming of skin prior to injury in order to control inflammation for the prevention of poor scarring outcome.

Keywords: skin scarring, wound healing, hypertrophic scars, keloid scars, inflammation, skin priming, pre-emptive skin priming

INTRODUCTION

The wound healing process is highly complex and is comprised of a series of well-defined stages that include inflammation, proliferation, and remodelling/scar formation (1). After an initial injury, clotting occurs and invading microbes activate an inflammatory response that is spread by the local release of chemotactic factors (2). There are multiple key players in the inflammatory process including neutrophils, monocytes, and other immune cells that are recruited to the wound site to clear cell debris and infections and aid in the tissue repair response (1–3). The length of response and the degree vary which has an effect on the final outcome. Certainly, there are significant benefits of producing an inflammatory response, but there are also negative aspects which can lead to non-healing wounds and excessive scarring, including hypertrophic scar and keloid formation (4–6). Many studies have suggested a direct association between the extent of injury/inflammation and the amount of scarring and there has been evidence that high levels of inflammation are associated with excessive scarring or development of abnormal scars, whereas inflammation is significantly diminished in wounds that heal without scars (7–11).

A number of immune cells have been associated with scar formation, including mast cells, macrophages and neutrophils as well as many inflammatory mediators have been shown to influence scar formation (12, 13) (**Figure 1**). In particular, macrophages, T cells, and mast cells have all been shown to be increased in abnormal scar tissue in particular in keloid, although in varying degrees. In keloid tissue, macrophages have been shown to have upregulated M2-associated genes which are highly relevant to tissue repair and remodelling (12, 13). While macrophages are indeed important for tissue repair, an overabundance on the other hand can be detrimental (14, 15). Current research has shown that T cells have a complex role in regulating scar formation, mainly due to the diverse T cell subsets (16, 17). Coculture of keloid fibroblasts with a Treg-enriched condition demonstrated reduced collagen synthesis in comparison to keloid fibroblasts cocultured with a Treg deficient T cell population (18). Neutrophils are the earliest leukocytes to arrive on the site of injury and they have been identified as the key cells in preventing microbes spreading and have a role in fibrosis (19) but there is a lack of *in vivo* evidence of the role of neutrophils in scar formation. Mast cells, however, are important in hypersensitivity responses and allergic reactions and their link with scar formation has also been studied (8, 20–22). Observations of their numbers and activation status were positively correlated with the degree of scar formation (23, 24). They have been identified as being significantly increased

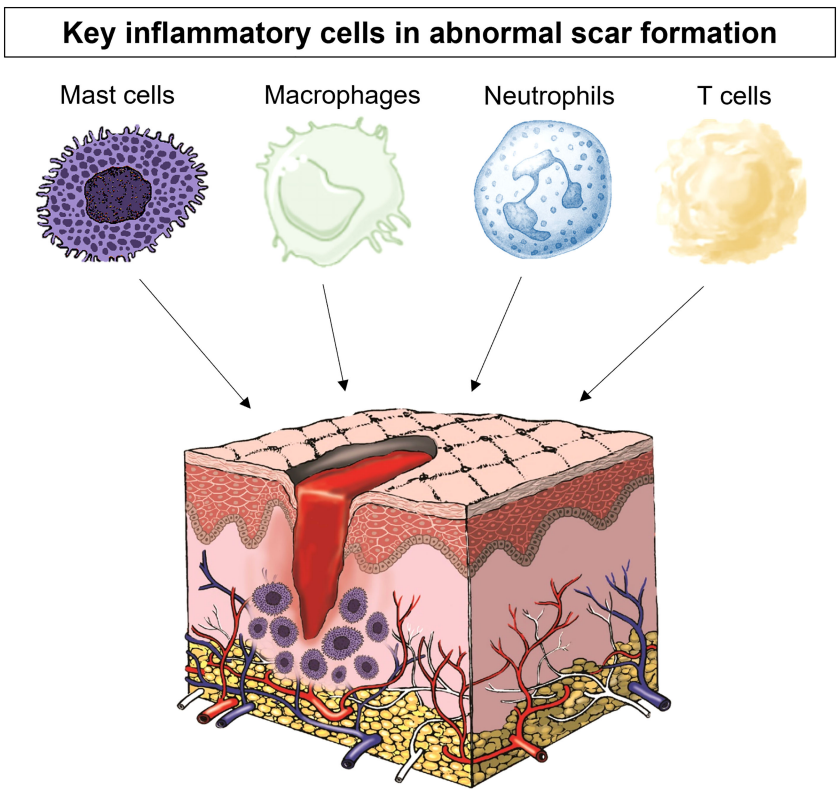

FIGURE 1 | The key inflammatory cells in scar formation include mast cells, macrophages, neutrophils and T cells.

in hypertrophic and keloid scars (8). Furthermore, our group has shown that not only is this a problem in excessive scarring but there are high numbers of mast cells in normal scarring compared to normal skin and this number is further increased after injury with levels not returning to normal even by week 8 post-injury (22).

In view of these important cell types being involved in the inflammatory process and their influence on the extent of scar formation, many scar therapies aim to target these cells in order to quench inflammation to improve scar outcome (25–29). However, most of these therapies have been evaluated in the remodelling phase of wound healing mainly due to the scar being most evident at this stage and the amount of inflammation is most noticeable when correlated to scar severity. Conversely, the evaluation of anti-inflammatory treatments at earlier stages (30, 31) have been limited, because there has been the assumption that inflammation in the early phase of healing is necessary and beneficial for infection prevention and neovasculature development in wound healing. Most current treatment strategies for the management of a newly formed skin scar often adopt a watch-and-wait approach prior to commencing targeted therapy (32, 33). However, in order to minimise the risk of developing a poor scar outcome, taking an early intervention prior to skin injury is desirable. Priming is defined as a substance that prepares the skin for use. Priming the skin prior to an invasive intervention for achieving an optimal result has been studied (34–40). However, the concept of pre-emptively priming the skin prior to injury has not been thoroughly evaluated. Therefore, the aim of this review was to evaluate the available literature regarding scar therapies which aim to target inflammation which are commenced after a scar has formed or immediately after injury, and we will particularly focus on the role of pre-emptive priming of skin prior to injury in order to control inflammation for the prevention of poor scarring outcome (**Figure 2**).

TARGETING INFLAMMATION TO TREAT EXISTING SKIN SCARRING

A number of anti-inflammatory treatments for skin scarring have been evaluated for existing scars including radiotherapy, compression (pressure therapy), laser and 5-fluorouracil therapy (40–43). These therapies have been thought to supress inflammation by inhibiting angiogenesis as inflammatory cells migrate through blood (5). A non-pharmacological treatment that has been used is onion extract ointment which is composed of phenolic compounds. This active ingredient can be converted to quercetin which is an anti-inflammatory derivative with its effects including mast cell stabilisation and anti-proliferative effects (44). This treatment has been used post-operatively to compare the efficacy of silicone gel containing onion extract and aloe vera to silicone gel sheets to prevent postoperative hypertrophic scars and keloids (45). Another study used onion extract on C-Section scars 4 weeks post-surgery and noted improved scar pigmentation and pliability (46).

There are a number of pharmacological treatments which have been used to target inflammation for scarring. Steroids are well known for their anti-inflammatory effect and are widely used for treatment of autoimmune diseases. They decrease inflammation by suppressing the activities of both myeloid and lymphoid cells (47). As increased inflammation promotes excessive scarring, steroid administration is one of the most commonly used treatments for keloid and hypertrophic scars (47). An anti-cancer drug named, Paclitaxel has been shown to regulate inflammatory responses and fibrosis. It has been found to inhibit the NF-kB pathway (48) and attenuate fibrosis by blocking STAT-3 signaling (49). This anti-inflammatory and anti-fibrosis effect has also been observed in animal models of keloid (50) and hypertrophic scars (51). *In vitro* studies have shown that the expression of IL-6 and TNF-a, as well as the production of a-SMA and collagen I, decreased in human keloid fibroblasts following paclitaxel administration (50).

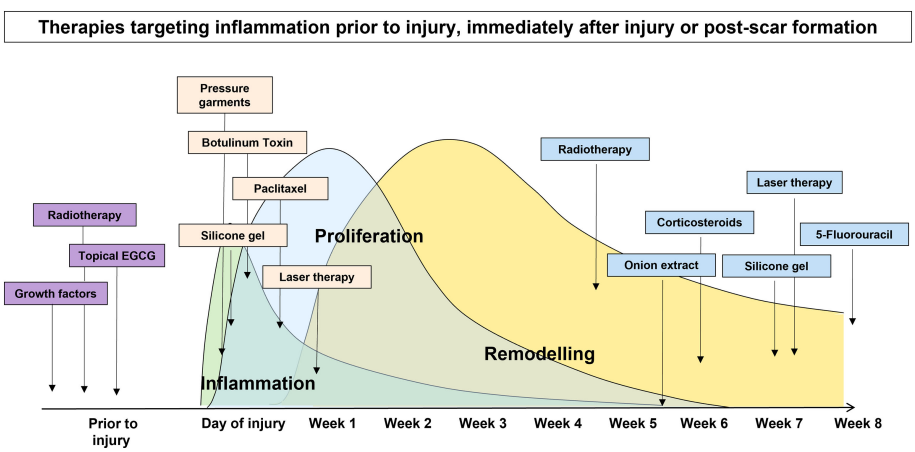

FIGURE 2 | Scar therapies which aim to target inflammation pre-emptively prior to injury, immediately after injury and post-scar formation.

Laser therapies have been used to target inflammation for existing scars. One study used a diode laser with an intralesional optical fibre delivery device in the treatment of hypertrophic and keloid scars and showed a significant reduction in pigmentation and blood perfusion levels (52). A PDL/Nd : YAG laser has also been used in the treatment of surgical scars and the short-term effects were evaluated by *in vivo* confocal microscopy and the long-term effects by clinical assessment of the scars appearance (53). The results demonstrated scar improvements with the laser treatment by showing lower numbers of vessels and decreased amount of collagen fibers.

TARGETING INFLAMMATION TO TREAT SCARS IMMEDIATELY POST-INJURY

A number of studies have aimed to explore the effects of early intervention of inflammation on scar formation with the outcomes varying by different approaches. Surgery, tapes, sheets, and pressure garments are considered useful in decreasing inflammation in the wound area by reducing the degree of tension at the wound edge and all have been used immediately during or after surgery/injury (54). Silicone gel is considered the first line of treatment for most scar management cases, including hypertrophic and keloid scars (55). This anti-scar activity could be partly attributed to the occlusive environment created by silicone gel dressings, and hydration is also believed to lead to the stabilisation of mast cells (16). This treatment is usually applied early once a scar has formed.

Laser therapies have been used both on existing scars and earlier in the healing process. In most studies, the recommended time frame for commencing scar treatment using fractional CO2 laser has remained relatively consistent at more than 2 months after surgery (56). However, recent studies have emphasised the importance of early treatment to reduce scar formation using fractional CO2 laser (56, 57). Resurfacing of scars using fractional CO2 laser with early interventional treatment has been shown to reduce scar formation (58–61). A meta-analysis has supported the efficacy of lasers in minimizing closed surgical scars when treated less than 1 month after surgery (62). There has also been reports on the use of intraoperative fractional CO2 laser treatment of wound edges, which significantly improved the appearance and texture of the scars (63). Erbium: YAG laser treatment, performed immediately after surgery, can also improve the appearance of a surgical scar (64). Thus, it appears that early treatment to the wound may lessen scar formation. Non-ablative fractional laser treatment has also been directly used on the wounded skin barrier immediately after punch biopsy collection, in order to improve scar appearance (65).

Botox which is the commercial name of botulinum toxin (BTX), a neurotoxin produced by clostridium botulinum has been shown to have anti-inflammatory effects on wound healing and scar formation (4, 66, 67). A meta-analysis evaluating intralesional injection of BTX-A versus corticosteroids and placebo in the treatment of hypertrophic scars and keloids showed that BTX-A was most effective (68). Another study compared the effects of inflammation intervention in earlier phases (on the day of operation) with that in later phase (2-week postoperatively) on scar formation after thyroidectomy (31). It has been suggested that by injecting BTX-A and its diffusion into the surrounding muscles at different times during the wound healing process this may have different effects on scar cosmesis by reducing the levels of inflammatory cytokines and mechanical tension on the wound edges (69–71). Although no difference was observed in scar size, early application of BTX-A achieved better scar appearance in relation to erythema, skin elasticity and patient satisfaction, compared to later application. However, the authors did not perform histopathologic assessments in order to evaluate the changes in inflammatory cell infiltration during specific phases of inflammation and structural changes of the skin.

Another study evaluated the effectiveness of intraoperative electro-abrasion for scar revision (72). This was a prospective, randomized, observer-blinded, split-scar study with 24 linear scar segments from patients undergoing Mohs micrographic surgery. After placement of dermal sutures, half of the wound was randomly treated with electro-abrasion whilst the other half was used as the control. Results showed improved scar topography but worsened erythema.

PRE-EMPTIVE PRIMING OF SKIN PRIOR TO INJURY

Several studies support the concept of pre-emptive priming of skin prior to cutaneous injury (34–39). For instance, research on the treatment of pigmented acne scars by ablative laser therapy advocates the use of priming agents to reduce wound healing time, decrease the risk of post-inflammatory hyperpigmentation and provide ultraviolet damage protection (34). Additionally, radiotherapy has been used as an adjuvant therapy for the treatment of keloid scarring both prior to extralesional excision and post-surgery and this has been shown to lead to lower recurrence rates (73).

Another option to target inflammation is by way of topical therapies which have been thought to be a viable therapeutic strategy for restricting scar tissue production and enhancing the cosmetic and functional clinical outcomes resulting from skin injury (74). Our group has conducted two double-blind randomised controlled clinical trials in humans to evaluate the concept of immediate versus delayed application of a topical formulation post-surgical wounding in an excisional punch-biopsy model (75) and the concept of pre-emptive priming of the wound site compared to immediate or delayed application (76). The objective was to deliver an active compound at the optimal time post-surgically induced injury, in order to maximise its impact and improve healing. The results from the first trial (75) demonstrated reduced mast cell numbers, scar thickness and angiogenesis plus increased hydration and

elasticity when an anti-scarring topical formulation was applied immediately to the zone of injury and with delayed application of topical two-weeks post-wounding. The topical formulation used epigallocatechin-3-gallate (EGCG) as the active ingredient. EGCG is the most potent anti-inflammatory anti-oxidant and active component and the most extensively studied green tea catechin (75). Our group have previously evidenced the transdermal delivery uptake of EGCG by using high-performance liquid chromatography and demonstrated this penetrated to the deep dermal tissue and remained in the dermis (74). The mechanism of action of EGCG in wound healing and scarring remain unclear but a number of *in vitro* studies have been conducted to identify the mechanism of action of EGCG on mast cells, angiogenesis and scar shrinkage (77–79).

The findings from the first study provoked the hypothesis that even earlier application of an active such as EGCG could have beneficial effects on the outcome of scarring. Therefore, the second double-blind randomized placebo-controlled trial used various modes of the same anti-scarring topical formulation (containing EGCG) application utilising a full-thickness excisional surgical biopsy approach to identify whether pre-emptive priming pre-surgically induced injury had a greater impact on scarring outcome compared to immediate or delayed application (76). This demonstrated that the effects were further maximised by targeting the source of inflammation earlier. Based on our data, early intervention with the application of topical EGCG particularly 7 days prior to injury demonstrated greater reduction in mast cells (**Figure 3**) and angiogenesis (**Figure 4**), increases in elastin (**Figure 5**) and antioxidant levels and reductions in scar thickness (**Figure 6**) compared to the other modes of topical application. The reduction in mast cell numbers and subsequent lower levels of angiogenesis are beneficial as by targeting these cell types it is thought that this will contain inflammation to achieve a better scar outcome. Additionally, healing requires a strong angiogenic response but high angiogenesis also directly influences scar formation so partial inhibition of the angiogenic response could reduce scar formation or the potential for the development of abnormal skin scarring (78). Furthermore, animal studies have suggested that knocking out mast cells are not detrimental to acute wound healing and there have been a number of studies that have blocked mast cell activation to improve scar formation (80–82).

The potential therapeutic benefits of priming with proangiogenic factors and cells prior to surgery with a combination of proangiogenic growth factors for wound healing in normoglycemic and diabetic mice has been investigated (38, 83). Priming with a combination of VEGF, fibroblast growth factor (FGF) and PDGF has been shown to lead to more rapid closure times, higher vessel densities and better functional outcomes (38). In addition to proangiogenic growth factors, endothelial progenitor cells (EPCs) have presented a potential pre-treatment option for diabetic wounds (83). A murine study showed beneficial effects with pre-treatment by pro-angiogenic growth factors in the healing of diabetic incisional wounds (83). They demonstrated that priming with proangiogenic growth factors and EPCs enhanced incisional wound healing, as defined by a more rapid wound re-epithelialization, higher wound vascularization and higher tensile strength. In particular, the assessment of time-to-closure and functional outcome revealed an advantage for the groups primed with EPCs in comparison to the control animals.

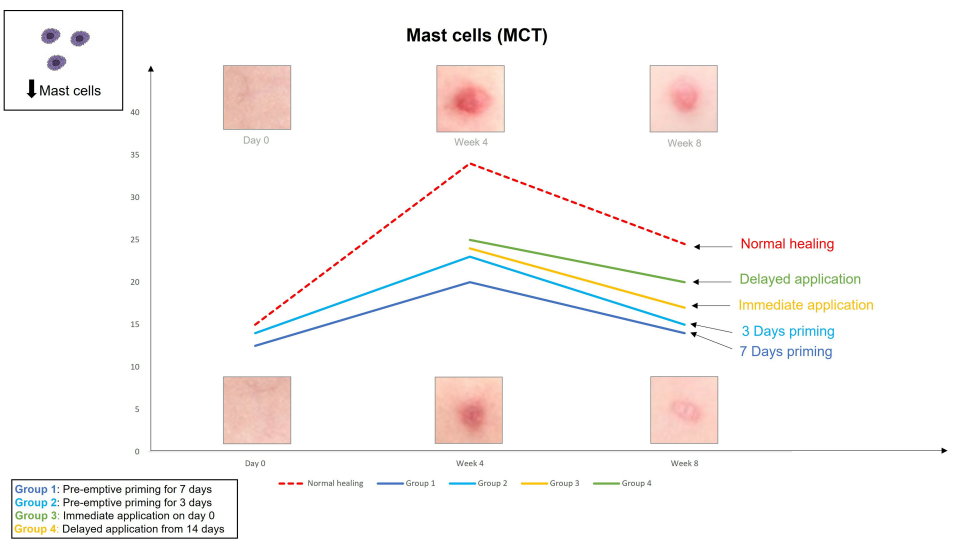

FIGURE 3 | We evaluated the pre-emptive, immediate and delayed intervention of topical Epigallocatechin-3-gallate (EGCG) on skin scarring by conducting a randomsied double blind controlled trial on 40 healthy volunteers over 8 weeks. Here, we demonstrate graphical representations of the trends. Application of topical EGCG, particularly 7 days prior to injury demonstrated greater reductions in mast cells, compared to the other modes of topical application.

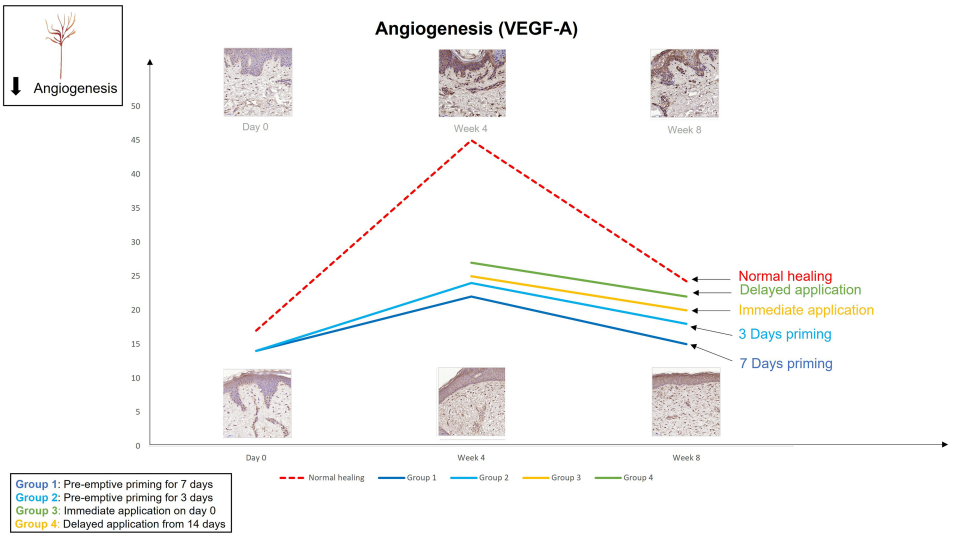

FIGURE 4 | We evaluated the pre-emptive, immediate and delayed intervention of topical Epigallocatechin-3-gallate on skin scarring by conducting a randomsied double blind controlled trial on 40 healthy volunteers over 8 weeks. Graphical representation of the trends for angiogenesis (VEGFA) which demonstrates that pre-emptively priming the skin 7 days prior to injury shows greater reductions in VEGFA compared to all other modes of application.

It is noted that while the 7 days pre-emptive treatment is feasible and beneficial for elective surgeries, this choice may not be available for traumatic injuries and emergency surgeries. Further research would be required to identify if application of this topical formulation for a short period of time, for example a number of hours prior to trauma surgery, could also be beneficial to the outcome of the scarring.

DISCUSSION

We cannot erase scarring, but we can modulate the course of healing, by reducing excessive inflammation, to achieve a better scar outcome. Normal wound healing requires inflammation and tissue remodelling mounting to appropriate degrees. Excessiveness of either of these two factors can lead to the

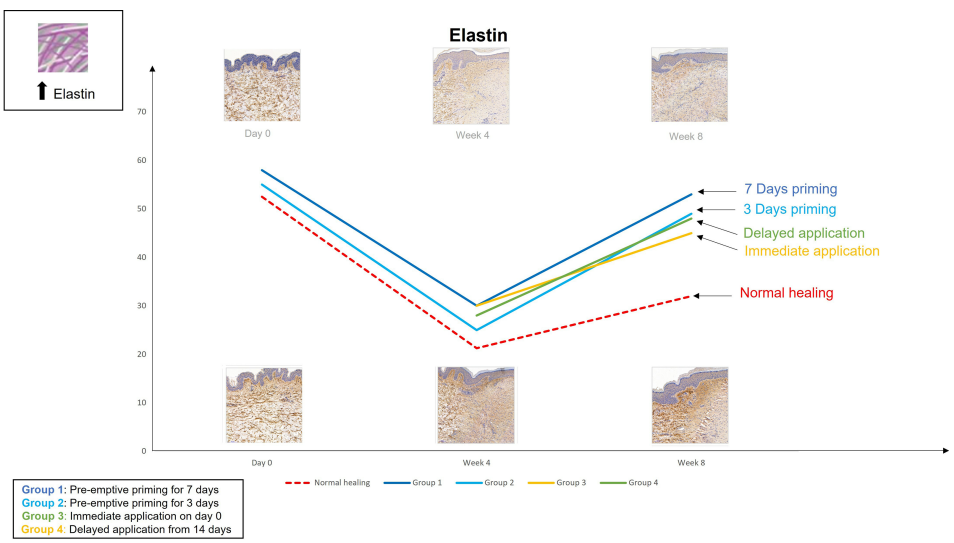

FIGURE 5 | We evaluated the pre-emptive, immediate and delayed intervention of topical Epigallocatechin-3-gallate on skin scarring by conducting a randomsied double blind controlled trial on 40 healthy volunteers over 8 weeks. Graphical representation of the trends for elastin which demonstrates that pre-emptively priming the skin 7 days prior to injury shows greater increases in elastin compared to all other modes of application.

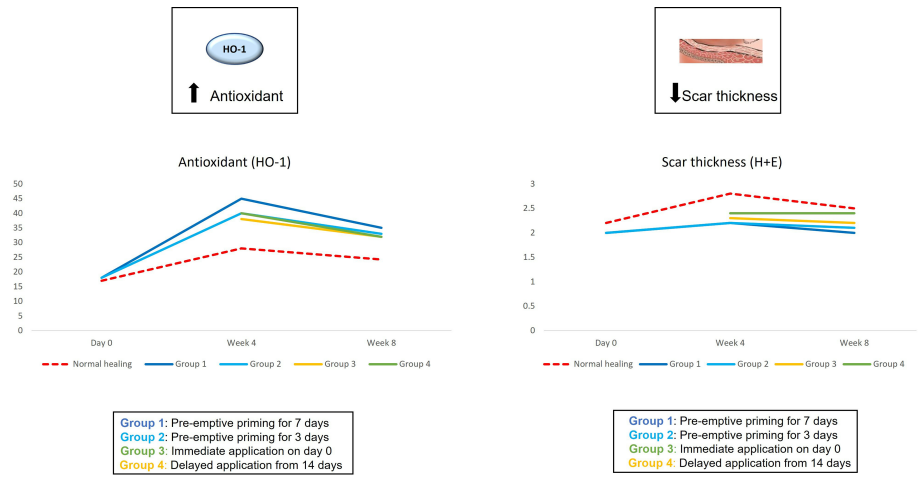

FIGURE 6 | We evaluated the pre-emptive, immediate and delayed intervention of topical Epigallocatechin-3-gallate on skin scarring by conducting a randomsied double blind controlled trial on 40 healthy volunteers over 8 weeks. Graphical representation of the trends for antioxidant levels and skin thickness which demonstrated that pre-emptively priming the skin 7 days prior to injury shows greater reductions in skin thickness and greater increases in antioxidant levels compared to all other modes of application.

development of keloid or hypertrophic scars. Particularly overabundance of inflammatory cells in the remodelling phase correlates with pathological scar formation, indicating the presence of a prolonged inflammatory phase overlapping with the later phases of healing. Inflammatory cell activation is vital for the prevention of infection in contaminated wounds particularly in the early stages of repair and can aid in cleaning the wound site and clearing debris (25, 26). Blocking the inflammatory pathway completely would be detrimental to this process therefore, instead of blocking, by reducing excessive inflammation this would allow infection prevention but not lead to abnormal scarring. However, blocking mast cell activation has been shown to not be detrimental to wound healing as there have been a number of studies that have blocked mast cells in order to improve scar formation (80–82). Furthermore, the concept of inducing altered inflammatory memory response in immune cells responding to injury or in tissue stem cells and epithelial cells has been studied. There have been suggestions that there are benefits in wound healing and tissue repair by priming these cell types to induce immune/inflammatory memory, characterized by epigenetic modifications, leading to increased responsiveness and more rapid inflammatory resolution upon secondary insult (84, 85). Further work could be carried out to elucidate the mechanisms involved in the therapeutic potential of inducing this inflammatory memory.

Early interventions targeting the source of inflammation have shown benefits in minimising scar formation. Many of the treatments used are general anti-inflammatory therapies, but more specific early interventions that target specific cell types such as reducing mast cells or supressing macrophage accumulation may be more optimal. Therefore, more research should be focussed on investigating the roles of the individual key players in inflammation and the effects of pre-emptive treatments to target these specific cell types to improve scar outcomes. By blocking certain pathways in the early phases of wound healing or prior to wounding this may have prophylactic effects for the prevention of abnormal skin scarring.

ETHICS STATEMENT

The studies involving human participants were reviewed and approved by University of Manchester Research Ethics Committee. The patients/participants provided their written informed consent to participate in this study.

AUTHOR CONTRIBUTIONS

SU-D drafted the manuscript. AB developed the concept and edited the manuscript. All authors contributed to the article and approved the submitted version.

ACKNOWLEDGMENTS

We would like to acknowledge the National Institute for Health Research Manchester Biomedical Research Centre (NIHR Manchester BRC) and Medical Research Council of South Africa for their support.

REFERENCES

1. Eming SA, Martin P, Tomic-Canic M. Wound Repair and Regeneration: Mechanisms, Signaling, and Translation. *Sci Transl Med* (2014) 6:265sr6. doi: 10.1126/scitranslmed.3009337
2. Gurtner GC, Werner S, Barrandon Y, Longaker MT. Wound Repair and Regeneration. *Nature* (2008) 453:314–21. doi: 10.1038/nature07039
3. Martin P. Wound Healing—Aiming for Perfect Skin Regeneration. *Science* (1997) 276:75–81. doi: 10.1126/science.276.5309.75
4. Wang ZC, Zhao WY, Cao Y, Liu YQ, Sun Q, Shi P, et al. The Roles of Inflammation in Keloid and Hypertrophic Scars. *Front Immunol* (2020) 11:603187. doi: 10.3389/fimmu.2020.603187
5. Ogawa R. Keloid and Hypertrophic Scars Are the Result of Chronic Inflammation in the Reticular Dermis. *Int J Mol Sci* (2017) 1018(3):606. doi: 10.3390/ijms18030606
6. Wilgus TA. Inflammation as an Orchestrator of Cutaneous Scar Formation: A Review of the Literature. *Plast Aesthet Res* (2020) 7:54. doi: 10.20517/2347-9264.2020.150
7. Wulff BC, Pappa NK, Wilgus TA. Interleukin-33 Encourages Scar Formation in Murine Fetal Skin Wounds. *Wound Repair Regen* (2019) 27(1):19–28. doi: 10.1111/wrr.12687
8. Bagabir R, Byers RJ, Chaudhry IH, Müller W, Paus R, Bayat A. Site-Specific Immunophenotyping of Keloid Disease Demonstrates Immune Upregulation and the Presence of Lymphoid Aggregates. *Br J Dermatol* (2012) 167(5):1053–66. doi: 10.1111/j.1365-2133.2012.11190.x
9. Lee S, Kim SK, Park H, Lee YJ, Park SH, Lee KJ, et al. Contribution of Autophagy-Notch1-Mediated NLRP3 Inflammasome Activation to Chronic Inflammation and Fibrosis in Keloid Fibroblasts. *Int J Mol Sci* (2020) 21 (21):8050. doi: 10.3390/ijms21218050
10. Fujita M, Yamamoto Y, Jiang JJ, Atsumi T, Tanaka Y, Ohki T, et al. NEDD4 Is Involved in Inflammation Development During Keloid Formation. *J Invest Dermatol* (2019) 139(2):333–41. doi: 10.1016/j.jid.2018.07.044
11. Liu XJ, Xu MJ, Fan ST, Wu Z, Li J, Yang XM, et al. Xiamenmycin Attenuates Hypertrophic Scars by Suppressing Local Inflammation and the Effects of Mechanical Stress. *J Invest Dermatol* (2013) 133(5):1351–60. doi: 10.1038/jid.2012.486
12. Shaker SA, Ayuob NN, Hajrah NH. Cell Talk: A Phenomenon Observed in the Keloid Scar by Immunohistochemical Study. *Appl Immunohistochem Mol Morphol AIMM* (2011) 19:153–9. doi: 10.1097/PAI.0b013e3181efa2ef
13. Gauglitz GG, Korting HC, Pavicic T, Ruzicka T, Jeschke MG. Hypertrophic Scarring and Keloids: Pathomechanisms and Current and Emerging Treatment Strategies. *Mol Med (Cambridge Mass)* (2011) 17:113–25. doi: 10.2119/molmed.2009.00153
14. Jin Q, Gui L, Niu F, Yu B, Lauda N, Liu J, et al. Macrophages in Keloid Are Potent at Promoting the Differentiation and Function of Regulatory T Cells. *Exp Cell Res* (2018) 362:472–6. doi: 10.1016/j.yexcr.2017.12.011
15. Mahdavian Delavary B, van der Veer WM, van Egmond M, Niessen FB, Beelen RH. Macrophages in Skin Injury and Repair. *Immunobiology* (2011) 216:753–62. doi: 10.1016/j.imbio.2011.01.001
16. Trace AP, Enos CW, Mantel A, Harvey VM. Keloids and Hypertrophic Scars: A Spectrum of Clinical Challenges. *Am J Clin Dermatol* (2016) 17:201–23. doi: 10.1007/s40257-016-0175-7
17. Chen Y, Jin Q, Fu X, Qiao J, Niu F. Connection Between T Regulatory Cell Enrichment and Collagen Deposition in Keloid. *Exp Cell Res* (2019) 383:111549. doi: 10.1016/j.yexcr.2019.111549
18. Murao N, Seino K, Hayashi T, Ikeda M, Funayama E, Furukawa H, et al. Tregenriched CD4+ T Cells Attenuate Collagen Synthesis in Keloid Fibroblasts. *Exp Dermatol* (2014) 23:266–71. doi: 10.1111/exd.12368
19. Chrysanthopoulou A, Mitroulis I, Apostolidou E, Arelaki S, Mikroulis D, Konstantinidis T, et al. Neutrophil Extracellular Traps Promote Differentiation and Function of Fibroblasts. *J Pathol* (2014) 233:294–307. doi: 10.1002/path.4359
20. Wilgus TA, Wulff BC. The Importance of Mast Cells in Dermal Scarring. *Adv Wound Care (New Rochelle)* (2014) 3(4):356–65. doi: 10.1089/wound.2013.0457
21. Wilgus TA, Ud-Din S, Bayat A. A Review of the Evidence for and Against a Role for Mast Cells in Cutaneous Scarring and Fibrosis. *Int J Mol Sci* (2020) 21 (24):9673. doi: 10.3390/ijms21249673
22. Ud-Din S, Wilgus TA, Bayat A. Mast Cells in Skin Scarring: A Review of Animal and Human Research. *Front Immunol* (2020) 11:552205. doi: 10.3389/fimmu.2020.552205
23. Zhang Q, Kelly AP, Wang L, French SW, Tang X, Duong HS, et al. Green Tea Extract and (-)-Epigallocatechin-3-Gallate Inhibit Mast Cell-Stimulated Type I Collagen Expression in Keloid Fibroblasts *via* Blocking PI-3k/AkT Signaling Pathways. *J Invest Dermatol* (2006) 126:2607–13. doi: 10.1038/sj.jid.5700472
24. Wulff BC, Parent AE, Meleski MA, DiPietro LA, Schrementi ME, Wilgus TA. Mast Cells Contribute to Scar Formation During Fetal Wound Healing. *J Invest Dermatol* (2012) 132:458–65. doi: 10.1038/jid.2011.324
25. Herndon D, Capek KD, Ross E, Jay JW, Prasai A, Ayadi AE, et al. Reduced Postburn Hypertrophic Scarring and Improved Physical Recovery With Yearlong Administration of Oxandrolone and Propranolol. *Ann Surg* (2018) 268:431–41. doi: 10.1097/SLA.0000000000002926
26. Al-Nimer MS, Hameed HG, Mahmood MM. Antiproliferative Effects of Aspirin and Diclofenac Against the Growth of Cancer and Fibroblast Cells: *In Vitro* Comparative Study. *Saudi Pharm J SPJ Off Publ Saudi Pharm Soc* (2015) 23:483–6. doi: 10.1016/j.jsps.2015.01.002
27. Wang Y, He G, Tang H, Shi Y, Kang X, Lyu J, et al. Aspirin Inhibits Inflammation and Scar Formation in the Injury Tendon Healing Through Regulating JNK/STAT-3 Signalling Pathway. *Cell Prolif* (2019) 52:e12650. doi: 10.1111/cpr.12650
28. Ud-Din S, Bowring A, Derbyshire B, Morris J, Bayat A. Identification of Steroid Sensitive Responders Versus Non-Responders in the Treatment of Keloid Disease. *Arch Dermatol Res* (2013) 305(5):423–32. doi: 10.1007/s00403-013-1328-7
29. Tawfic SO, El-Tawdy A, Shalaby S, Foad A, Shaker O, Sayed SS, et al. Evaluation of Fractional CO2 Versus Long Pulsed Nd:YAG Lasers in Treatment of Hypertrophic Scars and Keloids: A Randomized Clinical Trial. *Lasers Surg Med* (2020) 52(10):959–65. doi: 10.1002/lsm.23249
30. Lucas T, Waisman A, Ranjan R, Roes J, Krieg T, Muller W, et al. Differential Roles of Macrophages in Diverse Phases of Skin Repair. *J Immunol (Baltimore Md 1950)* (2010), 184:3964–77. doi: 10.4049/jimmunol.0903356
31. An MK, Cho EB, Park EJ, Kim KH, Kim LS, Kim KJ. Appropriate Timing of Early Postoperative Botulinum Toxin Type A Injection for Thyroidectomy Scar Management: A Split-Scar Study. *Plast Reconstr Surg* (2019) 144(4):659e–68e. doi: 10.1097/PRS.0000000000006064
32. Ud-Din S, Bayat A. Strategic Management of Keloid Disease in Ethnic Skin: A Structured Approach Supported by the Emerging Literature. *Br J Dermatol* (2013) 169(Suppl. S3):71–81. doi: 10.1111/bjd.12588
33. Bayat A, McGrouther DA, Ferguson MW. Skin scarring. *BMJ* (2003) 326 (7380):88–92. doi: 10.1136/bmj.326.7380.88
34. Arsiwala SZ, Desai SR. Fractional Carbon Dioxide Laser: Optimizing Treatment Outcomes for Pigmented Atrophic Acne Scars in Skin of Color. *J Cutan Aesthetic Surg* (2019) 12:85–94. doi: 10.4103/JCAS.JCAS_171_18
35. Du F, Yu Y, Zhou Z, Wang L, Zheng S. Early Treatment Using Fractional CO2 Laser Before Skin Suture During Scar Revision Surgery in Asians. *J Cosmet Laser Ther* (2018) 20:102–5. doi: 10.1080/14764172.2017.1358452
36. Antoniou GA, Onwuka CC, Antoniou SA, Russell D. Meta-Analysis and Trial Sequential Analysis of Prophylactic Negative Pressure Therapy for Groin Wounds in Vascular Surgery. *J Vasc Surg* (2019) 70:1700–1710.e6. doi: 10.1016/j.jvs.2019.01.083
37. Huang H-P, Zhao W-J, Pu J, He F. Prophylactic Negative Pressure Wound Therapy for Surgical Site Infection in Obese Women Undergoing Cesarean Section: An Evidence Synthesis With Trial Sequential Analysis. *J Matern Fetal Neonatal Med* (2019) 25:1–8. doi: 10.1080/14767058.2019.1668924
38. Ackermann M, Pabst AM, Houdek JP, Ziebart T, Konerding MA. Priming With Proangiogenic Growth Factors and Endothelial Progenitor Cells Improves Revascularization in Linear Diabetic Wounds. *Int J Mol Med* (2014) 33:833–9. doi: 10.3892/ijmm.2014.1630
39. Anitha B. Prevention of Complications in Chemical Peeling. *J Cutan Aesthetic Surg* (2010) 3:186–8. doi: 10.4103/0974-2077.74500
40. Yang X, Shao Y, Yu W, Zhang X, Sun Y, Zhang L, et al. A Novel Radiotherapy Approach for Keloids With Intrabeam. *BioMed Res Int* (2019) 2019:4693528. doi: 10.1155/2019/4693528
41. DeBruler DM, Zbinden JC, Baumann ME, Blackstone BN, Malara MM, Bailey JK, et al. Early Cessation of Pressure Garment Therapy Results in Scar

Contraction and Thickening. *PloS One* (2018) 13(6):e0197558. doi: 10.1371/journal.pone.0197558
42. Shi Y, Jiang W, Li W, Zhang W, Zou Y. Comparison of Fractionated Frequency-Doubled 1,064/532 Nm Picosecond Nd:YAG Lasers and Non-Ablative Fractional 1,540 Nm Er: Glass in the Treatment of Facial Atrophic Scars: A Randomized, Split-Face, Double-Blind Trial. *Ann Transl Med* (2021) 9(10):862. doi: 10.21037/atm-21-1715
43. Chen XE, Liu J, Bin Jameel AA, Valeska M, Zhang JA, Xu Y, et al. Combined Effects of Long-Pulsed Neodymium-Yttrium-Aluminum-Garnet Laser, Diprospan and 5-Fluorouracil in the Treatment of Keloid Scars. *Exp Ther Med* (2017) 13(6):3607–12. doi: 10.3892/etm.2017.4438
44. Saulis AS, Mogford JH, Mustoe TA. Effect of Mederma on Hypertrophic Scarring in the Rabbit Ear Model. *Plast Reconstr Surg* (2002) 110:177–83. doi: 10.1097/00006534-200207000-00029
45. Pangkanon W, Yenbutra P, Kamanamool N, Tannirandorn A, Udompataikul M. A Comparison of the Efficacy of Silicone Gel Containing Onion Extract and Aloe Vera to Silicone Gel Sheets to Prevent Postoperative Hypertrophic Scars and Keloids. *J Cosmet Dermatol* (2021) 20(4):1146–53. doi: 10.1111/jocd.13933
46. Conti V, Corbi G, Iannaccone T, Corrado B, Giugliano L, Lembo S, et al. Effectiveness and Tolerability of a Patch Containing Onion Extract and Allantoin for Cesarean Section Scars. *Front Pharmacol* (2020) 11:569514. doi: 10.3389/fphar.2020.569514
47. Rutkowski D, Syed F, Matthews LC, Ray DW, McGrouther DA, Watson RE, et al. An Abnormality in Glucocorticoid Receptor Expression Differentiates Steroid Responders From Nonresponders in Keloid Disease. *Br J Dermatol* (2015) 173(3):690–700. doi: 10.1111/bjd.13752
48. Zhang D, Li Y, Liu Y, Xiang X, Dong Z. Paclitaxel Ameliorates Lipopolysaccharide-Induced Kidney Injury by Binding Myeloid Differentiation Protein-2 to Block Toll-Like Receptor 4-Mediated Nuclear factor-kappaB Activation and Cytokine Production. *J Pharmacol Exp Ther* (2013) 345:69–75. doi: 10.1124/jpet.112.202481
49. Zhang L, Xu X, Yang R, Chen J, Wang S, Yang J, et al. Paclitaxel Attenuates Renal Interstitial Fibroblast Activation and Interstitial Fibrosis by Inhibiting STAT3 Signaling. *Drug Design Dev Ther* (2015) 9:2139–48. doi: 10.2147/DDDT.S81390
50. Wang M, Chen L, Huang W, Jin M, Wang Q, Gao Z, et al. Improving the Antikeloid Outcomes Through Liposomes Loading Paclitaxel-Cholesterol Complexes. *Int J Nanomed* (2019) 14:1385–400. doi: 10.2147/IJN.S195375
51. Huang L-P, Wang G-Q, Jia Z-S, Chen J-W, Wang G, Wang X-L. Paclitaxel Reduces Formation of Hypertrophic Scars in the Rabbit Ear Model. *Ther Clin Risk Manag* (2015) 11:1089–95. doi: 10.2147/TCRM.S82961
52. Li K, Nicoli F, Cui C, Xi WJ, Al-Mousawi A, Zhang Z, et al. Treatment of Hypertrophic Scars and Keloids Using an Intralesional 1470 Nm Bare-Fibre Diode Laser: A Novel Efficient Minimally-Invasive Technique. *Sci Rep* (2020) 10(1):21694. doi: 10.1038/s41598-020-78738-9
53. Vas K, Gaál M, Varga E, Kovács R, Bende B, Kocsis A, et al. Effects of the Combined PDL/Nd:YAG Laser on Surgical Scars: Vascularity and Collagen Changes Evaluated by *In Vivo* Confocal Microscopy. *BioMed Res Int* (2014) 2014:204532. doi: 10.1155/2014/204532
54. Ogawa R, Akaishi S, Kuribayashi S, Miyashita T. Keloids and Hypertrophic Scars Can Now Be Cured Completely: Recent Progress in Our Understanding of the Pathogenesis of Keloids and Hypertrophic Scars and the Most Promising Current Therapeutic Strategy. *J Nippon Med School = Nippon Ika Daigaku zasshi* (2016) 83:46–53. doi: 10.1272/jnms.83.46
55. Wang F, Li X, Wang X, Jiang X. Efficacy of Topical Silicone Gel in Scar Management: A Systematic Review and Meta-Analysis of Randomised Controlled Trials. *Int Wound J* (2020) 17(3):765–73. doi: 10.1111/iwj.13337
56. Lee SH, Zheng Z, Roh MR. Early Postoperative Treatment of Surgical Scars Using a Fractional Carbon Dioxide Laser: A Splitscar, Evaluator-Blinded Study. *Dermatol Surg* (2013) 2013-08-0139(8):1190–6. doi: 10.1111/dsu.12228
57. Jung JY, Jeong JJ, Roh HJ, Cho SH, Chung KY, Lee WJ, et al. Early Postoperative Treatment of Thyroidectomy Scars Using a Fractional Carbon Dioxide Laser. *Dermatol Surg* (2011) 37(2):217–23. doi: 10.1111/j.1524-4725.2010.01853.x
58. Bjorn M, Stausbol-Gron B, Braae OA, Hedelund L. Treatment of Acne Scars With Fractional CO2 Laser at 1-Month Versus 3-Month Intervals: An Intra-Individual Randomized Controlled Trial. *Lasers Surg Med* (2014) 46(2):89–93. doi: 10.1002/lsm.22165
59. Choi JE, Oh GN, Kim JY, Seo SH, Ahn HH, Kye YC. Ablative Fractional Laser Treatment for Hypertrophic Scars: Comparison Between Er: Yagand CO2 Fractional Lasers. *J Dermatolog Treat* (2014) 25(4):299–303. doi: 10.3109/09546634.2013.782090
60. Majid I, Imran S. Fractional CO2 Laser Resurfacing as Monotherapy in the Treatment of Atrophic Facial Acne Scars. *J Cutan Aesthet Surg* (2014) 7(2):87–92. doi: 10.4103/0974-2077.138326
61. Nguyen JK, Weedon J, Jakus J, Heilman E, Isseroff RR, Siegel DM, et al. Dose-Ranging, Parallel Group, Split-Face, Single-Blind Phase II Study of Light Emitting Diode-Red Light (LED-RL) for Skin Scarring Prevention: Study Protocol for a Randomized Controlled Trial. *Trials* (2019) 20(1):432. doi: 10.1186/s13063-019-3546-6
62. Kent RA, Shupp J, Fernandez S, Prindeze N, DeKlotz CMC. Effectiveness of Early Laser Treatment in Surgical Scar Minimization: A Systematic Review and Meta-Analysis. *Dermatol Surg* (2020) 46(3):402–10. doi: 10.1097/DSS.0000000000001887
63. Ozog DM, Moy RL. A Randomized Split-Scar Study of Intraoperative Treatment of Surgical Wound Edges to Minimize Scarring. *Arch Dermatol* (2011) 147(9):1108–10. doi: 10.1001/archdermatol.2011.248
64. Kolli H, Moy RL. Prevention of Scarring With Intraoperative Erbium: YAG Laser Treatment. *J Drugs Dermatol* (2020) 19(11):1040–3. doi: 10.36849/JDD.2020.5244
65. Taudorf EH, Haedersdal M. Early non-Ablative Fractional Laser Improves the Appearance of Punch Biopsy Scars: A Clinical Report. *J Eur Acad Dermatol Venereol* (2016) 30(3):550–52. doi: 10.1111/jdv.12955
66. Prodromidou A, Frountzas M, Vlachos DE, Vlachos GD, Bakoyiannis I, Perrea D, et al. Botulinum Toxin for the Prevention and Healing of Wound Scars: A Systematic Review of the Literature. *Plast Surg (Oakville Ont)* (2015) 23:260–4. doi: 10.1177/229255031502300402
67. Lee BJ, Jeong JH, Wang SG, Lee JC, Goh EK, Kim HW. Effect of Botulinum Toxin Type a on a Rat Surgical Wound Model. *Clin Exp Otorhinolaryngol* (2009) 2:20–7. doi: 10.3342/ceo.2009.2.1.20
68. Bi M, Sun P, Li D, Dong Z, Chen Z. Intralesional Injection of Botulinum Toxin Type A Compared With Intralesional Injection of Corticosteroid for the Treatment of Hypertrophic Scar and Keloid: A Systematic Review and Meta- Analysis. *Med Sci Monit Int Med J Exp Clin Res* (2019) 25:2950–8. doi: 10.12659/MSM.916305
69. Kim YS, Lee HJ, Cho SH, Lee JD, Kim HS. Early Postoperative Treatment of Thyroidectomy Scars Using Botulinum Toxin: A Split-Scar, Double-Blind Randomized Controlled Trial. *Wound Repair Regen* (2014) 22:605–12. doi: 10.1111/wrr.12204
70. Zhibo X, Miaobo Z. Potential Therapeutical Effects of Botulinum Toxin Type A in Keloid Management. *Med Hypotheses* (2008) 71:623. doi: 10.1016/j.mehy.2008.04.018
71. Hsu TS, Dover JS, Arndt KA. Effect of Volume and Concentration on the Diffusion of Botulinum Exotoxin a. *Arch Dermatol* (2004) 140:1351–4. doi: 10.1001/archderm.140.11.1351
72. Kannan S, de Golian E, Lee N, Smith J, Brian Jiang SI. A Split-Scar Study Investigating the Effectiveness of Early Intervention With Electroabrasion on Improving the Cosmetic Appearance of Postsurgical Scars. *Dermatol Surg* (2020) 46(10):1300–5. doi: 10.1097/DSS.0000000000002324
73. Stahl S, Barnea Y, Weiss J, Amir A, Zaretski A, Leshem D, et al. Treatment of Earlobe Keloids by Extralesional Excision Combined With Preoperative and Postoperative "Sandwich" Radiotherapy. *Plast Reconstr Surg* (2010) 125(1):88–92. doi: 10.1097/PRS.0b013e3181c2a46e
74. Sidgwick GP, McGeorge D, Bayat A. Functional Testing of Topical Skin Formulations Using an Optimised *Ex Vivo* Skin Organ Culture Model. *Arch Dermatol Res* (2016) 308:297–308. doi: 10.1007/s00403-016-1645-8
75. Ud-Din S, Foden P, Mazhari M, Al-Habba S, Baguneid M, Bulfone-Paus S, et al. A Double-Blind, Randomized Trial Shows the Role of Zonal Priming and Direct Topical Application of Epigallocatechin-3-Gallate in the Modulation of Cutaneous Scarring in Human Skin. *J Invest Dermatol* (2019) 139(8):1680–90.e16. doi: 10.1016/j.jid.2019.01.030
76. Ud-Din S, Wilgus TA, McGeorge DD, Bayat A. Pre-Emptive Priming of Human Skin Improves Cutaneous Scarring and Is Superior to Immediate and Delayed Topical Anti-Scarring Treatment Post-Wounding: A Double-Blind

Randomised Placebo-Controlled Clinical Trial. *Pharmaceutics* (2021) 13 (4):510. doi: 10.3390/pharmaceutics13040510
77. Wang Z, Dabrosin C, Yin X, Fuster MM, Arreola A, Rathmell WK, et al. Broad Targeting of Angiogenesis for Cancer Prevention and Therapy. *Semin Cancer Biol* (2015) 35(Suppl):S224–43. doi: 10.1016/j.semcancer.2015.01.001
78. Singh BN, Shankar S, Srivastava RK. Green Tea Catechin, Epigallocatechin-3-Gallate (EGCG): Mechanisms, Perspectives and Clinical Applications. *Biochem Pharmacol* (2011) 82(12):1807–21. doi: 10.1016/j.bcp.2011.07.093
79. Syed F, Bagabir RA, Paus R, Bayat A. *Ex Vivo* Evaluation of Antifibrotic Compounds in Skin Scarring: EGCG and Silencing of PAI-1 Independently Inhibit Growth and Induce Keloid Shrinkage. *Lab Invest* (2013) 93(8):946–60. doi: 10.1038/labinvest.2013.82
80. Weitzmann A, Naumann R, Dudeck A, Zerjatke T, Gerbaulet A, Roers A. Mast Cells Occupy Stable Clonal Territories in Adult Steady-State Skin. *J Invest Dermatol* (2020) 140(12):2433–41.e5. doi: 10.1016/j.jid.2020.03.963
81. Artuc M, Hermes B, Steckelings UM, Grützkau A, Henz BM. Mast Cells and Their Mediators in Cutaneous Wound Healing–Active Participants or Innocent Bystanders? *Exp Dermatol* (1999) 8(1):1–16. doi: 10.1111/j.1600-0625.1999.tb00342.x
82. Voss M, Kotrba J, Gaffal E, Katsoulis-Dimitriou K, Dudeck A. Mast Cells in the Skin: Defenders of Integrity or Offenders in Inflammation? *Int J Mol Sci* (2021) 22(9):4589. doi: 10.3390/ijms22094589
83. Ackermann M, Wolloscheck T, Wellmann A, Li VW, Li WW, Konerding MA. Priming With a Combination of Proangiogenic Growth Factors Enhances Wound Healing in Streptozotocin-Induced Diabetes in Mice. *Eur Surg Res* (2011) 47(2):81–9. doi: 10.1159/000328143
84. Gonzales KAU, Polak L, Matos I, Tierney MT, Gola A, Wong E, et al. Stem Cells Expand Potency and Alter Tissue Fitness by Accumulating Diverse Epigenetic Memories. *Science* (2021) 374(6571):eabh2444. doi: 10.1126/science.abh2444
85. Wilgus TA. Vascular Endothelial Growth Factor and Cutaneous Scarring. *Adv Wound Care (New Rochelle)* (2019) 8(12):671–8. doi: 10.1089/wound.2018.0796

Conflict of Interest: The authors declare that the research was conducted in the absence of any commercial or financial relationships that could be construed as a potential conflict of interest.

Publisher's Note: All claims expressed in this article are solely those of the authors and do not necessarily represent those of their affiliated organizations, or those of the publisher, the editors and the reviewers. Any product that may be evaluated in this article, or claim that may be made by its manufacturer, is not guaranteed or endorsed by the publisher.

frontiers | Frontiers in Immunology

TYPE Original Research
PUBLISHED 03 October 2022
DOI 10.3389/fimmu.2022.984045

OPEN ACCESS

EDITED BY
Gaby Palmer,
Université de Genève,
Switzerland

REVIEWED BY
Agnes Silvia Klar,
University Children's Hospital Zurich,
Switzerland
Carlo Chizzolini,
Université de Genève,
Switzerland

*CORRESPONDENCE
Jean-François Jégou
jean-francois.jegou@univ-poitiers.fr

SPECIALTY SECTION
This article was submitted to Inflammation, a section of the journal Frontiers in Immunology

RECEIVED 01 July 2022
ACCEPTED 01 September 2022
PUBLISHED 03 October 2022

CITATION
Cordier-Dirikoc S, Pedretti N, Garnier J, Clarhaut-Charreau S, Ryffel B, Morel F, Bernard F-X, Hamon de Almeida V, Lecron J-C and Jégou J-F (2022) Dermal fibroblasts are the key sensors of aseptic skin inflammation through interleukin 1 release by lesioned keratinocytes. *Front. Immunol.* 13:984045. doi: 10.3389/fimmu.2022.984045

Dermal fibroblasts are the key sensors of aseptic skin inflammation through interleukin 1 release by lesioned keratinocytes

Sevda Cordier-Dirikoc[1], Nathalie Pedretti[1], Julien Garnier[1], Sandrine Clarhaut-Charreau[1,2], Bernhard Ryffel[3], Franck Morel[2], François-Xavier Bernard[1], Valérie Hamon de Almeida[1], Jean-Claude Lecron[2,4] and Jean-François Jégou[2*]

[1]Qima-Bioalternatives (Qima Life Sciences), Gençay, France, [2]Université de Poitiers, Laboratoire Inflammation, Tissus Epithéliaux et Cytokines (LITEC), UR15560, Poitiers, France, [3]INEM, CNRS, UMR 7355, Orléans, France, [4]Service d'Immunologie et Inflammation, CHU de Poitiers, Poitiers, France

IL-1 plays a crucial role in triggering sterile inflammation following tissue injury. Although most studies associate IL-1 release by injured cells to the recruitment of neutrophils for tissue repair, the inflammatory cascade involves several molecular and cellular actors whose role remains to be specified. In the present study, we identified dermal fibroblasts among the IL-1R1-expressing skin cells as key sensors of IL-1 released by injured keratinocytes. After *in vitro* stimulation by recombinant cytokines or protein extracts of lysed keratinocytes containing high concentrations of IL-1, we show that dermal fibroblasts are by far the most IL-1-responsive cells compared to keratinocytes, melanocytes and endothelial cells. Fibroblasts have the property to respond to very low concentrations of IL-1 (from 10 fg/ml), even in the presence of 100-fold higher concentrations of IL-1RA, by increasing their expression of chemokines such as IL-8 for neutrophil recruitment. The capacity of IL-1-stimulated fibroblasts to attract neutrophils has been demonstrated both *in vitro* using cell migration assay and *in vivo* using a model of superficial epidermal lesion in IL-1R1-deficient mice which harbored reduced expression of inflammatory mediators and neutrophil skin infiltration. Together, our results shed a light on dermal fibroblasts as key relay cells in the chain of sterile inflammation induced after epidermal lesion.

KEYWORDS

keratinocytes, fibroblasts, IL-1, skin, sterile inflammation, epidermal lesion

Introduction

Skin is the outermost tissue of the human body that represents a primary interface with the external environment. It provides a protective barrier against mechanical, thermal and physical injuries and constitutes the first line of defense against pathogens. In this multilayered tissue, the epidermis plays a crucial role in the natural barrier function, in association with a wide repertoire of immune cells both from the innate and adaptive systems which contribute to host defense and the maintenance of skin homeostasis (1).

After a primary epidermal lesion in aseptic condition, keratinocytes have the capacity to trigger a sequence of events involving a wide diversity of molecular and cellular actors to initiate a dedicated inflammatory response, leading to local protection and repair mechanisms. The role of keratinocytes has been widely studied in the pathogenesis of chronic skin inflammatory pathologies such as psoriasis or atopic dermatitis (2, 3). However, much less is known about the contribution of keratinocytes in the early events of the innate immune response after a primary epidermal lesion and the downstream mechanisms that contribute to the development of a sterile inflammation characterized by the infiltration of injured tissues by immune cells. In a pathogen-free context, this epidermal innate immune response can be induced after a cellular stress by the passive release of alarmins such as heat-shock proteins (HSPs), adenosine triphosphate (ATP), S100 proteins or IL-33, which activate sterile inflammation (4). Among these mediators, interleukin 1α (IL-1α) is also considered as an alarmin and it has been known for a long time that keratinocytes are a potent source of proIL-1α, as well as proIL-1β (5, 6), which are both matured and released under their active forms in response to different cellular stresses to trigger sterile inflammation. IL-1α and IL-1β are both leader cytokines of the IL-1 family which encompasses 11 members, including 7 agonists with proinflammatory activities (IL-1α, IL-1β, IL-18, IL-33, IL-36α, IL-36β, andIL-36γ) and 4 antagonists (IL-1RA, IL-18BP, IL-37, and IL-38) with anti-inflammatory activities (7, 8). Keratinocytes were also reported to express and secrete IL-18 (9), IL-33 (10) and IL-36α/β/γ (11) in inflammatory conditions, but most studies reported a predominant contribution of IL-1α and IL-1β to cutaneous sterile inflammation. Thus, both cytokines were described be upregulated and secreted by damaged keratinocytes after UVB exposure (12, 13). IL-1α represents a signal for genotoxic stress when keratinocytes and fibroblasts are exposed to various DNA damage agents, thus initiating a sterile inflammatory cascade that contributes to efficient tissue repair and wound healing (14). The role of IL-1α and IL-1β has also been investigated in hypoxia-induced sterile inflammation, both *in vitro* and *in vivo* (15). In this study, Rider *et al.* demonstrated the contribution of the proIL-1α and mature IL-1β released by necrotic keratinocytes to recruit sequentially neutrophils and macrophages, respectively. In another mouse model of intraperitoneal sterile inflammation after injured cells injection, the acute neutrophilic inflammatory response required IL-1α and the IL-1R1-Myd88 pathway (16).

Although most studies converge to a central role of IL-1 released by injured cells to trigger sterile inflammation and the recruitment of neutrophils, less is known about the potential target cells in the skin that express IL-1 receptors and that could act as intermediate cells contributing to attract neutrophils at the site of tissue injury. In the present study, we have investigated the role of IL-1 in the induction of aseptic cutaneous inflammation after primary epidermal lesion by integrating the different skin compartments. We have analyzed and compared the expression of cytokines of the IL-1 family and their receptors in a panel of skin and immune cells, allowing us to confirm that keratinocytes are the main source of IL-1α/β and to identify dermal fibroblasts as central relay cells, highly sensitive to low levels of IL-1 α/β, even in the presence of high concentrations of the antagonist IL-1RA, and able to promote skin inflammation through the release of neutrophil-attracting chemokines.

Abbreviations: HMVEC, Human dermal microvascular endothelial cells; NHDF, Normal human dermal fibroblasts; NHEK, Normal human epidermal keratinocytes; NHEM, Normal human epidermal melanocytes; PBMC, Peripheral blood mononuclear cells; PMN, Polymorphonuclear cells; RHS, Reconstituted human skin; WT, Wild-type.

Materials and methods

Cell cultures, cytokines and reagents

Primary normal human epidermal keratinocytes (NHEK), normal human dermal fibroblasts (NHDF), normal human epidermal melanocytes (NHEM) and human dermal microvascular endothelial cells (HMVEC) were isolated from human skin and cultured as described in supplementary materials and methods (17–19). Peripheral blood mononuclear cells (PBMC) and polymorphonuclear neutrophils (PMN) were typically isolated from whole blood of healthy adult volunteers using Ficoll density gradient centrifugation. Subsequently, $CD4^+$ T cells and $CD14^+$ monocytes were isolated from PBMC through positive selection by magnetic cell sorting using MACS isolation kits (Miltenyi Biotec). Reconstituted human skins (RHS) were obtained from Qima-Bioalternatives (Gençay, France). Briefly, a collagen (from rat tail, Institut de Biotechnologies Jacques Boy) lattice containing fibroblasts is cast in a 0.5 cm^2 culture insert (Millipore). After polymerization, keratinocytes are seeded onto the lattice and the latter is incubated at 37°C/5% CO_2 for 48 h. The medium in the inserts is then removed allowing the reconstructed skins to be placed in an air/liquid interface condition. The reconstructed skins are then grown for 7 days, changing the medium under the inserts every 2 or 3 days. The epidermal surface of RHS was then scarified with a scalpel under

sterile condition and supernatants were collected 48 h after scarification for IL-8 measurements.

All recombinant cytokines (IL-1α, IL-1β, IL-36γ, IL-18, IL-33) were purchased from R&D systems. Anti-IL-1R1 polyclonal antibody (PA5-46930) and goat IgG isotype control were purchased from Thermo Fischer scientific.

ELISA for the detection of human IL-1α, IL-1β, IL-6, IL-8, IL-36γ, IL-18, IL-33, IL-1Ra, IL-18BPa, IL-36Ra and mouse CXCL-1, in cell culture supernatant or keratinocyte extract was carried out according to the manufacturer's instructions (R&D Systems).

RNA isolation and transcriptional analysis

Total RNA was extracted from cell cultures or mouse skin tissues using TriPure Isolation Reagent® (Roche, Merck) and treated with DNase I (0.05 U/ml; Clontech). RNA was reverse-transcribed with « Transcriptor Reverse Transcriptase » (Roche) and transcripts were amplified and quantified using the LightCycler-FastStart DNA Master Plus SYBR Green I kit on a LightCycler 480 instrument (Roche). Oligonucleotides were designed with Primer 3 and-Blast software and purchased from Merck (Sigma-Aldrich) or Eurogentec. Primer sequences to amplify human IL-8 were 5'-CTCTTGGCAGCCTTCCTG-3'(Forward) and 5'-TTGGGGTCCAGACAGAGC-3'(Reverse). Forward and reverse primer sequences for mouse gene amplification were indicated in Supplemental Table 1. Samples were normalized to the expression of the control housekeeping gene GAPDH.

For Affymetrix analysis, RNA was extracted using the NucleoSpin RNA kit (Macherey-Nagel), according to the manufacturer's instructions. The concentration and the quality of extracted RNA was determined for each sample using a 2100 bioanalyzer system (Agilent technologies). Probes were prepared and hybridized to the Affymetrix Human Genome U219 Array as recommended by the manufacturer. Equal amount and quality of RNA was used for each sample, constituting the first step of normalization. Data were obtained from measurements of the relative signal strength for probes containing ~30,000 transcripts. The raw intensity values are background corrected, log2 transformed and then quantile normalized according to the RMA algorithm. Then, a linear model is fit to the normalized data to obtain an expression measure for each probe set on each array. Data were submitted to the Gene Expression Omnibus Database (GSE111191) and to the Database for Annotation, Visualization and Integrated Discovery (DAVID) for clustering analysis (20).

Keratinocyte extract preparation

NHEK were seeded at 80,000 cells/cm2 in T25 Flasks in supplemented keratinocyte-SFM medium. The culture medium was renewed 24 hours later. The next day, the medium was replaced by keratinocyte-SFM medium containing no supplements and cells were incubated for 48 hours (8 ml/T25 Flask). The cell-free culture supernatant was collected and stored at -80 C until use. Cells were trypsinized, washed in PBS solution and then centrifuged. The cell pellet was lysed using freeze/thaw procedure and sonication in 8 ml of ultrapure water for each flask (this volume corresponding to the same volume as the initial culture medium volume). The obtained cell lysate was aliquoted and stored at -80 C until use. The concentration of IL-1α was determined for each keratinocyte extract and normalized from one preparation to another.

Cell stimulation with cytokines or keratinocyte extract

NHEK, NHDF, NHEM and HMVEC were all seeded at 150,000 cells/well in 24-well plates (Nunc). After 24 hours of incubation, the culture medium was renewed or replaced by assay medium, and cells were incubated for 24 hours. The next day, cells were incubated for 48 hours in presence or not of the cytokines or keratinocyte extract. On NHDF, keratinocyte extract was also tested in presence of an anti-IL1R1 neutralizing polyclonal antibody or the isotype control.

Blood cells were seeded in all assays at 200,000 cells/well in 96-well plates ($1x10^6$ cells/ml) and incubated for 48 hours in presence or not of the stimulants (interleukins of IL1Fm or keratinocyte extract). The treatments with the stimulants were performed one hour after the seeding for 48 h.

At the end of stimulation, cell culture supernatants were harvested for ELISA quantification of IL-8 and/or IL-6 and when necessary and cell layers were used for RNA extraction and gene expression profiling.

Cell migration assay

PMN migration was assessed using Boyden chamber transmigration system. Briefly, PMN freshly isolated from whole blood, were labeled using calcein-AM (Invitrogen, Thermo Fischer scientific), seeded onto the upper compartment of 3 µm-porous membrane inserts. Culture medium containing chemoattractant reference IL-8 or fibroblast culture supernatants was placed in the lower compartment and the cells were incubated for 90 minutes. Cells which have migrated through the membrane were quantified by measuring the fluorescence intensity (λ_{exc} 485 nm, λ_{em} 530 nm) of the recipient compartment using a fluorescent microplate reader (Spectramax, Molecular Devices).

In vivo experiments

Male and female wild-type and IL-1R1-deficient C57Bl/6 mice were bred in the specific pathogen-free animal facility at

CNRS (TAAM UPS44, Orleans, France). Mice were provided food and water ad libitum and maintained on a 12 h light/dark cycle. Experimental procedures were approved by French Government's ethical and animal experiment regulations and were submitted to the ethics committee for animal Experimentation of "CNRS Campus Orleans" (CCO) under number APAFIS#30196-2019021818223038.

For experiments, 8–14-week-old mice were transferred to experimental animal facility. Under anesthesia by intraperitoneal injection of a xylazine (10 mg/mL)/ketamine (1 mg/mL) solution (100 µL/10 g of animal weight), the back skin of mice was shaved, and remaining hairs were removed using a depilatory cream (Veet@, Reckitt Benckiser). The skin was antiseptically cleaned before gentle scarification with a sterile scalpel for epidermal lesion (star-shaped scar to facilitate the observation of lesions on skin sections for subsequent immunohistological analysis). Twenty-four hours later, mice were euthanized and both lesioned back skin and non-lesioned skin were collected and snap-frozen in liquid nitrogen and stored at -80°C for further transcriptional and immunohistofluorescence analysis.

Immunohistofluorescence

Immunohistofluorescence experiments were performed on cryopreserved mouse skin samples. Five-micrometer sections were cut from a tissue block. Sections were fixed in acetone/methanol and staining was performed using monoclonal antibodies against Mouse Gr1 (1:100; BD Biosciences; 550291) and vimentin (1:100; Abcam; ab92547). These stainings were detected using appropriate secondary antibodies (goat anti-rat IgG Alexa 488 conjugated secondary antibody for Gr1 and Alexa 568-conjugated goat anti-rabbit for vimentin). Sections were observed using a NIKON Ci microscope. The images were captured using a NIKON DS-Ri2 and processed with NIS Elements software.

For quantitative analyses, the intensity of Gr1 staining was measured in five representative areas for each section using the Image J software (National Institute of Health, USA).

Statistical analyses

Statistical analysis of significance was calculated using either Mann & Whitney's test or for *in vivo* experiments, the Kruskal-Wallis one-way ANOVA test with a Bonferroni post-test. The p values < 0.05 were considered as significant, and all data are represented as mean ± SEM. Statistical analyses were performed using Excel and GraphPad 9 software (Prism).

Results

Expression of cytokines and receptors of the IL-1 family by skin cells

Before modelling the epidermal lesion at the cellular level, we first determined the mRNA expression profiles of the IL-1 family members and their receptors by the most abundant skin cells, including primary epidermal keratinocytes, dermal fibroblasts, melanocytes, and dermal microvascular endothelial cells isolated from human skin, all cultivated *in vitro* in physiological conditions (Figures 1A–D). As expected, keratinocytes were found to express IL-1α, IL-1β, IL-18 and IL36G at high levels compared to the other skin cells studied in which the levels of the proinflammatory cytokines were low or undetectable. Keratinocytes were also the only skin cells to express significant levels of the regulatory/antagonist cytokines IL-1RA (IL-1RN) and IL-36RN. By contrast, dermal fibroblasts represented by far the cell population expressing the highest level of the IL-1R1 chain together with the IL-1RAP chain (also named IL-RAcP or IL-1R3) to form the functional receptor that binds both IL-1α and IL-1β (Figures 1A–D). The expression of receptors of the IL-1 family in the other cell types was detectable but at much lower levels. Of note, none of the analyzed skin cells expressed significant levels of IL-1R2, a decoy receptor for IL-1. For comparison, we also analyzed the expression of IL-1 family members in immune blood cells (PBMC, $CD4^+$ T cells, monocytes and polymorphonuclear cells (PMN), Supplementary Figure 1). Among proinflammatory cytokines, all blood cell types expressed significant amounts of IL-1β and IL-1α, although at a lesser extent than keratinocytes. Most blood cells also expressed regulatory/antagonist cytokines and significant levels of IL-1R1 receptor (together with IL-1RAP), but most strikingly the expression profile of blood cells clearly differed from skin cells due to the significant expression levels of the decoy receptor IL1-R2 (especially in monocytes and PMN).

In conclusion, this transcriptional analysis confirmed that epidermal keratinocytes are the main cells expressing the proinflammatory cytokines IL-1α and IL-1β in the skin and suggests that, among skin cells, dermal fibroblasts could be the strongest responders to IL-1 after epidermis injury in aseptic conditions.

Fibroblasts are the most responsive skin cells to lesioned keratinocytes

To test the hypothesis that dermal fibroblasts could be the strongest responder cells to IL-1, we compared *in vitro* the response of the different populations of cutaneous and immune cells after exposure to keratinocyte extracts. As keratinocytes do not release the proinflammatory cytokines IL-1α and IL-1β in

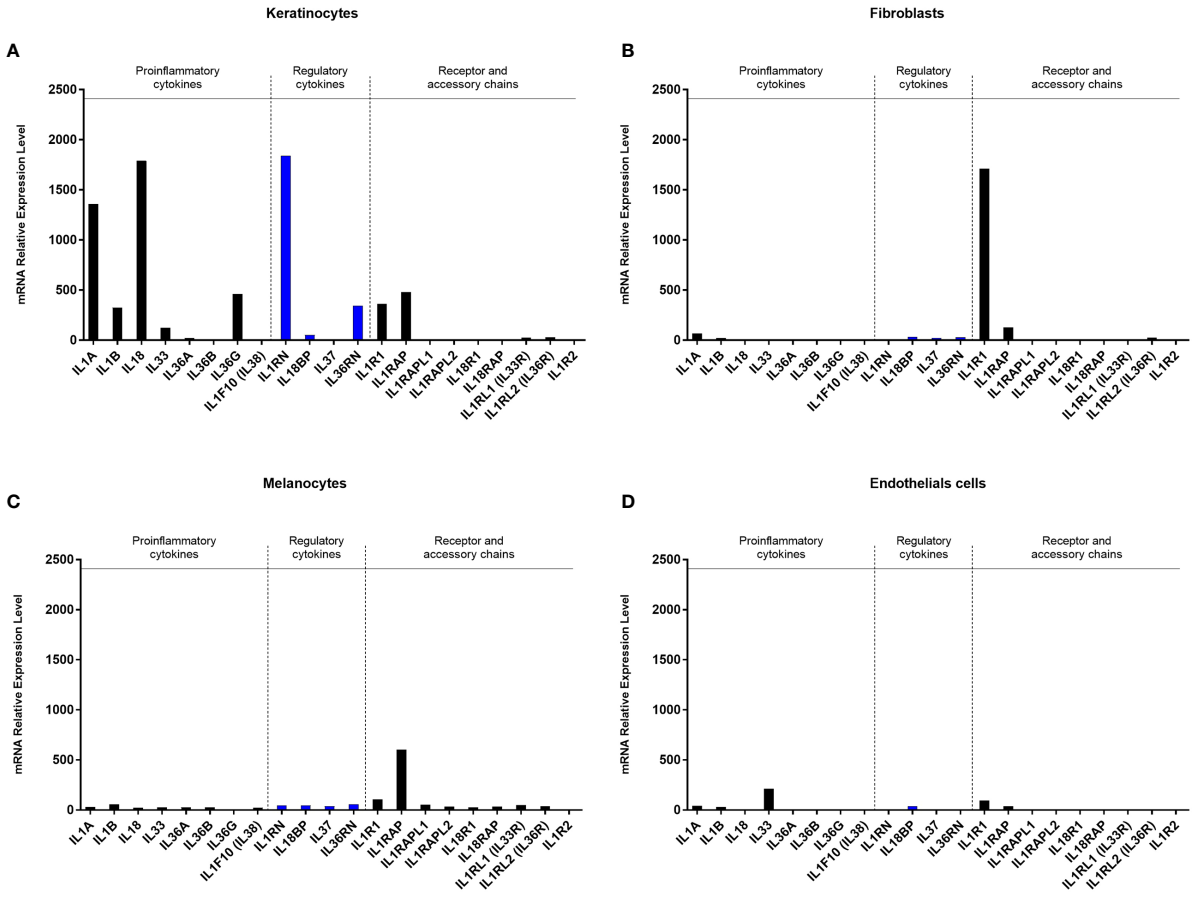

FIGURE 1
Gene expression profiles of proinflammatory cytokines, regulatory cytokines and receptors of the IL-1 family by different skin cell populations. The expression of the IL-1 family members and their receptors was analyzed at the transcriptional level by Affymetrix analysis (hU219 array) after mRNA extraction of primary cultures of epidermal keratinocytes **(A)**, dermal fibroblasts **(B)** melanocytes **(C)** and dermal microvascular endothelial cells **(D)**, all isolated from human skin and cultivated in healthy conditions. Averaged data obtained from 2 independent cultures for each cell type are presented in relative expression of the gene of interest.

homeostatic conditions (Figure 2A), we used keratinocyte lysates for cell stimulation, in which elevated concentrations of IL-1α, IL-1β, IL-18 and IL-36γ were detected (Figure 2B). It is noteworthy that significant concentrations of the secreted regulatory cytokines IL-1RA and IL-36RA were found in culture medium of keratinocytes but even stronger concentrations of IL-1RA were measured in keratinocyte extracts, ~100-fold higher than IL-1α concentrations (Figures 2A, B).

The response of individual skin and immune cells was analyzed by measuring IL-8 (Figure 2C) and IL-6 (Figure 2D) release in culture medium after stimulation with increasing doses of keratinocyte extracts. Our results clearly showed that dermal fibroblasts are the most responsive cells as demonstrated by the massive secretion of IL-8 and IL-6 in the presence of keratinocyte extracts at a dilution of 10% only, corresponding to an IL-1α/β concentration of 20 pg/ml, despite the presence of IL-1RA at a concentration of 2000 pg/ml. Only endothelial cells and monocytes were found to release detectable but much lower amounts of IL-8 and IL-6 after exposure to higher concentrations of keratinocyte extracts (dilutions between 20% to 50%, corresponding to IL-1 concentrations ranging from 40 to 100 pg/ml and IL-1RA concentrations ranging from 4 to 10 ng/ml). This experiment showed that, except fibroblasts, most of the skin cells studied, including keratinocytes, did not respond to keratinocyte extracts.

To model epidermal lesion *in vitro* in a more complex manner, we used a three-dimensional model of human reconstituted skin (RHS), composed of a stratified epidermis developed from human primary keratinocytes cultivated at the air-liquid interface, at the surface of a dermal equivalent (human primary dermal fibroblasts embedded in a collagen lattice). RHS were superficially scarified with a sterile scalpel to induce epidermis injury and IL-8 concentrations were measured in

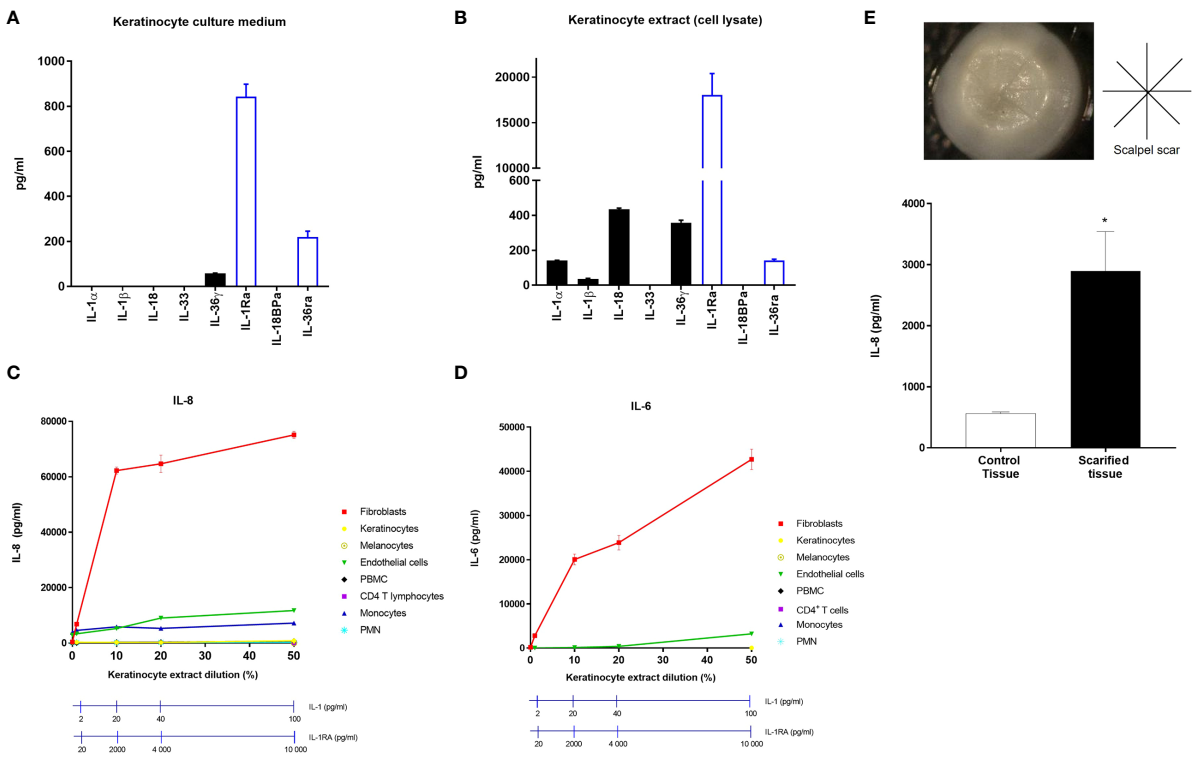

FIGURE 2
Dermal fibroblasts are stimulated by keratinocyte extracts. Concentrations of the IL-1 family members, IL-1α, IL-1β, IL-18, IL-33, IL-36γ, IL-1RA, IL-18BP and IL-36RA were measured by ELISA in culture medium of keratinocytes cultivated in healthy conditions **(A)** or in keratinocyte extracts after cell lysis **(B)**. Several cell types including fibroblasts, keratinocytes, melanocytes, endothelial cells, PBMC, CD4 T cells, monocytes and PMN were stimulated with different dilutions of keratinocyte extracts. IL-8 **(C)** and IL-6 **(D)** concentrations were measured by ELISA in culture medium of stimulated fibroblasts. Concentrations of IL-1 and IL-1RA were measured for each keratinocyte extract dilution and were indicated above **(C, D)**. Reconstituted human skins were scarified with a scalpel under sterile conditions according to the indicated cross-shaped scheme **(E)**. Scars are observable on the representative image of the reconstituted human skin. IL-8 concentrations were measured in the underlying culture medium, 48 h after scarification or in non-lesioned control tissue. Data are representative of three independent experiments done in triplicate. *$P < 0.05$, using the Mann & Whitney's test for comparison between groups.

the underlying culture medium 48 h after scarification (Figure 2E). The epidermal lesion induced a significant release of IL-8 by comparison to the non-lesioned control tissue.

Together, these findings demonstrate that dermal fibroblasts are the most responsive skin cells to epidermal injury in an aseptic context.

IL-1 released by keratinocytes is the most potent inducer of the fibroblast response

To confirm that the response of dermal fibroblasts to keratinocyte extracts is mainly mediated by IL-1, we compared the stimulating effect of single recombinant cytokines on fibroblasts, including IL-1α, IL-1β, IL-36G, IL-18 and IL-33 (Figure 3A). Among these IL-1 family members, IL-1α and IL-1β were the most potent cytokines to induce IL-8 release by fibroblasts, with an increasing effect at concentrations ranging from 10^{-5} to 10^{-1} ng/ml for both cytokines. The stimulating effect of IL-1α/IL-1β reached a plateau from 10^{-1} ng/ml with a massive induction of IL-8 release which remained constant at higher concentrations of IL-1α/IL-1β (IL-8 concentrations above 100 ng/ml). IL-36G was also able to stimulate IL-8 secretion but at higher concentrations than IL-1 (above 1 ng/ml), while IL-18 and IL-33 failed to stimulate fibroblasts. In comparison, a much weaker effect of IL-1α and IL-1β was observed in human primary keratinocytes on IL-8 secretion, with stimulating concentrations observed only above 10^{-1} ng/ml (Figure 3B). Also, the highest concentrations observed for IL-8 release by keratinocytes never exceeded 5 ng/ml.

Considering that IL-1α and IL-1β are the most powerful cytokines of the IL-1 family and that both members have a comparable and redundant activity by binding to the shared ILR1/IL-1RAP receptor, we compared the response of the different cell populations stimulated with IL-1α only, by analyzing IL-8 release in culture medium. We confirmed that dermal fibroblasts were the most responsive cells to IL-1α,

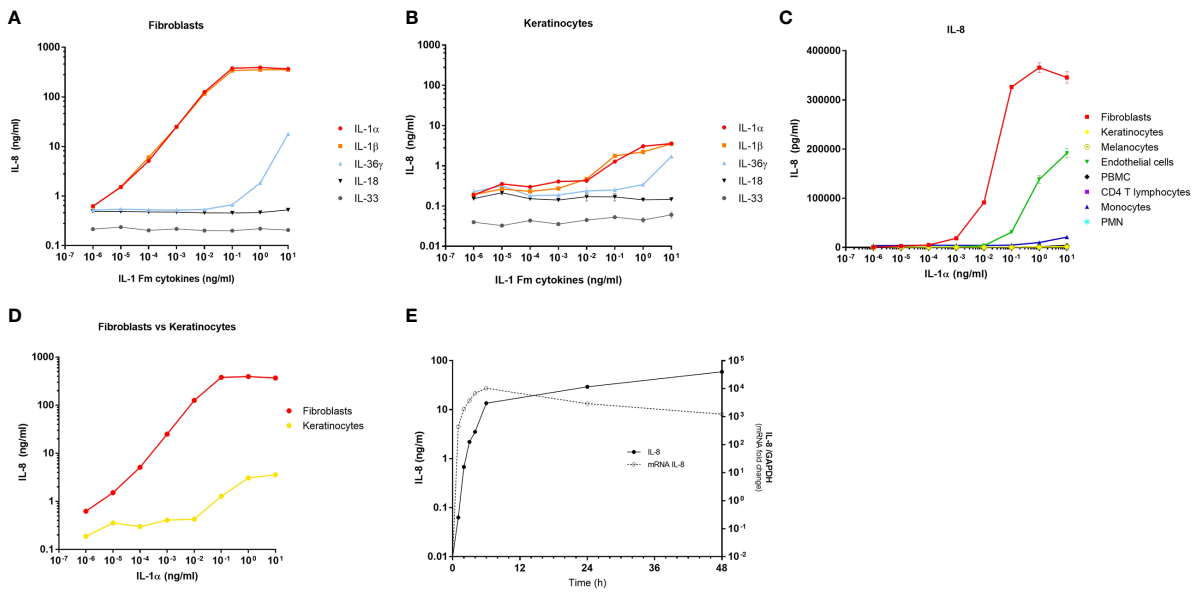

FIGURE 3
Dermal fibroblasts are the best responder skin cells to IL-1α/β. Dermal fibroblasts **(A)** and epidermal keratinocytes **(B)** were stimulated for 24 h with increasing concentrations of IL-1 family members including, IL-1α, IL-1β, IL-36γ, IL-18 and IL-33. The fibroblast response to cytokines was evaluated by measuring IL-8 concentrations in culture medium by ELISA. Several cell types including fibroblasts, keratinocytes, melanocytes, endothelial cells, PBMC, CD4 T cells, monocytes and PMN were stimulated for 24 h with increasing concentrations of IL-1α before measuring IL-8 concentrations in culture medium by ELISA **(C)**. Comparison between fibroblast and keratinocyte responses to increasing concentrations of IL-1α by IL-8 measurements in culture medium after 24 h of stimulation **(D)**. Kinetics of IL-8 mRNA expression and IL-8 protein release by fibroblasts stimulated with 100 pg/ml of IL-1α **(E)**. IL-8 mRNA expression was determined by RT-qPCR and data were presented as relative expression to the housekeeping gene GAPDH. IL-8 dosages in culture medium were performed by ELISA.

followed by endothelial cells, while the other cells were non-responders or low-responders (Figure 3C). This analysis was performed on several cultures of dermal fibroblasts isolated from different anatomical sites (breast, abdomen, ear, foreskin) and from patients with different ages (from 7 months to 51 years) to demonstrate that all fibroblasts tested have the same capacity to respond to IL-1α (Supplementary Figure 2). The comparison between fibroblasts and keratinocytes responses reveals that keratinocytes must be exposed to ~10.000-fold higher concentrations of IL-1α to secrete similar amounts of IL-8 by fibroblasts (Figure 3D). In addition, starting from the concentration of 10^{-3} ng/ml of IL-1α, the response of fibroblasts is already ~100-fold more elevated than those of keratinocytes. Finally, by measuring at several time points both IL-8 expression at the transcriptional level and IL-8 release at the protein level, we showed that the fibroblast response to IL-1α exposure is very fast, with a maximum effect observed in few hours only, including at the protein level (Figure 3E).

We next investigated whether the effect of keratinocyte extracts on dermal fibroblasts is mediated only by IL-1α/β or also by other potential proinflammatory mediators. We first compared the transcriptomic profiles of unstimulated and stimulated fibroblasts by analyzing the expression of ~30.000 transcripts by microarray experiments. Compared to control cells, fibroblasts stimulated by keratinocyte extracts or by recombinant IL-1α presented highly similar profiles of gene regulation, explaining why both stimulated conditions (e.g., keratinocyte extracts vs IL-1α) showed an overlaying profile (Figure 4A). Interestingly, among the top twenty genes whose expressions were the most upregulated, eight were coding for chemokines including many neutrophil-attracting chemokines (Supplementary Table 1). We further stimulated fibroblasts with increasing concentrations of keratinocyte extracts (Figure 4B) or recombinant IL-1α (Figure 4C) in the presence of a blocking anti-IL-1R1 antibody or an isotype control. Since the anti-IL-1R1 antibody blocked efficiently IL-8 secretion by fibroblasts after keratinocyte extracts stimulation, we can state that the biological effect of keratinocyte extracts was specifically mediated by IL-1α/β.

Fibroblasts are very sensitive to low concentrations of IL-1 even in the presence of high concentrations of IL-1Ra

The analysis of the composition of keratinocyte extracts realized above revealed high concentrations of the antagonist

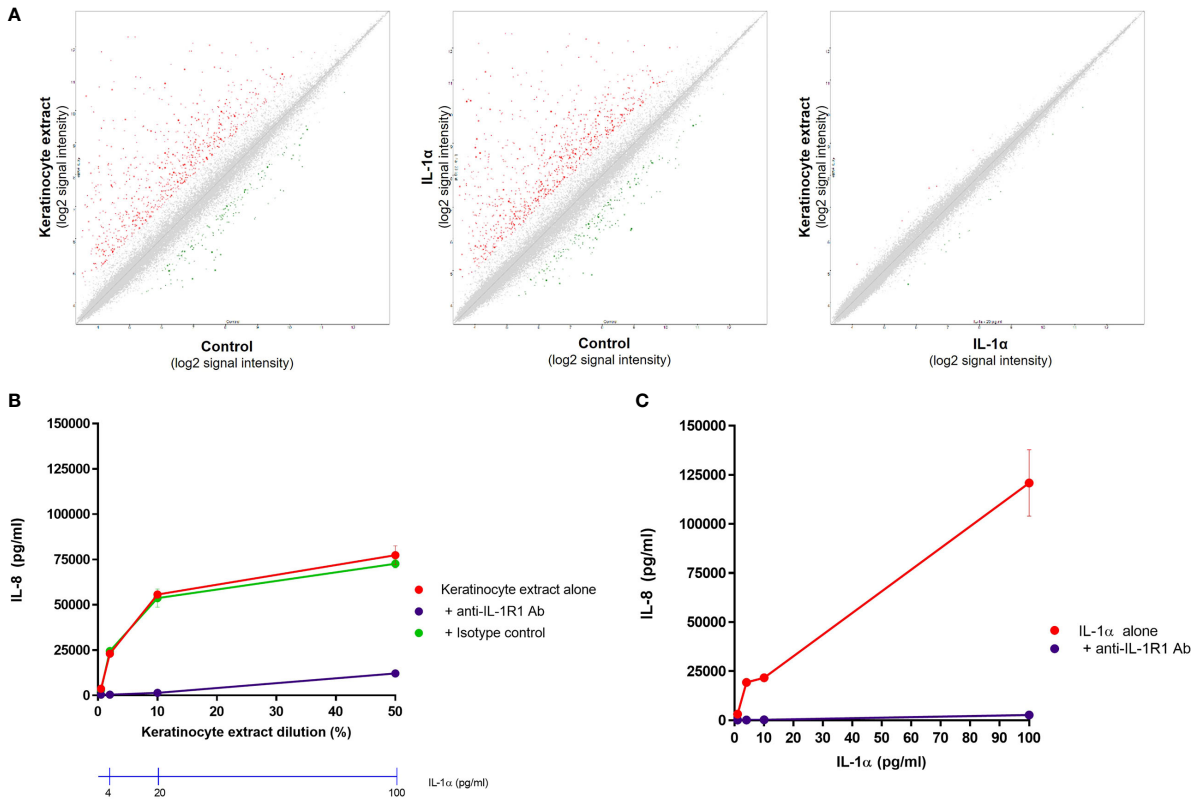

FIGURE 4
The response of dermal fibroblasts to keratinocyte extracts is mainly mediated by IL-1α/β. Complementary Affymetrix microarray experiments (hU219 array) were performed to analyze the expression of 36000 transcripts (corresponding to ~20000 genes) by normal dermal fibroblasts (control) and fibroblasts stimulated either by keratinocyte extracts (tested at a dilution of 10%, containing ~20 pg/ml of IL-1α) or IL-1α (tested at 20 pg/ml). Comparisons of the transcriptional profiles between two conditions were shown, with up-regulated genes shown in red and down-regulated genes in green **(A)**. Dermal fibroblasts were stimulated by different dilutions of keratinocyte extracts **(B)** or increasing concentrations of IL-1α **(C)** in the presence of an anti-IL-1R1 blocking antibody or an isotype control. Corresponding concentrations of IL-1α in keratinocyte extracts were also indicated **(B)**.

IL-1RA, which is known to bind to the IL-1α/β receptor and block its activity. However, although the concentrations of IL-1RA were 100-fold more elevated than IL-1 concentrations in keratinocyte extracts, we showed that the activity of IL-1α/β on fibroblastic cells was not abolished. This interesting finding led us to evaluate *in vitro* the responsiveness of dermal fibroblasts to IL-1α exposed to increasing doses of IL-1RA. Thus, we analyzed IL-8 release by fibroblasts, and keratinocytes for comparison, after stimulation with different concentrations of IL-1α (from 1 pg/ml to 10 ng/ml) in the presence of IL-1RA at different ratios (1, 2, 5, 10, 20 and 100) (Figure 5A). Up to an IL-1RA/IL-1α ratio of 10, the activity of IL-1α remained unaffected. The activity of IL-1α was significantly affected at all tested concentrations (except the lowest) only when the concentration of IL-1RA reached 100-fold the concentration of IL-1α (IL-1RA/IL-1α ratio of 100 as in the keratinocyte extracts), but it should be noted that the activity of IL-1α still remained elevated (similar to a 10 pg/ml IL-1α stimulation without IL-1RA with an IL-8 secretion above 10 ng/ml). By contrast, when keratinocytes were stimulated with IL-1α at concentrations of 1 and 10 ng/ml, a blocking effect of IL-1RA was rapidly observed already at an IL-1RA/IL-1α ratio of 1. For an IL-1RA/IL-1α ratio ≥ 10, the stimulating effect of IL-1α on IL-8 secretion was almost abolished (Figure 5B). Altogether, these results confirmed the high responsiveness of fibroblasts to IL-1α, even in presence of elevated concentrations of the antagonist IL-1RA, a feature which was not observed in keratinocytes.

IL-1-activated fibroblasts have the capacity to attract neutrophils both *in vitro* and *in vivo*

Finally, we carried out functional experiments to demonstrate that IL-1-activated fibroblasts have the capacity to

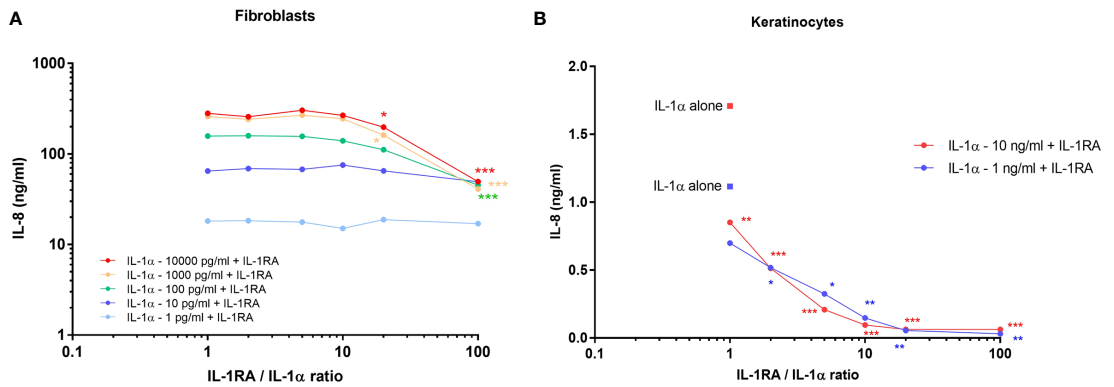

FIGURE 5
Dermal fibroblasts are highly sensitive to IL-1α despite the presence of elevated concentrations of IL-1RA. Dermal Fibroblasts **(A)** and keratinocytes **(B)** were stimulated for 24 h with increasing concentrations of IL-1α in presence of different concentrations of IL-1RA at IL-1RA/IL-1α ratios ranging from 1 to 100. The concentrations of IL-8 released by stimulated cells were measured by ELISA in culture medium. *P < 0.05, **P < 0.01, ***P < 0.001 using the Mann & Whitney's test.

elicit an inflammatory response by attracting immune cells on the site of injury after aseptic epidermal lesion. As previously shown, fibroblasts responded to IL-1α by overexpressing numerous neutrophil-attracting chemokines, particularly IL-8 which has been used constantly as a read-out parameter for our *in vitro* studies. To determine the capacity of activated fibroblasts to attract neutrophils, we firstly performed *in vitro* cell migration assays using Boyden chambers. PMN were seeded in the upper compartment, while the lower compartment contained different dilutions of culture supernatants of unstimulated fibroblasts (control supernatant), supernatants from fibroblasts stimulated either with keratinocyte extracts or IL-1α, or culture medium containing different concentrations of IL-8 (positive control). Culture supernatants of fibroblasts stimulated with 100 pg/ml of IL-1α or keratinocyte extract (containing approximatively 100 pg/ml of IL-1α), contained similar concentrations of IL-8 (~ 100 ng/ml), IL-6 (~ 50 ng/ml) (Figure 6A) and the metalloproteinase MMP- also involved in cell migration (~ 40 ng/ml, data not shown). Boyden chamber migration assays showed the capacity of 10%-diluted supernatants from stimulated-fibroblasts to attract neutrophils in the lower compartment at the same level as IL-8 at a concentration of 10 ng/ml (Figure 6B). A weak but significant cell migration could be observed when supernatants of stimulated fibroblast were used at a 1% dilution or IL-8 at a concentration of 1 ng/ml.

To confirm these results *in vivo* and to demonstrate the major role of IL-1 in aseptic skin inflammation, we modelled the epidermal lesion by scarifying superficially the epidermis of the depilated back skin of C57BL6/J wild-type (WT) mice or IL-1R1-deficient mice using a sterile scalpel (Figure 7A). In these transgenic mice, we previously verified *in vitro* that murine primary keratinocytes were unable to respond to IL-1 (Supplemental Figure 3). Twenty-four hours after scarification, the lesioned and unlesioned skins were collected and the detection of neutrophils was analyzed in skin sections by immunohistofluorescence using Gr1 antibody. A strong infiltration of Gr1-positive cells could be observed in the dermis of the lesioned skins of WT mice (Figures 7B, C); however, in the lesioned skin of IL-1R1-deficient mice, the infiltration of neutrophils was significantly lower and almost absent in unlesioned skins in both strains of mice. A transcriptional analysis of inflammatory mediators was also performed on unlesioned and lesioned skins of WT and IL-1R1-deficient mice 24 h after scarification (Figure 7D). While an overexpression of neutrophil-attracting chemokines (e.g., CXCL-1/2/3), inflammatory cytokines (e.g., oncostatin M, IL-6, TNFα, IL-1α, IL-1β) and the anti-inflammatory IL-1RA could be observed in the lesioned skin of WT mice, these overexpressions were almost abolished in the lesioned skins of IL-1R1-deficient mice at similar levels to those of unlesioned skins ($p < 0.01$ using the Mann & Whitney test for all genes tested, excepted for IL-6 ($p < 0.05$), and CD3 (no significant difference). Consistently with our observation by immunohistofluorescence, the expression of the Gr1 marker (Ly-6G) was also found reduced in the lesioned skin of IL-1R1-deficient mice compared to WT mice. By contrast, no difference in CD3 expression could be observed suggesting that the IL-1-mediated skin inflammation is not associated with T cells and adaptative immunity. Altogether, these *in vivo* results reinforce our *in vitro* data on the major contribution of IL-1α/β in sterile inflammation by attracting neutrophils to the site of epidermis injury.

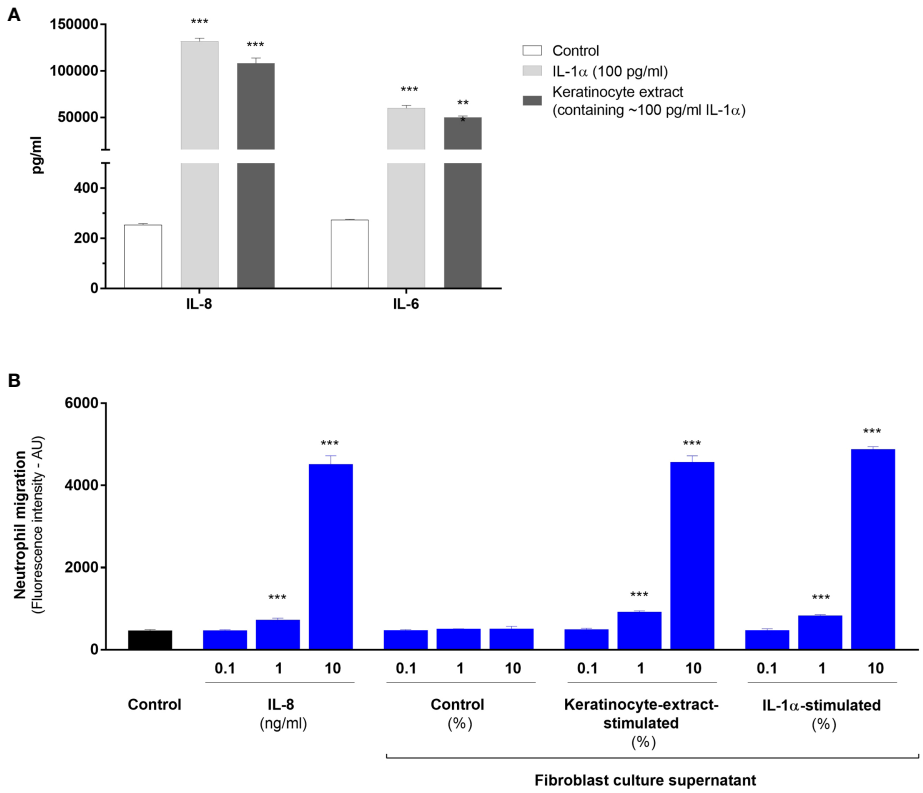

FIGURE 6
IL-1-activated fibroblasts have the capacity to attract neutrophils *in vitro*. Concentrations of IL-8 and IL-6 were determined by ELISA in culture supernatants from dermal fibroblasts stimulated with IL-1α at a concentration of 100 pg/ml or a half-diluted keratinocyte extract containing IL-1α at a similar concentration of 100 pg/ml **(A)**. Analysis of cell migration determined by Boyden chamber assays **(B)**. Polymorphonuclear cells were seeded in the upper compartment for migration and the lower compartment contained either culture medium (control), or different concentrations of IL-8, control supernatant of unstimulated fibroblasts or supernatants from fibroblasts stimulated either with IL-1α (100 pg/ml) or a half-diluted keratinocyte extract. Data were obtained from 2 independent experiments done in triplicate and presented as mean fluorescence intensity ± SEM. ***$P < 0.001$ using the Mann & Whitney's test.

Discussion

The role of IL-1 in inflammatory processes has been described for a long time and has led to substantial body of literature (21). In the context of sterile inflammation after tissue injury on which we have focused, Chen and colleagues reported that dying lymphoblastic cells have the capacity to drive an acute neutrophilic and monocytic inflammatory response when they were injected intraperitoneally to mice (16). They demonstrated that the neutrophil response was dependent on IL-1α and required IL-1R expression on non-bone marrow-derived cells, suggesting the involvement of IL-1-sensitive cells playing an intermediate role in the inflammatory cascade that remain to be determined. In a model of hypoxia-induced cell death, IL-1α and IL-1β were both shown to be released by dying keratinocytes to trigger sterile inflammation along with neutrophil and macrophage recruitment (15). However, the nature of the potential IL-1-responder cells was not determined in this study. Therefore, we have investigated the role of IL-1 released by keratinocytes after epidermal injury to provide new insights on the molecular and cellular mechanisms of sterile skin inflammation and to identify potential important relay cells in this process. We first analyzed the mRNA expression profiles of cytokines and receptors of the IL-1 family in different skin cell populations and in cells of hematopoietic origin for comparison. Unsurprisingly, we found that keratinocytes are the main source of IL-1α and IL-1β in the skin, as well as IL-18, IL-33 and IL-36γ, as previously described (5, 9–11). More interestingly, we show that dermal fibroblasts have the highest expression level of the IL-1R1 chain compared to keratinocytes, melanocytes and skin-isolated endothelial cells. Our results are in accordance with a previous study in which the expression of the IL-1R1 chain was analyzed in PBMC and skin-isolated cells (22). This expression level in fibroblasts was comparable to those of neutrophils, suggesting that these cells might be a good target for IL-1α and IL-1β released by injured keratinocytes. To test this

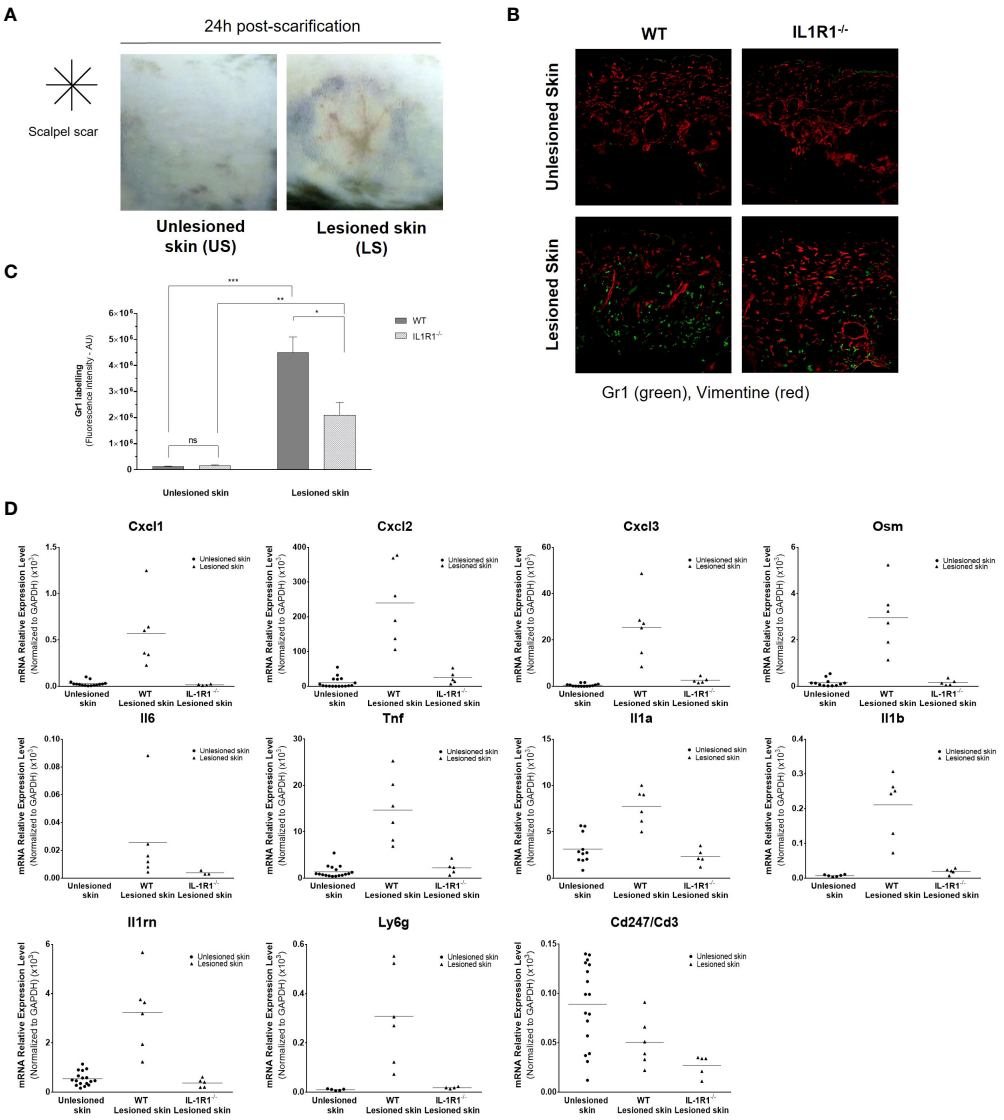

FIGURE 7
Aseptic epidermal lesion induces skin infiltration of neutrophils in an IL-1-dependent manner. The epidermis of the back skin of WT and IL-1R1-deficient (IL-1R1$^{-/-}$) mice was scarified in aseptic conditions using a sterile scalpel. Representative pictures of mouse unlesioned skin and the lesioned back skin of mice 24 h after a cross-shaped scarification **(A)**. Immunofluorescence staining of Gr1-positive neutrophils (in green) and the mesenchymal marker vimentin (in red), in skin sections of unlesioned and lesioned skins of WT and IL-1R1-deficient mice **(B)**. Quantitative analysis of Gr1-specific fluorescent labelling in unlesioned and lesioned skin sections of WT and IL-1R1-deficient mice **(C)**. Transcriptional analysis by RT-qPCR after mRNA extraction from lesioned back skins of WT and IL-1R1-KO mice and unlesioned skins (both from WT and IL-1R1-KO mice) 24 h after scarification **(D)**. The expression of *CXCL1*, *CXCL2*, CXCL3, *OSM*, *IL-6*, *TNFα*, *IL-1α*, *IL-1β*, *IL-1RA*, *Ly6G* and *CD3ζ (CD247)* was analyzed and expressed as mean ± SEM relative expression to the housekeeping gene *Gapdh*. *$P < 0.05$, **$P < 0.01$, ***$P < 0.001$ using the Mann & Whitney's test.

hypothesis, we exposed the different skin cells to protein extracts of lysed keratinocytes which contained significant concentrations of IL-1α, IL-1β, IL-18, IL-33 and IL-36γ, with IL-1α concentrations similar to those measured in supernatants of hypoxia-induced dying keratinocytes (15). Although these cytokine concentrations are elevated and certainly do not reflect *in vivo* conditions of physiological and/or pathological keratinocyte death, we exposed cells to different dilutions of keratinocyte extracts and demonstrated that, among these skin cells, dermal fibroblasts were by far the most responsive cells by releasing rapidly the neutrophil-attracting chemokine IL-8 and the proinflammatory cytokine IL-6. Using a more sophisticated *in vitro* model of injured reconstituted human skin, the superficial lesion of epidermis also resulted in IL-8 release. As injured keratinocytes could potentially release other danger-associated molecular patterns or alarmins in addition

to cytokines of the IL-1 family (4), we addressed the question of the real contribution of IL-1α and IL-1β to dermal fibroblast activation. Both cytokines have the highest capacity to stimulate dermal fibroblasts at very low concentrations (from 0.01 pg/ml). When fibroblasts were stimulated with keratinocyte extracts or recombinant cytokines in the presence of anti-IL-1R1 neutralizing antibodies, fibroblast activation was strongly abolished, demonstrating that sterile inflammation following epidermal injury is mainly driven by IL-1α and IL-1β. Of note, skin-derived endothelial cells were identified as the second-best responder cells but to higher concentrations of IL-1 and at a lower intensity than fibroblasts. The capacity of human dermal microvascular endothelial cells was already investigated thirty years ago by Kristensen et al., showing that endothelial cells produced very high, fibroblasts and monocytes intermediate, and keratinocytes low amounts of IL-8 mRNA using a dot blot mRNA hybridization method (23). Using more sensitive and specific techniques at the protein level, we can state that fibroblasts have a higher capacity to respond to IL-1 than endothelial cells.

The contribution of fibroblasts as relay cells in the cascade of sterile inflammation after tissue injury and their capacity to respond to IL-1 has always been neglected or underestimated, most studies focusing on the activity of IL-1 on PBMCs, in particular on neutrophils and monocytes whose activation is essential for tissue repair (15, 16). If keratinocyte-fibroblast interactions have been investigated in wound healing processes, the role of IL-1 released by injured keratinocytes was focused on the regulation of the TGF-β-induced transformation of dermal fibroblasts into myofibroblasts during wound contraction (24). In fact, most studies on dermal fibroblasts as a target of IL-1 were carried out in the context of chronic skin inflammatory diseases. In systemic sclerosis within the fibroblasts play a central role in the pathophysiology, the interplay between pathological keratinocytes and the underlying fibroblasts involving IL-1α was described to be important in the fibrotic process (25). IL-1β has been also found highly expressed in hidradenitis suppurativa skin lesions and targets fibroblasts to modulate gene expression of molecules involved in remodeling of the extracellular matrix, chemokines, adhesion molecules or cytokines (22). Interestingly, in this study, they identified, like us, dermal fibroblasts as the skin-resident cell type harboring the highest number of gene regulation after IL-1β stimulation.

Surprisingly, our results showed the capacity of dermal fibroblasts to respond to low concentrations of IL-1α and IL-1β in the presence of elevated concentrations of the antagonist IL-1RA, although it is known to bind to IL-1R in a competitive manner with IL-1α and IL-1β. Four isoforms of IL-1RA exist, one secreted form and three intracellular forms which can be released by dying cells and compete extracellularly for IL-1R1 binding in a manner similar to the secreted IL-1RA (26). Although our method for IL-1RA dosage do not allow to discriminate between these isoforms, we could detect 100-fold higher concentrations of IL-1RA compared to IL-1α and IL-1β concentrations in our keratinocytes extracts without affecting its capacity to strongly stimulate fibroblasts, whereas the response of keratinocyte to IL-1 was almost abolished in the presence of 10-fold higher concentrations of IL-1RA. This finding might be explained by the difference between IL-1R1 expression levels between both cell types. Only a small fraction of the cell surface heterodimeric IL-1R1/IL1-RAP receptor needs to be bound by IL-1 to induce an activation signal in fibroblasts, even if the majority of the IL-1R1 chains on fibroblast surface are mobilized for IL-1RA binding. Our observation is in agreement with a previous study showing that a 10^4-fold excess of IL1-RA over the level of IL-1α was required to significantly reduce the activity of the agonist cytokine on a murine fibroblastic cell line (27). As this particularity concerns fibroblasts only, this might suggest that IL1-RA released together with IL-1 should protect other skin-resident cells from activation and limit the local inflammatory response.

Finally, we show that dermal fibroblasts are important relay cells for neutrophil recruitment to the site of tissue injury through their capacity to release neutrophil-attracting chemokines. In response to IL-1 or keratinocyte extract exposure, CXCL-1/2/3 and IL-8 were found among the most up-regulated genes by stimulated fibroblasts. Our *in vitro* cell migration assay demonstrated the capacity of culture supernatant of stimulated fibroblasts to attract neutrophils efficiently. As well, our *in vivo* experiments of superficial epidermal lesions on the back skin of IL-1R1-deficient mice confirmed the crucial role of IL-1 in the development of a sterile inflammation and the recruitment of neutrophils in the underlying dermis. However, since neutrophil infiltration was reduced, but not abolished, in the lesioned skin of IL-1R1-deficient mice, this finding suggests that IL-1 is not the only relevant cytokine responsible for neutrophil recruitment and that other proinflammatory mediators may also be implicated. For instance, IL-18 and IL-36 were also found at high concentrations in our keratinocyte extracts. While IL-18 is mostly associated with macrophage recruitment *in vivo* (15), IL-36 has been reported to attract neutrophils in the skin (28). Altogether, our results are in accordance with the previous studies reporting the contribution of IL-1 in sterile inflammation induced by dying cells (15, 16).

In conclusion, we demonstrate that dermal fibroblasts are key relay cells in the cascade of sterile inflammation induced by epidermis injury. They are potent responder cells of IL-1 released by injured keratinocytes, extremely sensitive to low concentrations of IL-1 even in the presence of elevated concentrations of IL-1RA, and contribute to the recruitment of neutrophils involved in tissue repair *via* the secretion of relevant chemokines. Mostly underestimated in the inflammatory process, more attention should be paid to dermal fibroblasts considering their high sensitivity to IL-1, particularly in strategies which consist in regulating IL-1 activity through the use of IL-1RA or neutralizing anti-IL-1R1 antibodies.

Data availability statement

The datasets presented in this study can be found in online repositories. The name of the repository and accession number can be found below: NCBI Gene Expression Omnibus; GSE111191.

Ethics statement

Experimental procedures were approved by French Government's ethical and animal experiment regulations and were submitted to the ethics committee for animal Experimentation of "CNRS Campus Orleans" (CCO) and approved under APAFIS#30196-2019021818223038.

Author contributions

Conceived and designed the experiments: SC-D, F-XB, J-CL, FM and J-FJ. Performed the experiments: SC-D, NP, JG, SC-C, VH, J-FJ. Analyzed the data: SC-D, NP, JG, SC-C, F-XB, VH, J-FJ. Contributed reagents/materials/analysis tools/animals: BR. Wrote the paper: SC-D, VH, J-FJ. All authors contributed to the article and approved the submitted version.

Funding

This work was supported by grants from Qima-Bioalternatives, the University of Poitiers and CNRS, University of Orleans, 'Fondation pour la Recherche Médicale' (EQU202003010405) and European funding in Region Centre-Val de Loire (FEDER N° EX010381). Publication charges were supported by the 'Direction de la Recherche et de l'Innovation' of Poitiers Hospital (CHU de Poitiers).

Acknowledgments

We thank Stéphanie Rose (INEM, CNRS, UMR 7355, Orléans, France) for technical help for animal experimentation, and Sarah Collober (Qima-Bioalternatives) for formatting the figures and the tables of the article.

Conflict of interest

Authors SC-D, NP, JG, SC-C, F-XB and VHA were employed by Qima-Bioalternatives (Qima Life Sciences).

The remaining authors declare that the research was conducted in the absence of any commercial or financial relationships that could be construed as a potential conflict of interest.

The authors declare that this study received funding from Qima-Bioalternatives. The funder had the following involvement with the study: design, collection, analysis, interpretation of data, the writing of this article and the decision to submit it for publication.

Publisher's note

Supplementary material

The Supplementary Material for this article can be found online at: https://www.frontiersin.org/articles/10.3389/fimmu.2022.984045/full#supplementary-material

References

1. Nestle FO, Di Meglio P, Qin JZ, Nickoloff BJ. Skin immune sentinels in health and disease. *Nat Rev Immunol* (2009) 9(10):679–91. doi: 10.1038/nri2622

2. Bernard FX, Morel F, Camus M, Pedretti N, Barrault C, Garnier J, et al. Keratinocytes under fire of proinflammatory cytokines: Bona fide innate immune cells involved in the physiopathology of chronic atopic dermatitis and psoriasis. *J Allergy (Cairo).* (2012) 2012:718725. doi: 10.1155/2012/718725

3. Albanesi C, Madonna S, Gisondi P, Girolomoni G. The interplay between keratinocytes and immune cells in the pathogenesis of psoriasis. *Front Immunol* (2018) 9:1549. doi: 10.3389/fimmu.2018.01549

4. Bertheloot D, Latz E. HMGB1, IL-1alpha, IL-33 and S100 proteins: dual-function alarmins. *Cell Mol Immunol* (2017) 14(1):43–64. doi: 10.1038/cmi.2016.34

5. Kupper TS, Ballard DW, Chua AO, McGuire JS, Flood PM, Horowitz MC, et al. Human keratinocytes contain mRNA indistinguishable from monocyte interleukin 1 alpha and beta mRNA. keratinocyte epidermal cell-derived thymocyte-activating factor is identical to interleukin 1. *J Exp Med* (1986) 164 (6):2095–100. doi: 10.1084/jem.164.6.2095

6. England H, Summersgill HR, Edye ME, Rothwell NJ, Brough D. Release of interleukin-1alpha or interleukin-1beta depends on mechanism of cell death. *J Biol Chem* (2014) 289(23):15942–50. doi: 10.1074/jbc.M114.557561

7. Palomo J, Dietrich D, Martin P, Palmer G, Gabay C. The interleukin (IL)-1 cytokine family–balance between agonists and antagonists in inflammatory diseases. *Cytokine* (2015) 76(1):25–37. doi: 10.1016/j.cyto.2015.06.017

8. Supino D, Minute L, Mariancini A, Riva F, Magrini E, Garlanda C. Negative regulation of the IL-1 system by IL-1R2 and IL-1R8: Relevance in pathophysiology and disease. *Front Immunol* (2022) 13:804641. doi: 10.3389/fimmu.2022.804641

9. Naik SM, Cannon G, Burbach GJ, Singh SR, Swerlick RA, Wilcox JN, et al. Human keratinocytes constitutively express interleukin-18 and secrete biologically active interleukin-18 after treatment with pro-inflammatory mediators and dinitrochlorobenzene. *J Invest Dermatol* (1999) 113(5):766–72. doi: 10.1046/j.1523-1747.1999.00750.x

10. Sundnes O, Pietka W, Loos T, Sponheim J, Rankin AL, Pflanz S, et al. Epidermal expression and regulation of interleukin-33 during homeostasis and inflammation: Strong species differences. *J Invest Dermatol* (2015) 135(7):1771–80. doi: 10.1038/jid.2015.85

11. Johnston A, Xing X, Guzman AM, Riblett M, Loyd CM, Ward NL, et al. IL-1F5, -F6, -F8, and -F9: A novel IL-1 family signaling system that is active in psoriasis and promotes keratinocyte antimicrobial peptide expression. *J Immunol* (2011) 186(4):2613–22. doi: 10.4049/jimmunol.1003162

12. Feldmeyer L, Keller M, Niklaus G, Hohl D, Werner S, Beer HD. The inflammasome mediates UVB-induced activation and secretion of interleukin-1beta by keratinocytes. *Curr Biol* (2007) 17(13):1140–5. doi: 10.1016/j.cub.2007.05.074

13. Kondo S, Sauder DN, Kono T, Galley KA, McKenzie RC. Differential modulation of interleukin-1 alpha (IL-1 alpha) and interleukin-1 beta (IL-1 beta) in human epidermal keratinocytes by UVB. *Exp Dermatol* (1994) 3(1):29–39. doi: 10.1111/j.1600-0625.1994.tb00263.x

14. Cohen I, Rider P, Vornov E, Tomas M, Tudor C, Wegner M, et al. IL-1alpha is a DNA damage sensor linking genotoxic stress signaling to sterile inflammation and innate immunity. *Sci Rep 6 oct* (2015) 5:14756. doi: 10.1038/srep14756

15. Rider P, Carmi Y, Guttman O, Braiman A, Cohen I, Voronov E, et al. IL-1alpha and IL-1beta recruit different myeloid cells and promote different stages of sterile inflammation. *J Immunol* (2011) 187(9):4835–43. doi: 10.4049/jimmunol.1102048

16. Chen CJ, Kono H, Golenbock D, Reed G, Akira S, Rock KL. Identification of a key pathway required for the sterile inflammatory response triggered by dying cells. *Nat Med* (2007) 13(7):851–6. doi: 10.1038/nm1603

17. Boniface K, Lecron JC, Bernard FX, Dagregorio G, Guillet G, Nau F, et al. Keratinocytes as targets for interleukin-10-related cytokines: a putative role in the pathogenesis of psoriasis. *Eur Cytokine Netw* (2005) 16(4):309–19.

18. Gontier E, Cario-Andre M, Lepreux S, Vergnes P, Bizik J, Surleve-Bazeille JE, et al. Dermal nevus cells from congenital nevi cannot penetrate the dermis in skin reconstructs. *Pigment Cell Res* (2002) 15(1):41–8. doi: 10.1034/j.1600-0749.2002.00065.x

19. Huguier V, Giot JP, Simonneau M, Levillain P, Charreau S, Garcia M, et al. Oncostatin m exerts a protective effect against excessive scarring by counteracting the inductive effect of TGFβ1 on fibrosis markers. *Sci Rep 14 fevr* (2019) 9(1):2113. doi: 10.1038/s41598-019-38572-0

20. Huang da W, Sherman BT, Lempicki RA. Systematic and integrative analysis of large gene lists using DAVID bioinformatics resources. *Nat Protoc* (2009) 4(1):44–57. doi: 10.1038/nprot.2008.211

21. Di Paolo NC, Shayakhmetov DM. Interleukin 1alpha and the inflammatory process. *Nat Immunol* (2016) 17(8):906–13. doi: 10.1038/ni.3503 ni.3503

22. Witte-Handel E, Wolk K, Tsaousi A, Irmer ML, Mossner R, Shomroni O, et al. The IL-1 pathway is hyperactive in hidradenitis suppurativa and contributes to skin infiltration and destruction. *J Invest Dermatol* (2019) 139(6):1294–305. doi: 10.1016/j.jid.2018.11.018

23. Kristensen MS, Paludan K, Larsen CG, Zachariae CO, Deleuran BW, Jensen PK, et al. Quantitative determination of IL-1 alpha-induced IL-8 mRNA levels in cultured human keratinocytes, dermal fibroblasts, endothelial cells, and monocytes. *J Invest Dermatol* (1991) 97(3):506–10. doi: 10.1111/1523-1747.ep12481543

24. Werner S, Krieg T, Smola H. Keratinocyte-fibroblast interactions in wound healing. *J Invest Dermatol* (2007) 127(5):998–1008. doi: 10.1038/sj.jid.5700786

25. Aden N, Nuttall A, Shiwen X, de Winter P, Leask A, Black CM, et al. Epithelial cells promote fibroblast activation *via* IL-1alpha in systemic sclerosis. *J Invest Dermatol* (2010) 130(9):2191–200. doi: 10.1038/jid.2010.120

26. Martin P, Palmer G, Rodriguez E, Palomo J, Lemeille S, Goldstein J, et al. Intracellular IL-1 receptor antagonist isoform 1 released from keratinocytes upon cell death acts as an inhibitor for the alarmin IL-1alpha. *J Immunol* (2020) 204(4):967–79. doi: 10.4049/jimmunol.1901074

27. Dripps DJ, Brandhuber BJ, Thompson RC, Eisenberg SP. Interleukin-1 (IL-1) receptor antagonist binds to the 80-kDa IL-1 receptor but does not initiate IL-1 signal transduction. *J Biol Chem* (1991) 266(16):10331–6. doi: 10.1016/S0021-9258(18)99230-6

28. Giannoudaki E, Stefanska AM, Lawler H, Leon G, Hernandez Santana YE, Hassan N, et al. SIGIRR negatively regulates IL-36–driven psoriasiform inflammation and neutrophil infiltration in the skin. *J Immunol* (2021) 207:651–60. doi: 10.4049/jimmunol.2100237

frontiers | Frontiers in Immunology

TYPE Original Research
PUBLISHED 07 October 2022
DOI 10.3389/fimmu.2022.984016

OPEN ACCESS

EDITED BY
Ho Seong Seo,
Korea Atomic Energy Research Institute (KAERI), South Korea

REVIEWED BY
Jae Hyang Lim,
Ewha Womans University, South Korea
Carlo Chizzolini,
Université de Genève, Switzerland

*CORRESPONDENCE
Jean-Claude Lecron,
jean-claude.lecron@univ-poitiers.fr

SPECIALTY SECTION
This article was submitted to Cytokines and Soluble Mediators in Immunity, a section of the journal Frontiers in Immunology

RECEIVED 01 July 2022
ACCEPTED 20 September 2022
PUBLISHED 07 October 2022

CITATION
Lecron J-C, Charreau S, Jégou J-F, Salhi N, Petit-Paris I, Guignouard E, Burucoa C, Favot-Laforge L, Bodet C, Barra A, Huguier V, Mcheik J, Dumoutier L, Garnier J, Bernard FX, Ryffel B and Morel F (2022) IL-17 and IL-22 are pivotal cytokines to delay wound healing of *S. aureus and P. aeruginosa* infected skin. *Front. Immunol.* 13:984016. doi: 10.3389/fimmu.2022.984016

IL-17 and IL-22 are pivotal cytokines to delay wound healing of *S. aureus and P. aeruginosa* infected skin

Jean-Claude Lecron[1,2]*, Sandrine Charreau[1,3], Jean-François Jégou[1], Nadjet Salhi[1], Isabelle Petit-Paris[1], Emmanuel Guignouard[1], Christophe Burucoa[1,4], Laure Favot-Laforge[1], Charles Bodet[1], Anne Barra[1,2], Vincent Huguier[1,5], Jiad Mcheik[1,6], Laure Dumoutier[7], Julien Garnier[3], François-Xavier Bernard[1,3], Bernhard Ryffel[8] and Franck Morel[1]

[1]Laboratoire Inflammation, Tissus Epithéliaux et Cytokines, UR15560, Université de Poitiers, Poitiers, France, [2]Laboratoire Immunologie et Inflammation, Centre Hospitalier et Universitaire (CHU) de Poitiers, Poitiers, France, [3]Qima-Bioalternatives (Qima Life Sciences), Gençay, France, [4]Laboratoire de Bactériologie, Centre Hospitalier et Universitaire (CHU) de Poitiers, Poitiers, France, [5]Service de Chirurgie Plastique, Centre Hospitalier et Universitaire (CHU) de Poitiers, Poitiers, France, [6]Service de Chirurgie Pédiatrique, Centre Hospitalier et Universitaire CHU) de Poitiers, Poitiers, France, [7]De Duve Institute, Université catholique de Louvain, Brussels, Belgium, [8]Laboratoire d'Immunologie et Neurogénétique Expérimentales et Moléculaire (INEM) - Unité Mixte de Recherche (UMR) 7355, Centre National de la Recherche Scientifique (CNRS) et Université d'Orléans, Orléans, France

Introduction: Although the presence of pathogens in skin wounds is known to delay the wound healing process, the mechanisms underlying this delay remain poorly understood. In the present study, we have investigated the regulatory role of proinflammatory cytokines on the healing kinetics of infected wounds.

Methods: We have developed a mouse model of cutaneous wound healing, with or without wound inoculation with *Staphylococcus aureus* and *Pseudomonas aeruginosa*, two major pathogens involved in cutaneous wound bacterial infections.

Results: Aseptic excision in C57BL/6 mouse skin induced early expression of IL-1β, TNFα and Oncostatin M (OSM), without detectable expression of IL-22 and IL-17A/F. *S. aureus* and *P. aeruginosa* wound inoculation not only increased the expression of IL-1β and OSM, but also induced a strong cutaneous expression of IL-22, IL-17A and IL-17F, along with an increased number of infiltrating IL-17A and/or IL-22-producing γδ T cells. The same cytokine expression pattern was observed in infected human skin wounds. When compared to uninfected wounds, mouse skin infection delayed the wound healing process. Injection of IL-1α, TNFα, OSM, IL-22 and IL-17 together in the wound edges induced delayed wound healing similar to that induced by the bacterial infection. Wound

healing experiments in infected Rag2KO mice (deficient in lymphocytes) showed a wound healing kinetic similar to uninfected Rag2KO mice or WT mice. Rag2KO infected-skin lesions expressed lower levels of IL-17 and IL-22 than WT, suggesting that the expression of these cytokines is mainly dependent on γδ T cells in this model. Wound healing was not delayed in infected IL-17R/IL-22KO, comparable to uninfected control mice. Injection of recombinant IL-22 and IL-17 in infected wound edges of Rag2KO mice re-establish the delayed kinetic of wound healing, as in infected WT mice.

Conclusion: These results demonstrate the synergistic and specific effects of IL-22 and IL-17 induced by bacterial infection delay the wound healing process, regardless of the presence of bacteria *per se*. Therefore, these cytokines play an unexpected role in delayed skin wound healing.

KEYWORDS

skin, wound healing, cytokine, Th17, pathogen, inflammation

Introduction

The wound healing process is the final step to restore tissue integrity following the acute inflammation induced by a skin injury, when a chronic inflammatory step is not engaged. The mechanisms and controls of wound healing (proliferation, migration, extracellular matrix protein synthesis, angiogenesis…) are complex and involve collaborative efforts of many cell types (fibroblasts, keratinocytes, immune cells…) and numerous soluble factors (inflammatory mediators, growth factors, cytokines, antimicrobial peptides) produced at the lesion site (1). These mechanisms also depend on the environment of the wound, including the presence of germs capable of using skin wound as a gateway to colonize the body. These germs can modify the inflammatory response, the immune response and the healing process.

It is a common belief that wound bacterial infection is detrimental to wound healing, especially by delaying the process. Beside commensal skin microbiota regulating homeostasis of skin host immune response (2), wound infections can disrupt the host-bacteria equilibrium favoring bacterial growth toward altered wound healing processes. These processes depend on host immune response, bacterial count, species and virulence of bacteria, as well as the synergistic effect of the different species (3). The gram-positive bacteria *Staphylococcus aureus (S. aureus)* is a major pathogen of numerous skin infections such as cellulitis, impetigo or folliculitis that can be complicated by septicemia, whereas the gram-negative bacteria *Pseudomonas aeruginosa (P. aeruginosa)* is responsible for infection of chronic wounds associated with delayed wound healing and cutaneous starting point-nosocomial infections (4, 5). *P. aeruginosa* and *S. aureus* are the two most common causes of chronic wound infection. These both species are frequently found together in wounds and may exhibit synergistic interactions (6–10). Wound infection is a serious public health concern and could originate from operative procedures on the skin during surgery, acute trauma during accidents or chronic pressure ulcers in the context of diabetes.

Wound healing resolution is a medical and surgical challenge, especially in the case of skin infection, whereas wound healing delay or inhibition is a critical concern. The situation is nevertheless more complex since paradoxically, it is known to surgeons that an infected wound should not be closed, and that, if necessary, it be reopened to prevent abscess and bacterial dissemination, summarized about 40 years ago by the plastic surgeon Raymond Villain's famous aphorism "Paix sur la plaie aux germes de bonne volonté" (11).

However, the mechanisms slowing down the wound healing kinetic during infection remain poorly understood, especially if it is caused by bacteria or bacterial derived products intra se, or due to host immune response and the inflammatory mediators released. For about 15 years, the production and role of growth factors and proinflammatory cytokines over skin inflammatory processes have been extensively documented (12), albeit their precise role on the last phase of the inflammatory process –i.e., wound healing- remains partially known (13). Recent studies report potential involvement of IL-17 and/or IL-22 cytokinesin this process, with a delicate balance to secure the beneficial and deleterious effects of these cytokines (14).

By studying wound healing regulation by cinnamaldehyde, Ferro et al. reported that *P. aeruginosa* delayed wound healing and induced IL-17 expression (4). In agreement, exogenous IL-17 led to delayed wound closure (15), whereas this phenomenon is abolished in IL-17A KO mice or with IL-17 blocking mAbs (15, 16). In contrast, it has been suggested that IL-22 could be a

promising therapeutic agent for epithelial repair (17). In a model of type II diabetic db/db mice, systemic administration of IL-22-fc (a fusion protein that prolongs cytokine half-life *in vivo*) accelerated wound healing in S aureus infected wounds (18).

By studying the role of cytokines on cutaneous physiology and physiopathology, we and others have shown that the pro-inflammatory cytokines IL-22, IL-17A and Oncostatin M (OSM) are produced in inflammatory skin and that they target keratinocytes and fibroblasts. They induce the production of antimicrobial peptides (AMP), cytokines and chemokines, promote cell proliferation and migration and inhibit keratinocyte differentiation (19–24). In combination with TNFα and IL-1β, which are also reported to target keratinocytes, IL-22, IL-17A and OSM (M5 cocktail of cytokines) have a powerful synergistic effect on these functions (21, 23). Given their properties, in the present study we have investigated the expression of these cytokines during skin wound healing, and questioned their ability to modulate the process.

By using a mouse model of excisional cutaneous wounds co-infected or not with *S. aureus* and *P. aeruginosa*, we show that the infection specifically increases the expression of IL-17A, IL-17F and IL-22, and that these cytokines are responsible for the delayed wound healing observed in infected wounds. We discuss the beneficial effects of an acceleration or slowing down of the healing kinetics in view of developing new therapeutic approaches to skin infections and scarring.

Materials and methods

Bacterial strains and culture

Cultures of *S. aureus* (ATCC 29213) and *P. aeruginosa* (ATCC 27853) were prepared by inoculating Mueller-Hinton agar growth medium (Biorad) and incubated overnight at 37°C. For wound inoculation, a bacterial mixture containing both strains in equal proportions was prepared in 1X PBS (Dulbecco) by resuspending each strain at a final density of 2.5 x10^8 CFU/ml. Bacterial concentration was determined by measuring the absorbance at 600 nm using an Ultrospec-10 spectrophotometer (Amersham Biosciences) and by colony-forming unit (CFU) counts for each strain controlled by serial 10-fold dilutions of the bacterial suspensions and plating on either MH (Mueller Hinton)/vancomycin and CNA (Columbia Naladixic Acid) selective agar plates.

Animals

Eight to ten-week-old C57BL/6J mice were purchased from Janvier Labs (Le Genest, France). Mice were acclimatized for at least 1 week before experiments. Rag2KO, IL-17R and IL-17R/IL-22KO mice were provided by Marc Le Bert (INEM, CNRS, Orléans, France). IL-22KO mice were from L Dumoutier (de Duve Institute, Belgium) All transgenic mice and their WT littermates were bred and housed in the animal facility of Poitiers University (Prebios), under specific pathogen-free conditions and maintained on a 12 h light/dark cycle, with food and water ad libitum. Protocols and animals were approved by the regional ethics committee for animal experimentation (COMETHEA-CE86) under the agreement number CE-2012-21.

Excisional skin wounding, bacterial infections and measurement of wound areas

After anesthesia by an intraperitoneal injection of a xylazine (10 mg/ml)/ketamine (1 mg/ml) solution (100 µl of this solution/10 g of animal weight), the back skin of mice was shaved and remaining hairs were removed using a depilatory cream (Veet@, Reckitt Benckiser, France). Four excisional wounds were performed by puncturing the skin with a 4 mm-round punch (Stiefel) and removing the skin biopsy. Twenty microliters of the bacterial suspension (5X10^6 CFU) or the PBS control solution were directly applied on each wound. After spreading of the bacterial mixture on the wound, mice were housed individually to avoid grooming behavior of infected wounds.

To follow wound healing kinetics, the surface of each wound was measured daily using Image J software on pictures of back skin of mice including a meter stick as reference. The wound area was determined in mm^2.

To analyze the effect of cytokines on wound healing kinetics, three injections of 10 µl of carrier-free recombinant cytokine solution diluted in 1X PBS at a final concentration of 25 µg/ml (IL-17A, IL-17F, OSM, TNFα, IL-22 and IL-1α; all from R&D systems, Europe) or combinations were performed in each wound edges. Control mice received PBS injections.

For RNA isolation, each wound biopsy was collected using a 6 mm punch (Stiefel) after mouse euthanasia, rapidly snap-frozen and stored in liquid nitrogen. For flow cytometry analysis, the whole skin containing the four excisional wounds (representing an 8 cm^2 surface) was collected five days after excision and wound infection, in RPMI medium supplemented with 10% of Fetal Calf Serum (FCS), 1% penicillin/streptomycin (P/S) solution and 200 ng/ml of gentamycin (all products were purchased from Invitrogen) and stored at 4°C until cell dissociation. For bacterial analysis, the 6 mm punch was dissociated in 0.5ml PBS and cell count was performed as described above in bacterial strains and culture.

Patients

This study included adult patients presenting uninfected (n=12) or infected wounds (n=7). Skin biopsies were obtained

during surgical treatment of the wound. For uninfected wounds, sampling was performed from surgical edge wounds without pathological healing process. For infected wounds, edge sampling was performed during their surgical trimming before antibiotherapy. A swab was sampled for culture bacteriological analysis in the Microbiology Laboratory of the Poitiers Hospital. Two patient wounds were infected by three germs (hemolytic *Streptococcus-Proteus mirabilis-Corynebacterium spp and S. epidermitis- Propionobacterium acnes-S. aureus*) and the other ones were infected with *S. aureus*. Normal skin samples were obtained from surgical samples of abdominoplasty or breast reduction surgery and were used as controls (n=16). The biopsies were immediately frozen in liquid nitrogen before RNA extraction.

All of our studies involving human tissues were approved by the Institutional Ethics Committee on Human Experimentation (Comité de Protection des Personnes Ouest III) of the Poitou-Charentes Region. This study was conducted according to the Declaration of Helsinki principles, and oral informed consent was obtained from participants before inclusion.

RNA isolation and real-time quantitative RT-PCR

Skin total RNA was isolated and reverse transcribed as previously described (21). Quantitative real time PCR was carried using the LightCycler-FastStart DNA MasterPlus SYBR® Green I kit on LightCycler 480 (Roche Diagnostics, Meylan, France). The reaction components were 1X DNA Master Mix, and 0.5 µM of sense and anti-sense oligonucleotides purchased from Eurogentec (Eurogentec France, Angers, France), designed using Primer3 software. Samples were normalized to three independent control housekeeping genes (G3PDH, RPL13A and ACTB for human samples and G3PDH, HMBS and B2M for mouse samples) and reported according to the ΔΔCT method as RNA fold increase: 2ΔΔCT= 2ΔCT sample- ΔCT reference.

Cell preparation and flow cytometry

Collected skin biopsies comprising the four excisional wounds were cut into small pieces using scissors and scalpel before overnight treatment in a 2.5 U/ml solution of dispase diluted in complete RPMI at 4°C. Then, skin tissues were incubated in an enzymatic solution composed of 50 µg/mL of Liberase TM Research Grade (Roche Diagnostics, Basel, Switzerland), 25 ng/ml of collagenase I and 100 µg/mL of DNase I (Sigma-Aldrich, St. Louis, MO) for 4 hours at 37°C before filtration through a 100 µm cell strainer followed by a second filtration through a 40 µm cell strainer and two washes in complete RPMI by centrifugation at 1700 rpm for 10 min. After the last centrifugation, cell pellets were resuspended with 250 µl of StemPro Accutase solution (Gibco) for 2 min at 37°C. After washing, cells were resuspended in complete RPMI and stimulated for 4 hours in the presence of phorbol myristate acetate (PMA, 50 ng/ml), ionomycin (750 ng/ml) and Golgi Plug (1 µl for/10^6 cells; BD Biosciences). Before extracellular staining, cells were incubated with Fc Block (BD Biosciences) for 10 minutes and then for 15 minutes at 4°C with the following antibodies: V500-conjugated anti-CD45, BV421-conjugated anti-CD3ϵ, FITC-conjugated anti-TCRγδ (all from BD Biosciences) and Zombie NIR for cell viability (BioLegend, San Diego,CA). For intracellular staining, cells were permeabilized with the Cytofix/Cytoperm kit and labelled for 15 min at 4°C with PE-conjugated anti-IL-17A (BD Biosciences) and PercP-eFluor710-conjugated anti-IL-22 (eBioscience) antibodies. Data were collected on a FACS Verse instrument (BD Bioscience) and analyzed using FlowJo software.

Statistical analysis

Statistical analysis of significance was calculated using either the Mann-Whitney U-test or the Kruskal Wallis one-way analysis of variance by ranks followed by a Dunn's post-test. p values of 0.05 or less were considered as significant, and all data are represented as mean +/- SEM. Comparison study used the Spearman rank correlation test.

Results

S. aureus and *P. aeruginosa* inoculated in skin excisional wounds delay the wound healing process

The kinetics of macroscopic wound closure was studied after performing 4 mm excisional wounds on the back skin of mice. By measuring the surface of the lesions every 2 days, we observed a progressive closure with nearly complete healing on day 8 for control mice/uninfected wounds. In contrast, when wounds were co-infected with a mixture of *S. aureus* and *P. aeruginosa*, the wound closure was almost achieved at day 12, with significant differences with uninfected wound from day 2 to day 14 (Figures 1A, B).

IL-17 and IL-22 expression in infected wound

It is well-documented that different sets of proinflammatory cytokines are produced in injured skin, whatever the etiology. With multiple target cells in skin, these cytokines have pleiotropic properties, such as not only to amplify and

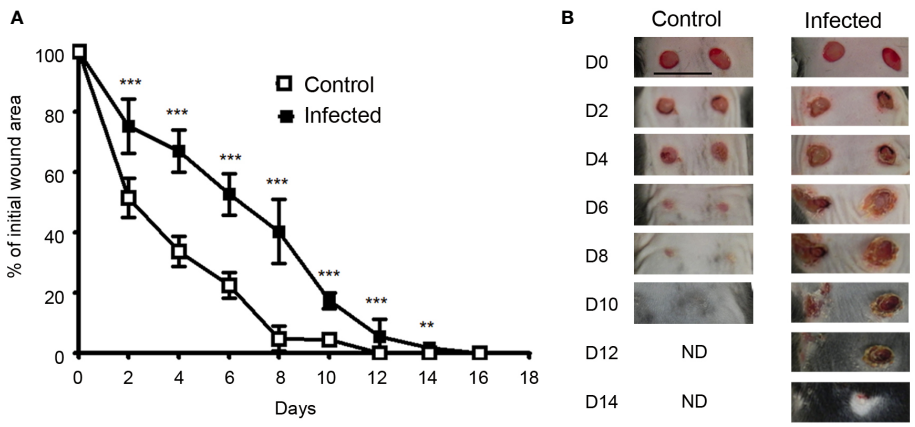

FIGURE 1
Wound closure is delayed in infected skin excisional wounds.**(A)**Time course of wound closure expressed as the percentage of initial wound area at each time point, in the control wound (□) or wound infected with a mixture of *S. aureus* and *P. aeruginosa* (■). The data are expressed as the mean +/- SEM of 5 independent experiments, with at least 4 mice/group; ** $p<0.01$, ***$p<0.001$. **(B)** Representative photographs of the control and infected wounds at days 0, 2, 4, 6, 8, 10, 12 and 14 after injury..

coordinate the inflammatory process, but also to have the ability to control it. We focused in the present study on the IL-22, IL-17, OSM, TNFα and IL-1β proinflammatory cytokines, which are produced in inflammatory human and murine skin and drive an inflammatory keratinocyte state. Taken together, their combination (M5 mixture) had a powerful synergistic biological effect on epidermal cells, stronger than other cytokine combinations studied (21, 23). Skin excision in aseptic condition induces the early skin expression of IL-1β, TNFα and OSM at day 2 and day 7, without detectable expression of IL-22, IL-17A and IL-17F (Figure 2A). In contrast, *S. aureus* and *P. aeruginosa* wound infection induced a strong expression of IL-22, IL-17A and IL-17F on day 2, which remained elevated on day 7. Under these conditions of infection, TNFα expression remained unchanged when compared to uninfected wound, while OSM increased about 5 times at day 7, and IL-1β enhanced at day 2 and day 7 (Figure 2A). As IL-22, IL-17A and IL-17F are mainly produced by T cells, we isolated CD45/CD3 immune cells from the skin of infected and non-infected mice collected at day 5 and analyzed cytokine expression by flow cytometry. This approach allows us to validate the mRNA cytokine expression pattern at the protein level and to precise the type of producing cells. We observed a significant increase in the number of IL-17A- and IL-22-producing T cells in the skin of infected mice compared to uninfected mice, while the slightly increased number of IL-17A/IL-22 double positive cells in the skin of infected mice was not significant (Figure 2B). These IL-17 and/or IL-22 positive CD3 T cells were 89.9% TCRγδ (Figure 2B).

Finally, we observed a close expression pattern in infected human skin wounds. Whereas IL-1β and OSM were similarly overexpressed in uninfected and infected wounds compared to normal skin, IL-17A and IL-22 expressions were enhanced only in infected wounds. In contrast to mice, TNFα levels were unchanged in wounds when compared to normal skin (Figure 2C).

IL-17 and IL-22 induced by bacterial infection have a key role in the delayed wound healing process

Since *S. aureus* and *P. aeruginosa* inoculation delayed skin wound healing and specifically induced IL-17 and IL-22 expression, we wondered if these cytokines could be responsible for the delayed healing. We studied the wound healing process in IL-17RKO or in IL-22KO infected mice and observed no significant difference with wound closure time course of infected WT mice (Supplementary Figure 1). In contrast, the wound healing process in infected IL-17R/IL-22 double knock-out mice (IL-17R/IL-22KO) is reduced and the wound closure time course similar to that of non-infected WT mice, highlighting the key role of the combination of IL-17 and IL-22 in this process (Figure 3A). To confirm their key roles, IL-17A/IL-17F and IL-22 alone or in combination were injected in four sites of each wound edge after skin excision, in the absence of bacteria. As indicated in Figure 3B, neither IL-17A/IL-17F nor IL-22 alone was able to modify the wound closure time course compared to the control group, whereas the combination of both cytokines weakly slowed down the healing process (Figure 3C), demonstrating that the simple combination of IL-17A/IL-17F and IL-22 was not sufficient to explain delayed closure of an infected wound. While TNFα, IL-1β and OSM are produced in non-infected skin lesions, IL-1β and OSM are produced much

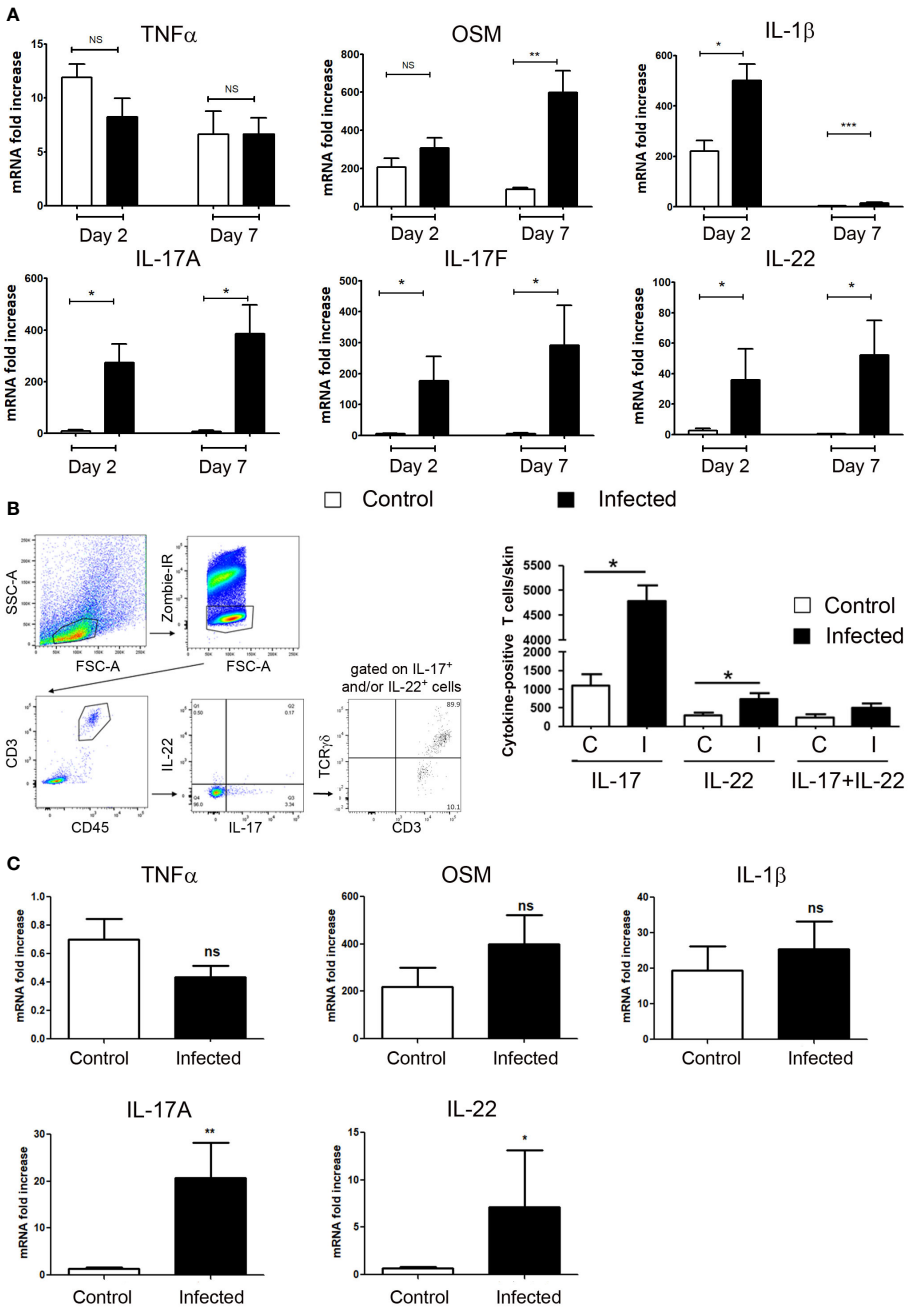

FIGURE 2
IL-17 and IL-22 are produced by T cells in infected skin excisional wounds. **(A)** Cytokine mRNA expression into control or *S. aureus* and *P. aeruginosa* infected wounds were determined by RT-qPCR at day 2 and day 7. Each bar represents the mRNA fold increase over normal skin, in control-wounded skin (white) or infected wounded skin (black). The data correspond to the mean +/- SEM of 4 independent experiments; * $p<0.05$, ** $p<0.01$, ***$p<0.001$; **(B)** Five days after wound infection by the bacterial mixture (infected, I) or application of a control PBS solution (uninfected, C), an 8 cm^2 biopsy of back skin including 4 excisional wounds was collected and underwent mechanical and enzymatic treatment for cell dissociation before analysis by flow cytometry. (B, left) Representative gating strategy to analyze IL-17 and IL-22 expressions in CD3-positive T cells and TCRγδ expression among this IL-17$^+$ and/or IL-22$^+$, CD3$^+$ T cell population. (B, right) Quantitative analysis of the number of IL-17-, IL-22- or IL-17/IL-22-positive T cells infiltrating infected or non-infected wounded skins. Data (mean +/- SEM) are representative of one out from three independent experiments including 5 mice per group. *p < 0.05. **(C)** IL-17A, IL-22, OSM, IL-1β and TNFα mRNA levels were determined by quantitative PCR in human wounds. Each bar represents the mRNA fold increase over normal human skin in uninfected (white) or infected wounded skin (black). The data correspond to the mean +/- SEM of 12 uninfected and 7 infected skin wound samples; * $p<0.05$, ** $p<0.01$, ***$p<0.001$. ns, not significant..

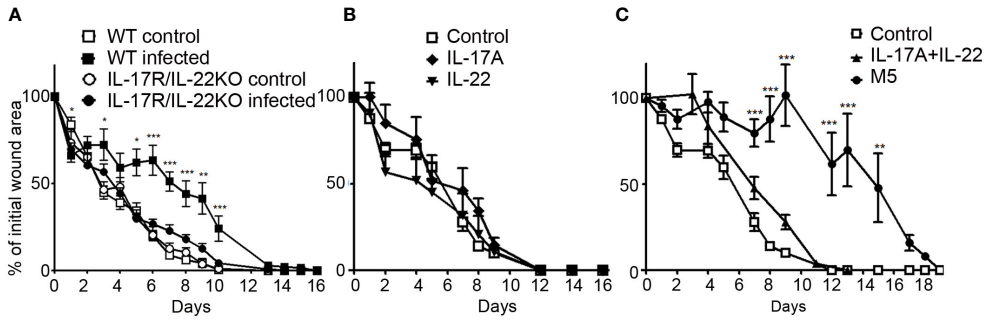

FIGURE 3
Combination of IL-17 and IL-22 are required for delayed closure in an infected skin wound. Time course of wound closure expressed as the percentage of initial wound area at each time point, **(A)** in the uninfected or infected wounds of WT mice (control □; infected ■) or IL-17R/IL-22KO mice (control ○; infected ●). **(B)** in the uninfected wound of WT mice injected with IL-17A (♦), IL-22 (▼). **(C)** in the uninfected wound of WT mice injected with IL-17A and IL-22 (▲), mix of IL-17A, OSM, TNFα, IL-22 and IL-1α (●) or PBS as a control (□). The data are expressed as the mean +/- SEM of 5 independent experiments, with at least 4 mice/group. * $p<0.05$, ** $p<0.01$, *** $p<0.001$..

more in infected wounds; given these findings, we wondered whether sufficient amounts of cytokines were necessary to reveal and potentiate the effects of IL-22 and IL-17A/IL-17F. Indeed, the injection of IL-1α, TNFα, OSM, IL-17A, and IL-22 mixture in the edge of uninfected lesions effectively delayed the wound healing process, as has been observed in the presence of bacteria (Figure 3C).

The wound healing process in Rag2KO mice is not delayed by bacterial infection

As IL-17A/IL-17F and IL-22 are produced mainly by T lymphocytes in infected wounds, we performed wound experiments in the presence or absence of bacteria in Rag2KO mice (deficient in mature lymphocytes). The wound healing process reported at day 7 after aseptic excisions was similar for WT and Rag2KO mice (Supplementary Figure 2) and wound healing achieve at day 12. In contrast to WT infected mice, the wound healing process in infected Rag2KO wounds was not delayed by infection, with a kinetics of healing comparable to that of uninfected WT wounds (Figure 4A and Supplementary Figure 2).

In uninfected Rag2KO wounds, IL-1β, TNFα and OSM mRNA levels were enhanced at days 2 and 7 when compared to uninjured Rag2KO skin (Figure 4B). In infected Rag2KO wounds, the levels of IL-1β, TNFα and OSM were comparable at day 2 to those of uninfected wounds, whereas their expression was enhanced at day 7 for TNFα and IL-1β (Figure 4B).

As for uninfected WT mice (Figure 2A), the expression of IL-22 and IL-17A/F was undetectable or low in uninfected Rag2KO wounds, except a discrete increase of IL-17F at day 2 when compared to normal skin (Figure 4B). *S. aureus* and *P. aeruginosa* wound inoculation did not significantly induce the expression of IL-17A, whereas they stimulated IL-22 on day 2 and IL-17F on day 7. OSM, IL-1β and IL-17A levels in Rag2KO infected wound remained significantly lower than in infected WT mice wounds (Figures 2A and 4B). In the same conditions, although TNFα and IL-17F levels were close in the two strains of mice, IL-22 levels were strongly reduced at day 7 in Rag2KO infected wounds (Figures 2A and 4B). It suggests that innate cells were also involved in the production of IL-17F and at least early for IL-22.

To further demonstrate the role of IL-22 and IL-17A/F amongst the proinflammatory cytokines able to delay wound healing, we injected exogenous recombinant IL-22 and IL-17 in the edges of infected wounds of Rag2KO mice. Whereas the healing kinetic of infected Rag2KO wounds was as fast as that of uninfected WT wounds, the combination of exogenous IL-22 and IL-17A/IL-17F delayed the wound healing process in infected Rag2KO mice at the same level as with infected WT mice (Figure 4A).

Regulation of the inflammatory response by infection during wound healing process

In the course of the wound healing in Rag2KO mice compared to WT, we further evaluated markers of the inflammatory response such as the antimicrobial peptides β-defensin 3 (BD3) and S100A9, the chemokine CXCL2 or neutrophil infiltration, all of which were strongly induced by the M5 mixture (21). In WT mice, BD3 expression was significantly induced in wounds infected by *S. aureus* and *P. aeruginosa* at day 2 and to an even greater extent at day 7, but not in uninfected wounds. (Figure 4C). In contrast, S100A9 and CXCL2 expressions were already highly induced in uninfected

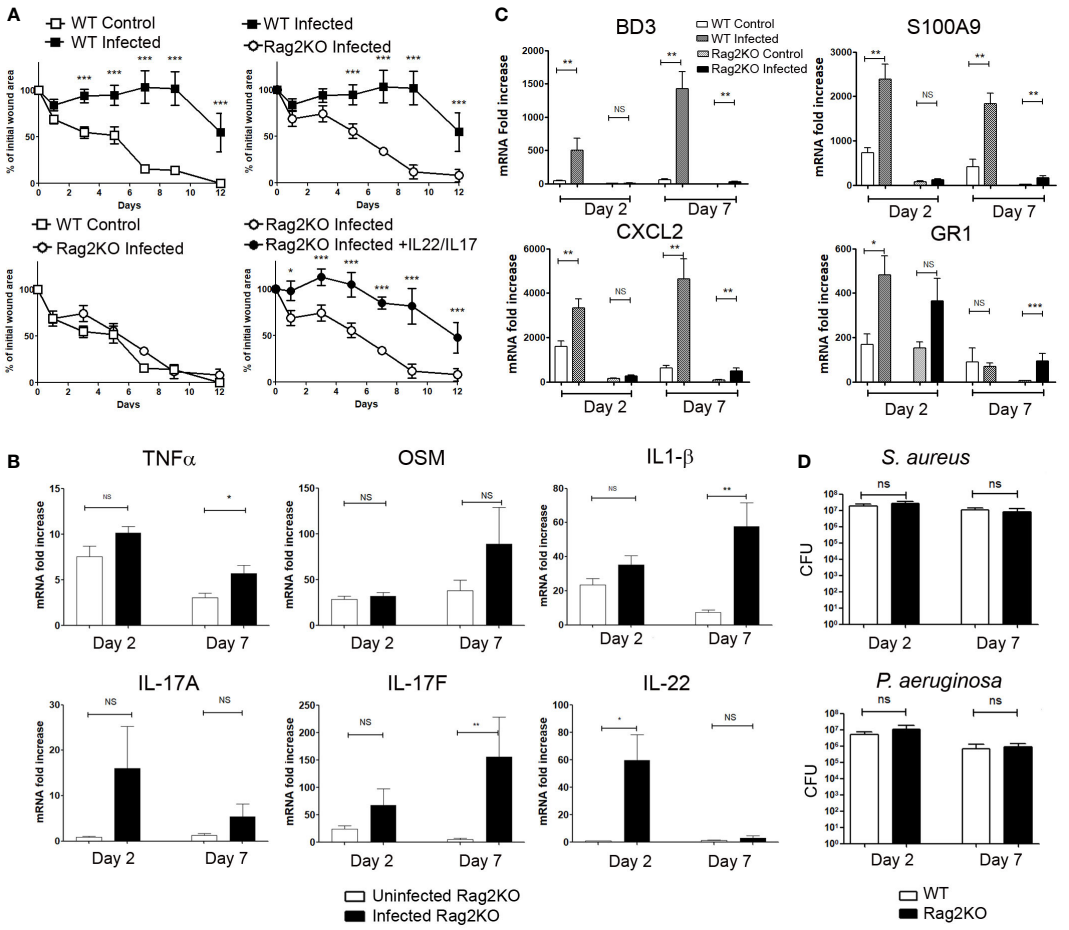

FIGURE 4
Wound closure is not delayed in infected skin excisional wounds of Rag2KO mice, and exogenous IL-17A/F and IL-22 make up for this delay. Time course of wound closure expressed as the percentage of initial wound area at each time point, **(A)** in the uninfected (□) or infected (■) wounds of WT mice, infected Rag2KO mice (○) or infected Rag2KO mice with exogenous IL-17A and IL-22 (●). The data are expressed as the mean +/- SEM of 6 independent experiments, with at least 4 mice/group; ** p<0.01, ***p<0.001. ns, not significant. **(B)** Cytokine mRNA expression into control or infected wounds of Rag2KO mice was determined by RT-qPCR at day 2 and day 7. Each bar represents the mRNA fold increase over normal skin, in control-wounded skin (white) or infected wounded skin (black). The data correspond to the mean +/- SEM of 3 independent experiments; * $p<0.05$, ** $p<0.01$, ***$p<0.001$. ns, not significant. **(C)** BD3, S100A9, CXCL2, GR1 mRNA expression into control or infected wounds of WT and Rag2KO mice were determined by RT-qPCR at day 2 and day 7. Each bar represents the mRNA fold increase over normal skin in control-wounded WT mice skin (white), infected wounded WT mice skin (hatched), in control-wounded Rag2KO mice skin (dotted), infected wounded Rag2KO mice skin (black). The data correspond to the mean +/- SEM of 3 independent experiments; * $p<0.05$, ** $p<0.01$, ***$p<0.001$. ns, not significant. **(D)** The bacterial load after inoculation in skin wounds is unchanged between WT and Rag2KO mice. CFU determination for *S. aureus* and *P. aeruginosa* in wounded WT and Rag2KO mice skin 2 and 7 days after inoculation of *S. aureus* and *P. aeruginosa*. The data correspond to the mean +/- SEM of 3 independent experiments, ns, not significant.

wounds of WT mice at day 2 as well as day 7, and these levels were much more highly increased by infection. The same induction was observed in infected wounds of Rag2KO mice in particular at day 7, but at levels much lower than those of WT mice (Figure 4C). Regarding the neutrophil GR1 marker, mRNA levels increased in non-infected WT and Rag2KO wounds at day 2 (Figure 4C). Application of *S. aureus* and *P. aeruginosa* mixture on wounds resulted in further GR1 mRNA overexpression at day 2 for WT mice and at day 7 for Rag2KO mice (Figure 4C).

Lastly, we compared the impact of the time course of wound healing on the bacterial load 2 and 7 days after inoculation of skin wounds. We detected approximately 2.10^7 *S. aureus* CFU/wound in WT mice at day 2 and 1.10^7 at day 7, and 8.10^6 P. *aeruginosa* CFU/wound at day 2 and 8.10^5 at day 7. Surprisingly, we could not point out any clear-cut differences between WT and Rag2KO mice, either at day 2 or at day 7, both for *S. aureus* and *P. aeruginosa* (Figure 4D). Furthermore, no suggestive signs of infection were observed in wounds of mice receiving PBS as a control, and neither *S. aureus* nor *P. aeruginosa* were detected.

Discussion

Skin wound healing is a regulated sequence of events controlled by multiple factors in view of restoring integrity, and it has been known by surgeons and nurses for over a century that this mechanism is delayed or stopped by bacterial wound contamination. In addition to the bacterial count and species, it depends on the number and virulence of the species present, and on the synergy between them. The wound healing process is also dependent on host immune response (3). However, despite numerous studies, the signals slowing down this healing of infected wounds remain partially understood. The role of soluble factors associated with inflammatory response is suggested by delayed wound healing in mice with sepsis induced by *P. aeruginosa* (25).

In this study, we reported that *S. aureus* and *P. aeruginosa* inoculated in skin excisional wounds of WT conventional mouse delay the wound healing process as reported with *P. aeruginosa* (4) and *S. aureus* (5, 26). In contrast to *S. aureus*, authors recently reported that *P. aeruginosa* did not delay healing, although the ulcers were larger than non-colonized ulcers (26). In accordance with our results in mice, the presence of different species such as Pseudomonas and Staphylococcus together correlates positively with nonhealing in humans (3). Interestingly, Canesso et al. showed that skin wound healing is accelerated in the absence of commensal microbiota in germ-free mice when compared to conventional mice, suggesting that commensal microbiota can delay the wound healing process (27).

We showed that if IL-1β, TNFα and OSM were present in uninfected excisional skin lesions, IL-17A, IL-17F and IL-22 were specifically produced after *S. aureus* and *P. aeruginosa* co-infection of the lesions. The combined action of IL-17, IL-22, IL-1β, TNFα and OSM delayed wound healing to a level comparable to the application of both *S. aureus* and *P. aeruginosa* in wounds. In accordance, numerous studies have reported the production of IL-17A, IL-17F and/or IL-22 in *S. aureus* (28–30) or *P. aeruginosa* infected mouse skins (4). These two species have the ability to promote cutaneous inflammation and to induce T cell-recruiting chemokine production (31, 32). Given that IL-1β, TNFα and OSM are mainly produced by innate immune cells and other skin resident cells, it would seem that the inflammatory process of an aseptic skin excisional lesion is primarily linked to an innate immunity process. By contrast, infection of the lesion with *S. aureus* and *P. aeruginosa* led to T cell recruitment/activation, mainly TCRγδ, and IL-17 and IL-22 production, evidencing the involvement of an additional adaptive immune response.

Finally, we observed a close expression pattern in infected human skin wounds, despite the differences between T cell skin infiltrates between mice and humans. T cell infiltrate in human skin is dominated by αβ Tcells, with less than 10% γδT cells both present in epidermis and dermis, whereas mouse skin is dominated by γδ T cells (50-70% in the dermis and more than 90% in the epidermis). In the epidermis, these γδ Tcells are represented by a majority of highly specialized cell subsets with a dendritic morphology termed DETC (dendritic epidermis T cells) with an invariant Vγ5Vδ1 TCR, not clearly evidenced in humans. Dermic γδ Tcells were mainly Vγ4 or 6. Thus, these γδ cells were characterized by a restricted TCR. Activation of γδ T cells can be performed both by innate and adaptive ligands, making these cells intermediate between innate and adaptive immunity (33). These cells have been reported to produce growth factors and to be involved in wound healing. Taking into account the differences between skin human and mouse T cells, the question of the IL-17/IL-22-producing cells in human wounded skin remains an opened question. αβ T cells, strongly present in human skin could be candidates. In *tcrδ*$^{-/-}$mice, skin resident γδ DETC were replaced by αβ DETC with polyclonal αβ TCRs, as in humans (34). In humans, both αβ and γδ T cells participate to acute wound healing (35)."

The central role of IL-17 and IL-22 in delayed wound healing is underlined by the accelerated skin wound healing kinetics in infected IL-17R/IL-22KO mice when compared to infected WT mice, and it overlaps with those of uninfected WT mice. Whereas exogenous recombinant IL-17A and F and/or IL-22 injected in the edges of uninfected wounds did not modify the healing kinetic, the IL-1α-TNFα-OSM-IL-17A-IL-22 combination (the M5 combination) strongly delayed it and overlapped with those of infected mice. Since IL-1β and OSM were produced in non-infected skin lesions but much more in infected wounds, we suggest that additional exogenous cytokines are required to synergize with IL-17 and IL-22. In accordance, the M5 combination in other inflammatory skin models has a huge synergistic effect to induce *in vitro* a critical inflammatory phenotype on keratinocytes and a powerful skin inflammation *in vivo* in mice (21, 23). In a model of excisional wound, Thomay et al. reported that disruption of IL-1 signaling (IL-1RKO mice) improves the quality of skin architecture when compared to WT mice, but does not change the wound healing kinetics (36). In a model of subcutaneous infection by *S. aureus* in mice, Chan *et al.* reported that IL-17A and IL-22 have complementary roles in host defense (28). Using the same model, Cho *et al.* reported an increase of IL-17A, IL-17F, and IL-22 in the infected lesions, and that IL-17RKO mice developed lesions with increased size (30). Despite controversial data reporting pro-reparative effects for IL-17 cytokine family, most of the recent studies highlight the role of IL-17 in pathogenesis and its anti-reparative effects (review in 37). By using IL-17A KO mice and/or IL-17-blocking mAb in models of non-infected wound, two recent studies reported that IL-17A delayed wound closure (15, 16 and reviewed in 37), also reported in obese diabetic mouse (37, 38). It was suggested to target IL-17A in a near future to promote wound healing. However, Hadian et al. indicated that the studies on the involvement of IL-17 in wound healing are performed on non-infected models, and have been to be continued in infected

ones, especially "since chronic wounds display increase relative abundance of *S. aureus* and *P. aeruginosa*" (39)

Regarding IL-22, and in disagreement with our data, another study reported that C57BL/6 mice deficient for IL-22R display a delay on day 14 wound healing (18). In contrast with this report, the same study indicated that IL-22-Fc promotes wound healing in db/db diabetic mice and *S. aureus* wound infected C57BL/6 mice (18). The differences could be due to different strategies; while we studied the behavior of an opened infected wound, Koluman et al. closed the wound and used dressing, which meant that two different healing conditions were to be evaluated.

In an attempt to summarize and even though these studies involved models and conditions (type of lesion, infection or not, independently studied cytokines…) different from ours, IL-17 increases skin lesion size and delays wound healing in the same way as in our results, and IL-22 appears to be beneficial to healing.

In agreement, by using Rag2KO mice, which fail to generate mature B and T lymphocytes, the healing kinetics of infected wound were faster compared to infected WT mice and overlapped with those of uninfected WT mice or infected IL-17R/IL-22KO mice. If wounds of Rag2KO mice significantly expressed IL-1α, IL-17F, TNFα and OSM, the production of IL-17Aand IL-22 was reduced and transient. This is in accordance with the prominence of γδ T lymphocytes in IL-17A, and IL-22 production in infected wounds of WT mice. In Rag2KO mice, we detected a residual production of IL-17F at day 2, suggesting that other cells such as innate immune cells are able to produce the cytokine. We suggest that ILC3 cells can participate to this production, in agreement with Li et al. reporting that dermis RORγ ILC3 produced IL-17F into wounded dermis (40).

Finally, the injection of exogenous recombinant IL-17 and IL-22 delayed the wound healing of infected Rag2KO to a similar degree as that of infected WT mice.

However, it was surprising that infected wounds of mice devoid of mature B and T cells were able to heal faster than those of infected WT mice, and we may wonder whether such processes are beneficial or detrimental. Moreover, the bacterial load of *S. aureus* and *P. aeruginosa* in the wounds of WT mice and Rag2KO mice were almost the same during the healing process, suggesting that adaptive immunity had a limited effect on this process. Regarding innate immunity, the production of BD3 and S100A9 was strongly reduced in Rag2KO wounds when compared to WT, as was that of the neutrophil-attracting chemokine CXCL2. However, the expression of the neutrophil marker GR1 was strongly enhanced in uninfected and infected wounds when compared to normal skin, and similar between infected wounds of WT and Rag2KO mice. By using a model of pneumonia induced by methicillin-resistant *S. aureus* in Rag2KO mice, Parker et al. reported that adaptive immunity is involved in lung pathology, and ascribe these deleterious effects to inflammatory cytokines (41). They described comparable levels of neutrophils in both WT and Rag2KO mice as in the present study, and that the clearance of bacteria is more effective in Rag2KO mice. It reminds, if necessary, the central role of neutrophils at least in such infectious models. In a model of colitis induced by *Citrobacter rotendium*, Vallance et al. reported that colitis, crypt hyperplasia and inflammation were attenuated in Rag1KO mice compared to WT, and suggest that adaptive immune response can be deleterious for tissues (42). In contrast to Parker et al. and the present study, bacteria were not cleared in these KO mice, but show few signs of disease. Taken together, these studies demonstrate that the adaptive immunity can also have paradoxical effects during bacterial defense, as deleterious impact on tissues, in part mediated by cytokines production by lymphocytes. Depending of the models, bacteria clearance can be delayed in lung or unaffected in lesional skin of RagKO mice.

Different reports have indicated that neutrophils are able to delay the wound healing process (43–45). This dependence of neutrophils is observed not for young mice (2-month-old) but only for older mice (6 to 20 months), whose wound healing is delayed when compared to young mice (43, 45). However, a reduced accumulation of neutrophils is observed in skin wounds of germ-free mice with accelerated wound healing compared to conventional mice (27). As we studied young mice (2.5 months), we suggest that the cytokine-delayed wound healing reported in our model could be independent of neutrophils

The ultimate goal is to evaluate the beneficial/deleterious effects of an acceleration or a slowing down of the healing kinetics in infected wounds. By studying regeneration after skin excision in the African spiny mice (Acomys), which is characterized by skin autonomy (capacity to regenerate missing skin), Seifert et al. suggested that too much inflammation would be detrimental, whereas no inflammation was not helpful either (46). We can hypothesize that in the case of acute infected wounds, slowed healing would allow a control of the infection by avoiding sepsis and would be beneficial. By contrast, in the case of chronic ulcers, we may wonder if IL-17 and IL-22 are involved in the lack of wound closure, which can consequently be deleterious. The deleterious effect of inflammatory cytokines in skin has been reported in hypertensive leg ulcer (HLU) and associated with impaired wound healing, displaying skin IL-1β and OSM hyperexpression. Furthermore, injection of exogenous IL-1β and OSM in the skin of mice mimics the skin characteristics of HLU (47).

This unexpected role of the proinflammatory cytokines IL-17 and IL-22 in control of the healing process provides new directions in control of kinetic wound healing by cytokines. Taken together, we have described new properties for IL-17 in association with IL-22 in control of skin wound healing kinetics. In inflamed tissues, it is always not one but a complex "cytokine network" that leads to a specific signature and response. In the present study, we have reported a specific cytokine signature associated with aseptic or infected wound skin, and demonstrated that IL-17 and IL-22 act synergistically with IL-1, TNFα and OSM are responsible for the delayed healing

observed in infected wounds. Depending on the context -infected or not-, -acute or chronic wound inflammation- we suggest that these cytokines could be used to slow down the wound healing process, or could be blocked to accelerate the process, in view of developing new therapeutic approaches to treat skin infections and scarring. In this perspective, a recombinant human IL-22 dimer (F-652) has been designed and tested safety in phase I studies, with the purpose of controlling epithelial repair (48). We are looking forward to observing its effects on wound healing kinetics.

By extension, such approaches to modulate wound healing could facilitate and accelerate skin grafts, an emerging strategy that remains to be explored (49).

However, the precarious balance between beneficial and deleterious properties of numerous cytokines, depending on the target cells, the inflammatory and/or the infectious states, should make us more cautious before using them for beneficial adjuvant therapies.

Data availability statement

The original contributions presented in the study are included in the article/Supplementary Material. Further inquiries can be directed to the corresponding author.

Ethics statement

All of our studies involving human tissues were approved by the Institutional Ethics Committee on Human Experimentation (Comité de Protection des Personnes Ouest III) of the Poitou-Charentes Region. The patients/participants provided their written informed consent to participate in this study. Protocols and animals were approved by the regional ethics committee for animal experimentation (COMETHEA-CE86) under the agreement number CE-2012-21.

Author contributions

J-CL, FM and F-XB contributed to conception and design of the study. EG, IPP, SC, and LFL performed the *in vivo* experiments, transcriptomic studies, and data management. NS, AB,JG and J-FJ performed and analyzed the *in vitro*, flow cytometry Experiments and data managements. CBu and CBo organize the bacterial studies and altogether wrote sections of the manuscript. VH and JM provided the human samples and wrote sections of the manuscript. FM performed the statistical analysis. BR and LD generate the transgenic mice and wrote sections of the manuscript. J-CL wrote the first draft of the manuscript. All authors contributed to manuscript revision, read, and approved the submitted version.

Funding

This study was supported by grants from University of Poitiers, a clinical research program from Poitiers University Hospital (PHRC), CNRS and University of Orleans and European funding in Region Centre-Val de Loire (FEDER N° 2016-00110366).

Acknowledgments

We thank Martine Garnier for her excellent technical support, Adriana Delwail (ImageUP platform, University of Poitiers) for technical help for flow cytometry and the members of the animal facility of the University of Poitiers (Prebios) and CNRS/University of Orléans. We thank Jeffrey Arsham (CHU Poitiers, France) for careful reviewing and editing the original English language manuscript. The authors thank the European Union for benefiting from its equipment grant program for research laboratories and platforms and the Poitiers University Hospital (CHU) for his grant for publication support.

Conflict of interest

The authors declare that the research was conducted in the absence of any commercial or financial relationships that could be construed as a potential conflict of interest.

Publisher's note

Supplementary material

The Supplementary Material for this article can be found online at: https://www.frontiersin.org/articles/10.3389/fimmu.2022.984016/full#supplementary-material

References

1. Martin P. Wound healing–aiming for perfect skin regeneration. *Science* (1997) 276(5309):75–81. doi: 10.1126/science.276.5309.75

2. Scholz F, Badgley BD, Sadowsky MJ, Kaplan DH. Immune mediated shaping of microflora community composition depends on barrier site. *PloS One* (2014) 9 (1):e84019. doi: 10.1371/journal.pone.0084019

3. Edwards R, Harding KG. Bacteria and wound healing. *Curr Opin Infect Dis* (2004) 17(2):91–6. doi: 10.1097/00001432-200404000-00004

4. Ferro TAF, Souza EB, Suarez MAM, Rodrigues JFS, Pereira DMS, Mendes SJF, et al. Topical application of cinnamaldehyde promotes faster healing of skin wounds infected with pseudomonas aeruginosa. *Molecules* (2019) 24(8):1627. doi: 10.3390/molecules24081627

5. Halbert AR, Stacey MC, Rohr JB, Jopp-McKay A. The effect of bacterial colonization on venous ulcer healing. *Australas J Dermatol* (1992) 33(2):75–80. doi: 10.1111/j.1440-0960.1992.tb00083.x

6. Bessa LJ, Fazii P, Di Giulio M, Cellini L. Bacterial isolates from infected wounds and their antibiotic susceptibility pattern: Some remarks about wound infection. *Int Wound J* (2015) 12(1):47–52. doi: 10.1111/iwj.12049

7. DeLeon S, Clinton A, Fowler H, Everett J, Horswill AR, Rumbaugh KP. Synergistic interactions of pseudomonas aeruginosa and staphylococcus aureus in an *in vitro* wound model. *Infect Immun* (2014) 82(11):4718–28. doi: 10.1128/IAI.02198-14

8. Fazli M, Bjarnsholt T, Kirketerp-Moller K, Jorgensen B, Andersen AS, Krogfelt KA, et al. Nonrandom distribution of pseudomonas aeruginosa and staphylococcus aureus in chronic wounds. *J Clin Microbiol* (2009) 47(12):4084–9. doi: 10.1128/JCM.01395-09

9. Gjodsbol K, Christensen JJ, Karlsmark T, Jorgensen B, Klein BM, Krogfelt KA. Multiple bacterial species reside in chronic wounds: A longitudinal study. *Int Wound J* (2006) 3(3):225–31. doi: 10.1111/j.1742-481X.2006.00159.x

10. Trivedi U, Parameswaran S, Armstrong A, Burgueno-Vega D, Griswold J, Dissanaike S, et al. Prevalence of multiple antibiotic resistant infections in diabetic versus nondiabetic wounds. *J Pathog* (2014) 2014:173053. doi: 10.1155/2014/173053

11. Villain R. *Plaies, Brulures Et Nécroses*. éditions Baillière JB, ed. 2 Cité Paradis, 75010 Paris, France: Les cahiers Baillièr (1980).

12. Pasparakis M, Haase I, Nestle FO. Mechanisms regulating skin immunity and inflammation. *Nat Rev Immunol* (2014) 14(5):289–301. doi: 10.1038/nri3646

13. Barrientos S, Brem H, Stojadinovic O, Tomic-Canic M. Clinical application of growth factors and cytokines in wound healing. *Wound Repair Regener* (2014) 22(5):569–78. doi: 10.1111/wrr.12205

14. Brockmann L, Giannou AD, Gagliani N, Huber S. Regulation of Th17 cells and associated cytokines in wound healing, tissue regeneration, and carcinogenesis. *Int J Mol Sci* (2017) 18(5):1033. doi: 10.3390/ijms18051033

15. Takagi N, Kawakami K, Kanno E, Tanno H, Takeda A, Ishii K, et al. Il-17a promotes neutrophilic inflammation and disturbs acute wound healing in skin. *Exp Dermatol* (2017) 26(2):137–44. doi: 10.1111/exd.13115

16. Rodero MP, Hodgson SS, Hollier B, Combadiere C, Khosrotehrani K. Reduced Il17a expression distinguishes a Ly6clomhciihi macrophage population promoting wound healing. *J Invest Dermatol* (2013) 133(3):783–92. doi: 10.1038/jid.2012.368

17. Gao B, Xiang X. Interleukin-22 from bench to bedside: A promising drug for epithelial repair. *Cell Mol Immunol* (2019) 16(7):666–7. doi: 10.1038/s41423-018-0055-6

18. Kolumam G, Wu X, Lee WP, Hackney JA, Zavala-Solorio J, Gandham V, et al. Il-22r ligands il-20, il-22, and il-24 promote wound healing in diabetic Db/Db mice. *PloS One* (2017) 12(1):e0170639. doi: 10.1371/journal.pone.0170639

19. Boniface K, Bernard FX, Garcia M, Gurney AL, Lecron JC, Morel F. Il-22 inhibits epidermal differentiation and induces proinflammatory gene expression and migration of human keratinocytes. *J Immunol* (2005) 174(6):3695–702. doi: 10.4049/jimmunol.174.6.3695

20. Boniface K, Diveu C, Morel F, Pedretti N, Froger J, Ravon E, et al. Oncostatin m secreted by skin infiltrating T lymphocytes is a potent keratinocyte activator involved in skin inflammation. *J Immunol* (2007) 178(7):4615–22. doi: 10.4049/jimmunol.178.7.4615

21. Guilloteau K, Paris I, Pedretti N, Boniface K, Juchaux F, Huguier V, et al. Skin inflammation induced by the synergistic action of il-17a, il-22, oncostatin m, il-1{Alpha}, and tnf-{Alpha} recapitulates some features of psoriasis. *J Immunol* (2010) 184:5256–70. doi: 10.4049/jimmunol.0902464

22. Pohin M, Guesdon W, Mekouo AA, Rabeony H, Paris I, Atanassov H, et al. Oncostatin m overexpression induces skin inflammation but is not required in the mouse model of imiquimod-induced psoriasis-like inflammation. *Eur J Immunol* (2016) 46(7):1737–51. doi: 10.1002/eji.201546216

23. Rabeony H, Petit-Paris I, Garnier J, Barrault C, Pedretti N, Guilloteau K, et al. Inhibition of keratinocyte differentiation by the synergistic effect of Il-17a, Il-22, Il-1alpha, Tnfalpha and Oncostatin M. *PloS One* (2014) 9(7):e101937. doi: 10.1371/journal.pone.0101937

24. Wilson NJ, Boniface K, Chan JR, McKenzie BS, Blumenschein WM, Mattson JD, et al. Development, cytokine profile and function of human interleukin 17-producing helper T cells. *Nat Immunol* (2007) 8(9):950–7. doi: 10.1038/ni1497

25. Rico RM, Ripamonti R, Burns AL, Gamelli RL, DiPietro LA. The effect of sepsis on wound healing. *J Surg Res* (2002) 102(2):193–7. doi: 10.1006/jsre.2001.6316

26. Sahu K, Verma Y, Sharma M, Rao KD, Gupta PK. Non-invasive assessment of healing of bacteria infected and uninfected wounds using optical coherence tomography. *Skin Res Technol* (2010) 16(4):428–37. doi: 10.1111/j.1600-0846.2010.00451.x

27. Canesso MC, Vieira AT, Castro TB, Schirmer BG, Cisalpino D, Martins FS, et al. Skin wound healing is accelerated and scarless in the absence of commensal microbiota. *J Immunol* (2014) 193:5171–80. doi: 10.4049/jimmunol.1400625

28. Chan LC, Chaili S, Filler SG, Barr K, Wang H, Kupferwasser D, et al. Nonredundant roles of interleukin-17a (Il-17a) and il-22 in murine host defense against cutaneous and hematogenous infection due to methicillin-resistant staphylococcus aureus. *Infect Immun* (2015) 83(11):4427–37. doi: 10.1128/IAI.01061-15

29. Miller LS, Cho JS. Immunity against staphylococcus aureus cutaneous infections. *Nat Rev Immunol* (2011) 11(8):505–18. doi: 10.1038/nri3010

30. Cho JS, Pietras EM, Garcia NC, Ramos RI, Farzam DM, Monroe HR, et al. Il-17 is essential for host defense against cutaneous staphylococcus aureus infection in mice. *J Clin Invest* (2010) 120(5):1762–73. doi: 10.1172/JCI40891

31. Damour A, Robin B, Deroche L, Broutin L, Bellin N, Verdon J, et al. Phenol-soluble modulins alpha are major virulence factors of staphylococcus aureus secretome promoting inflammatory response in human epidermis. *Virulence* (2021) 12(1):2474–92. doi: 10.1080/21505594.2021.1975909

32. Garcia M, Morello E, Garnier J, Barrault C, Garnier M, Burucoa C, et al. Pseudomonas aeruginosa flagellum is critical for invasion, cutaneous persistence and induction of inflammatory response of skin epidermis. *Virulence* (2018) 9 (1):1163–75. doi: 10.1080/21505594.2018.1480830

33. Hu W, Shang R, Yang J, Chen C, Liu Z , Liang G, et al. Skin GammaDelta T cells and their function in wound healing. *Front Immunol* (2022) 13:875076. doi: 10.3389/fimmu.2022.875076

34. Binz C, Bubke A, Sandrock I, Prinz I. Alphabeta T cells replacing dermal and epidermal GammaDelta T cells in tcrd(-/-) mice express an mhc-independent tcr repertoire. *Eur J Immunol* (2021) 51(11):2618–32. doi: 10.1002/eji.202149243

35. Toulon A, Breton L, Taylor KR, Tenenhaus M, Bhavsar D, Lanigan C, et al. A role for human skin-resident T cells in wound healing. *J Exp Med* (2009) 206 (4):743–50. doi: 10.1084/jem.20081787

36. Thomay AA, Daley JM, Sabo E, Worth PJ, Shelton LJ, Harty MW, et al. Disruption of interleukin-1 signaling improves the quality of wound healing. *Am J Pathol* (2009) 174:2129–36. doi: 10.2353/ajpath.2009.080765

37. Zhang F, Liu Y, Wang S, Yan X, Lin Y , Chen D, et al. Interleukin-25-Mediated-IL-17RB upregulation promotes cutaneous wound healing in diabetic mice by improving endothelial cell functions. *Front Immunol* (2022) 13:809755. doi: 10.3389/fimmu.2022.809755

38. Lee J, Rodero MP, Patel J, Moi D, Mazzieri R, Khosrotehrani K. Interleukin-23 regulates interleukin-17 expression in wounds, and its inhibition accelerates diabetic wound healing through the alteration of macrophage polarization. *FASEB J* (2018) 32:2086–94. doi: 10.1096/fj.201700773R

39. Hadian Y, Bagood MD, Dahle SE, Sood A, Isseroff RR. Interleukin-17: Potential target for chronic wounds. *Mediators Inflamm* (2019) 2019:1297675. doi: 10.1155/2019/1297675

40. Li Z, Hodgkinson T, Gothard EJ, Boroumand S, Lamb R, Cummins I, et al. Epidermal Notch1 recruits rorgamma (+) group 3 innate lymphoid cells to orchestrate normal skin repair. *Nat Commun* (2016) 7:11394. doi: 10.1038/ncomms11394

41. Parker D, Ryan CL, Alonzo F3rd, Torres VJ, Planet PJ, Prince AS. Cd4+ T cells promote the pathogenesis of staphylococcus aureus pneumonia. *J Infect Dis* (2015) 211:835–45. doi: 10.1093/infdis/jiu525

42. Vallance BA, Deng W, Knodler LA, Finlay BB. Mice lacking T and b lymphocytes develop transient colitis and crypt hyperplasia yet suffer impaired bacterial clearance during citrobacter rodentium infection. *Infect Immun* (2002) 70:2070–81. doi: 10.1128/IAI.70.4.2070-2081.2002

43. Brubaker AL, Rendon JL, Ramirez L, Choudhry MA, Kovacs EJ. Reduced neutrophil chemotaxis and infiltration contributes to delayed resolution of cutaneous wound infection with advanced age. *J Immunol* (2013) 190(4):1746–57. doi: 10.4049/jimmunol.1201213

44. Dovi JV, He LK, DiPietro LA. Accelerated wound closure in neutrophil-depleted mice. *J Leukoc Biol* (2003) 73(4):448–55. doi: 10.1189/jlb.0802406

45. Phillipson M, Kubes P. The healing power of neutrophils. *Trends Immunol* (2019) 40(7):635–47. doi: 10.1016/j.it.2019.05.001

46. Seifert AW, Kiama SG, Seifert MG, Goheen JR, Palmer TM, Maden M. Skin shedding and tissue regeneration in African spiny mice (Acomys). *Nature* (2012) 489(7417):561–5. doi: 10.1038/nature11499

47. Giot JP, Paris I, Levillain P, Huguier V, Charreau S, Delwail A, et al. Involvement of il-1 and oncostatin m in acanthosis associated with hypertensive leg ulcer. *Am J Pathol* (2013) 182(3):806–18. doi: 10.1016/j.ajpath.2012.11.030

48. Tang KY, Lickliter J, Huang ZH, Xian ZS, Chen HY, Huang C, et al. Safety, pharmacokinetics, and biomarkers of f-652, a recombinant human interleukin-22 dimer, in healthy subjects. *Cell Mol Immunol* (2019) 16(5):473–82. doi: 10.1038/s41423-018-0029-8

49. Magne B, Dedier M, Nivet M, Coulomb B, Banzet S, Lataillade JJ, et al. Il-1beta-Primed mesenchymal stromal cells improve epidermal substitute engraftment and wound healing *via* matrix metalloproteinases and transforming growth factor-Beta1. *J Invest Dermatol* (2020) 140(3):688–98. doi: 10.1016/j.jid.2019.07.721

frontiers | Frontiers in Immunology

TYPE Original Research
PUBLISHED 20 October 2022
DOI 10.3389/fimmu.2022.1025499

OPEN ACCESS

EDITED BY
Alicia R Mathers,
University of Pittsburgh, United States

REVIEWED BY
Nathan K. Archer,
Johns Hopkins Medicine, United States
Ronald Sluyter,
University of Wollongong, Australia

*CORRESPONDENCE
Samuel T. Hwang
sthwang@ucdavis.edu

SPECIALTY SECTION
This article was submitted to Autoimmune and Autoinflammatory Disorders : Autoimmune Disorders, a section of the journal Frontiers in Immunology

RECEIVED 23 August 2022
ACCEPTED 05 October 2022
PUBLISHED 20 October 2022

CITATION
Yamada D, Vu S, Wu X, Shi Z, Morris D, Bloomstein JD, Huynh M, Zheng J and Hwang ST (2022) Gain-of-function of TRPM4 predisposes mice to psoriasiform dermatitis.
Front. Immunol. 13:1025499.
doi: 10.3389/fimmu.2022.1025499

Gain-of-function of TRPM4 predisposes mice to psoriasiform dermatitis

Daisuke Yamada[1], Simon Vu[2], Xuesong Wu[1], Zhenrui Shi[3], Desiree Morris[4], Joshua D. Bloomstein[1], Mindy Huynh[1], Jie Zheng[2] and Samuel T. Hwang[1]*

[1]Department of Dermatology, University of California, Davis, Sacramento, CA, United States, [2]Department of Physiology and Membrane Biology, University of California, Davis, Davis, CA, United States, [3]Department of Dermatology, Sun Yat-sen Memorial Hospital, Sun Yat-sen University, Guangzhou, China, [4]Kirk Kerkorian School of Medicine at University of Nevada, Las Vegas, Las, Vegas, NV, United States

Transient receptor potential melastatin 4 (TRPM4) is a Ca^{2+}-activated, monovalent cation channel that is expressed in a wide range of cells. We previously reported two gain-of-function (GoF) mutations of TRPM4 as the cause of progressive symmetric erythrokeratodermia (PSEK), which shares similar clinical and histopathological features with psoriasis. Using CRISPR/Cas9 technology, we generated TRPM4^{I1029M} mice that have the equivalent mutation to one of the two genetic mutations found in human PSEK (equivalent to human TRPM4^{I1033M}). Using this mutant mice, we examined the effects of TRPM4 GoF at the cellular and phenotypic levels to elucidate the pathological mechanisms underlying PSEK. In the absence of experimental stimulation, TRPM4^{I1029M} mice did not show a phenotype. When treated with imiquimod (IMQ), however, TRPM4^{I1029M} mice were predisposed to more severe psoriasiform dermatitis (PsD) than wild-type (WT), which was characterized by greater accumulation of CCR6-expressing γδ T cells and higher mRNA levels of *Il17a*. In TRPM4^{I1029M} mice, dendritic cells showed enhanced migration and keratinocytes exhibited increased proliferation. Moreover, a TRPM4 inhibitor, glibenclamide, ameliorated PsD in WT and TRPM4^{I1029M} mice. Our results indicate elevated TRPM4 activities boosted susceptibility to cutaneous stimuli, likely through elevation of membrane potential and alteration of downstream cellular signaling, resulting in enhanced inflammation. Our results further suggest a possible therapeutic application of TRPM4 inhibitors in psoriasis.

KEYWORDS

TRPM4, keratinocyte, dendritic cell, psoriasis, imiquimod (IMQ), mouse model, progressive symmetric erythrokeratodermia, glibenclamide

Introduction

Transient receptor potential melastatin 4 (TRPM4) is a Ca^{2+}-activated nonselective cation (CAN) channel involved in diverse physiological processes and implicated in several human hereditary diseases (1, 2). Increase in TRPM4 activity induced by elevating intracellular Ca^{2+} concentration is expected to depolarize the membrane potential and induce subsequent cellular response (3). Like most transient receptor potential (TRP) channels, TRPM4 is thought to be tetramer made of four subunits, each of which containing six transmembrane segments and intracellularly located N- and C-terminal. Recently, its cryo-EM structure was reported by four independent groups, showing a four-fold symmetrical complex (4–7). TRPM4 proteins are found in various cell types and determine important functions, including insulin secretion in pancreatic beta cells, cardiac excitability in ventricular cells, immune response in lymphocytes, dendritic cells (DCs), and mast cells as well as excitability and contractility in vascular smooth muscle cells (8–14). Several heterozygous mutations of TRPM4, leading to gain-of function (GoF) have been identified in familial heart conduction diseases (15, 16), signifying its importance in maintaining cellular homeostasis. Recently, two GoF mutations (p.I1033M and p.I1040T) in TRPM4 were found in patients with an autosomal dominant-inherited skin disease termed progressive symmetric erythrokeratodermia (PSEK). Both of the mutation sites are located in ion permeation pore region. The mutant channels were found to induce increased sensitivity to Ca^{2+} leading to elevation of resting membrane potential and keratinocyte proliferation (17). These new findings suggest TRPM4 may be important in the maintenance of skin homeostasis as well as response to inflammatory stimuli.

Abnormalities in the immune response are involved in many dermatoses, including potentially PSEK. TRPM4 affects the function of various types of immune cells. For example, TRPM4 has been demonstrated to regulate migration, but not the maturation, of DCs (13). Inhibition of *TRPM4* by siRNA in Jurkat T cells resulted in enhanced IL-2 production (18), and inhibition of *TRPM4* expression led to increased Ca^{2+} influx and oscillatory levels in Th2 cells, but decreased Ca^{2+} influx and oscillations in Th1 cells. Inhibition of *TRPM4* expression also significantly altered T cell cytokine production and motility (12). Other studies indicate that TRPM4 affected the function of monocytes, macrophages (19) and mast cells (14, 20), but does not alter intracellular Ca^{2+} mobilization in neutrophils (19).

In vivo roles of TRPM4 have been explored in several experimental animal models using TRPM4 knockout ($TRPM4^{-/-}$) mice. $TRPM4^{-/-}$ mice have shown increased mortality in a model of sepsis induced by cecal ligation and puncture (19), as well as more severe IgE-mediated acute cutaneous anaphylactic response (14). Additionally, they showed reduced axonal and neuronal degeneration and attenuated clinical disease scores in mice models of experimental autoimmune encephalomyelitis (EAE), but this occurred without altering EAE-relevant immune function (21). While these studies highlighted the role of TRPM4 in maintaining cellular homeostasis including the immune system, it remains unclear how TRPM4 GoF mutants lead to PSEK and other human diseases. To address this question, we generated TRPM4 GoF mice using the CRISPR/Cas9 method which have the equivalent mutation to one of the two genetic mutations found in human PSEK (equivalent to human $TRPM4^{I1033M}$). The mutation site is located in ion permeation pore region (Supplementary Figure 1). The TRPM4 GoF mice did not show any skin phenotype in the absence of stimulation, however, the results of our *in vitro* experiments indicated that this mutation affects the membrane potential and proliferation of keratinocytes, suggesting that cells harboring GoF mutant TRPM4 channels might be more susceptible to disease-causing environmental stimuli. Considering that the skin manifestations and histopathological findings of PSEK are similar to those of psoriasis (17) as manifested by thickened, red scaly plaques, we employed an imiquimod (IMQ)-induced PsD model. When stimulated by IMQ, TRPM4 GoF mice showed enhanced cutaneous inflammation. Both GoF mice and wild-type (WT) littermates showed reduction of IMQ-induced dermatitis when treated with glibenclamide, a TRPM4 inhibitor. Thus, TRPM4 plays a critical role in regulating psoriasis-like features in mice, which possibly explains the resemblance of the skin lesions in PSEK patients to human psoriasis and may point to TRPM4 as a relevant target in psoriasis.

Abbreviations: TRPM4, transient receptor potential melastatin 4; GoF, gain-of-function; PSEK, progressive symmetric erythrokeratodermia; CRISPR/Cas9, clustered regularly interspaced short palindromic repeats and CRISPR-associated protein 9; IMQ, imiquimod; PsD, psoriasiform dermatitis; IL, interleukin; DC, dendritic cell; EAE, experimental autoimmune encephalomyelitis; WT, wild-type; gRNA, guide RNA; HDR, homology directed repair; p-STAT3, phosphorylated signal transducer and activator of transcription 3; SUR, sulfonylurea receptor; IHC, Immunohistochemistry; H&E, hematoxylin and eosin; γδ-low, TCR γδ-low expressing; Th, T helper; CCR6, CC chemokine receptor-6.

Materials and methods

Generation of TRPM4 mutant (I1029M) mice (C57BL/6J background)

To generate TRPM4 I1029M mice, we obtained purified Cas9, a TRPM4-targeting guide RNA (gRNA; 5'-CAGGTTGAGCA ACAGGATATTGG-3') that targets Cas9 to a site near the I1029 codon, and donor oligos for HDR resulting in p.I1029M (c.C3087G) mutations (HDR donor sequence; 5'-

CCCAGTATGCCAACTGGCTGGTGGTGTTGCTCCTTATCG TCTTCTTGCTGGTGGC CAATATGCTGTTGCTCAACCT GCTCATCGCCATGTTCAGGTGTGCCT-3'). Purified Cas9, TRPM4-targeting gRNA, and HDR oligos were procured from Integrated DNA Technologies. All three products were injected into C57BL/6J zygotes at the University of California, Davis mouse biology program. C57BL/6J mice were purchased from Jackson laboratories. The resulting pups were genotyped by amplifying a 374 bp region flanking the I1029M site and subsequent Sanger sequencing. Heterozygous mice from the founder line were then intercrossed to produce litters with WT, heterozygous, and homozygous animals. Mice were maintained under specific pathogen free conditions throughout this study. For the genotyping of the mice, we used RT-qPCR of mutant *TRPM4*, i.e., homozygous mouse expressed twice as high mutant *TRPM4* as heterozygous mice whereas no mutant *TRPM4* was detected in WT mouse. All animal experiments were performed under protocols (#20960) approved by the Institutional Animal Care and Use Committee at the University of California, Davis.

Primary keratinocyte isolation and culture

Adult mouse keratinocytes were cultured following the procedure described by Li (22). Briefly, the tail skin from an adult mouse was digested in dispase digestion buffer, which contains 4 mg/ml dispase II in supplemented KC growth medium (KC basal medium with 0.06 mM CaCl2, Defined Growth Supplement, antibiotics) overnight 4°C. Epidermal sheet was removed, digested in trypsin-based digestion solution. Then cells were filtered and seeded in supplemented KC growth medium in culture dishes pre-coated with a collagen-based coating material. For WST-1 assay, cells were seeded at $1.0x10^5$ cells/well in a 96-well plate. After 24 hours of incubation, medium was changed and thereafter WST-1 (Sigma-Aldrich, St. Louis, MO) was added to each well. For cell counting, $1.0x10^5$ cells/well were seeded in a 24-well plate. After 4 days of incubation, cell numbers were counted using a hemocytometer.

Electrophysiology

Recordings were performed using a HEKA EPC10 amplifier with PatchMaster software. The bath solution consisted of 140 mM NaCl, 5 mM KCl, 1 mM $CaCl_2$, 1 mM $MgCl_2$, 10 mM HEPES, 10 mM Glucose, pH 7.4; the pipette solution consisted of 150 mM K-Asp, 5 mM KCl, 10 mM HEPES, 10 μM PIP2, 2 mM EGTA, 1.8 mM $CaCl_2$, pH 7.4 (resulting in 10 μM free Ca^{2+}, calculated by MAXCHELATOR program, http://maxchelator.stanford.edu). Patch pipettes were fashioned from borosilicate glass and fire polished within the range of 3-5 MΩ. All recordings were performed at room temperature (~22°C). Membrane potential was recorded in the whole-cell patch configuration. The liquid junction potentials were tested experimentally and adjusted accordingly.

Cell cycle assay

Cell cycle assay was performed following the procedure described by Kim (23). Briefly, primary keratinocytes isolated from adult mouse tail were fixed in ice cold 70% ethanol. Then, the cells were stained with anti-Ki-67 antibody (Cat# 151211, BioLegend) and propidium iodide containing RNase (Cat# 4087, Cell Signaling Technologies).

IMQ-induced PsD model

IMQ-induced PsD model was described previously (24). 50 mg of 5% IMQ (Aldara; 3M Pharmaceuticals) in total was applied once daily to both sides of both ears for 5 consecutive days. Vanicream (Pharmaceutical Specialties, Cleveland, GA, USA) was applied on ears of WT mice as a vehicle control.

Scoring severity of skin inflammation

To score the severity of inflammation of the ear skin, an objective scoring system was used as described before (24). Briefly, erythema, scaling, and thickening were scored independently on a scale from 0 to 4: 0, none; 1, slight; 2, moderate; 3, marked; 4, very marked. We calculated the cumulative score (erythema plus scaling plus thickening) as psoriasis severity index (PSI) score (scale 0–12). Ear skin thickness was measured with a thickness gauge (Peacock, Ozaki, MFG.CO., LTD, Japan) having 0.01 mm accuracy.

Histopathological analysis and immunohistochemistry

Formaldehyde-fixed, paraffin-embedded ear skin samples were stained with H&E using standard procedures. Images were acquired using a Nikon Optiphot 2 microscope (Nikon, Tokyo, Japan). Epidermal thickness was measured with a computer-assisted image analysis software. For immunohistochemical analysis, skin sections were incubated with primary antibodies against murine p-STAT3, followed by the appropriate secondary antibodies. Rinsed sections were counterstained with hematoxylin.

DNFB-induced contact hypersensitivity

One day after shaving the back hair with electrical clippers, the back skin was treated with 50 μl of 0.5% DNFB (1-fluoro-2,4-dinitrobenzene) (Sigma-Aldrich, St. Louis, MO) in a 4:1 mixture

of acetone and olive oil. Five days later, the mice were challenged with 40 µl 0.2% DNFB. WT mice without sensitization served as a control group. Ear thickness was evaluated before challenge and after challenge (24 hours, 48 hours, and 72 hours).

Croton oil-induced irritant contact dermatitis

25 µl of 2% croton oil (in a 4:1 mixture of acetone and olive oil) was applied to the dorsal side of the ear. Ear thickness was evaluated 2, 4, 6, and 24 hours after challenge. WT mice applied with 4:1 mixture of acetone and olive oil served as a vehicle control group.

Flow cytometry

Anti–mouse γδ-TCR (clone GL3), CD3 (17A2), CD45 (30-F11), CCR6 (29-2L17), CD11b (M1/70), CD11c (N418), and Ly6G (IA8) antibodies were from BioLegend (San Diego, CA). Anti-mouse IL-17A (eBio17B7) antibody was from eBioscience (San Diego, CA). Flow cytometry was performed and analyzed using an Accuri C6 (BD Biosciences, San Jose, CA). After recovery of mouse ears, the ears were cut into small pieces with a blade. To obtain cell suspensions, small pieces of ear skin were digested with Liberase TM (Roche, Mannheim, Germany) and DNase I (Sigma-Aldrich, St. Louis, MO) with addition of 5% fetal bovine serum for 90 minutes before passing tissue through a 100-µm cell strainer. Anti-mouse CD16/32 (BD, San Jose, CA) were added to cells prior to staining to block binding to Fc receptors. Flow gating for $CCR6^+$ γδ-low T cells was performed using a gating strategy described in detail in our previous reports (25, 26). Representative flow gating for the population is shown in Supplementary Figure 2. Intracellular staining for IL-17A was done after incubating cells for 5 hours with cell stimulation cocktail plus protein transport inhibitors (eBioscience 00-4975-93).

Quantitative real-time PCR

Total RNA of mouse ear skin was extracted using a RNeasy Fibrous Tissue Kit (Qiagen, Hilden, Germany). Quantitative real-time PCR was performed using CFX connect Real-Time PCR Detection System (Bio-Rad, Hercules, CA). Predesigned primers were obtained from Integrated DNA Technologies, Inc (Skokie, IL).

DC migration assay

We applied 100µl of 1% FITC (Sigma-Aldrich, St. Louis, MO) solution in acetone and dibutyl phthalate (1:1) on mouse ears to label phagocytic antigen presentation cells, such as dermal and epidermal DCs, and quantified their migration from skin to regional LN. Six hours after the FITC application, we collected the cervical LNs and quantified the $FITC^+$ DCs by flow cytometry.

Glibenclamide treatment

We administered 10 µg glibenclamide daily by intraperitoneal injections to all mice in the treatment group (21). We daily dissolved 25 mg glibenclamide (Sigma-Aldrich, St. Louis, MO) in 5 ml DMSO and diluted 200 µl of this solution in 9.8 ml PBS. Mice received 100 µl of this solution or 2% DMSO in PBS as vehicle control.

Statistical analysis

All data are shown as mean ± SEM. Data were analyzed using GraphPad Prism version 8 (GraphPad Software, San Diego, CA). A two-sided unpaired Student's t-test was used to compare two groups, and one-way analysis of variance (27) with Tukey's *post hoc* test was used for multiple comparisons unless otherwise indicated. A p-value less than 0.05 was considered statistically significant.

Results

TRPM4 I1029M mutant mice show minimum phenotype without stimulation

To examine if mice harboring the human PSEK mutation can spontaneously exhibit a similar skin phenotype, we generated TRPM4 I1029M mutant mice using CRISPR/Cas9 methodology (Figure 1A; see Materials and Methods). This mutation is equivalent to human I1033M mutation. Briefly, purified Cas9, TRPM4-targeting guide RNA (gRNA), and homology directed repair (HDR) oligos were injected into C57BL/6J zygotes. The resulting pups were genotyped by amplifying a 374 bp region flanking the I1029M site and subsequent Sanger sequencing. Since clinical manifestations of PSEK are erythematous hyperkeratotic plaques at hands, foots, or periorificial sites, we observed those sites carefully. TRPM4 I1029M GoF mice, housed under standard specific-pathogen free conditions, did not show an obvious skin phenotype throughout the first 5 months of their lives (Figure 1B). Because other TRPM4 mutations in humans have been associated with familial heart block (9), we performed electrocardiograms in our mutant mice and found no abnormalities compared to WT siblings (data not shown). This is consistent with clinical observations from PSEK patients who do not have cardiac abnormalities (17).

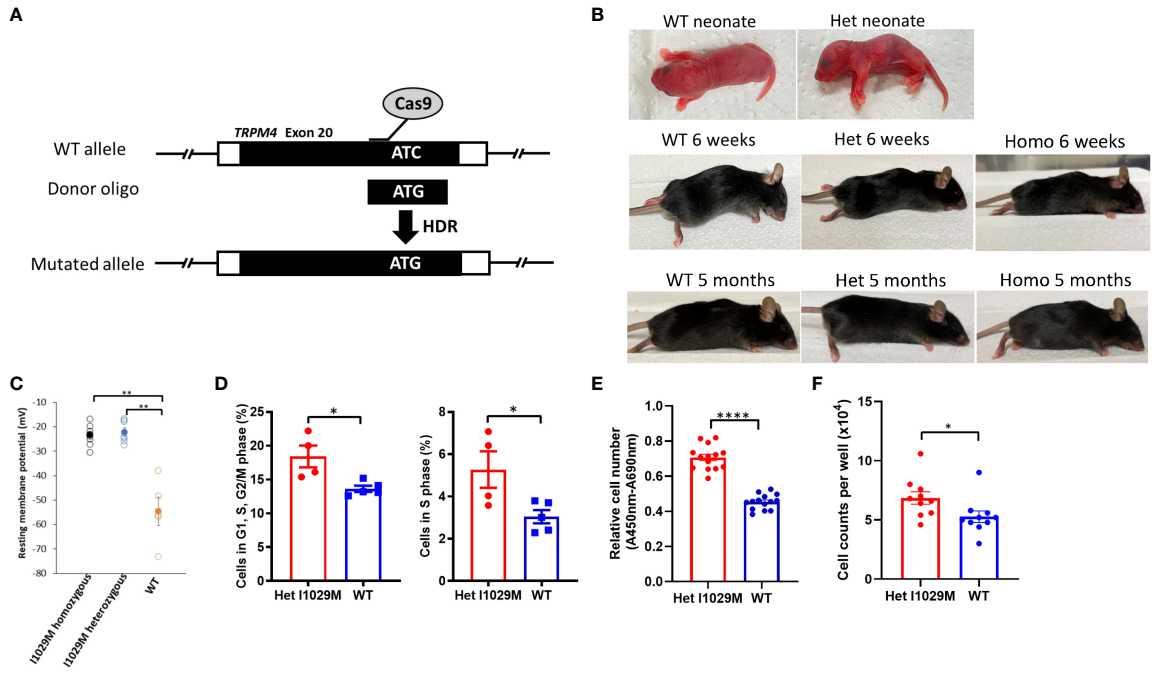

FIGURE 1
Het I1029M mice do not show phenotype without stimulation, however keratinocytes derived from the mutant mice are more proliferative. **(A)** Schematic diagram showing the site-directed mutation of ATC, encoding I1029, to ATG, encoding an M, using CRISPR/Cas9 technology. **(B)** Representative images of mice at neonate, 6-weeks, and 5-month. **(C)** Primary keratinocytes were isolated from the skin of I1029M homozygous, heterozygous, or WT mouse. Resting membrane potential was measured using patch-clamp technique with intracellular Ca^{2+} concentration of 100 μM (n = 5-8). **(D)** Left: Percentages of cells in G1, S, and G2/M phase. Right: Percentages of cells in S phase (n = 4-5). **(E)** The relative cell numbers of WT mice or Het mice-derived keratinocytes, determined by WST-1 assay (n = 14). **(F)** Cell numbers of WT mice or Het mice-derived keratinocytes, determined by cell counting (n = 8-10). Viable cell number was evaluated using WST-1 assay (n = 14). The data are presented as mean ± SEM. Data are representative of two independent experiments. *p < 0.05, **p < 0.01, ****p < 0.0001 by using one-way ANOVA with Tukey's test in multiple comparison, Student's T test in two group comparison.

TRPM4 I1029M mutant keratinocytes exhibit an elevated resting membrane potential

Since we did not find obvious skin changes in TRPM4 GoF mice *in vivo*, we next asked if cells harboring this mutation show any changes compared to WT cells *in vitro*. Previously, we reported that the two TRPM4 missense mutations (I1033M, I1040T; human) exhibited an elevated resting membrane potential in HEK293 cells (17). To determine if this phenomenon occurs in TRPM4 mutant cells *in vitro*, we compared the resting membrane potential in isolated primary keratinocytes from TRPM4 I1029M mutant (and WT) mice. Indeed, the resting membrane potential was elevated in homozygous and heterozygous keratinocytes compared to WT (-23.6 ± 4.3 mV, -22.2 ± 3.7 mV, -54.6 ± 5.8 mV; homozygous, heterozygous, and WT, respectively) (Figure 1C). These results confirmed that TRPM4 activity is indeed enhanced (as expected) with the I1029M mutation. Notably, there was no obvious difference between homozygous and heterozygous mutation with regard to the resting membrane potential. Thus, despite similarities in baseline skin characteristics in TRPM4 mutant and WT mice *in vivo*, keratinocytes from the GoF mutant show elevated resting membrane potential.

TRPM4 I1029M mutant keratinocytes exhibit enhanced proliferation

Since one of the major histological characteristics of PSEK is epidermal hyperplasia, we next asked whether TRPM4 I1029M mutation alters keratinocyte proliferation. In the electrophysiological study, we observed no substantial difference in resting membrane potential between homozygous and heterozygous keratinocytes (Figure 1C). This suggested that a single heterozygous mutation was enough to alter cellular physiology and was consistent with the autosomal dominant

genetic inheritance of PSEK. While homozygous mutant mice were generated along with heterozygous TRPM4 GoF mutant mice, our *in vivo* experiments focused on heterozygous mice (Het I1029M) in order to replicate the human PSEK disease, which is only known to occur in the heterozygous state. Comparing Het I1029M and WT keratinocytes, we found that I1029M keratinocytes were more likely to be in G1, S, G2/M phase or S phase (Figure 1D). WST-1 assay was performed to examine the number of viable cells after 24 hours of incubation with equal numbers of either Het mice-derived or WT mice-derived keratinocytes. The relative cell number of Het mice-derived keratinocytes was significantly higher than those of WT mice-derived keratinocytes (Figure 1E). We performed cell counting, which also confirmed Het keratinocytes were more proliferative (Figure 1F).

Thus, these results show that the Het I1029M mutation stimulated keratinocytes proliferation *in vitro*.

Het I1029M mice exhibit enhanced susceptibility to IMQ-induced psoriasiform dermatitis

Although Het I1029M mice did not display any skin phenotype in the absence of stimulation (Figure 1 B), the results of our *in vitro* experiments indicate that this mutation affects the membrane potentials and proliferation of keratinocytes (Figures 1C–F), suggesting that cells harboring GoF mutant TRPM4 channels might be more susceptible to disease-causing environmental stimuli. The skin manifestations and histopathological findings of PSEK are similar to those of psoriasis (17). Thus, to determine if there is a difference between Het I1029M and WT mice in response to stimulation, we used an IMQ-induced PsD model. As a vehicle control group, we applied Vanicream to WT mice. To see if the application of Vanicream alone can cause any difference between WT and Het I1029M mice, we compared WT and Het I1029M with applying Vanicream only and there was no difference between WT and Het I1029M (Supplementary Figure 3). Firstly, to determine if TRPM4 is expressed in psoriasis skin, we analyzed a publicly available RNA sequencing dataset and found that TRPM4 was expressed in both psoriasis skin lesions and healthy skin controls (Gene Expression Omnibus GSE117405). Het I1029M mice showed more severe inflammation that was characterized by increased ear thickening, erythema, and scale (Figures 2A, B). Changes in ear thickness and clinical score (as assessed by psoriasis severity index score, PSI score) were larger in Het I1029M mice versus their WT littermates (Figure 2B). Consistent with the observation that Het I1029M keratinocytes were more proliferative (Figure 1D–F), epidermal thickness was greater in Het I1029M mice than WT controls (Figure 2C). Interestingly, other parameters such as erythema and scale that reflect inflammation rather than keratinocyte proliferation also showed significant differences (Figure 2B), suggesting that this mutation could affect other aspects of inflammation in this mouse model.

Het I1029M mice do not show altered phenotype in croton oil-induced irritant contact dermatitis or DNFB-induced allergic contact dermatitis

We next asked if TRPM4 GoF mice have susceptibility to other stimuli using two other dermatitis models, i.e., croton oil-induced irritant contact dermatitis and di-nitro-fluoro-benzene (DNFB)-induced allergic contact dermatitis. However, Het I1029M mice did not show altered phenotype in these contact dermatitis models (Supplementary Figures 4, 5). In the croton oil-induced model, WT mice were treated with a 4:1 mixture of acetone and olive oil and served as a vehicle control group. In the DNFB-induced model, WT mice which received DNFB challenge only served as a control group. The results indicate that the effect of TRPM4 GoF had relatively specific functional effects in the PsD-related IMQ model compared to the other two models.

Enhanced inflammation observed in Het I1029M mice is characterized by accumulation of CCR6-expressing γδ-low T cells and higher expression levels of *Il17a*

We next sought to characterize the immunological features of the enhanced skin inflammation observed in Het I1029M mice. One day following the last application of IMQ (day 5), mice were sacrificed and cell suspensions from the ears were prepared. We have previously shown that CC chemokine receptor-6 positive ($CCR6^+$) γδ-low T cells are one of the dominant sources of IL-17A and play an important role in IMQ-induced PsD (28–30). We first evaluated this cell subset by flow cytometry. Het I1029M mice showed an increased proportion of $CCR6^+$ γδ-low T cells as well as neutrophils among $CD45^+$ cells (Figure 2D). We next evaluated mRNA expression levels from mouse ears. mRNA expression levels of *Il17a* were greater in Het I1029M mice than WT (Figure 2E). This was consistent with the IHC staining of p-STAT3 where Het I1029M mice showed higher expression of p-STAT3 (Figure 2A), which is a downstream signaling of IL-17A and plays important roles in psoriatic keratinocytes (31). mRNA expression levels of other cytokines such as *Il6* did not show a difference (data not shown). We next asked if IL-$17A^+$ T cells in the regional lymph node (LN) were increased in Het I1029M mice. IMQ was applied on the mouse ears for 2 days, 24 hours after the second IMQ application, mice were sacrificed and cell suspension from cervical LNs was prepared. Indeed, greater numbers of IL-$17A^+$ $CD3^+$ T cell or IL-$17A^+$ γδ T cells were observed in Het I1029M mice (Figure 2F). LN cells from non-stimulated WT or Het I1029M mice had similar rate of IL-$17A^+$ γδ T cells (Supplementary Figure 6). Collectively, at the immunological level, Het I1029M mice displayed augmented skin inflammation mainly characterized by enhanced Th17

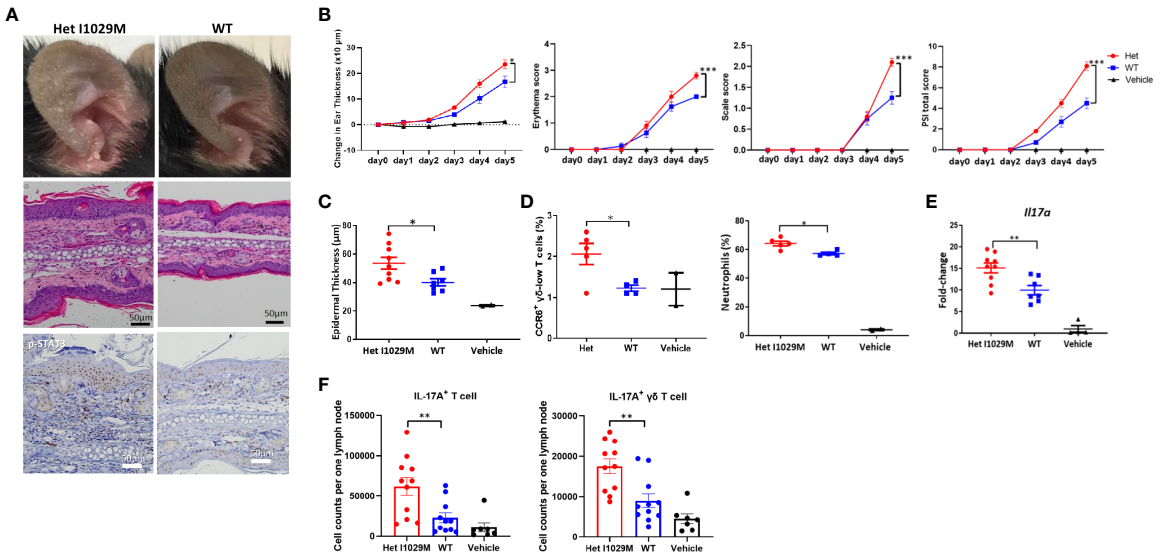

FIGURE 2
Het I1029M mice have enhanced susceptibility to PsD in response to IMQ treatment with more accumulation of CCR6 expressing γδ-low T cells and higher expression levels of *Il17a*. IMQ was applied to the ears of Het I1029M or WT mice for five consecutive days. **(A)** Representative photographs, images of H&E section (scale bars, 50 μm), and images of immunohistochemistry for p-STAT3. **(B)** Changes in ear thickness, erythema score, scale score, and total PSI score (n = 8-10, vehicle; n = 4). **(C)** Histological analysis of epidermal thickness (n = 8-10, vehicle; n = 2). **(D)** Left: proportions of $CCR6^+$ γδ-low T cells among $CD45^+$ cells, right: proportions of neutrophils among $CD45^+$ cells in the lesional skin, determined by flow cytometry (n = 4-5, vehicle; n =2). **(E)** *Il17a* expression levels in the ear skin (n = 8-10, vehicle; n =4). **(F)** Cell from the regional lymph node were collected and evaluated by flow cytometry (n = 11). Vanicream was applied on ears of WT mice as a vehicle control (vehicle; n = 7). The data are presented as mean ± SEM. Data are representative of two independent experiments. *p < 0.05, **p < 0.01, ***p < 0.001 by using Student's t-test.

response compared to WT counterparts following application of IMQ.

Enhanced accumulation of DC in Het I1029M mice

We next sought to identify a functional explanation for the enhanced dermatitis in Het I1029M mice. Since TRPM4 contributes to efficient migration of DC (13), we hypothesized that DC migration is accelerated in Het I1029M mice. To test this idea, we applied 1% FITC solution on mouse ears to both label phagocytic antigen presentation cells, such as dermal and epidermal DC, to measure the efficiency of their migration from skin to regional LN. Six hours after the FITC application, we collected the cervical LNs and determined the $FITC^+$ DC. Indeed, significantly increased numbers of $FITC^+$ DC were observed in Het I1029M mice (Figure 3A), indicating that DC migration is enhanced in Het I1029M mice compared to WT mice. Moreover, this increased DC migration in Het I1029M mice was also observed under the skin was stimulated with IMQ (Figure 3B). Because DCs are one of the key players in PsD, it is possible that this increased migration of DCs contributes to the more severe inflammation observed in the mutant mice.

Glibenclamide, a TRPM4 inhibitor, attenuates IMQ-induced PsD in Het I1029M and WT mice

Since TRPM4 GoF predisposes mice to more active PsD, we predicted that a TRPM4 inhibitor may ameliorate PsD. Glibenclamide, a classic diabetes drug, is known to also act as an inhibitor of TRPM4 (21). Het I1029M and WT mice received daily IMQ application and glibenclamide i.p. injection for 5 days. Indeed, glibenclamide ameliorated IMQ-induced PsD clinically and histologically in both groups of mice (Figures 4A–C). Clinical evaluation represented by the changes in ear thickness revealed that glibenclamide significantly ameliorated IMQ-induced PsD both in WT and Het I1029M mice (Figure 4B). In addition, glibenclamide treatment reduced the epidermal thickness in Het I1029M mice. Flow cytometry of mouse ear showed that the numbers of $CCR6^+$ γδ-low T cells and neutrophils tended (although not reaching statistical significance) to be reduced by glibenclamide in Het I1029M mice (Figure 4D). Furthermore, mRNA levels of *Tnf* were reduced by glibenclamide both in WT and Het I1029M mice, and *Il17a*, *Il17f*, *Cxcl1*, and *K16* were reduced by glibenclamide in Het I1029M mice. (Figure 5). Lastly, we sought to investigate if DC migration is inhibited by glibenclamide. Glibenclamide was intraperitoneally injected, then IMQ was

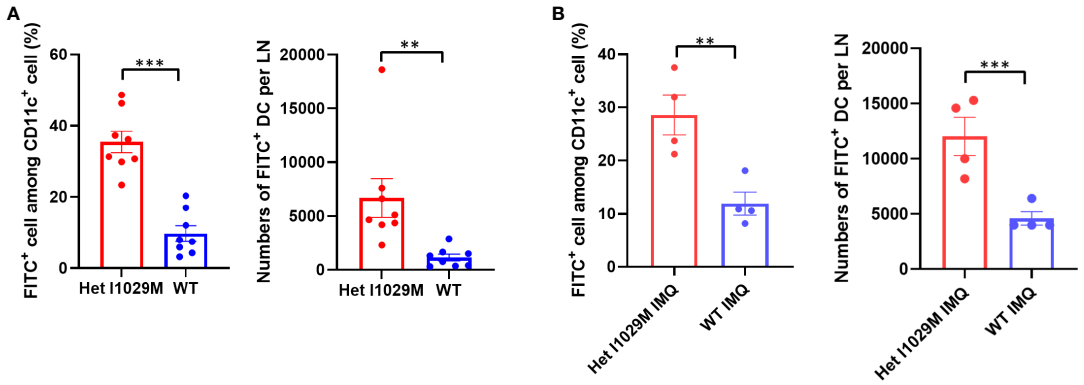

FIGURE 3
Enhanced accumulation of DCs is observed in Het I1029M mice. **(A)**100µl of 1% FITC solution was applied on mouse ears. Six hours after the FITC application, cervical LNs were collected. Left: increased $FITC^+$ rate among $CD11c^+$ cells, right: increased numbers of $FITC^+$ DCs were observed in Het I1029M mice compared to WT (n = 8). **(B)** DC migration assay was conducted under IMQ applied condition. Left: increased $FITC^+$ rate among $CD11c^+$ cells, right: increased numbers of $FITC^+$ DCs were observed in Het I1029M mice compared to WT (n = 4). Data are presented as mean ± SEM and are representative of two independent experiments. **p < 0.01, ***p < 0.001 by using Student's T test.

applied on mice ear. On the next day of the IMQ application, 1% FITC solution was applied on mice ear. Six hours after FITC application, the regional LN was collected and evaluated by flow cytometry. Indeed, DC migration was inhibited by glibenclamide (Figure 6). Thus, a known inhibitor of TRPM4 ameliorates PsD in TRPM4 mutant as well as WT mice, suggesting that TRPM4 may have a regulatory role in PsD and possibly introducing this protein as a therapeutic target in psoriasis.

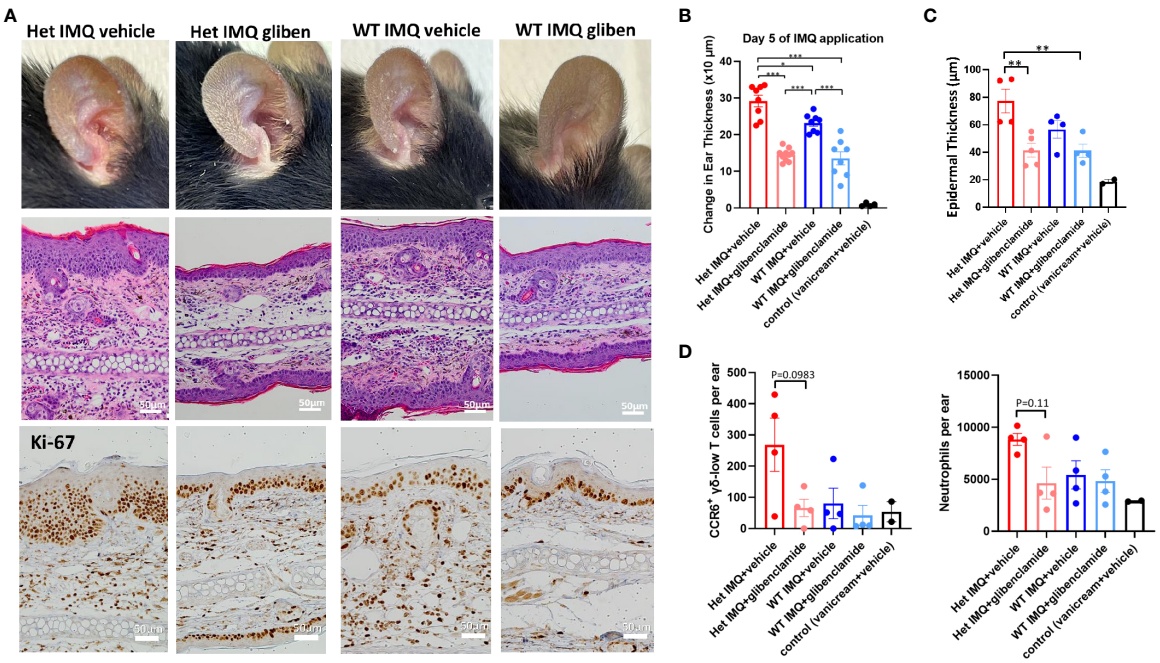

FIGURE 4
Glibenclamide, a TRPM4 inhibitor, attenuates IMQ-induced PsD in Het I1029M and WT mice. Het I1029M mice or WT mice received daily imiquimod application and daily glibenclamide i.p. injection for 5 days. **(A)** Representative photographs, histology images, and immunohistochemical images for Ki-67. **(B)** Changes in ear thickness (n = 8, vehicle; n = 4). **(C)** Histological analysis of epidermal thickness (n = 4, vehicle; n = 2). **(D)** Left: numbers of $CCR6^+$ γδ-low T cells per ear, right: numbers of neutrophils per ear in the lesional skin (n = 4, vehicle; n = 2), determined by flow cytometry. The data are presented as mean ± SEM. Data are representative of two independent experiments. *p < 0.05, **p < 0.01, ***<0.001 by using one-way ANOVA with Tukey's test.

10.3389/fimmu.2022.1025499

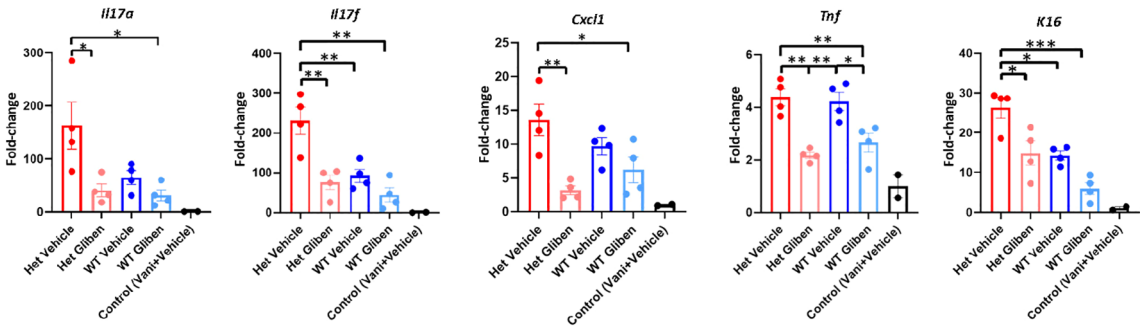

FIGURE 5
Glibenclamide ameliorates proinflammatory cytokine expressions. Het I1029M mice or WT mice received daily imiquimod application and daily glibenclamide i.p. injection for 5 days. RNA was extracted from mice ear skin. RT-qPCR was performed for *Il17a, Il17f, Cxcl1, Tnf, and K16*. The data are presented as mean ± SEM (n = 4, control; n = 2). Data are representative of two independent experiments. *p < 0.05, **p < 0.01, ***<0.001 by using one-way ANOVA with Tukey's test.

Discussion

Recently, we and our collaborators reported two TRPM4 GoF mutations that we suggest are the genetic basis of PSEK (17). Though PSEK is a genetic disease, it is clinically characterized by keratotic erythema that resembles the ones observed in inflammatory skin conditions such as psoriasis (32). Therefore, we hypothesized TRPM4 was involved in not only PSEK but could potentially play a regulatory role in other inflammatory skin diseases. To investigate the role of TRPM4 in the physiology and pathophysiology of dermatitis and PSEK, we generated TRPM4 GoF mutant mice (I1029M) that have an equivalent mutation to human PSEK.

Since PSEK is a disease that develops spontaneously during early childhood without known triggers or stimulation, we carefully observed the mutant mice from birth. Interestingly, our mutant mice did not show an obvious skin phenotype (Figure 1B) despite our observation that Het I1029M keratinocytes showed increased proliferation (Figures 1D–F). We speculate that compensatory mechanisms may inhibit the tendency of the mutant keratinocytes to undergo enhanced proliferation. Another important fact is that PSEK is a spontaneously resolving disease. We hypothesize that some unknown inflammatory trigger that is present in humans (and not present in mice) may be the necessary trigger for the development of PSEK. We further hypothesize that this stimulus may resolve spontaneously as children get older, leading to the eventual disappearance of the PSEK skin disease in older patients. While we have not identified the exact trigger in human PSEK, it is worthwhile noting that several common skin diseases, including atopic dermatitis and acne, that have complex interactions with skin microbiota, occur in younger individuals and tend to resolve in adults.

When subjected to IMQ topical application, a standard model of human psoriasis, Het I1029M mice showed exacerbated inflammation compared to WT (Figure 2A). This inflammation was characterized by higher mRNA expression levels of *Il17a* and accumulation of CCR6$^+$ γδ T cells that is reported to be a major source of IL-17A in this model (Figures 2D, E). Then, we sought to investigate what cells are affected and contribute to the exacerbated inflammation in Het I1029M mice. Among the inflammatory cells, DCs are known to have a pivotal role in psoriasis. Importantly, TRPM4 is reported to be essential for DC migration (13). Our migration assay results clearly demonstrated that DC migration is enhanced in Het I1029M mice. In summary, the TRPM4 mutation may have two independent impacts on the exacerbation of PsD *via* increased proliferation of keratinocytes and enhanced migration of DCs. In Het I1029M mice, DC migration to the regional LN is enhanced (Figure 3A). These migrated DCs potentially stimulate LN T cells leading to expand IL-17A producing γδ T cells. As a result, increased accumulation of IL-17A producing γδ T cells in the lesions could lead to IL-17A-mediated dermatitis. Because keratinocytes are not the predominant cells that directly respond to IMQ, other cell types such as DCs expressing TLR7 should be activated by IMQ, resulting in the production of proinflammatory cytokines that then secondarily activate keratinocytes that express TRPM4. Recently in microglia, TRPM4-mediated NLRP3 inflammasome activation was reported (33). It is possible that TRPM4 GoF may mediate inflammasome-mediated signaling in the context of skin inflammation although this should be tested in future studies.

Interestingly, exaggerated inflammation in Het I1029M mice was only observed in IMQ-induced psoriasiform dermatitis model, but not observed in the croton oil-induced or DNFB-induced dermatitis models. Our results at least showed that DC migration and keratinocyte proliferation are associated with TRPM4 GoF. We

10.3389/fimmu.2022.1025499

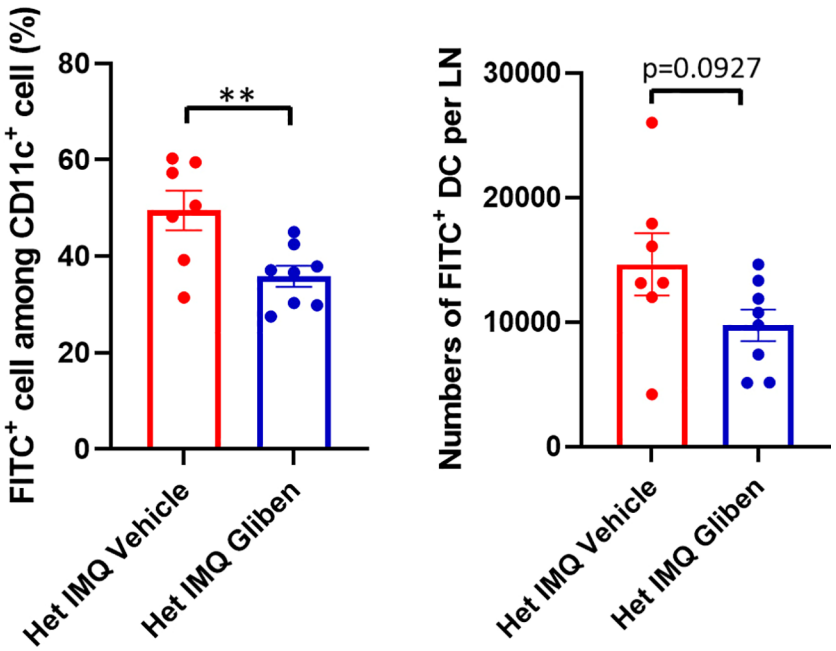

FIGURE 6
DC migration was attenuated by glibenclamide treatment. Glibenclamide was intraperitoneally injected, then IMQ was applied on mice ear. On the next day of the IMQ application, 1% FITC solution was applied on mice ear. Six hours after FITC application, the regional LN was collected, and evaluated by flow cytometry. Left: $FITC^+$ rate among $CD11c^+$ cells, right: numbers of $FITC^+$ DCs. Data are presented as mean ± SEM (n = 7-8) and are representative of two independent experiments. **p < 0.01 by using Student's T test.

speculate that diseases in which DC migration and keratinocyte proliferation play important roles would be greatly affected by TRPM4 GoF. As both DC migration and keratinocyte proliferation are the important features in psoriasis-like skin inflammation, that may explain why this GoF mutation specifically enhanced IMQ-induced skin inflammation. Clearly, other models of skin inflammation (such as tape-stripping) could be tested in the future to examine the specificity of TRPM4-mediated signaling.

Consequently, an important question is whether or not this exacerbated PsD in Het I1029M mice or spontaneous PsD in WT mice can be ameliorated by a TRPM4 inhibitor. TRPM4 channels can exist as homomers or assemble with sulfonylurea receptors (SURs) as complexes (34, 35). Glibenclamide inhibits SUR-TRPM4 heteromeric channels (34), but it may also directly inhibit TRPM4 channels (36, 37). Glibenclamide clearly ameliorated PsD both in Het I1029M and WT (Figures 4A–D, 5). Moreover, glibenclamide clearly inhibited DC migration to the regional LN (Figure 6). These results help to re-affirm that the enhanced PsD observed in Het mice is a direct consequence of the TRPM4 channel. Since both WT and Het TRPM4 mice had reduced PsD when treated with glibenclamide, we suggest that TRPM4 may be a new and relevant target for psoriasis in humans.

There are several limitations in this study. One of the limitations is some of the results showed trends, but did not reach statistical significance due to the lack of availability of larger numbers of mutant mice. However, we note that these trends were observed in multiple experiments. Furthermore, we used only glibenclamide as a TRPM4 inhibitor because it is most widely used TRPM4 inhibitor used *in vivo*. Future studies using TRPM4 inhibitors other than glibenclamide are warranted. Lastly, while we were able to study keratinocytes and dendritic cells in greater detail, one limitation of this study is that we were not able to assess the biochemical characteristics of other immune cells such as T cells that might also be impacted by TRPM4 function. Because of multiple known functions of TRPM4 in different cell types, it is possible that TRPM4 GoF mutation regulates PsD in several ways, but, of note, a TRPM4 inhibitor blocks PsD in WT as well as TRPM4 GoF mice. Overall, these data indicate that TRPM4 may contribute to PsD in humans and that it warrants further study as a target in human psoriasis.

Data availability statement

The original contributions presented in the study are included in the article/Supplementary Materials, further inquiries can be directed to the corresponding author/s.

Ethics statement

The animal study was reviewed and approved by Institutional Animal Care and Use Committee, University of California, Davis.

Author contributions

DY, SV, JZ, and SH designed the experiments, analyzed the data and wrote the manuscript. XW, ZS, and MH acquired, analyzed and interpreted the data. DM and JB analyzed and interpreted the data. All authors contributed to the article and approved the submitted version.

Funding

Research reported in this publication was supported by the National Institutes of Health under award number 1R01NS128180-01 (to JZ) and Department of Dermatology Seed Grant (to SH).

Conflict of interest

The authors declare that the research was conducted in the absence of any commercial or financial relationships that could be construed as a potential conflict of interest.

Publisher's note

All claims expressed in this article are solely those of the authors and do not necessarily represent those of their affiliated organizations, or those of the publisher, the editors and the reviewers. Any product that may be evaluated in this article, or claim that may be made by its manufacturer, is not guaranteed or endorsed by the publisher.

Supplementary material

The Supplementary Material for this article can be found online at: https://www.frontiersin.org/articles/10.3389/fimmu.2022.1025499/full#supplementary-material

References

1. Kruse M, Pongs O. TRPM4 channels in the cardiovascular system. *Curr Opin Pharmacol* (2014) 15:68–73. doi: 10.1016/j.coph.2013.12.003

2. Syam N, Chatel S, Ozhathil LC, Sottas V, Rougier JS, Baruteau A, et al. Variants of transient receptor potential melastatin member 4 in childhood atrioventricular block. *J Am Heart Assoc* (2016) 5:e001625. doi: 10.1161/JAHA.114.001625

3. Launay P, Fleig A, Perraud AL, Scharenberg AM, Penner R, Kinet JP. TRPM4 is a Ca2+-activated nonselective cation channel mediating cell membrane depolarization. *Cell* (2002) 109:397–407. doi: 10.1016/s0092-8674(02)00719-5

4. Winkler PA, Huang Y, Sun W, Du J, Lu W. Electron cryo-microscopy structure of a human TRPM4 channel. *Nature* (2017) 552:200–4. doi: 10.1038/nature24674

5. Guo J, She J, Zeng W, Chen Q, Bai XC, Jiang Y. Structures of the calcium-activated, non-selective cation channel TRPM4. *Nature* (2017) 552:205–9. doi: 10.1038/nature24997

6. Autzen HE, Myasnikov AG, Campbell MG, Asarnow D, Julius D, Cheng Y. Structure of the human TRPM4 ion channel in a lipid nanodisc. *Science* (2018) 359:228–32. doi: 10.1126/science.aar4510

7. Duan J, Li Z, Li J, Santa-Cruz A, Sanchez-Martinez S, Zhang J, et al. Structure of full-length human TRPM4. *Proc Natl Acad Sci U S A.* (2018) 115:2377–82. doi: 10.1073/pnas.1722038115

8. Gonzales AL, Garcia ZI, Amberg GC, Earley S. Pharmacological inhibition of TRPM4 hyperpolarizes vascular smooth muscle. *Am J Physiol Cell Physiol* (2010) 299:C1195–202. doi: 10.1152/ajpcell.00269.2010

9. Wang C, Naruse K, Takahashi K. Role of the TRPM4 channel in cardiovascular physiology and pathophysiology. *Cells* (2018) 7. doi: 10.3390/cells7060062

10. Cheng H, Beck A, Launay P, Gross SA, Stokes AJ, Kinet JP, et al. TRPM4 controls insulin secretion in pancreatic beta-cells. *Cell Calcium.* (2007) 41:51–61. doi: 10.1016/j.ceca.2006.04.032

11. Earley S. TRPM4 channels in smooth muscle function. *Pflugers Arch* (2013) 465:1223–31. doi: 10.1007/s00424-013-1250-z

12. Weber KS, Hildner K, Murphy KM, Allen PM. Trpm4 differentially regulates Th1 and Th2 function by altering calcium signaling and NFAT localization. *J Immunol* (2010) 185:2836–46. doi: 10.4049/jimmunol.1000880

13. Barbet G, Demion M, Moura IC, Serafini N, Leger T, Vrtovsnik F, et al. The calcium-activated nonselective cation channel TRPM4 is essential for the migration but not the maturation of dendritic cells. *Nat Immunol* (2008) 9:1148–56. doi: 10.1038/ni.1648

14. Vennekens R, Olausson J, Meissner M, Bloch W, Mathar I, Philipp SE, et al. Increased IgE-dependent mast cell activation and anaphylactic responses in mice lacking the calcium-activated nonselective cation channel TRPM4. *Nat Immunol* (2007) 8:312–20. doi: 10.1038/ni1441

15. Kruse M, Schulze-Bahr E, Corfield V, Beckmann A, Stallmeyer B, Kurtbay G, et al. Impaired endocytosis of the ion channel TRPM4 is associated with human progressive familial heart block type I. *J Clin Invest.* (2009) 119:2737–44. doi: 10.1172/JCI38292

16. Liu H, El Zein L, Kruse M, Guinamard R, Beckmann A, Bozio A, et al. Gain-of-function mutations in TRPM4 cause autosomal dominant isolated cardiac conduction disease. *Circ Cardiovasc Genet* (2010) 3:374–85. doi: 10.1161/CIRCGENETICS.109.930867

17. Wang H, Xu Z, Lee BH, Vu S, Hu L, Lee M, et al. Gain-of-Function mutations in TRPM4 activation gate cause progressive symmetric erythrokeratodermia. *J Invest Dermatol* (2019) 139:1089–97. doi: 10.1016/j.jid.2018.10.044

18. Launay P, Cheng H, Srivatsan S, Penner R, Fleig A, Kinet JP. TRPM4 regulates calcium oscillations after T cell activation. *Science* (2004) 306:1374–7. doi: 10.1126/science.1098845

19. Serafini N, Dahdah A, Barbet G, Demion M, Attout T, Gautier G, et al. The TRPM4 channel controls monocyte and macrophage, but not neutrophil, function for survival in sepsis. *J Immunol* (2012) 189:3689–99. doi: 10.4049/jimmunol.1102969

20. Shimizu T, Owsianik G, Freichel M, Flockerzi V, Nilius B, Vennekens R. TRPM4 regulates migration of mast cells in mice. *Cell Calcium.* (2009) 45:226–32. doi: 10.1016/j.ceca.2008.10.005

21. Schattling B, Steinbach K, Thies E, Kruse M, Menigoz A, Ufer F, et al. TRPM4 cation channel mediates axonal and neuronal degeneration in experimental autoimmune encephalomyelitis and multiple sclerosis. *Nat Med* (2012) 18:1805–11. doi: 10.1038/nm.3015

22. Li F, Adase CA, Zhang LJ. Isolation and culture of primary mouse keratinocytes from neonatal and adult mouse skin. *J Vis Exp* (2017) 125:56027. doi: 10.3791/56027

23. Kim KH, Sederstrom JM. Assaying cell cycle status using flow cytometry. *Curr Protoc Mol Biol* (2015) 111:28601–11. doi: 10.1002/0471142727.mb2806s111

24. van der Fits L, Mourits S, Voerman JS, Kant M, Boon L, Laman JD, et al. Imiquimod-induced psoriasis-like skin inflammation in mice is mediated *via* the IL-23/IL-17 axis. *J Immunol* (2009) 182:5836–45. doi: 10.4049/jimmunol.0802999

25. Shi Z, Garcia-Melchor E, Wu X, Getschman AE, Nguyen M, Rowland DJ, et al. Targeting the CCR6/CCL20 axis in entheseal and cutaneous inflammation. *Arthritis Rheumatol* (2021) 73:2271–81. doi: 10.1002/art.41882

26. Shi Z, Wu X, Santos Rocha C, Rolston M, Garcia-Melchor E, Huynh M, et al. Short-term Western diet intake promotes IL-23Mediated skin and joint inflammation accompanied by changes to the gut microbiota in mice. *J Invest Dermatol* (2021) 141:1780–91. doi: 10.1016/j.jid.2020.11.032

27. Gerzanich V, Woo SK, Vennekens R, Tsymbalyuk O, Ivanova S, Ivanov A, et al. *De novo* expression of Trpm4 initiates secondary hemorrhage in spinal cord injury. *Nat Med* (2009) 15:185–91. doi: 10.1038/nm.1899

28. Cai Y, Shen X, Ding C, Qi C, Li K, Li X, et al. Pivotal role of dermal IL-17-producing gammadelta T cells in skin inflammation. *Immunity* (2011) 35:596–610. doi: 10.1016/j.immuni.2011.08.001

29. Mabuchi T, Takekoshi T, Hwang ST. Epidermal CCR6+ gammadelta T cells are major producers of IL-22 and IL-17 in a murine model of psoriasiform dermatitis. *J Immunol* (2011) 187:5026–31. doi: 10.4049/jimmunol.1101817

30. Yu S, Wu X, Zhou Y, Han D, Anderson LS, Simon SI, et al. Is CCR6 required for the development of psoriasiform dermatitis in mice? *J Invest Dermatol* (2019) 139:485–8. doi: 10.1016/j.jid.2018.07.036

31. Furue M, Furue K, Tsuji G, Nakahara T. Interleukin-17A and keratinocytes in psoriasis. *Int J Mol Sci* (2020) 21:1275. doi: 10.3390/ijms21041275

32. Nir M, Tanzer F. Progressive symmetric erythrokeratodermia. *Dermatologica* (1978) 156:268–73. doi: 10.1159/000250927

33. He Y, Chang Y, Peng Y, Zhu J, Liu K, Chen J, et al. Glibenclamide directly prevents neuroinflammation by targeting SUR1-TRPM4-Mediated NLRP3 inflammasome activation in microglia. *Mol Neurobiol* (2022) 59:6590–607. doi: 10.1007/s12035-022-02998-x

34. Woo SK, Kwon MS, Ivanov A, Gerzanich V, Simard JM. The sulfonylurea receptor 1 (Sur1)-transient receptor potential melastatin 4 (Trpm4) channel. *J Biol Chem* (2013) 288:3655–67. doi: 10.1074/jbc.M112.428219

35. Malysz J, Maxwell SE, Yarotskyy V, Petkov GV. TRPM4 channel inhibitors 9-phenanthrol and glibenclamide differentially decrease guinea pig detrusor smooth muscle whole-cell cation currents and phasic contractions. *Am J Physiol Cell Physiol* (2020) 318:C406–C21. doi: 10.1152/ajpcell.00055.2019

36. Demion M, Bois P, Launay P, Guinamard R. TRPM4, a Ca2+-activated nonselective cation channel in mouse sino-atrial node cells. *Cardiovasc Res* (2007) 73:531–8. doi: 10.1016/j.cardiores.2006.11.023

37. Ozhathil LC, Delalande C, Bianchi B, Nemeth G, Kappel S, Thomet U, et al. Identification of potent and selective small molecule inhibitors of the cation channel TRPM4. *Br J Pharmacol* (2018) 175:2504–19. doi: 10.1111/bph.14220

frontiers | Frontiers in Immunology

TYPE Original Research
PUBLISHED 24 October 2022
DOI 10.3389/fimmu.2022.991797

OPEN ACCESS

EDITED BY
Camelia Quek,
Melanoma Institute Australia, Australia

REVIEWED BY
Julin Xie,
The First Affiliated Hospital of Sun Yat-sen University, China
Tiancheng Zhang,
Fudan University, China
Yan Zhang,
Nankai University, China

*CORRESPONDENCE
Wenying Zhong
sczjhzzwy@126.com
Xinhua Liu
liuxinhua@tmu.edu.cn

†These authors have contributed equally to this work

SPECIALTY SECTION
This article was submitted to Cancer Immunity and Immunotherapy, a section of the journal Frontiers in Immunology

RECEIVED 12 July 2022
ACCEPTED 03 October 2022
PUBLISHED 24 October 2022

CITATION
Yang J, Xu Y, Xie K, Gao L, Zhong W and Liu X (2022) CEBPB is associated with active tumor immune environment and favorable prognosis of metastatic skin cutaneous melanoma. *Front. Immunol.* 13:991797. doi: 10.3389/fimmu.2022.991797

CEBPB is associated with active tumor immune environment and favorable prognosis of metastatic skin cutaneous melanoma

Jingrun Yang[1,2†], Yang Xu[3†], Kuixia Xie[4†], Ling Gao[3], Wenying Zhong[4*] and Xinhua Liu[3,5*]

[1]Department of General Surgery, The First Medical Center of Chinese People's Liberation Army (PLA) General Hospital, Beijing, China, [2]Key Laboratory of Bio-inspired Materials and Interfacial Science, Technical Institute of Physics and Chemistry, Chinese Academy of Sciences, Beijing, China, [3]Department of Biochemistry and Molecular Biology, School of Basic Medical Sciences, Hangzhou Normal University, Hangzhou, China, [4]Department of Dermatology, The Affiliated Hospital of Hangzhou Normal University, Hangzhou, China, [5]Key Laboratory of Aging and Cancer Biology of Zhejiang Province, Hangzhou Normal University, Hangzhou, China

Metastatic skin cutaneous melanoma (SKCM) is a common malignancy that accounts for low morbidity but high mortality of skin cancer. SKCM is characterized by high lymphocytic infiltration, whereas the states of infiltrated cells are variable in patients leading to a heterogeneous prognosis and hindering appropriate clinical decisions. It is therefore urgent to identify markers associated with lymphocytic infiltration, cellular conditions, and the prognosis of SKCM. In this study, we report that CEBPB, a transcriptional factor, is mainly expressed in macrophages in metastatic SKCM and associated with an active tumor immune environment and a favorable prognosis through integrated analysis of single-cell and bulk RNA-seq datasets. High CEBPB expression is significantly associated with active inflammation and immune response pathways in both macrophages and bulk SKCM tumor tissues. A signature based on CEBPB-associated genes that are specifically expressed in macrophages could robustly and prognostically separate different metastatic SKCM patients. In addition, the associations between the metastatic SKCM tumor signature and microenvironment with respect to T-cell recruitment and state, inflammation response, angiogenesis, and so on were also determined. In conclusion, we present here the first report on CEBPB in tumor immune environment and prognosis regulation in metastatic SKCM and construct a reliable signature, which should provide a useful biomarker for stratification of the patient's prognosis and therapeutic selection.

KEYWORDS

CEBPb, SKCM, tumor immune microenvironment, single cell RNAseq, immune subtype

Introduction

Skin cutaneous melanoma (SKCM), which occurs in the skin, is the most common type of melanoma. SKCM is one of the most aggressive and lethal malignancies, which accounts for only 3–5% of morbidity but almost 75% of mortality of skin cancer (1). Surgical resection followed by adjuvant chemotherapy or radiotherapy to control tumor spread represents the optimal therapeutic method for localized SKCM (2). Additionally, the development of targeted therapy and immunotherapy has significantly prolonged the overall survival (OS) of SKCM patients (3, 4). However, metastasis continues to pose a great threat to the prognosis of SKCM patients, and the probability of 5-year OS of metastatic SKCM is only approximately 19% (5). Systemic treatment, including chemotherapy and a combination of chemotherapy and biochemotherapy, has been extensively used in metastatic SKCM, but only low clinical benefits have been achieved and were often accompanied by great toxicity (6). A high level of lymphocytic infiltration in both primary lesions and metastatic sites enables SKCM to be an ideal candidate for immunotherapy, which aims to modulate the immune environment of tumor tissue, and a significant improvement and less toxicity compared to conventional chemotherapy are obtained (7). In contrast, great heterogeneities of response to immunotherapy exist in metastatic SKCM patients, largely due to the heterogeneous tumor microenvironment (TME) (8, 9). As a result, the identification of molecular biomarkers for metastatic SKCM stratification with different TME would be helpful for appropriate clinical decision-making.

The TME is a complex community composed of multiple cell types and interactions among them. Lymphocytes and myeloid cells could infiltrate the solid tumor tissue through tumor vasculature or other means, consisting of the immune part of the TME (9). Infiltration levels and states of cells are dynamically regulated by various factors. For example, the migration of T cells from the second lymphoid organ to the solid tumor tissue is regulated by some chemokines (10). High expression of PD-1, CTLA4 on the T cell surface, or PD-L1/L2 on the malignant cell surface could induce the exhaustion of T cells, resulting in the reduction and even the loss of their cytotoxicity on malignant cells (11). Cell–cell interactions *via* an autocrine or paracrine manner could also influence the states of infiltrated cells in the TME. Such malignant cells could induce the differentiation of fibroblasts into cancer-associated fibroblasts (CAFs) and promote tumor metastasis. Macrophage polarization to the M2 subtype induced by CAFs could in turn result in a suppressed immune environment mainly through manipulation of T-cell states (12). Additionally, it turned out that a growing number of molecules were involved in the regulation of the TME. For example, PTEN has been extensively studied solely in the epithelial context as a tumor suppressor, whereas its indispensable role in CAF regulation in the TME has recently been identified and approved for participation in cancer progression (13). CDR1, as a circular RNA, was found to be closely associated with the infiltration and state of immune cells in multiple cancers (14). However, the understanding of TME regulation in cancers, including metastatic SKCM, is far from complete, which represents an obstacle to the development of therapeutic methods and the determination of appropriate treatments.

CEBPB is a transcriptional factor (TF) that has three subtypes, namely, LAP-1, LAP-2, and LIP. LAP-1 and LAP-2 play important roles in transcriptional activation, while LIP is mainly involved in transcriptional repression (15). One of the most known functions of CEBPB is immune modulation in multiple inflammatory diseases, including sepsis (16, 17) and skin or fibrotic diseases (18–20). Furthermore, it has been demonstrated that CEBPB is the master regulator of macrophage differentiation, which could define the macrophage identity by marking the macrophage-specific chromatin regulatory elements for the following TF binding (21). The regulatory roles of CEBPB in the onset of cancer and the progression of its transcriptional regulatory function in malignant cells have also been uncovered (22, 23). A few studies have also reported potential associations between CEBPB and metastasis (24) or treatment response in melanoma (25). However, relationships between CEBPB and tumor immune landscape as well as the prognosis of metastatic SKCM have never been systemically reported.

In this study, we report that CEBPB is mainly expressed as macrophages in the TME of metastatic SKCM and is associated with an active immune environment. A signature based on CEBPB-regulated genes that are expressed specifically in macrophages could robustly separate prognostically and immunologically different metastatic SKCM patients.

Materials and methods

Datasets, normal fibroblast, and melanoma cell line

A total of three metastatic SKCM datasets were used for survival analysis in this study. The TCGA-SKCM cohort contains a total of 472 samples including one adjacent normal tissue sample, out of which 349 metastatic ones, including distant metastasis, regional lymph node metastasis, and regional skin metastasis, with complete prognosis information, were retained in this study. Another metastatic SKCM cohort was obtained from the study of Garraway et al. (26) and abbreviated as DFCI2015 hereafter, which contains 40 metastatic SKCM samples with transcriptome and complete survival information freely available. Notably, all 40 patients of the DFCI2015 cohort experimented with anti-CTLA4 treatment and the molecular data were obtained before the treatment. GSE59455 (27) from the Gene Expression Omnibus (GEO;

https://www.ncbi.nlm.nih.gov/geo/) contains 141 SKCM samples including 39 primary and 102 metastatic ones, only those metastatic samples were retained for analysis, and all the samples were deceased at the end of the follow-up. Additionally, GSE46517 (28) contains 121 samples including 73 metastatic SKCM samples, 31 primary SKCM samples, nine nevus samples, and seven normal skin samples, and one normal epithelial melanocyte sample was also included in this study for CEBPB expression comparison. CEBPB mRNA level was compared between the 73 metastatic SKCM and the seven normal skin samples. Gene Expression Profiling Interactive Analysis (GEPIA; http://gepia.cancer-pku.cn/) online tool was also adopted to estimate the difference in CEBPB mRNA level by including the SKCM tumor samples from The Cancer Genome Atlas (TCGA) and normal skin samples from Genotype-Tissue Expression (GTEx; https://www.gtexportal.org/). A single-cell RNA-seq dataset GSE115978 (29), which contains gene expression profiles of 7,186 cells from 31 melanoma samples, was used for CEBPB cell-specific expression analysis.

Normal dermal fibroblast was obtained from a 67-year-old male keloid patient in a Chinese PLA hospital with signed consent obtained. The ethics committee of PLA General Hospital approved this study (Ethics Approval No. S2018-223-02). The details for fibroblast extraction and culture could be found in our previous study (30). Additionally, skin melanoma cell lines A375 and SK-MEL-2 were obtained from the RE-STEM cell bank (Jiangsu, China).

Cell culture

A375 cells were cultured in a complete medium (DMEM: serum:double antibody = 100:10:1) and placed in a 5% CO_2, 37° C incubator for culture. Subculture was carried out every 3 days, and seeds were grown on plates.

Transfection

A total of 1×10^5 cells were plated on a 6-well plate and transfected with 2 μg of either pcDNA3.1-3×Flag as mock control or CEBPB-pcDNA3.1-3×Flag. Transfection was done using 4 μl of PEI 40000 following the manufacturer's protocol. Cells were transfected overnight for cell proliferation assay.

Reverse transcription–PCR

Total RNA was extracted using the Steady Pure Quick RNA Extraction Kit (AG) according to the manufacturer's instructions and used for first-strand cDNA synthesis using the Evo M-MLVRT Mix Kit (AG). The quantification of all gene transcripts was performed on a QuantStudioTM5 Real-Time PCR Instrument (Applied Biosystems Inc., Foster City, CA, USA) using the SYBR R Green Premix Pro Taq HS qPCR Kit (Rox Plus, Hunan, China) (AG), and RNA levels were normalized to those of 18S rRNA. $2^{-\Delta\Delta ct}$ was applied to analyze the data. Three parallel duplicate wells were designed for the experiment, and all samples were tested three times. Error bars represent the mean ± standard deviation (SD) from three independent experiments. The primer sequences used were as follows: 18S rRNA forward: 5′-GTAACCCGTTGAACCCCATT-3′, reverse: 5′-CCATCCAATCCGTAGTAGCG-3′; CEBPB, forward: 5′ TTTCGAAGTTGATGCAATCGG-3′, reverse: 5′-CGTAGGAACATCTTTAAGCGA-3′.

Assessment of cell proliferation with cell counting kit-8 test

Cells were divided into the control group and the overexpression-CEBPB group. The cells were spread in 96-well plates with 3,000 cells per well, and then an appropriate amount of Cell Counting Kit-8 (CCK-8) reagent was added to detect the absorbance of each experimental group, so as to measure the proliferation activity at different times.

Differential expression analysis

Differential expression analysis between metastatic SKCM samples with higher and lower CEBPB mRNA levels was performed by using the DESeq2 R package (31) based on the raw count data. For the single-cell RNA-seq, which provides fragments per kilobase of transcript per million mapped reads (FPKM) data for each cell, the limma R package (https://bioconductor.org/packages/release/bioc/html/limma.html) was applied for differential expression analysis between cells with CEBPB FPKM > 1 and those without CEBPB detected. Threshold of absolute log2(Fold Change) (|log2FC|) > 1 and false discovery rate (FDR) adjusted p-value<0.05 was used as the criteria for screening significantly differentially expressed genes (DEGs).

Functional enrichment analysis

Significantly enriched Kyoto Encyclopedia of Genes and Genomes (KEGG) pathways were obtained by using the clusterProfiler R package (32) to the DEGs with the threshold of Benjamini–Hochberg (BH) adjusted p-value<0.05. In addition, Gene Set Enrichment Analysis (GSEA) was also adopted to identify hallmarks (gene signatures) that are associated with CEBPB expression in both bulk metastatic SKCM tissue and the macrophages in the TME by using GSEA software (33) with the threshold of nominal p-value<0.05.

Construction of death risk signature

Univariate Cox regression analysis was first applied to the candidate genes, namely, CEBPB-regulated genes in macrophages, to identify prognostically significant genes based on the metastatic melanoma samples in the TCGA-SKCM cohort with the threshold of p-value<0.05. Least absolute shrinkage and selection operator (LASSO) Cox regression analysis by using the glmnet R package (https://cran.r-project.org/web/packages/glmnet/) was then performed to further prioritize genes from the significant ones in univariate Cox regression analysis for death risk signature construction. The signature was finally constructed as an equation for the estimation of death risk for each metastatic SKCM patient: risk score (RS) = $\sum_{i=1}^{n} Coe_i \times E_i$, in which Coe_i and E_i represent the LASSO Cox coefficient and mRNA level of the ith gene, respectively.

Survival analysis

Kaplan–Meier (KM) analysis by using the survival R package (https://CRAN.R-project.org/package=survival) was used for determining the significance of the difference in OS probability between metastatic SKCM patients with higher and lower CEBPB expression as well as with higher and lower RS. p-Value<0.05 was used as the significant threshold.

Statistical analysis and visualization

A comparison of expression of CEBPB and antigen presentation-related genes between different patient groups was performed by using the Wilcoxon test with the threshold of p-value<0.05. Visualization of gene expression boxplot and volcano plot of differential expression analysis was performed through the ggplot2 R package (https://ggplot2-book.org/). The KM survival probability plot was visualized through the survminer R package (https://cran.r-project.org/web/packages/survminer/). The expression heatmap was visualized through the pheatmap R package (https://cran.rstudio.com/web/packages/pheatmap/). All the statistical analyses of this study were performed in R version 4.0.2 (https://www.r-project.org/).

Results

CEBPB is downregulated in metastatic skin cutaneous melanoma and associated with favorable prognosis

To explore alterations of CEBPB expression in SKCM initiation, we first performed a comparison analysis through GEPIA online tool (http://gepia.cancer-pku.cn/), which includes SKCM tumor tissue samples from TCGA and normal tissue samples from GTEx. As a result, CEBPB was significantly downregulated in SKCM tumor tissues (Figure 1A), which was further confirmed by another independent cohort GSE46517, which included 73 metastatic SKCM samples and seven normal skin samples (primary and nevus samples were excluded from this study) (Figure 1B). To validate the downregulation of CEBPB in melanoma, we performed RT-PCR of CEBPB in dermal fibroblast from the normal skin of a keloid patient and A375 and SK-MEL-2 melanoma cells. As a result, the CEBPB mRNA level was significantly lower in A375 and SK-MEL-2 cells compared with that in dermal fibroblast (Figure 1C). To confirm the repression of CEBPB protein expression in SKCM tissue, we obtained the immunohistochemical staining results of CEBPB in three normal skin and three tumor tissues of malignant melanoma patients from the Human Protein Atlas (HPA; https://www.proteinatlas.org/). The staining intensity of CEBPB is obviously higher in normal skin samples than that in melanoma tumor tissues (Figure S1). Additionally, a high CEBPB mRNA level was proved to be associated with a favorable prognosis, namely, longer overall survival here, of metastatic SKCM in both the TCGA cohort (Figure 1D) and DFCI2015, another independent patient cohort (Figure 1E, not significant, which might be attributed to its relatively small sample size, but the survival probability difference between the two groups is obvious). These indicated that CEBPB could inhibit the initiation and progression of SKCM.

To explore if CEBPB has any influence on melanoma proliferation, we overexpressed CEBPB in both A375 and SK-MEL-2 cell lines and performed a CCK-8 assay. Strikingly, CEBPB overexpression (OE-CEBPB) almost had no influence on the proliferation ability of the two cell lines (Figure S2). We speculated that CEBPB might affect skin melanoma mainly by influencing other cell types in the tumor microenvironment rather than the malignant cell itself.

CEBPB is associated with immune pathway activity in metastatic skin cutaneous melanoma

CEBPB is a transcription factor that plays important roles in gene expression regulation. To identify genes regulated by CEBPB in metastatic SKCM tumor tissue, we selected the 10 metastatic SKCM tumor tissues that have the highest CEBPB expression (CEBPB_High) and the 10 with the lowest CEBPB expression (CEBPB_Low) from the TCGA cohort and conducted differential gene expression analysis between the two sample groups. As a result, a total of 2,039 DEGs, including 842 downregulated and 1,197 upregulated genes, were obtained in CEBPB_High compared with CEBPB_Low samples (Figure 2A). Functional enrichment analysis of those

DEGs obtained many immune-related or TME regulation-related pathways, such as cytokine–cytokine interaction, JAK–STAT signaling pathway, and TNF signaling pathway (Figure 2B; Supplementary Table 1). GSEA indicated that immune response-related pathways were significantly activated in CEBPB_High metastatic SKCM samples (Figure 2C; Supplementary Table 2). These indicate that CEBPB participates in the immune activation in metastatic SKCM.

CEBPB is mainly expressed in macrophages of metastatic skin cutaneous melanoma tumor tissue and is associated with immune activation

To explore if CEBPB was specifically expressed in some cell types in the TME of metastatic SKCM tumor tissue, we analyzed its mRNA level in a single cell RNA-seq dataset (GSE115978) of metastatic SKCM patients across multiple cell types. Strikingly, it was mainly expressed in macrophages but nearly depleted in other cell types (Figure 3A). CEBPB has been previously reported to be a master regulator in macrophages; we here proposed to explore genes regulated by CEBPB in macrophages of metastatic SKCM TME. We first identified macrophage-specific genes in the TME by comparing the gene expression in macrophages with other cell types with the threshold of |log2(Fold Change)| > 0.5 and FDR-adjusted p-value<0.05, which obtained a total of 2,516 genes (Figure 3B), and CEBPB was expectedly identified. Then we selected the macrophages that have no CEBPB mRNA detected and those with FPKM of CEBPB > 1 and performed differential expression analysis between those two macrophage groups. As a result, a total of 41 upregulated and seven downregulated genes in addition to CEBPB itself were identified in CEBPB_High macrophages compared with those without CEBPB detected (Figure 3C). Additionally, GSEA indicated that immune response-related pathways, such as inflammatory response and IL6–JAK–STAT3 signaling pathway, were significantly activated in CEBPB_High macrophages (Figure 3D; Supplementary Table 3), which was consistent with the bulk tumor tissue analysis. These indicated that CEBPB might manipulate the TME of metastatic SKCM by influencing the macrophage state.

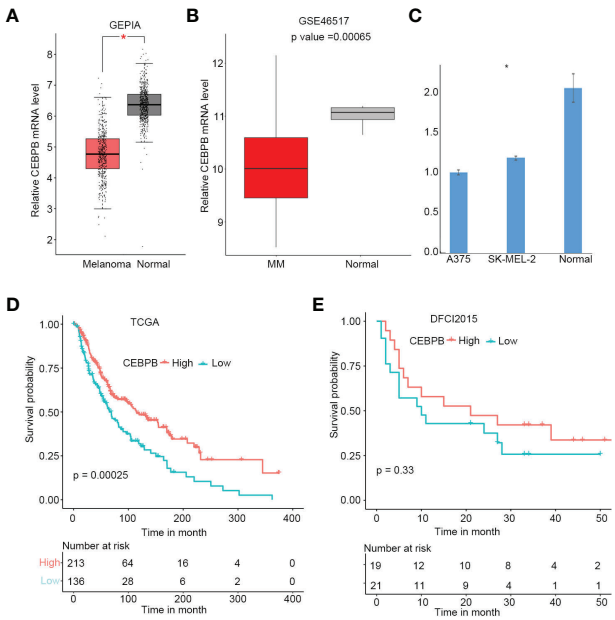

FIGURE 1
CEBPB is downregulated in metastatic SKCM and associated with superior prognosis. **(A)** Boxplot of relative CEBPB mRNA level in SKCM tumor samples from TCGA and normal skin samples from GTEx analyzed based on GEPIA. Asterisk indicates significant difference. **(B)** Boxplot of relative CEBPB mRNA level in metastatic SKCM tumor samples and normal skin samples from GSE46517. Exact p-value was provided. **(C)** Relative mRNA level of CEBPB in normal dermal fibroblast, A375, and SK-MEL-2 melanoma cell lines. **(D, E)** The KM survival probability curve of metastatic SKCM patients from TCGA-SKCM and DFCI2015 cohorts. The patients were grouped according to the best cut-point of CEBPB expression obtained through survminer R package. p-Value was determined by using log-rank test. SKCM, skin cutaneous melanoma; TCGA, The Cancer Genome Atlas; GTEx, Genotype-Tissue Expression; GEPIA, Gene Expression Profiling Interactive Analysis; KM, Kaplan–Meier.

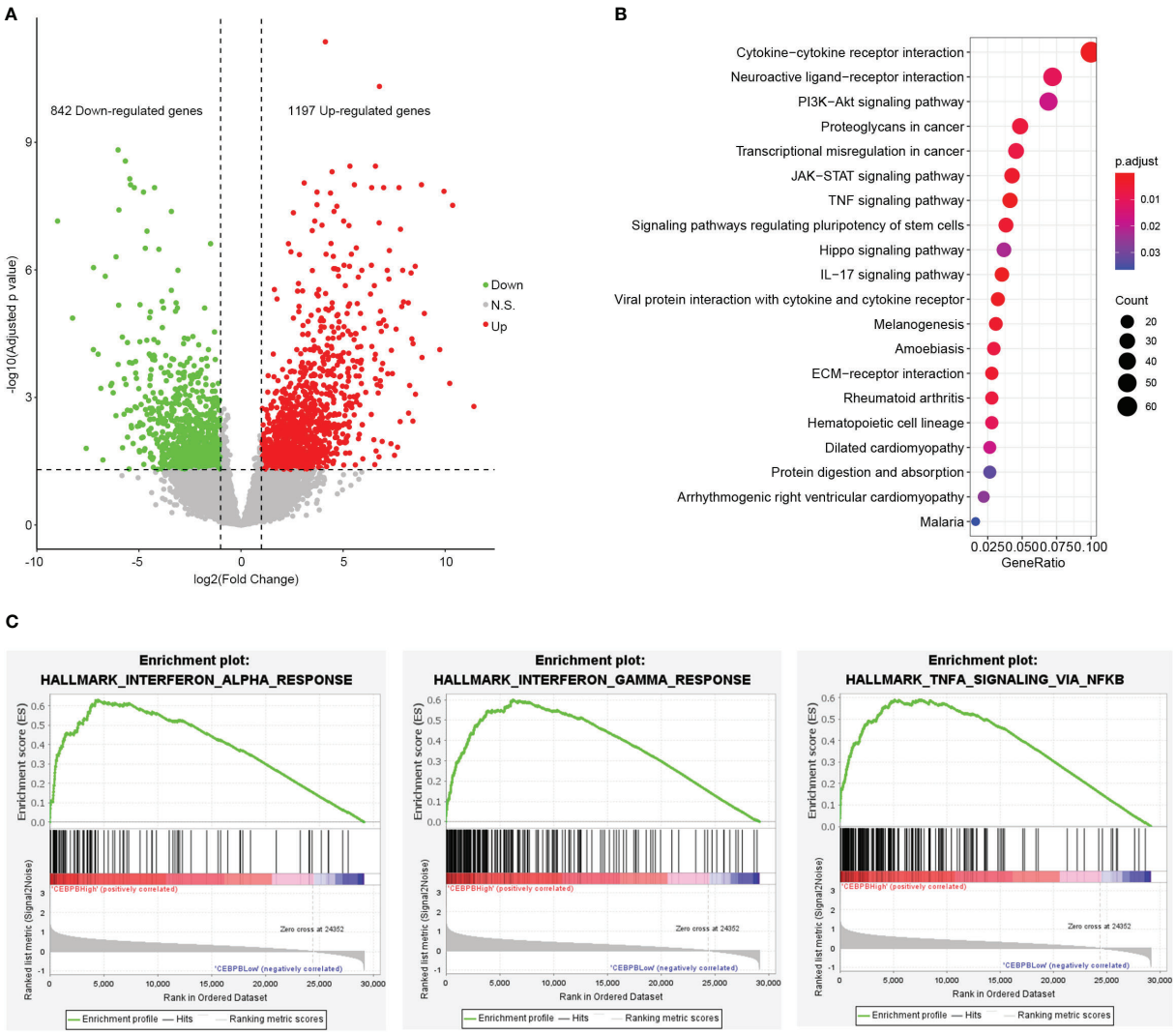

FIGURE 2
CEBPB is closely associated with immune response in metastatic SKCM tumor tissue. **(A)** Volcano plot of differential expression analysis between the 10 metastatic SKCM patients with the highest CEBPB expression (CEBPB_High) and the 10 with the lowest CEBPB expression (CEBPB_Low) from TCGA-SKCM cohort. Green, red, and gray dots represent significant downregulated, upregulated, and non-significant genes in CEBPB_High samples compared with CEBPB_Low samples. x-Axis and y-axis are log2FC and log10-based FDR-adjusted p-value, respectively. **(B)** The top 20 most significantly enriched KEGG pathways of the 2,039 DEGs in CEBPB_High samples. Dot size and color illustrate the number of genes included in the corresponding pathway and significance, respectively. Full list of significant KEGG pathways is provided in Supplementary Table 1. **(C)** Enrichment plot of three hallmark gene sets that are significantly enriched and specifically activated in the CEBPB_High samples compared with CEBPB_Low samples. The full list of significantly enriched gene sets in CEBPB_High samples is provided in Supplementary Table 2. SKCM, skin cutaneous melanoma; FDR, false discovery rate; KEGG, Kyoto Encyclopedia of Genes and Genomes; DEGs, differentially expressed genes.

A macrophage-specific CEBPB-associated gene signature could robustly distinguish prognostically different metastatic skin cutaneous melanoma patients

As TME state is closely associated with the prognosis of multiple cancers, we here proposed to explore if the CEBPB-associated genes could predict the prognosis of metastatic SKCM patients. We performed a univariate Cox regression analysis of the 48 DEGs in macrophages that were regulated by CEBPB along with CEBPB itself for their association with OS probability of metastatic SKCM patients from TCGA, which identified 36 prognostic-related genes. The top 20 most significant genes along with their hazard ratio and p-value were provided as a forest plot in Figure 4A. To further

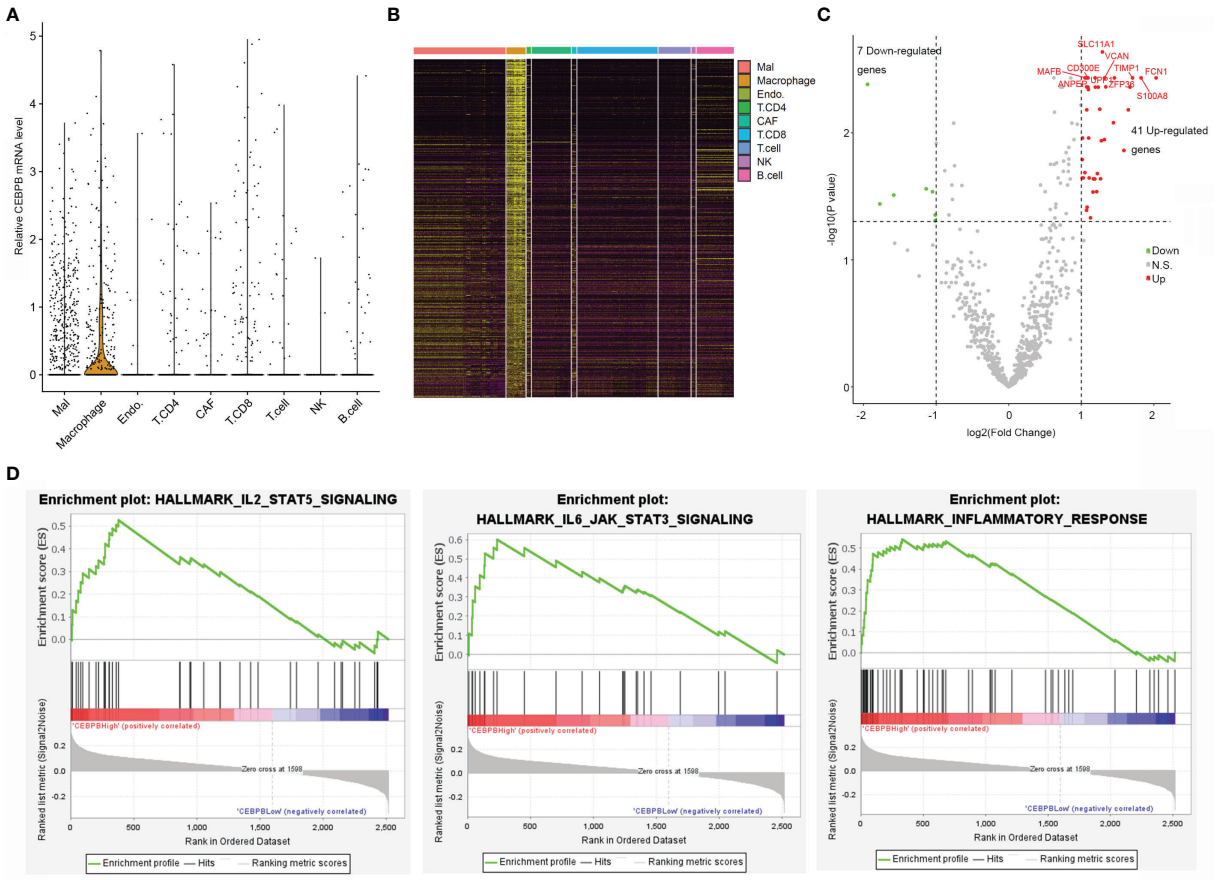

FIGURE 3
CEBPB is mainly expressed in macrophages of metastatic SKCM TME and associated with the immune activity of macrophages. **(A)** Distribution of CEBPB expression across different cell types in the metastatic SKCM TME. **(B)** Heatmap illustrating the expression of macrophage-specific markers across different cell types in the metastatic SKCM TME. **(C)** Volcano plot of differential expression analysis between macrophages with CEBPB FPKM > 1 and those macrophages without CEBPB detected. Only macrophage-specific genes were included in this analysis, and CEBPB itself was not included in this plot. Green, red, and gray dots represent genes that were significantly downregulated, upregulated, and non-significant in CEBPB FPKM > 1 macrophage compared with those without CEBPB detected. **(D)** Enrichment plot of three significantly enriched, specifically activated hallmark gene sets in CEBPB FPKM > 1 macrophage compared with macrophages without CEBPB detected. The full list of significantly enriched hallmark gene sets is provided in Supplementary Table 3. SKCM, skin cutaneous melanoma; TME, tumor microenvironment.

prioritize genes for prognostic signature construction, we applied the LASSO Cox regression method to the 36 prognostically significant genes, which finally retained five genes (Figure 4B), including FPR2, AIF1, LILRB2, SOD2, and FCGR2C, and the death RS of metastatic SKCM patients could be calculated by the sum of multiply–accumulate of each gene's relative expression, namely, log2-based raw sequencing reads, and its regression coefficient: RS = −0.0194 × FPR2 − 0.0202 × AIF1 − 0.0254 × LILRB2 − 0.0387 × SOD2 − 0.1226 × FCGR2C. We calculated the RS for the metastatic SKCM patients in TCGA cohort and found that patients with high RS had relatively short OS than those with low RS (Figure 4C). Additionally, KM analysis also illustrated the association between high RS and inferior OS of metastatic SKCM patients in TCGA cohort as well as another two independent validation metastatic SKCM patient cohorts (Figure 4D). Receiver operating characteristic (ROC) curve analysis for the prediction ability of RS for 3-year OS probability of metastatic SKCM patients obtained the area under the curve (AUC) of TCGA, DFCI2015, and GSE59455 as 0.690, 0.677, and 0.669, respectively (Figure 4E), which indicated the good performance of RS in prognosis prediction.

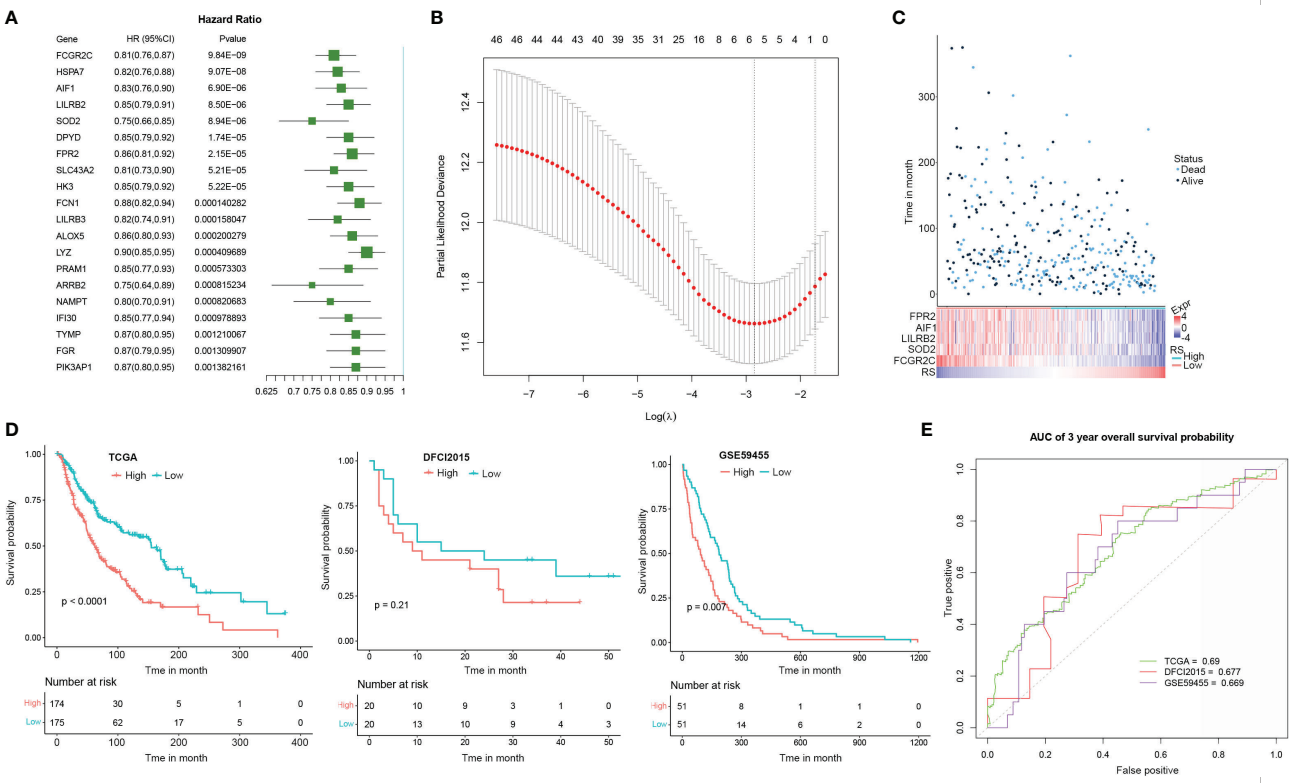

FIGURE 4
The signature based on the CEBPB-regulated genes in macrophages could robustly distinguish prognostically different metastatic SKCM patients. **(A)** Forest plot illustrating the hazard ratio (HR) and significance of the top 20 most significant CEBPB-regulated genes in macrophages in univariate Cox regression analysis of their association with overall survival probability of metastatic SKCM patients in TCGA-SKCM cohort. **(B)** LASSO Cox regression plot showing the optimal number of genes to be included in the death risk score (RS) signature. **(C)** RS and the overall survival time (month) as well as the survival status of each metastatic SKCM patient in TCGA-SKCM were altogether provided as a dot plot along with a heatmap. Each dot represents a patient, with dot color indicating the survival status, and the corresponding RS could be obtained through the last row of the heatmap. The relative expression of genes included in the signature was also illustrated in the heatmap. **(D)** KM survival probability curve of metastatic SKCM patients in TCGA-SKCM (left panel), DFCI2015 (middle panel), and GSE59455 (right panel) cohorts. The patients were grouped by the median RS value. p-Value was determined by using log-rank test. **(E)** Survival ROC curve for estimating the reliability of the RS in predicting the 3-year overall survival probability. The curve color represents the dataset used as indicated in the plot. SKCM, skin cutaneous melanoma; LASSO, least absolute shrinkage and selection operator; KM, Kaplan–Meier; ROC, receiver operating characteristic.

CEBPB-associated risk score is related to tumor immune landscape in metastatic skin cutaneous melanoma

RS could robustly separate prognostically different metastatic SKCM patients, and the TME plays fundamental roles in cancer initiation, progression, and drug resistance, so we proposed to explore the potential association between RS and TME landscape in metastatic SKCM tissues. First, the relative infiltration level of lymphocyte, myeloid cell, and the stromal cell was determined by the MCPCounter algorithm and compared between metastatic SKCM patients of the TCGA cohort stratified by their median RS. As a result, T cells, CD8 T cells, cytotoxic lymphocytes, NK cells, and monocytic lineage cells were among the most differential cell types, which had significantly high infiltration levels in SKCM patients with low RS. In contrast, neutrophils, endothelial cells, and fibroblasts only showed a slight difference between the two patient groups (Figure 5A). We then comprehensively collected genes closely related to TME modulation, including cytokines and chemokines associated with immune activity, namely, T-cell chemotaxis and activation and tertiary lymphoid structures here, and those associated with immune suppressive, including T cell-specific suppression, angiogenesis, and immunosuppression, and we compared their expressions between metastatic SKCM patients with high and low RS. Expectedly, mRNA levels of all the genes related to T-cell chemotaxis and activation as well as tertiary lymphoid structures (TLSs) were significantly higher in metastatic SKCM patients with low RS than those with high RS. Strikingly, most of the genes related to immune suppressive also showed higher expression in RS_low patients except angiogenesis-related

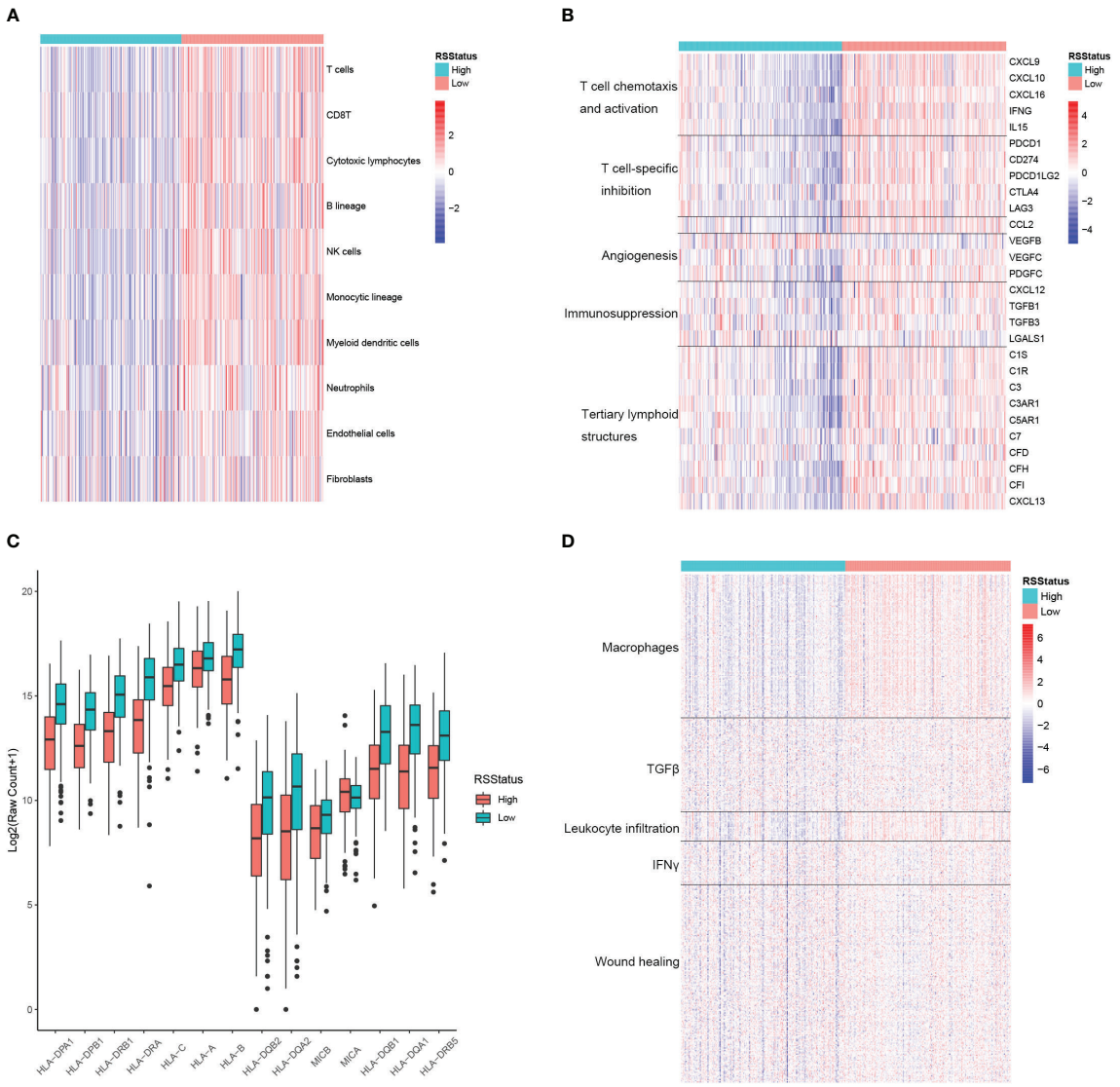

FIGURE 5
The signature based on the CEBPB-regulated genes in macrophages is closely associated with immune activity in metastatic SKCM TME. **(A)** Relative abundance of lymphocytes, myeloid cells, and stromal cells in metastatic SKCM patients' tumor samples of the TCGA-SKCM cohort stratified by the median RS value. **(B)** Relative expression of genes of several immunologically suppressive and active signatures in metastatic SKCM patients' tumor samples of the TCGA-SKCM cohort stratified by the median RS value. **(C)** Relative expression of antigen presentation-related genes in metastatic SKCM patients' tumor samples of the TCGA-SKCM cohort with higher and lower RS stratified by the median RS value. Asterisk indicates a significant difference, namely, p-value< 0.05. n.s. represents non-significance. **(D)** Relative expression of genes used for defining immune cluster in the study of Shmulevich et al. (34) in the metastatic SKCM patients' tumor tissues of the TCGA-SKCM cohort stratified by the median RS value. RSStatus, risk score status based on the median RS value; SKCM, skin cutaneous melanoma; TME, tumor microenvironment.

VEGFB and immunosuppression-related LGALS1, which were significantly higher in patients with higher RS (Figure 5B). This was partially controversial, for lower RS was associated with superior OS (Figure 4). We speculated that the immune active environment might stimulate the response of immunosuppression signals of multiple origins, such as high expression of immune checkpoint ligand gene in malignant cells and chemokine cascade secreted from tumor-associated macrophage (TAM) for regulatory T-cell recruitment. Antigen presentation (AP) is a core process for the recognition and the following cytotoxicity of T cells for malignant cells. Hence, we collected a comprehensive list of AP-related genes and compared their mRNA levels in metastatic SKCM patients from the TCGA cohort stratified by the median RS. As a result, 13 of the 14 genes showed significantly higher expressions in patients with low RS (RS_low) than in those with high RS (RS_high) as shown in Figure 5C, indicating that the RS_low

patients had a more intact AP system, which might underlie the better OS of those patients. Additionally, Shmulevich et al. grouped cancer patients into five immune clusters according to gene expression signatures associated with immune activity (34). To explore the relationship between RS and the immune cluster, we collected the genes used for defining each immune cluster and compared their mRNA levels between RS_low and RS_high metastatic SKCM patients. As a result, genes enriched in the macrophage and leukocyte infiltration cluster showed obviously higher expressions in RS_low patients than RS_high patients, whereas differences in expressions of TGFβ, IFNγ, and wound healing-related genes were nearly indistinguishable between the two patient groups (Figure 5D). These indicated that low RS is associated with high immune activity and might have predictive value for immunotherapy response.

Discussion

Metastatic SKCM is a common malignancy worldwide that accounts for low morbidity but very high mortality in all skin cancers (35). High exposure to UV irradiation represents the most common pathogenesis, which induces a high accumulation of mutation and in turn causes aggressive lymphocytic infiltration (36). Systemic treatment, including radiotherapy, chemotherapy, and the recently developed immunotherapy, are the most adopted therapeutics, and they provide some clinical benefits to metastatic SKCM, but heterogeneous clinical outcomes stand in the way of widespread adoption (37, 38). Therefore, it is urgently necessary to identify biomarkers or signatures that may immunologically and prognostically distinguish different patients.

In this study, we reported the associations between CEBPB and prognosis as well as the TME landscape of metastatic SKCM patients, and a genetic signature associated with CEBPB was developed for immune activity and stratification of OS probabilities. The results showed that high CEBPB expression is associated with a favorable prognosis of metastatic SKCM and activated immune response-related pathways in bulk tumor tissue as well as pure macrophages. It has been extensively reported that CEBPB participates in immune regulation (16, 39), and CEBPB contributes to immune activation in many scenarios and relates to the occurrence of many autoimmune diseases (40, 41). Particularly, it represents a master regulator for macrophage identity determination (21). Indeed, CEBPB has proven to be nearly specifically expressed in the macrophages of metastatic SKCM tissues and regulates several immune response-related pathways in both macrophage and bulk tumor tissue in this study. Macrophages exhibit controversial roles at different tumor stages. For example, macrophages could cause tumor regression by directly killing malignant cells or promoting the presentation of tumor cells to T cells. In contrast, macrophages might transform into TAMs and promote tumorigenesis, progression, metastasis, and drug resistance when type 2 T helper cell dominates the TME contexture (12). Above all, we speculated that CEBPB could prompt the polarization of macrophages to the immunologically stimulative subtype in metastatic SKCM TME and in turn inhibit tumor progression. In addition, the CEBPB mRNA level was significantly lower in melanoma cells than in normal dermal fibroblasts. In contrast, CEBPB overexpression almost had no influence on the proliferation ability of melanoma cells. CEBPB therefore might affect the initiation and progression of melanoma through the modulation of the tumor microenvironment rather than the malignant cell itself. In contrast, correlations between the change in malignant cells caused by CEBPB inhibition and tumor microenvironment perturbation should still be further studied.

For the important roles of macrophages in the determination of a relationship between the TME and tumor progression, we specially screened the macrophage-specific genes that were regulated by CEBPB in the metastatic SKCM and constructed a prognostic signature by using several CEBPB-regulated genes. The robustness of the gene signature in prognosis stratification was confidently validated with the assistance of three independent patient cohorts. In addition, we found obvious differences in the TME landscape between the signature-derived RS in high and low patients. Generally, the RS_low metastatic SKCM patients illustrated a more active immune environment than RS_high patients with respect to T-cell infiltration and state as well as antigen presentation. Unexpectedly, certain genes related to immunosuppression and angiogenesis also showed higher mRNA levels in the RS_low patient group than in the RS_high group. The TME is a complex contexture in which immunologically active and suppressive signals coexist and transition from high tumor immunity in the initial tumor to low tumor immunity in the late-stage tumor, which could occur in tumor progression (42, 43). In quantitative terms, the relative increment in the expression of immunologically active-related genes in RS_low samples compared to RS_high samples is much higher than that of immunologically suppressive-related genes, which might indicate that the RS could discriminate between patients with dominant immunoactive TME versus those with dominant immunosuppressants.

Immunotherapy is a recently developed therapeutic that aims to modulate the TME, and significant prognostic improvement has been achieved. However, the efficacy of immunotherapy is highly heterogeneous across different cancers and among individuals of the same cancer with

differences in their immune environment (44). Some biomarkers, such as tumor mutation burden, neoantigen load, and lymphocytic infiltration, have been proposed to be associated with immunotherapy responses (45, 46). However, there is evidence that the predictive values are limited in numerous investigations. In this study, the RS is closely associated with TME state: the lower the RS, the more active the immunity. In addition, the DFCI2015 patient cohort is comprised of immunotherapy-experienced metastatic SKCM patients, and the RS could robustly discriminate against the different prognostic patients. These indicate the potential predictive value of the RS in the immunotherapy response of metastatic SKCM patients.

This study also has several limitations. First of all, the conclusion about the influence of CEBPB on the tumor microenvironment of melanoma patients was mainly based on the prediction of the immune cell infiltration ratio in tumor tissues. An animal model with an intact immune system along with CEBPB perturbation would be more precise for exploring associations between CEBPB and the tumor microenvironment. Another limitation of this study was the lack of normal melanocytes for validation of CEBPB mRNA level, which was superseded by dermal fibroblast, although the CEBPB expression was indeed very low in A375 and SK-MEL-2 melanoma cells. These efforts will continue into the future.

Conclusion

In conclusion, we validated the positive role of CEBPB in metastatic SKCM patients and its function in enabling the immune response pathway in both bulk SKCM tissue and macrophages of SKCM TME for the first time. Additionally, a signature based on genes regulated by CEBPB in macrophages was also constructed, which could robustly distinguish prognostically and immunologically different metastatic SKCM patients. It might be a potentially useful marker for immunotherapy response.

Data availability statement

The original contributions presented in the study are included in the article/Supplementary Material. Further inquiries can be directed to the corresponding authors.

Author contributions

KX performed data curation and formal analysis. LG performed formal analysis. WZ performed the investigation. XL performed the writing – review and editing. JY and YX performed experiments and writing of the revised manuscript. All authors contributed to the article and approved the submitted version.

Funding

This work was supported by the research start-up funds of Hangzhou Normal University (No. 4125C50221204039) and National Natural Science Foundation of China (No. 82203471).

Conflict of interest

The authors declare that the research was conducted in the absence of any commercial or financial relationships that could be construed as a potential conflict of interest.

Publisher's note

Supplementary material

The Supplementary Material for this article can be found online at: https://www.frontiersin.org/articles/10.3389/fimmu.2022.991797/full#supplementary-material

SUPPLEMENTARY FIGURE 1
Immunohistochemical staining of CEBPB in normal skin samples and melanoma tumor tissues from HPA database. Patient ID in HPA were provided for each staining image.

SUPPLEMENTARY FIGURE 2
Cell proliferation ability detected by CCK-8 assay for control and OE-CEBPB A375 (A) and SK-MEL-2 (B) cell lines.

References

1. Shenenberger DW. Cutaneous malignant melanoma: a primary care perspective. *Am Fam Phys* (2012) 85(2):161–8.

2. Berk-Krauss J, Stein JA, Weber J, Polsky D, Geller AC. New systematic therapies and trends in cutaneous melanoma deaths among US whites, 1986-2016. *Am J Public Health* (2020) 110(5):731–3. doi: 10.2105/AJPH.2020.305567

3. Lugowska I, Teterycz P, Rutkowski P. Immunotherapy of melanoma. *Contemp Oncol (Pozn)* (2018) 22(1A):61–7. doi: 10.5114/wo.2018.73889

4. Kee D, McArthur G. Targeted therapies for cutaneous melanoma. *Hematol Oncol Clin North Am* (2014) 28(3):491–505. doi: 10.1016/j.hoc.2014.02.003

5. Miller KD, Nogueira L, Mariotto AB, Rowland JH, Yabroff KR, Alfano CM. Cancer treatment and survivorship statistics, 2019. *CA Cancer J Clin* (2019) 69 (5):363–85. doi: 10.3322/caac.21565

6. Bhatia S, Tykodi SS, Thompson JA. Treatment of metastatic melanoma: an overview. *Oncol (Williston Park)* (2009) 23(6):488–96.

7. Paijens ST, Vledder A, de Bruyn M, Nijman HS. Tumor infiltrating lymphocytes (TIL) therapy in metastatic melanoma: boosting of neoantigen-specific T cell reactivity and long-term follow-up. *J Immunother Cancer* (2020) 8 (2):1–11. doi: 10.1136/jitc-2020-000848

8. Tao T, Liu Y, Zhang J, Huang L, Tao Y. Dynamic observation: Immune-privileged microenvironment limited the effectiveness of immunotherapy in an intraocular metastasis mouse model. *Ophthal Res* (2022) 53. doi: 10.1159/000524485

9. Tschernia NP, Gulley JL. Tumor in the crossfire: Inhibiting TGF-beta to enhance cancer immunotherapy. *BioDrugs* (2022) 36(2):153–80. doi: 10.1007/s40259-022-00521-1

10. Harlin H, Meng Y, Peterson AC, Zha Y, Tretiakova M, Slingluff C, et al. Chemokine expression in melanoma metastases associated with CD8+ T-cell recruitment. *Cancer Res* (2009) 69(7):3077–85. doi: 10.1158/0008-5472.CAN-08-2281

11. Jiang Y, Li Y, Zhu B. T-Cell exhaustion in the tumor microenvironment. *Cell Death Dis* (2015) 6:e1792. doi: 10.1038/cddis.2015.162

12. Lopez-Yrigoyen M, Cassetta L, Pollard JW. Macrophage targeting in cancer. *Ann N Y Acad Sci* (2021) 1499(1):18–41. doi: 10.1111/nyas.14377

13. Lefler JE, Seward C, Ostrowski MC. PTEN in cancer associated fibroblasts. *Adv Cancer Res* (2022) 154:203–26. doi: 10.1016/bs.acr.2022.01.002

14. Zou Y, Zheng S, Deng X, Yang A, Xie X, Tang H, et al. The role of circular RNA CDR1as/ciRS-7 in regulating tumor microenvironment: A pan-cancer analysis. *Biomolecules* (2019) 9(9):1–13. doi: 10.3390/biom9090429

15. Sterken BA, Ackermann T, Muller C, Zuidhof HR, Kortman G, Hernandez-Segura A, et al. C/EBPbeta isoform-specific regulation of migration and invasion in triple-negative breast cancer cells. *NPJ Breast Cancer* (2022) 8(1):11. doi: 10.1038/s41523-021-00372-z

16. Xu C, Xu J, Lu L, Tian W, Ma J, Wu M. Identification of key genes and novel immune infiltration-associated biomarkers of sepsis. *Innate Immun* (2020) 26 (8):666–82. doi: 10.1177/1753425920966380

17. McPeak MB, Youssef D, Williams DA, Pritchett CL, Yao ZQ, McCall CE, et al. Frontline science: Myeloid cell-specific deletion of cebpb decreases sepsis-induced immunosuppression in mice. *J Leukoc Biol* (2017) 102(2):191–200. doi: 10.1189/jlb.4HI1216-537R

18. Qie C, Jiang J, Liu W, Hu X, Chen W, Xie X, et al. Single-cell RNA-seq reveals the transcriptional landscape and heterogeneity of skin macrophages in vsir (-/-) murine psoriasis. *Theranostics* (2020) 10(23):10483–97. doi: 10.7150/thno.45614

19. Satoh T, Nakagawa K, Sugihara F, Kuwahara R, Ashihara M, Yamane F, et al. Identification of an atypical monocyte and committed progenitor involved in fibrosis. *Nature* (2017) 541(7635):96–101. doi: 10.1038/nature20611

20. Vittal R, Mickler EA, Fisher AJ, Zhang C, Rothhaar K, Gu H, et al. Type V collagen induced tolerance suppresses collagen deposition, TGF-beta and associated transcripts in pulmonary fibrosis. *PloS One* (2013) 8(10):e76451. doi: 10.1371/journal.pone.0076451

21. Kuznetsova T, Prange KHM, Glass CK, Winther MPJ. Transcriptional and epigenetic regulation of macrophages in atherosclerosis. *Nat Rev Cardiol* (2020) 17 (4):216–28. doi: 10.1038/s41569-019-0265-3

22. Shao K, Pu W, Zhang J, Guo S, Qian F, Glurich I, et al. DNA Hypermethylation contributes to colorectal cancer metastasis by regulating the binding of CEBPB and TFCP2 to the CPEB1 promoter. *Clin Epigenet* (2021) 13 (1):89. doi: 10.1186/s13148-021-01071-z

23. Wang S, Xia D, Wang X, Cao H, Wu C, Sun Z, et al. C/EBPbeta regulates the JAK/STAT signaling pathway in triple-negative breast cancer. *FEBS Open Bio* (2021) 11(4):1250–8. doi: 10.1002/2211-5463.13138

24. Swoboda A, Soukup R, Eckel O, Kinslechner K, Wingelhofer B, Schörghofer D, et al. STAT3 promotes melanoma metastasis by CEBP-induced repression of the MITF pathway. *Oncogene* (2021) 40(6):1091–105. doi: 10.1038/s41388-020-01584-6

25. Vidarsdottir L, Fernandes RV, Zachariadis V, Das I, Edsbäcker E, Sigvaldadottir I, et al. Silencing of CEBPB-AS1 modulates CEBPB expression and resensitizes BRAF-inhibitor resistant melanoma cells to vemurafenib. *Melanoma Res* (2020) 30(5):443–54. doi: 10.1097/CMR.0000000000000675

26. Van Allen EM, Miao D, Schilling B, Shukla SA, Blank C, Zimmer L, et al. Genomic correlates of response to CTLA-4 blockade in metastatic melanoma. *Science* (2015) 350(6257):207–11. doi: 10.1126/science.aad0095

27. Budden T, Davey RJ, Vilain RE, Ashton KA, Braye SG, Beveridge NJ. Repair of UVB-induced DNA damage is reduced in melanoma due to low XPC and global genome repair. *Oncotarget* (2016) 7(38):60940–53. doi: 10.18632/oncotarget.10902

28. Kabbarah O, Nogueira C, Feng B, Nazarian RM, Bosenberg M, Wu M, et al. Integrative genome comparison of primary and metastatic melanomas. *PloS One* (2010) 5(5):e10770. doi: 10.1371/journal.pone.0010770

29. Jerby-Arnon L, Shah P, Cuoco MS, Rodman C, Su M-J, Melms JC, et al. A cancer cell program promotes T cell exclusion and resistance to checkpoint blockade. *Cell* (2018) 175(4):984–997.e24. doi: 10.1016/j.cell.2018.09.006

30. Xie K, Peng Y, Zhong W, Liu X. KMT2C is a Potential Biomarker of Anti-PD-1 Treatment Response in Metastatic Melanoma. *Front Biosci (Landmark Ed)* (2022) 27(3):103. doi: 10.31083/j.fbl2703103

31. Love MI, Huber W, Anders S. Moderated estimation of fold change and dispersion for RNA-seq data with DESeq2. *Genome Biol* (2014) 15(12):550. doi: 10.1186/s13059-014-0550-8

32. Yu G, Wang LG, Han Y, He Q-Y. clusterProfiler: an r package for comparing biological themes among gene clusters. *OMICS* (2012) 16(5):284–7. doi: 10.1089/omi.2011.0118

33. Subramanian A, Tamayo P, Mootha VK, Mukherjee S, Ebert BL, Gillette MA, et al. Gene set enrichment analysis: a knowledge-based approach for interpreting genome-wide expression profiles. *Proc Natl Acad Sci U.S.A.* (2005) 102(43):15545–50. doi: 10.1073/pnas.0506580102

34. Thorsson V, Gibbs DL, Brown SD, Wolf D, Bortone DS, Ou Yang T-H, et al. The immune landscape of cancer. *Immunity* (2018) 48(4):812–830.e14. doi: 10.1016/j.immuni.2018.03.023

35. Strickley JD, Jenson AB, Jung JY. Cutaneous metastasis. *Hematol Oncol Clin North Am* (2019) 33(1):173–97. doi: 10.1016/j.hoc.2018.08.008

36. Wang J, Perry CJ, Meeth K, Thakral D, Damsky W, Micevic G, et al. UV-Induced somatic mutations elicit a functional T cell response in the YUMMER1.7 mouse melanoma model. *Pigment Cell Melanoma Res* (2017) 30(4):428–35. doi: 10.1111/pcmr.12591

37. Ralli M, Botticelli A, Visconti IC, Angeletti D, Fiore M, Marchetti P, et al. Immunotherapy in the treatment of metastatic melanoma: Current knowledge and future directions. *J Immunol Res* (2020), 9235638. doi: 10.1155/2020/9235638

38. Lee AY, Brady MS. Neoadjuvant immunotherapy for melanoma. *J Surg Oncol* (2021) 123(3):782–8. doi: 10.1002/jso.26229

39. Li W, Tanikawa T, Kryczek I, Xia H, Li G, Wu K, et al. Aerobic glycolysis controls myeloid-derived suppressor cells and tumor immunity via a specific CEBPB isoform in triple-negative breast cancer. *Cell Metab* (2018) 28(1):87–103.e6. doi: 10.1016/j.cmet.2018.04.022

40. Chen J-Y, Wang C-M, Ma C-C, Chow Y-H, Luo S-F. The -844C/T polymorphism in the fas ligand promoter associates with Taiwanese SLE. *Genes Immun* (2005) 6(2):123–8. doi: 10.1038/sj.gene.6364158

41. Lin Y, Huang M, Wang S, You X, Zhang L, Chen Y, et al. PAQR11 modulates monocyte-to-macrophage differentiation and pathogenesis of rheumatoid arthritis. *Immunology* (2021) 163(1):60–73. doi: 10.1111/imm.13303

42. Duan Q, Zhang H, Zheng J, Zhang L. Turning cold into hot: Firing up the tumor microenvironment. *Trends Cancer* (2020) 6(7):605–18. doi: 10.1016/j.trecan.2020.02.022

43. Weber CE, Kuo PC. The tumor microenvironment. *Surg Oncol* (2012) 21 (3):172–7. doi: 10.1016/j.suronc.2011.09.001

44. De Cicco P, Ercolano G, Ianaro A. The new era of cancer immunotherapy: Targeting myeloid-derived suppressor cells to overcome immune evasion. *Front Immunol* (2020) 11:1680. doi: 10.3389/fimmu.2020.01680

45. Schumacher TN, Schreiber RD. Neoantigens in cancer immunotherapy. *Science* (2015) 348(6230):69–74. doi: 10.1126/science.aaa4971

46. Paijens ST, Vledder A, de Bruyn M, Nijman HW. Tumor-infiltrating lymphocytes in the immunotherapy era. *Cell Mol Immunol* (2021) 18(4):842–59. doi: 10.1038/s41423-020-00565-9

frontiers | Frontiers in Immunology

TYPE Original Research
PUBLISHED 16 November 2022
DOI 10.3389/fimmu.2022.1033498

OPEN ACCESS

EDITED BY
Fu Wang,
Xi'an Jiaotong University, China

REVIEWED BY
Yunfan He,
Southern Medical University, China
Guangchao Li,
Guangzhou Bio-gene Technology Co., Ltd, China
Yixi Yang,
Third Affiliated Hospital of Guangzhou Medical University, China
Vivek Choudhary,
Georgia Regents Medical Center, United States

*CORRESPONDENCE
Jie Yang
13337564169@163.com
Youshu Lin
linyoushu718@163.com

†These authors have contributed equally to this work and share first authorship

SPECIALTY SECTION
This article was submitted to Inflammation, a section of the journal Frontiers in Immunology

RECEIVED 31 August 2022
ACCEPTED 28 October 2022
PUBLISHED 16 November 2022

CITATION
Lu X, Wang H, Wang H, Xie F, Jiang C, Shen D, Zhang H, Yang J and Lin Y (2022) Indirubin combined with umbilical cord mesenchymal stem cells to relieve psoriasis-like skin lesions in BALB/c mice. *Front. Immunol.* 13:1033498. doi: 10.3389/fimmu.2022.1033498

Indirubin combined with umbilical cord mesenchymal stem cells to relieve psoriasis-like skin lesions in BALB/c mice

XiaoJuan Lu[1†], Hao Wang[2†], Hongwei Wang[2], Fan Xie[2], Cuibao Jiang[2], Danpeng Shen[2], Hongpeng Zhang[2], Jie Yang[3*] and Youshu Lin[3*]

[1]Department of Dermatology, Guangzhou Red Cross Hospital of Jinan University, Guangzhou, China, [2]Lab Animal Research Center, Asia Stem Cell Regenerative Pharmaceutical Co. Ltd., Shanghai, China, [3]Department of Dermatology, The Fifth People's Hospital of Hainan Province, Haikou, China

Objective: To investigate the efficacy of indirubin combined with human umbilical cord mesenchymal stem cells (hUC-MSCs) in the treatment of psoriatic lesions in BALB/c mice and to explore the related mechanism of indirubin in the treatment of psoriasis.

Methods: A BALB/c mouse psoriasis model induced by imiquimod was established and randomly divided into the control group, model group, indirubin group, hUC-MSCs group, and indirubin combined with hUC-MSCs group. Psoriasis area and severity index (PASI) score was used to observe skin lesion changes in the psoriasis-like mouse model. The epidermal scale, the degree of keratinization, and the infiltration of inflammatory cells were observed by hematoxylin eosin (HE) staining. The concentrations of TNF-α, IFN-γ, IL-17A, and IL-23 in serum of mice were measured using enzyme-linked immunosorbent assay (ELISA).

Results: The PASI integral trend chart indicates that hUC-MSCs and indirubin and the combination of drugs could relieve the appearance of skin lesions and accelerate the recovery of skin lesions. The indirubin group had the best effect in improving the scale of skin lesions. HE staining showed that the number of parakeratosis cells in the three treatment groups was significantly reduced, the degree of erythrocyte extravasation dermis hyperplasia and inflammatory cell infiltration was significantly lower than that in the model group, and the skin thickness and spleen index of the combined treatment group exhibited the most noticeable improvement. ELISA showed that the concentrations of TNF-α, IFN-γ, IL-17A, and IL-23 in serum of mice in the hUC-MSCs treatment group, indirubin group, and combined administration group were all decreased compared with those in the model group, and the concentrations of IFN-γ, IL-17A, and IL-23 could be decreased significantly in the indirubin group.

10.3389/fimmu.2022.1033498

Conclusions: Both hUC-MSCs and indirubin can effectively reduce psoriasis-like lesions in BALB/c mice, and the combined administration of these drugs has the best effect.

KEYWORDS

psoriasis, indirubin, umbilical cord mesenchymal stem cells, combined administration, inflammatory factor

1 Introduction

Psoriasis is an immune-mediated chronic, recurrent, inflammatory skin disease. It's typical clinical manifestations are scaly erythema or plaques, which may be localized or widely distributed. The etiology of psoriasis involves various factors such as heredity, immunity, and environment. Excessive proliferation of keratinocytes or inflammation of synovial cells and chondrocytes in joints is caused by the immune response mediated mainly by T lymphocytes and jointly participated by various immune cells. Psoriasis is an incurable disease, and many therapeutic drugs and methods are available at present. The treatment plan of psoriasis should be determined according to the symptoms of patients; mild patients can undergo external treatment, moderate and severe patients can use system treatment, and patients that respond poorly to traditional systemic drug treatment can choose targeted biological treatment. The selection of drugs and methods suitable for patients is important to control the disease and maintain long-term efficacy (1).

Although great progress has been made in the study of the pathogenesis of psoriasis in recent years, there is still a long way to go before the pathogenesis of psoriasis is fully elucidated. The high responsiveness of Th1 and Th17, the dysregulation of Tregs, and the complex relationship among immune system cells, keratinocytes, and vascular endothelial cells play an important role in the pathogenesis of psoriasis (2). The interleukin-23/Th17/IL-17 axis and Th1/IFN-γ axis play a key role in the inflammation of psoriasis. A series of biologics has been developed and put into use for the above immune mechanisms. However, the current biologics targeted therapy cannot completely cure psoriasis, which manifests in a small number of patients who are not sensitive to drugs or gradually develop treatment resistance. Therefore, the treatment of psoriasis is still under constant exploration (2).

The role of stem cells has attracted increasing attention. The effects of epidermal stem cells and stem cells on T cells have been found. The dysfunction of various types of stem cells may be the main reason for the dysregulation of inflammatory response in psoriasis (3, 4). Human umbilical cord mesenchymal stem cells (hUC-MSCs) are characterized by low immunogenicity, high expansion rate *in vitro*, and pluripotent differentiation potential, and they can be used as the ideal choice of mesenchymal stem cells for the treatment of psoriasis. Previous studies found that hUC-MSCs can produce IL-35 and induce the proliferation of Treg cells, thereby reducing the active expression of Th17 and Th1 cells (5, 6). Study also found that subcutaneous injection of hUC-MSCs may reduce the production of IL-17 by inhibiting γδT cells, thereby inhibiting skin inflammation and having therapeutic effects on psoriasis (7).

Due to the increasing application of Traditional Chinese Medicine in diseases, a variety of Traditional Chinese Medicine ingredients have been proved to have therapeutic effects on psoriasis, such as total glucosides of paeony, coptis coptidis, curcumin and so on (8, 9). Indigo naturalis has the functions of heat clearing, detoxifying, cooling blood, and calming nerves, and it is widely used in modern medicine to treat inflammation-related and autoimmune diseases. The external application of indigo naturalis ointment can significantly improve the erythema, scale, and infiltration of skin lesions in patients with psoriasis vulgaris and significantly reduce the psoriasis area and severity index (PASI) score. Its efficacy is proportional to the use time and concentration of indigo naturalis, and its safety is good (10, 11). Qingdai oil can improve psoriasis damage to nails (12, 13). Indirubin is a bisindole compound extracted from the leaves of indigo, which together with indigo constitutes the main active component of indigo naturalis. Many studies have shown that indirubin can inhibit inflammatory response and reduce psoriasis-like skin injury in mice (14, 15). Indirubin is stable and effective in the treatment of psoriasis, and can be used as a new topical agent for the treatment of psoriasis.

By observing the therapeutic effect of indirubin combined with stem cells in the treatment of psoriasis-like skin lesions in BALB/C mice, this paper aims to elucidate the immune mechanism of indirubin combined with stem cells in the treatment of psoriasis and the mechanism of regulating psoriasis-like inflammation.

2 Experimental materials and methods

2.1 Primary reagent

For the experiments, 5% imiquimod cream (Batch No. 17010139) was purchased from Sichuan Mingxin Lidi Co.,

LTD. Recombinant mouse interleukin-12 (RMIL-12 p70) was purchased from BD Pharmingen Inc (Batch No. 6278771, specification: 5 μg). Lipopolysaccharide (LPS) lyophilized powder was purchased from Sigma Company, USA (Batch No. 045M4087V; specification: 10 mg). IL-17A, IL-12 enzyme-linked immunosorbent assay (ELISA) kits were purchased from Shenzhen Dakewe Bioengineering Co., LTD (Batch No. DKW12-2170-048, DKW12-2020-048). Indirubin (Batch No. 110717-201805) was purchased from China Institute for Food and Drug Control and diluted at 0.5% CMC for use. Multiple Electrolytes Injection was purchased from Shanghai Kelun Pharmaceutical Co., Ltd. (Batch No. T14102120).

HUC-MSCs were produced by the GMP laboratory of Shanghai Quansheng Biotechnology Co., Ltd. The umbilical cord donor had signed an informed consent form for donation for scientific research and passed infectious disease tests. The collected umbilical cord tissue was cut and separated by cell climbing. After passage culture and expansion, 1×10^8 cells/mL saline cell suspension was prepared (Batch No. 20191201). The extracted hUC-MSCs were cultured in DMEM medium supplemented with 10% fetal bovine serum and 100 U/ml penicillin/streptomycin. After passing the quality inspection of sterility, mycoplasma, endotoxin, and molecular phenotyping, it was used in this experiment. The experimental instruments were provided by Shanghai Quansheng Biotechnology Co., Ltd.

2.2 Experiment animals

Fifty SPF male BALB/c mice aged 6–8 weeks and weighing about 20 g were purchased from Beijing Weitong Lihua Laboratory Animal Co., Ltd. Experimental animals were kept in the laboratory for at least 1 week and then tested under standard feeding conditions (room temperature 25°C–27°C) with alternating 12 h light and dark cycles. Free access to food (standard pellet feed) and water was allowed. Experiments were performed under a project license (No. 2016LL003) granted by institutional board of The Fifth People's Hospital of Hainan Province, in compliance with The Fifth People's Hospital of Hainan Province guidelines for the care and use of animals.

2.3 Animal model establishment and grouping

Animal protection and use guidelines were followed during the experiment. Fifty SPF male BALB/c mice were randomly divided into five groups: group A (blank group), group B (model group), group C (hUC-MSCs group), group D (indirubin group), and group E (indirubin + hUC-MSCs group), with 10 animals in each group. In group B, 5% imiquimod cream was applied to the back of the mice at 62.5 mg/day for 7 days. At the beginning of modeling, RMIL-12 10 ng (5 μL) and LPS 20 μg (5 μL) were injected subcutaneously once to make the psoriasis-like rash of mice more durable and typical (16). On the basis of the same modeling as group B, 2×10^7/kg hUC-MSCs were injected through the tail vein in group C on the first day. Group D was given the indirubin solution (50 mg/kg, 200 μL, 0.5% CMC dilution) by gavage once a day. In group E, stem cell preparation was injected once through the tail vein on day 1, and indirubin solution (50 mg/kg, 200 μL, 0.5% CMC dilution) was administered by gavage once a day. All mice were sacrificed after observation on day 7, and the blood and skin tissue were collected for use. The spleen was taken and weighed, and the spleen index (spleen mass/body mass) was calculated.

2.4 Stemness identification of hUC-MSCs

Fluid identification: The second passage cells were collected and digested with 0.25% TrypLE trypsin (Gibco), and the appropriate amount of cells was incubated with CD73, CD90, CD105, CD34, CD45, and HLA-DR antibodies (1 μg/100 μL, CST) conjugated to PE luminescent groups for 30 min on ice. Flow cytometry (Beckmancoulter) was used to detect the level of antibodies on the cell surface.

Osteogenic induction: hUC-MSCs were seeded in a six-well plate at a density of 1×10^5 cells/well. In addition, 10 mmol/L β-sodium glycerophosphate, 1 μmol/L dexamethasone, and 50 μmol/L vitamin C were added to the conventional medium as the osteogenic induction medium. Cells were cultured in osteogenic induction medium for 4 weeks, and mineral bone nodules were detected using Alizarin Red S dye.

Adipogenic induce supplements: hUC-MSCs were seeded in a six-well plate at a density of 1×10^5 cells/well. The conventional medium was supplemented with 0.5 mmol/L isobutyl methyl xanthine, 200 μmol/L indomethacin, 1 μmol/L dexamethasone, and 10 μmol/L insulin as adipogenic induction medium. After the cells were cultured in adipogenic induction medium for 1 week, lipid droplets were detected using oil Red O dye.

Chondrogenic induction: hUC-MSCs cells were seeded in a six-well plate at a density of 1×10^5 cells/well. The conventional medium was supplemented with 10 μg/L transforming growth factor-β1, 0.1 μmol/L dexamethasone, 100 μmol/L ascorbic acid, 200 mmol/L glutamine, and 1% ITS as chondrogenic induction medium.

2.5 Appearance scoring detection

The skin lesions of mice in each group were observed with naked eye and photographed with camera every day before drug administration. PASI was used to evaluate the appearance of mice, including three subscales of erythema, scale and skin hypertrophy. The total PASI score was obtained by adding the

scores of the three subscales. At the same time, two professional technicians besides the experimenter were asked to evaluate the degree of skin injury of the mice in a blind way. The scoring criteria are shown in Table 1.

2.6 Pathological evaluation

The skin tissue from the back of mice was fixed with 4% paraformaldehyde, embedded in paraffin, and sectioned with a thickness of 5 μm. Tissue sections were dewaxed with alcohol, stained with hematoxylin, differentiated with alcohol hydrochloride, and stained with eosin. Finally, the slices were washed and dehydrated by adding absolute ethanol. The slices were sealed, and the histopathological changes of mice were observed and photographed using a microscope. After pictures were taken, the thickness of the epidermis was measured. After photography, epidermal thickness of histopathological sections was measured by a chief of pathology using ORIGIN 8.0 software and light microscopy, and the measurement process was performed in a blind manner.

2.7 Immunological evaluation

Serum from mice was collected and a serum sample of 50 μL was taken from each group of mice and diluted with 1×Dilution buffer R (DAKEWE). The diluted serum samples were added to the culture plates, and antibody solution was added to detect the concentrations of Th1 and Th17 related immune molecules TNF-α, IFN-γ, IL-17A and IL-23 in mouse serum. The experimental procedure was performed according to the instructions of the ELISA kit (DAKEWE) manufacturer.

TABLE 1 PASI scoring criteria.

Symptom	Standard for evaluation
Erythema	0 points: No erythema
	1 points: Blush
	2 points: Red
	3 points: Deep red
	4 points: Very dark red
Skin hypertrophy	0 points: The lesions are level with normal skin.
	1 points: The skin lesions are slightly higher than the normal skin surface.
	2 points: The skin lesions have a medium elevation.
	3 points: The skin lesions were hypertrophic and eminently raised.
	4 points: The skin lesion was highly thickened, with several obvious ridges.
Scale	0 points: No scale on the surface.
	1 points: The surface of some lesions is covered with fine scales.
	2 points: The surface of most lesions is covered with flaky scales.
	3 points: The surface of most lesions is covered with non-viscous thick scales.
	4 points: All lesions were covered with viscous extremely thick scales.

2.8 Data collection and statistical analysis

Statistical software SPSS13.0 was used to process the data, and the measurement data were expressed as mean ± standard deviation, and comparison between groups was performed by ANOVA analysis and linear regression analysis. The Dunnett's test was used as *post-hoc* test of the data. $P < 0.05$ was considered statistically significant.

3 Result

3.1 Identification of HUCMSCs

Flow cytometry analysis confirmed that the positive rates of hUC-MSCs surface markers CD73, CD90 and CD105 were all more than 90%, while the positive rates of CD14, CD19, CD34, CD45 and HLA-DR were all less than 5% and negative (Figures 1A–H). The analysis of oil red O staining, alizarin red staining and alcian blue staining showed that HUC-MSCs could be successfully trans-differentiated into adipocytes, osteocytes and chondrocytes (Figures 1I–K). The results showed that hUC-MSCs had high purity and excellent differentiation potential.

3.2 Gross findings and skin lesion score results

Linear regression analysis was conducted with time as the independent variable and the scores of each part of PASI as the dependent variable. The erythema, scale, skin lesion thickness, and total score were linearly correlated with time ($P < 0.001$). Table 2 shows the results. The coefficient of determination of erythema, scale, skin lesion thickness, total score, and time were 0.99, 0.99, 0.97, and 0.99, respectively. The score of skin lesions in group B continued to increase over time, and the model was successfully established.

Changes in skin lesions on the back of mice were observed with the naked eye (Figure 2). Erythema began to appear on the skin of the back of the mice 1 day after modeling, significant scale formation was observed on the third to fourth day after modeling, and the scales on the surface of the back began to increase on the fifth day after modeling. On the sixth day after modeling, the skin erythema of mice in the model group (group B) aggravated, the infiltration thickened obviously, and the surface scales continued

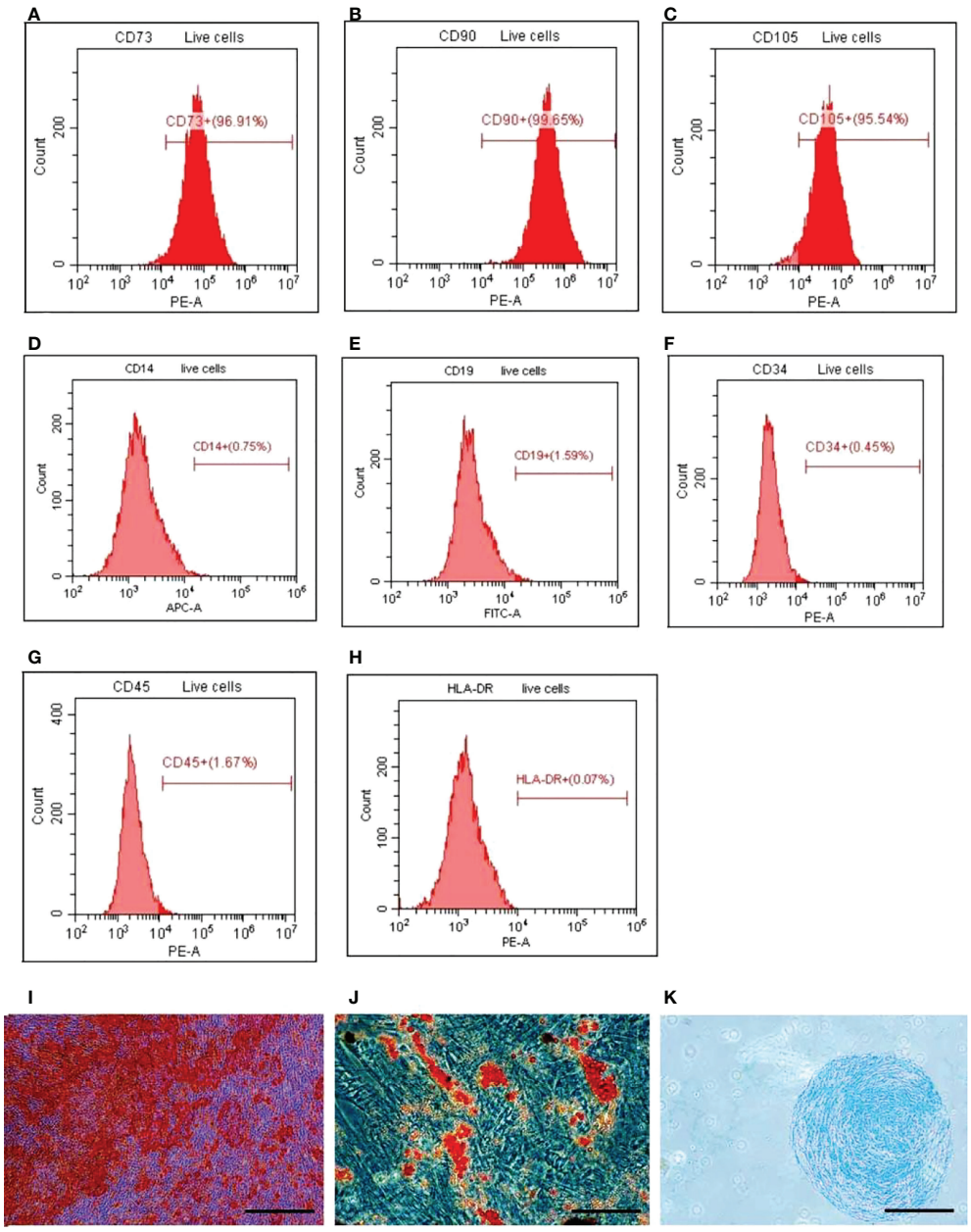

FIGURE 1
Detection of surface markers, osteogenesis, adipogenesis, and cartilage-induced differentiation of HUCMSCs. FACS was used to detect the surface markers and ICC was used to detect the differentiation. **(A–C)** The expression of positive surface marker CD73, CD90, and CD105. **(D–H)** The expression of surface negative markers CD14, CD19, CD34, CD45, HLA-DR. **(I)** The cells osteogenic differentiation was analyzed by alizarin red staining (scale bar = 20 μm). **(J)** The cells adipogenic differentiation was analyzed by oil red O staining (scale bar = 20 μm). **(K)** The cells chondrogenic differentiation was analyzed by alcian blue staining (scale bar = 100 μm). HUCMSCs, human umbilical cord mesenchymal stem cells.

to increase. The skin rash was similar to the appearance of human psoriasis. The psoriasis model induced by imiquimod cream +LPS/IL-12 was established.

The differences in erythema scores, scale score, skin lesion thickness score, PASI score among the four groups were compared. The results of ANOVA showed that there were differences in erythema score, scale score, skin lesion thickness score and PASI score among the four groups on day 7. ($P < 0.001$) (Figure 3).

The difference of infiltration score among the four groups was compared. ANOVA results showed a difference in

TABLE 2 Results of correlation analysis between PASI score and time in model group B.

	Intercept	β	SE	t	p	R-squared
Erythema	0.04167	0.44881	0.02077	21.61	6.41E−07	0.9873
Scale	0	0.52143	0.02143	24.33	3.17E−07	0.99
Skin lesion thickness	0.30833	0.41548	0.02878	14.438	6.92E−06	0.972
Total score	0.325	1.30714	0.06165	21.2	7.18E−07	0.9868

SE, standard error.

infiltration score among the four groups on day 7 ($F = 6.842$, $P < 0.001$) (Table 3). Further pairwise comparisons were performed, and Tukey's method was used to adjust the multiplicity. The results showed significant differences between groups C and B, groups D and B, and groups E and B, and relative differences of −0.7 ($P = 0.04$), −0.8 ($P = 0.015$), and −1.1 ($P < 0.001$), respectively. No significant difference was found among groups D, E, and C (Table 4). The results showed no difference between the indirubin group and the stem cell group.

3.3 Spleen index results

At the end of the experiment, spleens of each group were measured, and the spleen index (spleen index = spleen mass/body mass) was calculated (Figure 4A). The experimental results showed that the spleen size and spleen index of each group were significantly higher than those of control group A, and statistical differences existed between model group B and the combined administration group E ($P < 0.01$) (Figures 4A, B). The mean

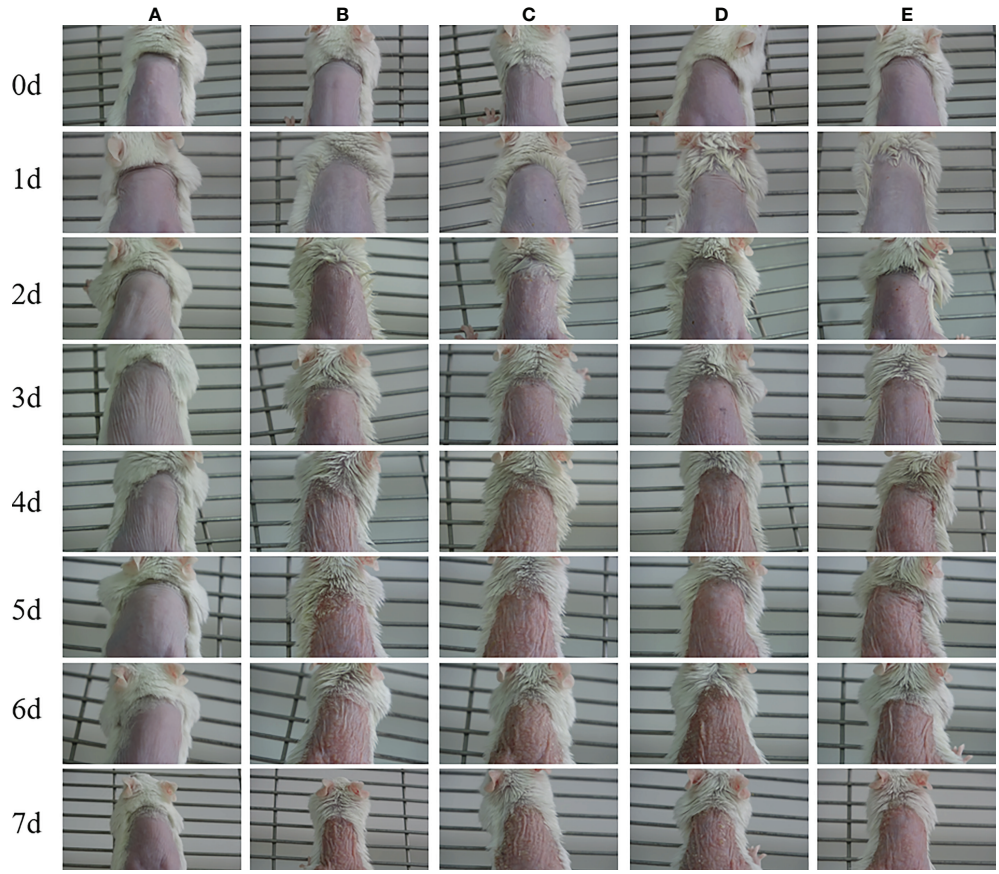

FIGURE 2
Representative images of psoriasis-like rash in each experimental group from 0 to 7 days after modeling. **(A)** Control-A; **(B)** Model-B; **(C)** hUC-MSMCs-C; **(D)** Indirubin-D; **(E)** Indirubin+hUC-MSCs-E.

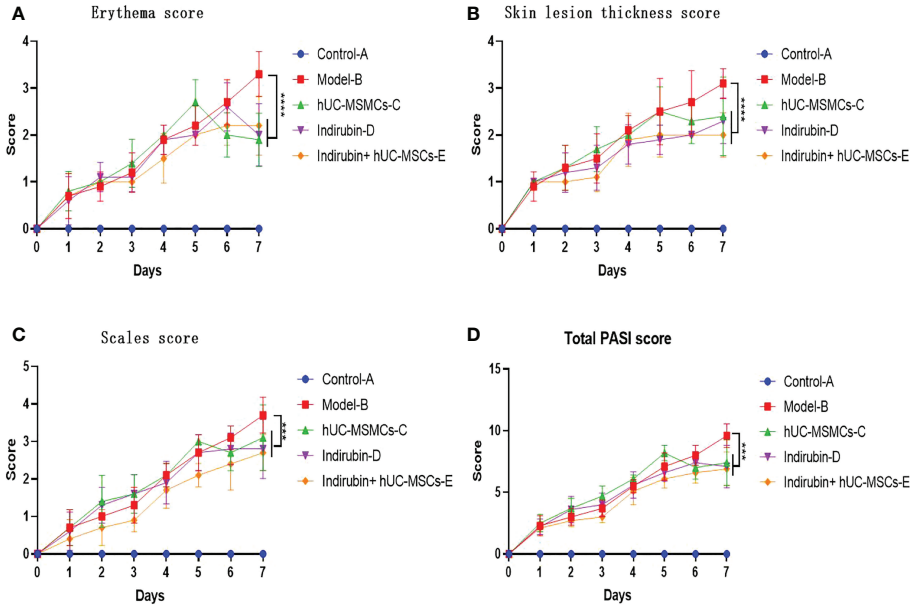

FIGURE 3
The erythema, scale, infiltration and PASI score of animals from 0 to 7 days after modeling. **(A)** Erythema score of mice in each group. **(B)** Skin lesion thickness score of mice in each group. **(C)** Scale score of mice in each group. **(D)** Total PASI score of mice in each group (one-way ANOVA/Dunnett's test). ****P < 0.0001, ***P < 0.0001, compared with model B.

TABLE 3 Results of ANOVA of infiltration score.

	ν	SS	MS	F	P
Group	3	6.5	2.1667	6.842	0.000914
Residuals	36	11.4	0.3167		

SS, sum of square; MS, mean square.

spleen index of group A was 0.302, and that of group B was 1.338; the difference between the two groups was 1.036 (t = −11.558, P < 0.001), thus indicating significant differences. Xenogeneic exogenous stem cells in the combined administration group may cause stress response activation of the immune system of experimental animals, leading to splenomegaly, so the spleen index in the combined administration group will increase. Moreover, compared with model-B group, the spleen index of indirubin group was lower, which proved that indirubin had a certain therapeutic effect on spleen enlargement in mice.

The difference of spleen index among the four groups was compared. ANOVA results showed a difference in spleen index among the four groups on day 7 (F = 8.98, P < 0.001) (Table 5). Further pairwise comparisons were performed, and Tukey's method was used to adjust the multiplicity. The results showed significant differences between groups E and B, groups C and E, and

TABLE 4 Results of pairwise comparison of infiltration score among groups.

	Relative difference	Lower confidence limits	Upper confidence limits	P
Groups C and B	−0.7	−1.3777806	−0.02221936	0.0407417
Groups D and B	−0.8	−1.4777806	−0.12221936	0.0153569
Groups E and B	−1.1	−1.7777806	−0.42221936	0.0005615
Groups D and C	−0.1	−0.7777806	0.57778064	0.9784162
Groups E and C	−0.4	−1.0777806	0.27778064	0.3972374
Groups E and D	−0.3	−0.9777806	0.37778064	0.6357029

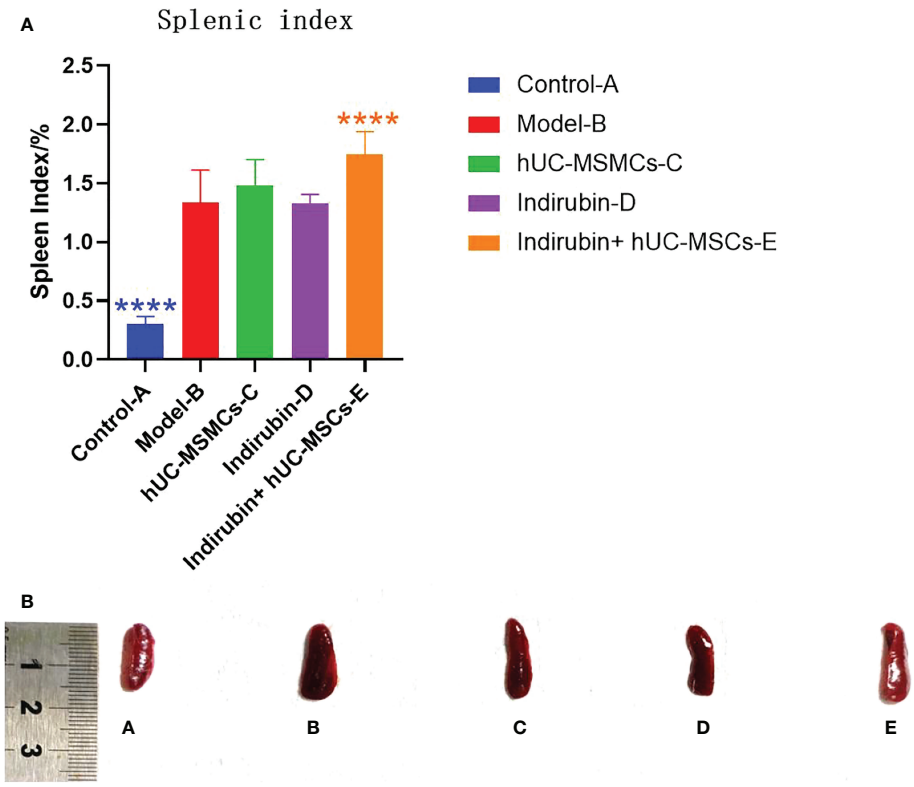

FIGURE 4
The spleen index (spleen mass/body mass) was calculated on day 7 in each group. **(A)** Spleen index of mice in each group (one-way ANOVA/Dunnett's test). **(B)** Comparison of spleen size. ****P < 0.0001, compared with model B. A, Control-A; B, Model-B; C, hUC-MSMCs-C; D, Indirubin-D; E, Indirubin+hUC-MSCs-E.

groups D and E, and the relative differences were 0.409 (P = 0.005), 0.268 (P = 0.03), and 0.42 (P < 0.001), respectively. No significant difference was found among groups C, D, and B, and between groups E and C (Table 6). The results showed that the combined group was superior to the stem cell group and was different from the indirubin group, and the stem cell and indirubin groups were not different from the model group.

3.4 Pathology results

3.4.1 Pathological features

An observation of the dorsal skin of mice in each group (Figure 5A) shows that the epidermal layer of mice in control-A group is thin, and the morphology of epidermal cells is roughly normal. The epidermis of other groups was significantly thickened, being thicker than normal skin epidermis. In the model-B group, it was observed that the epidermic cells hyperkeratosis with integration parakeratosis, acanthosis cell layer thickening, epidermal sudden downward extension of in-depth dermis, and a large number of inflammatory cells were infiltrated in the dermis, which were basically the same as the pathological changes of human psoriasis. Compared with the model-B group, the hUC-MSCs-C group, indirubin-D group had significantly fewer keratinized cells, acanthosis cell layer mild hyperplasia, epidermal sudden downward extension reduced, and the inflammatory cell infiltration was significantly reduced. Compared with model-B group, the epidermal thickness of mice was reduced after drug treatment,

TABLE 5 Results of ANOVA of spleen index.

	ν	SS	MS	F	P
Group	3	1.146	0.3821	8.98	0.000142
Residuals	36	1.532	0.0425		

SS, sum of square; MS, mean square.

TABLE 6 Results of pairwise comparison of spleen index among groups.

	Relative difference	Lower confidence limits	Upper confidence limits	P
Groups C and B	−0.1405282	−0.10791124	−0.38896755	0.4344881
Groups D and B	−0.0110871	−0.25952650	0.23735229	0.9993672
Groups E and B	0.4089165	0.16047707	0.65735587	0.0004679
Groups D and C	−0.1516153	−0.40005465	0.09682414	0.3678707
Groups E and C	0.2683883	0.01994892	0.51682771	0.0300334
Groups E and D	0.4200036	0.17156417	0.66844297	0.0003287

and the epidermal thickness in hUM-MCSs combined with indirubin group was the lowest, but still higher than that of control group-A group. In indirubin+hUM-MCSs group, some mild hyperkeratinized cells were observed in the epidermis, but no inkeratinized cells were observed, the acanthosis cell layer was mildly hyperplasia. Therefore, hUM-MCSs combined with indirubin has the best effect in inhibiting skin damage and epidermal thickening of psoriasis.

3.4.2 Epidermal measurement results

The thickness of the epidermal layer of the mice in each group was measured, and the results were as follows: group B

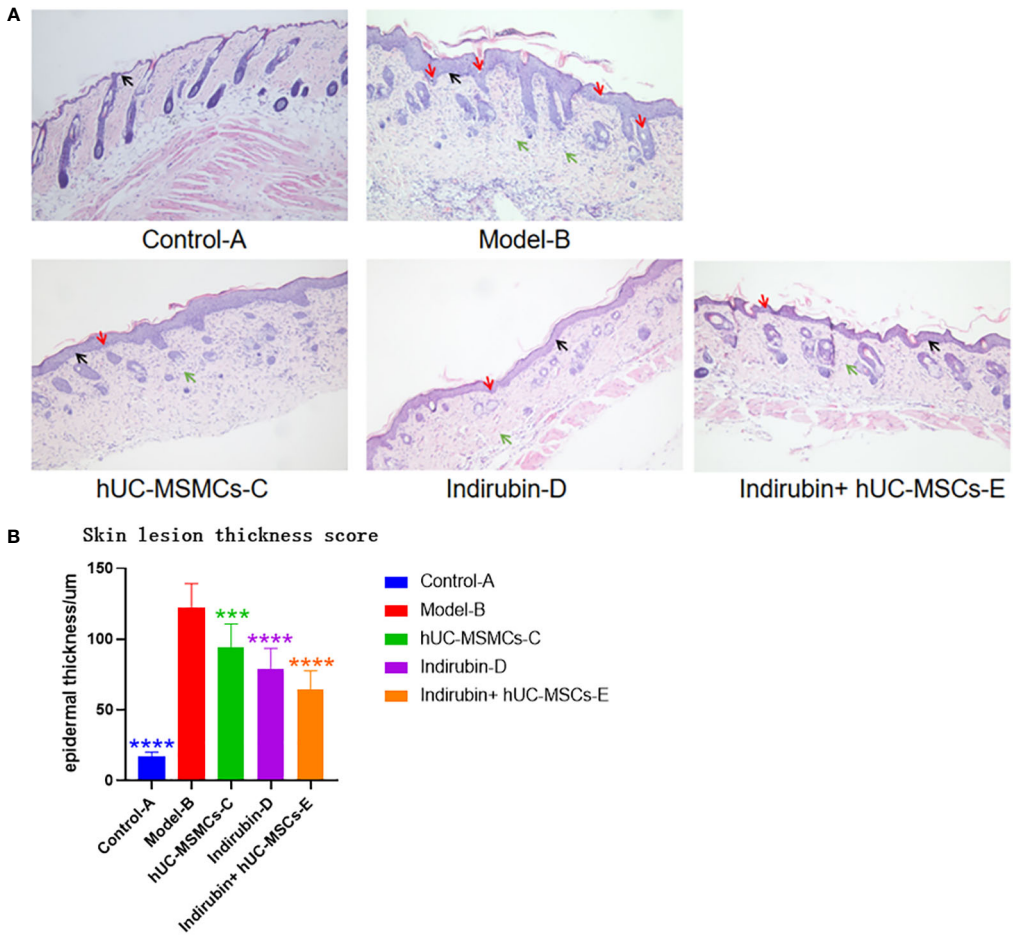

FIGURE 5
Thickness of epidermal layer was measured by H & E staining images of mice in each group. **(A)** HE staining results of pathological changes of skin tissues of mice in each group (200×). **(B)** Thickness of epidermal layer of mice in each group (one-way ANOVA/Dunnett's test). ****P < 0.0001, ***P < 0.001, compared with model **(B)** Red arrow: Munro microabscess; Black arrow: spinous cells; Green arrow: inflammatory cells.

(122 ± 17.0 μm) > group C (79 ± 14.3 μm) > group D (78 ± 8.7 μm) > group E (64 ± 13.1 μm) (Figure 5B). Statistically significant differences were found between each treatment group and model group B ($P < 0.01$). Compared with the other treatment groups, the combined treatment group E had the smallest epidermal thickness.

3.5 ELISA test results

ELISA was used to detect the concentrations of Th1- and Th17-related immune molecules TNF-α, IFN-γ, IL-17A, and IL-23 in serum of mice in each group (as shown in Tables 7–14 and Figure 6). The expression concentrations of cytokines in group B were higher than those in other groups. The concentrations of the four factors in serum of mice in each group were significantly different from those of group B ($P < 0.01$).

The mean IFN-γ of group A was 369.261, and the mean IFN-γ of group B was 666.478; the difference between the two groups was 17.803, which was significant ($t = -8.1453$, $P < 0.001$) (Figure 6A).

The difference of IFN-γ among the four groups was compared. ANOVA results showed a difference in IFN-γ among the four groups on day 7 ($F = 17.82$, $P < 0.001$) (Table 7). Further pairwise comparisons were performed, and Tukey's method was used to adjust the multiplicity. The results showed significant differences between groups D and B, groups E and B, and groups D and C, and the relative differences were −134.824 ($P = 0.005$), 0.250.822 ($P < 0.001$), and −115.998 ($P = 0.019$), respectively. No significant difference was observed between groups E and C, and groups E and D (Table 8). The results showed that the indirubin group had stronger IFN-γ intervention than the stem cell group.

The mean value of TNF-α in group A was 378.823, and that in group B was 605.863; the difference between the two groups was 17.733, which was significant ($t = -8.3208$, $P < 0.001$) (Figure 6B).

The difference of TNF-α among the four groups was compared. ANOVA results showed a difference in TNF-α among the four groups on day 7 ($F = 16.3$, $P < 0.001$) (Table 9). Further pairwise comparisons were performed, and Tukey's method was used to adjust the multiplicity. The results showed significant differences among groups C, D, E, and B, and the relative differences were −117.253 ($P = 0.001$), −164.291 ($P < 0.001$), and −183.553 ($P < 0.001$). No significant difference was found among groups D, E, and C (Table 10). No difference existed between the indirubin group and the stem cell group.

The mean value of IL-17A in group A was 17.583, and that in group B was 29.766; the difference between the two groups was 17.861, which was significant ($t = -9.8441$, $P < 0.001$) (Figure 6C).

The difference of IL-17A among the four groups was compared. ANOVA results showed a difference in IL-17A

TABLE 7 Results of ANOVA of IFN-γ.

	ν	SS	MS	F	P
Group	3	376322	125441	17.82	2.95×10^{-7}
Residuals	36	253431			

SS, sum of square; MS, mean square.

TABLE 8 Results of pairwise comparison of IFN-γ.

	Relative difference	Lower confidence limits	Upper confidence limits	P
Groups C and B	−134.82388	−235.88094	−33.76682	0.0051310
Groups D and B	−250.82234	−351.87940	−149.76528	0.0000005
Groups E and B	−218.86098	−319.91805	−117.80392	0.0000068
Groups D and C	−115.99846	−217.05552	−14.94140	0.0191699
Groups E and C	−84.03710	−185.09416	17.01996	0.1316457
Groups E and D	31.96136	−69.09571	133.01842	0.8292858

TABLE 9 Results of ANOVA of TNF-α.

	ν	SS	MS	F	P
Group	3	203527	67842	16.3	7.43×10^{-7}
Residuals	36	149858	4163		

SS, sum of square; MS, mean square.

TABLE 10 Results of pairwise comparison of TNF-α.

	Relative difference	Lower confidence limits	Upper confidence limits	P
Groups C and B	−117.25312	−194.96316	−39.54309	0.0013716
Groups D and B	−164.29147	−242.00150	−86.58143	0.0000103
Groups E and B	−183.55267	−261.26271	−105.84264	0.0000013
Groups D and C	−47.03834	−124.74838	30.67169	0.3750147
Groups E and C	−66.29955	−144.00958	11.41048	0.1174843
Groups E and D	−19.26120	−96.97124	58.44883	0.9085997

TABLE 11 Results of ANOVA of IL-17A.

	ν	SS	MS	F	P
Group	3	621.3	207.09	37.16	4.05×10^{-11}
Residuals	36	200.6	5.57		

SS, sum of square; MS, mean square.

TABLE 12 Results of pairwise comparison of IL-17A.

	Relative difference	Lower confidence limits	Upper confidence limits	P
Groups C and B	−5.9159186	−8.759176	−3.0726615	0.0000136
Groups D and B	−9.7532558	−12.596513	−6.9099986	0.0000000
Groups E and B	−9.5193331	−12.362590	−6.6760760	0.0000000
Groups D and C	−3.8373371	−6.680594	−0.9940800	0.0045776
Groups E and C	−3.6034145	−6.446672	−0.7601573	0.0083306
Groups E and D	0.2339227	−2.609334	3.0771798	0.9960904

TABLE 13 Results of ANOVA of IL-23.

	ν	SS	,MS	F	P
Group	3	3713	1237.6	26.57	4.05×10^{-11}
Residuals	36	1677	46.6		

SS, sum of square; MS, mean square.

TABLE 14 Results of pairwise comparison of IL-23.

	Relative difference	Lower confidence limits	Upper confidence limits	P
Groups C and B	−14.631466	−22.851869	−6.4110625	0.0001597
Groups D and B	−24.827428	−33.047832	−16.6070250	0.0000000
Groups E and B	−22.081641	−30.302044	−13.8612373	0.0000001
Groups D and C	−10.195963	−18.416366	−1.9755593	0.0100991
Groups E and C	−7.450175	−15.670578	0.7702284	0.0873333
Groups E and D	2.745788	−5.474616	10.9661909	0.8050746

among the four groups on day 7 ($F = 37.16$, $P < 0.001$) (Table 11). Further pairwise comparisons were performed, and Tukey's method was used to adjust the multiplicity. The results showed no significant difference between groups D and E, while significant differences existed between the other two groups (Table 12). No difference was observed between the indirubin group and the combined group, and the indirubin group was superior to the stem cell group.

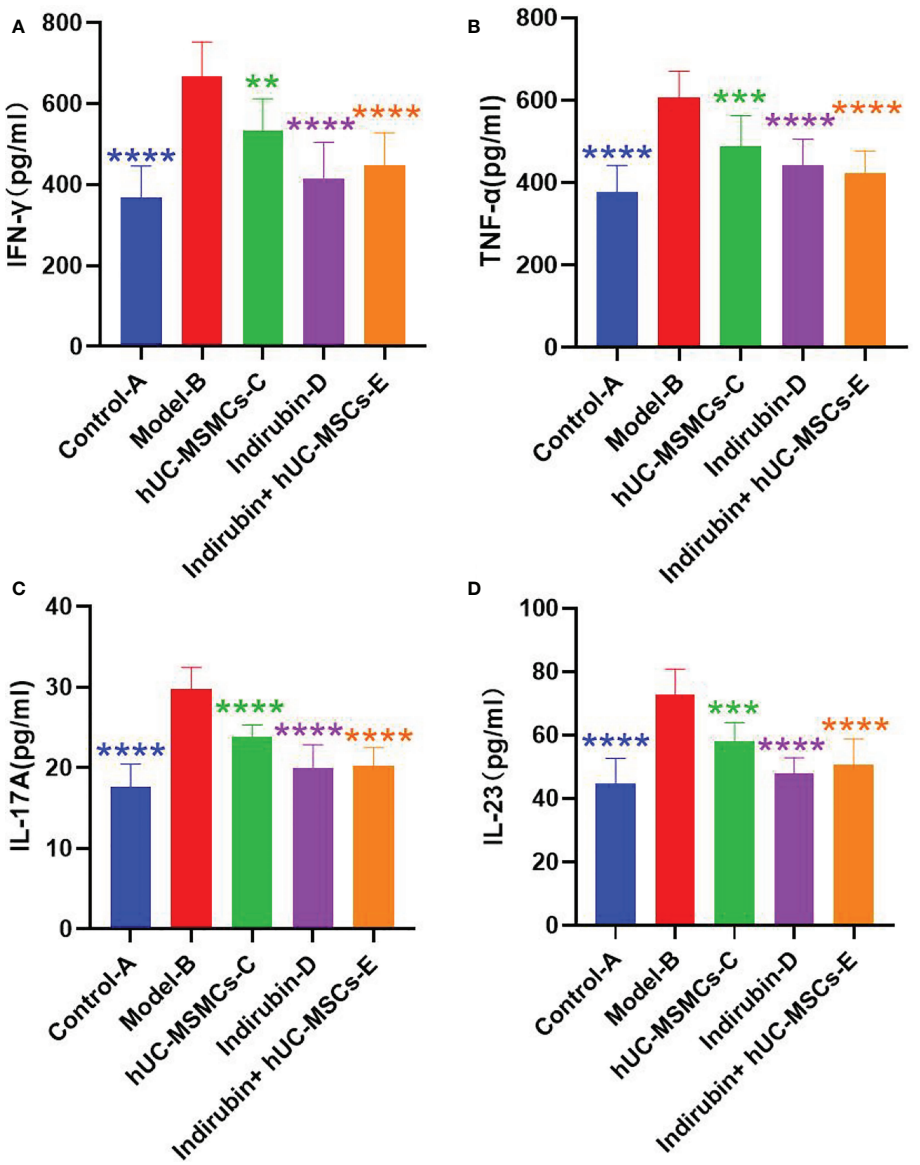

FIGURE 6
Concentrations of Th1- and Th17-related immune molecules TNF-α, IFN-γ, IL-17A, and IL-23 were detected by relative Elisa kits. **(A)** Concentrations of cytokine IFN-γ in serum of mice in each group. **(B)** Concentrations of cytokine TNF-α in serum of mice in each group. **(C)** Concentrations of cytokine IL-17A in serum of mice in each group. **(D)** Concentrations of cytokine IL-23 in serum of mice in each group (one-way ANOVA/Dunnett's test). ****P < 0.0001, ***P < 0.001, **P < 0.01, compared with model B.

The mean value of IL-23 in group A was 44.60, and that in group B was 72.77; the difference between the two groups was 17.996, which was significant (t = −7.833, P < 0.001) (Figure 6D).

The difference of IL-23 among the four groups was compared. ANOVA results showed a difference in IL-23 among the four groups on day 7 (F = 26.57, P < 0.001) (Table 12). Further pairwise comparisons were performed, and Tukey's method was used to adjust the multiplicity. The results showed no significant difference among groups C, D, and E, whereas significant differences were found between the other two groups (Table 14). No difference existed between the indirubin group and the stem cell group and between the indirubin group and the combined group. The combined group was superior to the stem cell group.

4 Discussion

Psoriasis, like most autoimmune diseases, is an immune-mediated skin disease influenced by genetic and epigenetic

modifications that can be triggered by environmental factors. To date, several important immune cell subsets have been found to play a role in the pathogenesis of psoriasis and other autoimmune diseases, including Th1, Th2, Treg, and Th17 cells, and the corresponding cytokines may involve IFN-γ, TNF-α, IL-23, and IL-17 (17).

hUC-MSCs are cells with self-renewal and multi-differentiation potential. They can promote tissue repair and regulate immune function by secreting a variety of cytokines. They also have low immunogenicity and have many advantages in the treatment of immune-related diseases. Reports have indicated that hUC-MSCs transplantation can treat psoriasis patients (4). hUC-MSCs are a safer psoriasis treatment option than topical glucocorticoids and can effectively avoid the adverse reactions caused by topical glucocorticoids on the epidermis. Electron microscopy showed that the epidermis of psoriasis cured by hUC-MSCs had uniform thickness, complete epidermis layers, clear boundary between the dermis and the epidermis, complete basement membrane, and no gap between tightly connected basal layer cells and basement membrane. Moreover, hUC-MSCs treatment could also reduce the expression of CD4, CD8 and CD31 in T cells (18). hUC-MSCs can significantly reduce the severity and development of psoriasis, inhibit the infiltration of immune cells into the skin, and downregulate the expression of various proinflammatory cytokines and chemokines, including first inhibiting neutrophil function and then downregulating the production of type I interferon in plasmacytoid dendritic cells (19). In this study, hUC-MSCs were used to treat imiquimod-induced BALB/c psoriasis mouse model. hUC-MSCs could significantly reduce the skin lesion score of the psoriasis mouse model and also reduce the epidermal thickness of skin lesions. In addition, Th1 cytokines (TNF-α and IFN-γ) and IL-27 and Th17 cytokines (IL-17A and IL-23) in serum of mice could be significantly inhibited by hUC-MSCs. Compared with the model group, hUC-MSCs in this experiment did not significantly reduce the spleen index of mice (20), which may be due to the different experimental protocols. The difference is that the spleen index of mice was directly proportional to the concentration of UC-MSCs in previous studies (6), this may be because xenogeneic exogenous stem cells introduced into mice may activate the immune system stress response in mice, leading to spleen enlargement, and then increase the spleen index of mice. Therefore, UC-MSCs in the combined administration group may lead to the increase of spleen index in mice. Compared with the model group, the spleen index in the indirubin group showed a downward trend, which proved that indirubin could improve the prognosis of mice. Considering that the mechanism of UC-MSCs in the treatment of psoriasis is different from immunosuppression, spleen index cannot be simply used as a measurement index, which will be further discussed in subsequent research.

Indirubin is one of the main active components in indigo naturalis. Current studies have shown that indirubin has a dose-dependent therapeutic effect on alleviating psoriasis-like skin lesions in mice (21), among which CD274 is a regulatory factor of indirubin-mediated effect on psoriasis-like skin lesions in mice (14). Indirubin attenuates imiquimod-induced psoriatic dermatitis mainly by reducing the inflammatory response mediated by γδT cells generated by IL-17A involving Jak3/Stat3 activation (22). Therefore, indirubin and its preparations may be developed as new drugs for the treatment of psoriasis. An *in vitro* experiment found that indirubin could significantly reduce the mRNA expression levels of proinflammatory cytokines IL-1β, IL-6, and TNF-α in HaCaT cells and cell culture supernatant, and the differences were statistically significant ($P < 0.05$). Moreover, the inhibitory effect was enhanced with the increase in the concentration of indirubin. A certain concentration dependence is observed (23). According to relevant literature analysis, the scholar treated mice with 50 mg/kg indirubin instillation to explore the therapeutic effect of indirubin on CD274 and skin lesions. The experimental results were clear and the mice had normal activity (22). Therefore, mice treated with 50 mg/kg indirubin in this experiment showed normal activity without obvious toxic and side effects, and the experimental results were significant.

This study confirmed that the three groups had significant inhibitory effects on IFN-γ, IL-17A, and IL-23 in mouse serum. However, further intergroup comparison indicated that the indirubin group had more obvious effects on the above three indicators than the hUC-MSCs group did. These results suggest that indirubin has a strong inhibitory effect on the psoriasis-related IL-23/Th17/IL-17 axis and Th1/IFN-γ axis. In addition, although the improvement of PASI score was significantly different among the three groups, the indirubin group was significantly better than the hUC-MSCs group in reducing scale, considering that indirubin can inhibit the mitosis of cells in psoriatic lesions and regulate cell keratinization. The systematic use of UC-MSCs therapy combined with indirubin external preparation may further improve the efficacy.

After the combination of hUC-MSCs and indirubin, the epidermis was the thinnest in the pathological sections of mice, thereby suggesting that the combination of hUC-MSCs and indirubin could exert a synergistic effect to better inhibit the proliferation of psoriasis epidermis. The spleen index of mice increased significantly after the combination of drugs, but single treatment of indirubin or hUC-MSCs had no obvious effect on the spleen index of mice, which may be due to the synergistic effect of the two groups of drugs in strengthening the regulation of immune function.

In general, according to the PASI score and pathological analysis of skin lesions, this study confirmed that hUC-MSCs, traditional Chinese medicine indirubin, and the combination of the above two groups had therapeutic and intervention effects on skin lesions of mice with psoriasis. Moreover, the concentrations of IFN-γ, TNF-α, IL-17A, and IL-23 in skin lesions and serum of mice decreased significantly, suggesting that hUC-MSCs and indirubin are involved in the process of immune regulation in the treatment of psoriasis, and the targets and focuses are

different. This subject needs to be further explored in future research.

Data availability statement

The original contributions presented in the study are included in the article/supplementary materials. Further inquiries can be directed to the corresponding authors.

Ethics statement

Experiments were performed under a project license (No. 2016LL003) granted by institutional board of The Fifth People's Hospital of Hainan Province, in compliance with The Fifth People's Hospital of Hainan Province guidelines for the care and use of animals.

Author contributions

(I) Conception and design: JY; (II) Administrative support: HW; (III) Provision of study materials or patients: HW, YL, and XL; (IV) Collection and assembly of data: XL; (V) Data analysis and interpretation: All authors; (VI) Manuscript writing: JY; (VII) Final approval of manuscript: All authors.

Funding

This work was supported by Hainan Province Clinical Medical Center and the funding project "Effects of indigo naturalis and Arnebia on differentiation and barrier function of epidermal stem cells in psoriasis response research (Hainan Natural Science Foundation, 20158342)"

Conflict of interest

Authors HW, HW, FX, CJ, DS, and HZ were employed by Asia Stem Cell Regenerative Pharmaceutical Co. Ltd.

The remaining authors declare that the research was conducted in the absence of any commercial or financial relationships that could be construed as a potential conflict of interest.

Publisher's note

References

1. Zhang XJ. Chinese Guidelines for the diagnosis and treatment of psoriasis (2018 complete version). *Chin J Dermatol* (2019) 52(10):667–710. doi: 10.35541/cjd.20190847

2. Iskandar I, Warren RB, Lunt M, Mason KJ, Evans I, McElhone K, et al. Differential drug survival of second-line biologic therapies in patients with psoriasis: Observational cohort study from the British association of dermatologists biologic interventions register (BADBIR). *J Invest Dermatol* (2018) 138(4):775–84. doi: 10.1016/j.jid.2017.09.044

3. Owczarczyk-Saczonek A, Krajewska-Wlodarczyk M, Kruszewska A, Placek W, Maksymowicz W, Wojtkiewicz J. Stem cells as potential candidates for psoriasis cell-replacement therapy. *Int J Mol Sci* (2017) 18(10):2182. doi: 10.3390/ijms18102182

4. Ahn H, Lee SY, Jung WJ, Pi J, Lee KH. Psoriasis treatment using minimally manipulated umbilical cord-derived mesenchymal stem cells: A case report. *World J Clin cases* (2021) 9(23):6798–803. doi: 10.12998/wjcc.v9.i23.6798

5. Cheng L, Wang S, Peng C, Zou X, Yang C, Mei H, et al. Human umbilical cord mesenchymal stem cells for psoriasis: a phase 1/2a, single-arm study. *Signal Transduct Target Ther* (2022) 7(1):263. doi: 10.1038/s41392-022-01059-y

6. Lin Y, Wang H, Jiang C, Chen C, Shen D, Xie F, et al. Effects of different concentrations of human umbilical cord mesenchymal stem cells to ameliorate psoriasis-like skin lesions in BALB/c mice. *Ann Transl Med* (2022) 10(2):86. doi: 10.21037/atm-22-4

7. Chen Y, Hu Y, Zhou X, Zhao Z, Yu Q, Chen Z, et al. Human umbilical cord-derived mesenchymal stem cells ameliorate psoriasis-like dermatitis by suppressing IL-17-producing γδ T cells. *Cell Tissue Res* (2022) 388(3):549–63. doi: 10.1007/s00441-022-03616-x

8. Zhang L, Wei W. Anti-inflammatory and immunoregulatory effects of paeoniflorin and total glucosides of paeony. *Pharmacol Ther* (2020) 207:107452. doi: 10.1016/j.pharmthera.2019.107452

9. Meng S, Lin Z, Wang Y, Wang Z, Li P, Zheng Y. Psoriasis therapy by Chinese medicine and modern agents. *Chin Med* (2018) 13:16. doi: 10.1186/s13020-018-0174-0

10. Lin YK, Chang CJ, Chang YC, Wong WR, Chang SC, Pang JH. Clinical assessment of patients with recalcitrant psoriasis in a randomized, observer-blind, vehicle-controlled trial using indigo naturalis. *Arch Dermatol* (2008) 144(11):1457–64. doi: 10.1001/archderm.144.11.1457

11. Lin YK, See LC, Huang YH, Chang YC, Tsou TC, Leu YL, et al. Comparison of refined and crude indigo naturalis ointment in treating psoriasis: randomized, observer-blind, controlled, intrapatient trial. *Arch Dermatol* (2012) 148(3):397–400. doi: 10.1001/archdermatol.2011.1091

12. Lin YK, See LC, Huang YH, Chang YC, Tsou TC, Lin TY, et al. Efficacy and safety of indigo naturalis extract in oil (Lindioil) in treating nail psoriasis: a randomized, observer-blind, vehicle-controlled trial. *Phytomedicine* (2014) 21(7):1015–20. doi: 10.1016/j.phymed.2014.02.013

13. Mcdermott L, Madan R, Rupani R, Siegel D. A review of indigo naturalis as an alternative treatment for nail psoriasis. *J Drugs Dermatol* (2016) 15(3):319–23.

14. Xue X, Wu J, Li J, Xu J, Dai H, Tao C, et al. Indirubin attenuates mouse psoriasis-like skin lesion in a CD274-dependent manner: an achievement of RNA sequencing. *Biosci Rep* (2018) 38(6):BSR20180958. doi: 10.1042/BSR20180958

15. Zhao J, Xie X, Di T, Liu Y, Qi C, Chen Z, et al. Indirubin attenuates IL-17A-induced CCL20 expression and production in keratinocytes through repressing TAK1 signaling pathway. *Int Immunopharmacol* (2021) 94:107229. doi: 10.1016/j.intimp.2020.107229

16. Xiu Y, Xiang C, Shao Z. Establishment of modified psoriasis mouse model. *China Pharm* (2019) 30(09):1187–91. doi: 10.6039/j.issn.1001-0408.2019.09.08

17. Deng Y, Chang C, Lu Q. The inflammatory response in psoriasis: a comprehensive review. *Clin Rev Allergy Immunol* (2016) 50(3):377–89. doi: 10.1007/s12016-016-8535-x

18. Attia SS, Rafla M, El-Nefiawy NE, Abdel Hamid HF, Amin MA, Fetouh MA. A potential role of mesenchymal stem cells derived from human umbilical cord blood in ameliorating psoriasis-like skin lesion in the rats. *Folia Morphol (Warsz)* (2021) 81(3):614–31. doi: 10.5603/FM.a2021.0076

19. Chen M, Peng J, Xie Q, Xiao N, Su X, Mei H, et al. Mesenchymal stem cells alleviate moderate-to-Severe psoriasis by reducing the production of type I interferon (IFN-I) by plasmacytoid dendritic cells (pDCs). *Stem Cells Int* (2019) 2019:6961052. doi: 10.1155/2019/6961052

20. Kim CH, Lim CY, Lee JH, Kim KC, Ahn JY, Kim CH, et al. Human embryonic stem cells-derived mesenchymal stem cells reduce the symptom of psoriasis in imiquimod-induced skin model. *Tissue Eng Regener Med* (2019) 16 (1):93–102. doi: 10.1007/s13770-018-0165-3

21. Lin YK, See LC, Huang YH, Chi CC, Hui RC. Comparison of indirubin concentrations in indigo naturalis ointment for psoriasis treatment: a randomized, double-blind, dosage-controlled trial. *Br J Dermatol* (2018) 178(1):124–31. doi: 10.1111/bjd.15894

22. Xie XJ, TT Di, Wang Y, Wang MX, Meng YJ, Lin Y, et al. Indirubin ameliorates imiquimod-induced psoriasis-like skin lesions in mice by inhibiting inflammatory responses mediated by IL-17A-producing gammadelta T cells. *Mol Immunol* (2018) 101:386–95. doi: 10.1016/j.molimm.2018.07.011

23. Li Q, Liu S, Lin J, Chen YF. Effect of indirubin on the expression of proinflammatory cytokines in keratinocytes. *Diagnosis Ther J Dermato-Venereol* (2021) 28(03):182–5. doi: 10.3969/j.issn.1674-8468.2021.03.005

frontiers | Frontiers in Immunology

TYPE Mini Review
PUBLISHED 25 November 2022
DOI 10.3389/fimmu.2022.1038744

OPEN ACCESS

EDITED BY
Eva Reali,
University of Milano-Bicocca, Italy

REVIEWED BY
H. Robert Frost,
Dartmouth College, United States

*CORRESPONDENCE
Wei Li
liweihx_hxyy@scu.edu.cn

SPECIALTY SECTION
This article was submitted to Inflammation, a section of the journal Frontiers in Immunology

RECEIVED 07 September 2022
ACCEPTED 27 October 2022
PUBLISHED 25 November 2022

CITATION
Xia D, Wang Y, Xiao Y and Li W (2022) Applications of single-cell RNA sequencing in atopic dermatitis and psoriasis. *Front. Immunol.* 13:1038744. doi: 10.3389/fimmu.2022.1038744

Applications of single-cell RNA sequencing in atopic dermatitis and psoriasis

Dengmei Xia[1,2,3], Yiyi Wang[1,3], Yue Xiao[1,3] and Wei Li[1,3]*

[1]Department of Dermatology, Rare Diseases Center, West China Hospital, Sichuan University, Chengdu, Sichuan, China, [2]Department of Dermatology, The Affiliated Hospital of Southwest Medical University, Luzhou, Sichuan, China, [3]Institutes for Systems Genetics, Frontiers Science Center for Disease-related Molecular Network, National Clinical Research Center for Geriatrics, West China Hospital, Sichuan University, Chengdu, Sichuan, China

Single-cell RNA sequencing (scRNA-seq) is a novel technology that characterizes molecular heterogeneity at the single-cell level. With the development of more automated, sensitive, and cost-effective single-cell isolation methods, the sensitivity and efficiency of scRNA-seq have improved. Technological advances in single-cell analysis provide a deeper understanding of the biological diversity of cells present in tissues, including inflamed skin. New subsets of cells have been discovered among common inflammatory skin diseases, such as atopic dermatitis (AD) and psoriasis. ScRNA-seq technology has also been used to analyze immune cell distribution and cell-cell communication, shedding new light on the complex interplay of components involved in disease responses. Moreover, scRNA-seq may be a promising tool in precision medicine because of its ability to define cell subsets with potential treatment targets and to characterize cell-specific responses to drugs or other stimuli. In this review, we briefly summarize the progress in the development of scRNA-seq technologies and discuss the latest scRNA-seq-related findings and future trends in AD and psoriasis. We also discuss the limitations and technical problems associated with current scRNA-seq technology.

KEYWORDS

single-cell RNA sequencing, inflammation, atopic dermatitis, psoriasis, transcriptomics

Introduction

Inflammatory skin diseases are induced by skin barrier disorders and dysregulation of innate and adaptive immunity. Atopic dermatitis (AD) and psoriasis are two of the most common chronic inflammatory skin diseases (1, 2). The Global Burden of Disease study showed that AD is the 15th most common non-fatal disease and the skin disorder

with the highest disease burden, with a prevalence of 15% to 20% among children and up to 10% in adults (3). Approximately 125 million people worldwide are estimated to have psoriasis (4). Although genetic, immune dysregulation, and environmental factors play important roles in the pathogenesis of AD and psoriasis (1, 2), the detailed mechanisms of AD and psoriasis remain unclear. In recent years, specific immune component targeted therapies have been reported in AD and psoriasis, with substantially positive effects. However, some patients do not respond to these treatments, have a secondary failure, or relapse after drug withdrawal; thus, the underlying mechanisms regarding the treatment of these diseases remain unclear.

Bulk RNA sequencing is an indispensable tool for analyzing transcriptional variations, which determine the average gene expression among pooled populations of cells and reported as single data. However, tissues consist of multiple cell types in various states; hence, the results of such a technique can be misleading. Newly developed single-cell RNA sequencing (scRNA-seq) technologies facilitate the analysis of transcriptional activity at the single-cell level (5). scRNA-seq facilitates the assessment of cellular heterogeneity, identification of new or rare cell populations, and clarification of cellular transition states at a high resolution. In addition, Thus, organ- or tissue-specific transcriptomic characteristics of keratinocytes (KCs), fibroblasts, endothelial cells, and immune cells hosted within or infiltrated after inflammation can be assessed to elucidate the function of cell heterogeneity in AD and psoriasis.

A brief introduction to single-cell RNA sequencing

scRNA-seq is a powerful tool for providing precision and detail to individual cells (6). The workflow of scRNA-seq usually includes sample preparation, single-cell capture, reverse transcription of full-length mRNA, cDNA amplification, preparation of a sequencing library, high-throughput sequencing, and bioinformatics analyses. Single-cell isolation and amplification of cDNA are the main steps in various single-cell sequencing strategies.

Methods of traditional single-cell isolation have eventually developed after many optimizations. Micromanipulation is a classic technique for manually capturing under a microscope (7, 8). It can accurately select single cells under microscopic observation and is suitable for analyzing a limited number of cells (9). However, this method is time-consuming, has low throughput, and may cause cellular injury due to mechanical shearing (10). Laser capture microdissection (LCM) is another approach for obtaining single cells from solid tissue. In this technique, a laser beam is used to capture the cells of interest from the tissue specimen quickly and accurately, attaching these cells to a thin and transparent film (11). Here, the spatial positional information of the target cells is retained (12); however, in addition to being laborious and inconvenient, there is a risk of destroying the integrity of cells and damaging cellular RNA (13), which could impact subsequent analyses. Fluorescence-activated cell sorting (FACS) is a specialized type of flow cytometry that sorts large numbers of cells based on cell surface markers and physicochemical properties and completes quantitative analyses quickly (14). Time consumption and low throughput limit the use of these traditional technologies. To circumvent this, scRNA-seq technology platforms have been rapidly developed based on the application of microfluidic and single-cell identification technologies.

Novel single-cell capture methods based on microfluidics include integrated fluidic circuits (IFCs), droplets, microwells, traps, and the SlipChip (15). Popular platforms have recently enabled droplet-based scRNA-seq, which sorts cells into aqueous compartments in a lipid suspension (16). Using this system, the cell capture rate of a single sample can be as high as 65%, and 80,000 cells can be simultaneously isolated and amplified in minutes (17). Split pool ligation-based transcriptome sequencing (SPLiT-Seq) uses combinatorial barcodes to label individual cells (18), which is expected to decrease operational costs and does not involve microfluidic devices. The development of these technologies has led to the widespread use of scRNA-seq. The advantages and disadvantages of these single-cell isolation methods are summarized in Table 1.

Single-cell bioinformatics analysis, typically involves fundamental analytical procedures such as quality control, normalization, dimensionality reduction, differential expression gene analysis, visualization, clustering, and cell type annotation. Thus, this analysis can obtain the basic single-cell landscape of specific disease. Some advanced analyses, such as trajectory and cell-cell communications, can help us further capture specific disease-related cells, genes, functional pathways, and cell-cell interactions. scRNA-seq technology has been applied in skin cancer and autoimmune skin diseases. For example, ferroptosis-related genes and resident memory CD8+ T cells in regional lymph nodes have been identified to predict the prognosis of melanoma using scRNA-seq analyses (19, 20). Moreover, patterns of dedifferentiation in melanoma are predictive of the response to immune checkpoint inhibitor therapy (21). Type 1 cytokine signaling plays a central role in vitiligo, and Treg cells inhibit disease progression in non-lesional skin (22). A unique cluster of CXCL13+ T cells identified *via* scRNA-seq appears to promote B- cell responses within the inflamed skin of patients with systemic sclerosis (23). These data provide critical insights into the pathogenesis of melanoma, vitiligo, and systemic sclerosis, respectively.

TABLE 1 Comparison of the advantages and disadvantages of single-cell isolation methods.

Techniques	Automation level	Impact on cell integrity	Advantages	Disadvantages
Micromanipulation (8–10)	Manual	Gentle	Precise capturing of single cells under direct visualization. Low cost.	Time-consuming and low throughout.
Laser capture microdissection (LCM) (11–13)	Manual	Often impairing	Isolation of single cells from solid samples, not need the preparation of cell suspensions.	Time-consuming, low throughout. and influence subsequent amplification.
Fluorescence-activated cell sorting (FACS) (14)	Automatic	Often impairing	Suitable for sorting different types of cells. High throughout.	Hard to detect cellular characteristics expressed at a low level and differentiate with similar marker expressions.
Integrated fluidic circuits-based microfluidics (15)	Automatic	Few	Capture and process 800 small or medium-size single cells simultaneously.	High cost.
Microdroplet-based microfluidics (16, 17)	Automatic	Few	Isolation and amplification of 80,000 cells imultaneously in minutes.	A risk of blockage.
Microwell-based microfluidics (15)	Automatic	Few	Single cells settled by gravity and microwells replaced droplets. Simultaneously capture approximately 10,000 single cells.	May not provide adequate space for the proliferation and movement of the cells.
Split pool ligation-based transcriptome sequencing (SPLiT-Seq) (18)	Automatic	/	Independent to microfluidic devices and low cell requirement of samples.	/

/: Not mentioned.

Applications of single-cell RNA sequencing in inflammatory skin diseases

Atopic dermatitis

Atopic dermatitis (AD) is one of the most common inflammatory skin diseases. The prevalence of AD has been reported up to 20% among children and 10% among adults (24), and the causes are complex. Genetic susceptibility, a dysfunctional epidermal barrier, skin microbiome abnormalities, and type-2 immune dysregulation predominantly play a role in the pathogenesis of AD (2). The endotype is the molecular mechanism underlying the disease phenotypes (25, 26). Aside from the presence of IgE that can distinguish between intrinsic and extrinsic AD, AD is characterized by a highly diverse endotype repertoire, including the dysregulation of Th1/Th2/Th17/Th22 cells and impaired epidermal barrier integrity (27).

In addition to the unclear specific pathogenic mechanisms of AD, the treatment options for this disease vary. Targeted therapies for specific AD endotypes, such as those directed against Th2/Tc2, and Th17 cells and general anti-inflammatory agents, have been proved by the FDA or are currently in different phases of clinical trials (28). Additionally, addressing the unsatisfactory efficacy of current therapies and identifying biomarkers that will improve therapy selection for biological agents and small-molecule drugs should be the focus for AD.

RNA sequencing and gene microarray analysis of skin biopsy specimens have provided insights into AD pathogenesis (29, 30). scRNA-seq was performed on lesional and non-lesional samples from patients with AD and skin from healthy individuals. It was found that *COL6A5*$^{+}$*COL18A1* $^{+}$ fibroblast, which express the cytokines CCL2 and CCL19, were a novel cell subpopulation unique to AD lesional skin. A dendritic cell population that expresses the CCL19 receptor CCR7 is also unique to AD lesions (31). Prx1+ fibroblasts overexpressing the eosinophilic chemokine CCL11 may also contribute to the pathogenesis of AD by dysregulating *IKKβ/NF-κB* signaling; hence, targeting CCL11 upregulation in Prx1+ fibroblasts may be a way to treat AD-like skin diseases (32). Whether these subpopulations of fibroblasts recruit T cells and other inflammatory cells into the local lesions or play a role in the initiation, maintenance, and regression phases needs further research.

Meanwhile, myeloid dendritic cells (DCs), including inflammatory dendritic epidermal cells, form the most expanded immune cell population in AD lesions (33). It has been demonstrated that unique inflammatory fibroblasts may interact with immune cells, such as DCs expressing CCR7, to regulate type 2 inflammation. Moreover, innate lymphoid cells (ILC), especially ILC2, have been implicated in AD pathogenesis. ILC2s are activated by various tissue-derived factors and exhibit different functions in both the steady- state and inflammation. The number of ILC2s in lesional skin biopsies from patients with AD was significantly higher than in healthy individuals (34, 35). Skin ILC2s were further sub-classified into skin-resident and circulating ILC2s through scRNA-seq in a transgenic mouse line expressing skin-specific IL-33 expression. Here, these transgenic mice showed ILC2- dependent atopic dermatitis-like skin

inflammation (36). Patients with AD have a high percentage of ILC2s in their peripheral blood that respond better to IL-4/13 inhibitors, such as dupilumab (37). Furthermore, ILC2s in lesional AD skin have been shown to be biologically heterogeneous and are involved in the IL-33 signaling pathway. ILC2s are flexible and co-express typical genes, either type 2 or type 3/17 immunity markers, within individual cells (38). It is well known that type3/17 immunity is associated with the development of psoriasis. However, whether the plasticity of ILC2s is responsible for psoriasis-related dermatitis remains unclear.

AD typically starts in infancy or early childhood, showing spontaneous regression after puberty in a subset of patients while waxing and waning for life in many others. However, the factors that modify the natural course of spontaneous remission remain to be elucidated. The overall cell composition of patients with spontaneously healed AD was comparable to that of healthy individuals. Compared to healthy controls, melanocytes exhibit many differentially expressed genes in all cell types in spontaneously healed atopic dermatitis. Specifically, the expression of the potential anti-inflammatory, maker PLA2G7 (Lipoprotein-associated phospholipase A2 or "platelet-activating factor acetylhydrolase) is increased. Regulatory markers are also upregulated in conventional T-cells (39). Moreover, skin-resident memory T cells showed the greatest transcriptional dysregulation in AD (40), which may be responsible for the recurrence of the disease. KCs also play an important role in the pathogenesis of AD. Epidermal proliferation and chemokines (CCL2 and CCL27) were significantly upregulated in the KCs of lesional AD. Such KCs were found to be enriched during epidermis development and immune responses (31).

Based on previous studies, innate immune cells (ILC2s and DCs), fibroblasts, and KCs, as well as their interplay and interactions, play a role in AD development. Melanocytes and skin-resident memory T cells may contribute to the specific regulatory microenvironment in the spontaneous remission and recurrence of AD, respectively.

Psoriasis

Psoriasis is also a common, chronic inflammatory skin disease, and its incidence in ethnic groups and countries is significantly different (41). The pathogenesis of psoriasis is complex and multifactorial, involving genetic, immune, and environmental factors. The IL-23/Th17 pathway is thought to be the predominant pathway governing the progression and development of psoriasis (42). Biologics that target IL-17/IL-17 receptor and IL-23 have shown significant clinical efficacy in patients with psoriasis (43, 44). Cutaneous type 17 T-cells showed markedly different g transcriptome profiles depending on various cytokines, including IL-17A, IL-17F, and IL-10 (45). CD8+ T cells are increased in abundance within psoriatic lesions (46) and are found to produce inflammatory cytokines, such as IL-17, at sites of the active phase of psoriasis (47). However, CD8+ T cells are phenotypically heterogeneous and have distinct functional properties with cytotoxic and cytokine-producing features (48). Two pathogenic cytotoxic type 17 T-cell (Tc17) subsets of CD8+ T cells were identified in psoriatic skin from lesional skin biopsies of 11 patients with psoriasis and five healthy control individuals *via* single-cell transcriptomics. CXCL13- expressing Tc17 cells appear to be specific to psoriatic lesions and are associated with disease severity (49). Up to 30% patients with psoriasis may develop psoriatic arthritis (PsA), presenting with peripheral arthritis, enthesitis, and (or) dactylitis (50). The expansion of memory CD8+ T cells in the joints of PsA patients was significantly higher than that in their peripheral blood. CD8+ T cells have also been previously reported in the synovial fluid of PsA patients (51). single-cell sequencing showed that in the synovial fluid, CD8+T cells that express CXCR3, a tissue-homing receptor, are increased in abundance and that the expression of its ligands (CXCL9 and CXCL10) were elevated, providing molecular insight into the cellular immune mechanism of PsA (52). Compared to healthy, patients with psoriasis are characterized by T_{reg} expansion and CD8 + T cell exhaustion. Moreover, differentially expressed genes in skin-resident memory T cells have been recently reported to discriminate psoriasis vulgaris from AD. Other T cell subsets, such as dysfunctional T cells that regulate and express NR4A1, are also involved in psoriasis (53).

In addition to adaptive immunity, innate immunity plays an important role in the pathogenesis of psoriasis. Cutaneous antigen-presenting cells (APCs) are divided into three groups: Langerhans cells in the epidermis, classical dendritic cell type 1 (cDC1) and cDC2 in the dermis, and macrophages (54). A new subset of inflammatory DCs expressing CD5-CD163+CD14+ (DC3) was identified in human blood (55). CD14+ DC3 cells expressing genes related to IL-17 and neutrophil activation signaling were enriched in psoriatic lesions, which were considered potential promoters of inflammation in psoriasis. Higher proportions of macrophage-expressing genes related to inflammatory chemokines and cytokines (CXCL8 and CXCL2) were found in psoriatic lesions compared to non-lesional skin (56). ILC3s have been reported in human and mouse psoriatic lesions (57, 58). The response to therapeutic compounds has decreased the number of ILC3 cells (59). Fate mapping analysis suggested that ILC3-like cells may arise from quiescent-like cells and ILC2s, highlighting the flexibility of skin ILC responses and driving the pathological remodeling process (60).

Even though immune cell infiltration plays a fundamental role in cutaneous inflammation, KCs can also influence the inflammatory microenvironment (61). scRNA-seq analysis showed that aberrant inflammatory transcription of A20 in KCs in psoriasis is related to the IL-17 and tumor necrosis

factor-α(TNF-α) signaling pathways (62), suggesting a potential targeted therapy. Hence, Th17 cells, CD8+ T cells, DC3 cells, macrophages, ILCs and KCs play an important role in the development of psoriasis. And Tc17 cells, a subtype of CD8+ T cells, are associated with disease activity.

Discussion

Since 2009, the first conceptual and technical breakthrough of the single-cell RNA sequencing method was made by Tang et al. (8). An increasing number of improved scRNA-seq technologies were developed to introduce essential modifications and improvements in sample collection, single-cell capture, barcoded reverse transcription, cDNA amplification, library preparation, sequencing and streamlined bioinformatics analysis. Freshly tissues, high cost of per sample and scRNA-seq data analysis still remain challenge. Subsequent studies are expected to explore fixed tissue sample and to downregulate costs. And automatic scRNA-seq data analysis pipelines and visualization platforms are expected to be available in the future.

Most of studies related in this review prepare the libraries and sequence depending on 10X Genomics platform. These findings highlight KCs, fibroblasts, and different types of immune cells in mechanisms for coping with the different stages of AD and psoriasis. scRNA-seq offers a novel method to identify the receptors, ligands, and cytokines expressed in each cell type to further highlight intercellular communication in the skin microenvironment. However, the detailed mechanisms driving the pathogenicity of these cells and the relationship between them require further study. And the clinical characteristics of AD and psoriasis varied. Therefore, more specific studies are necessary to elucidate the characteristics of AD and psoriasis based on the differences in the stages and subtypes of these diseases. Patients with clinical characteristics of both AD and psoriasis have been described as having psoriasis dermatitis, typically found in children (63). In addition to the co-existence of both AD and psoriasis, disease co-occurrence but alternating flare-ups or co-occurrence at different life stages may also be observed (64). The overlap condition not only presented in children but also in adult patients. With the increasing application of biologics agents, the psoriasiform reaction during dupilumab therapy has been reported in AD, and an eczematous reaction to anti-interleukin (IL)-17 treatment has been reported in psoriasis (65, 66). However, the pathophysiology should be further clarified. Moreover, it will be beneficial to analyze cell lineage trajectories and patient-specific cell heterogeneity using scRNA-seq data.

Analyzing the non-coding RNAs (ncRNAs) with scRNA-seq and combining proteomics with epigenomics will get closer to a ture global examination of single cell. In addition, the analysis of minimally invasive or non-invasive samples, such as blood or urine specimens, may also hold promise in diagnosis process and treatment response prediction. Considering the rapid development of sequencing methods, scRNA-seq can be expected to enter the clinics soon and facilitate personalized therapeutic decisions for patients with inflammatory skin diseases.

Limitations of single-cell RNA sequencing

Although scRNA-seq can identify cell type-specific transcriptional regulation and cellular heterogeneity, its limitations can be challenged. Firstly, high-throughput single-cell analysis requires cell dissociation, quality control, and are largely tend to examine freshly isolated cells. More research will use such technology to explore cryopreserved and fixed tissue samples. And the preparation of single-cell suspensions destroys spatial information of tissues. In addition, researchers have mostly focused on protein-coding RNA. An increasing number of studies have indicated that ncRNAs have important roles in cell function and specialization (67–69). Even though it has been neglected in previous scRNA-seq studies, nanopore sequencing and Smart-seq-total technology may also address current gaps in the technology (70, 71). Bioinformatics analysis of DEGs in scRNA-seq strongly depends on the cell count in each identified cluster, whether the transcriptional changes obtained *via* scRNA-seq are specific biological findings, or a biased subset clustering data that is prone to misinterpretation (72, 73). The development of scRNA-seq technology has raised a wide range of computational and analytical challenges. Even though several methods have now been designed to efficiently perform upstream (quality control and normalization) and downstream (cell-, gene- and pathway-level) analyses of scRNA-seq data (74), there are limited guidelines on how to define quality control standards, remove technical artifacts, and interpret results. Deep-learning based methods, such as machine learning, may also provide more benefits than traditional statistical models in dealing with high-dimensional data.

Conclusions

In recent years, transcriptomics has made a great leap from bulk RNA-seq, which measures the average gene expression, to analyzing gene expression data in individual cells. This mini-review summarizes and discusses the applications of scRNA-seq in AD and psoriasis (Figure 1). Single-cell RNA sequencing has provided new insights into inflammatory skin disease heterogeneity, revealed complex interactions between cell types, and allowed a more comprehensive understanding of inflammatory skin disease initiation, progression, and

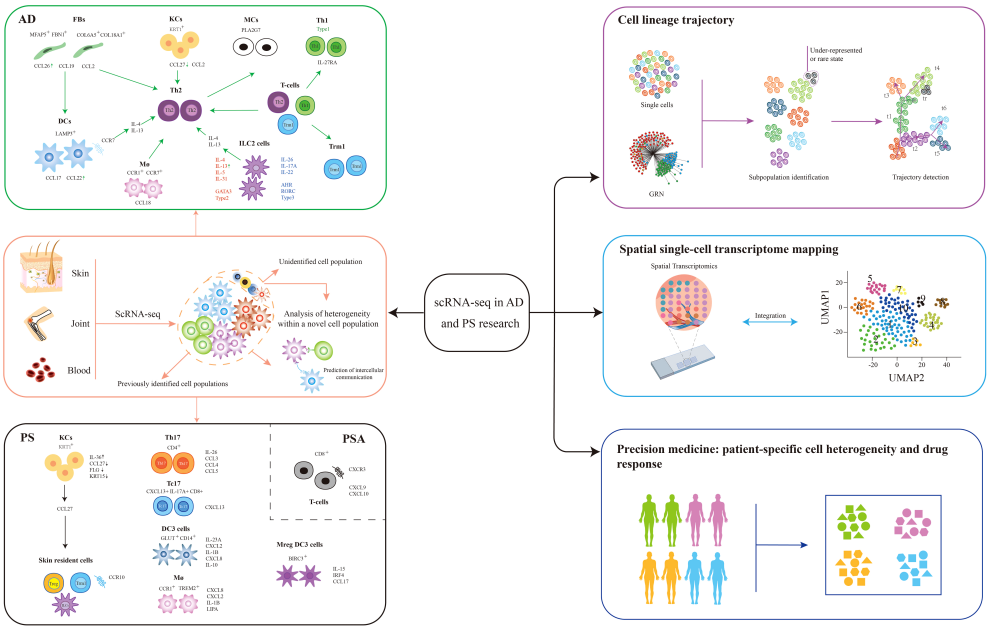

FIGURE 1
Application of scRNA-seq in AD and PS. Single-cell RNA sequencing (scRNA-seq) is especially useful in the detection of rare cell populations, identifying cell-to-cell interactions, reconstructing skin cell trajectories, spatial transcriptomic mapping of skin (75), and developing more precision medicine tools for the better prediction of patient-specific drug responses. The future trends involved cell-to-cell communication, skin cell trajectories, spatial transcriptomic mapping of skin, and precision medicines in these diseases. AD, atopic dermatitis; PS, psoriasis; FBs, fibroblasts; KCs, keratinocytes; MCs, melanocytes; Th1, T helper 1; Th17, T helper 17; Tc17, expressing IL-17 cytotoxic CD+8 T cell; Trm, skin-resident memory T cell; Treg, regulatory T cell; DC, dendritic cell; Mreg DC, mature dendritic cell enriched in immunoregulatory molecules; ILC, innate lymphoid cell; Mø, macrophage; CCL, CC chemokine ligand; CXCL, C-X-C motif ligand; GRN, gene regulatory network; t-SNE, t-distributed stochastic neighbor embedding.

regression. New insights are crucial for developing targeted and innovative therapeutic strategies, to advance precision medicine for inflammatory skin diseases. Although some limitations remain, scRNA-seq will pave the way for personalized medicine once solving the challenges.

Author contributions

DX wrote the manuscript. YW, YX, and WL contributed to the revision of the manuscript. All authors approved the final submitted version.

Funding

1·3·5 project for disciplines of excellence, West China Hospital, Sichuan University.

Conflict of interest

The authors declare that the research was conducted in the absence of any commercial or financial relationships that could be construed as a potential conflict of interest.

Publisher's note

References

1. Boehncke W-H, Schön MP. Psoriasis. *Lancet* (2015) 386(9997):983–94. doi: 10.1016/s0140-6736(14)61909-7

2. Langan SM, Irvine AD, Weidinger S. Atopic dermatitis. *Lancet* (2020) 396 (10247):345–60. doi: 10.1016/s0140-6736(20)31286-1

3. Laughter MR, Maymone MBC, Mashayekhi S, Arents BWM, Karimkhani C, Langan SM, et al. The global burden of atopic dermatitis: Lessons from the global burden of disease study 1990-2017. *Br J Dermatol* (2021) 184(2):304–9. doi: 10.1111/bjd.19580

4. World Health Organization. *Global report on psoriasis: World health organization* (2016). Available at: https://apps.who.int/iris/handle/10665/204417 (Accessed February 13, 2020).

5. Shapiro E, Biezuner T, Linnarsson S. Single-cell sequencing-based technologies will revolutionize whole-organism science. *Nat Rev Genet* (2013) 14 (9):618–30. doi: 10.1038/nrg3542

6. Qi R, Ma A, Ma Q, Zou Q. Clustering and classification methods for single-cell rna-sequencing data. *Brief Bioinform* (2020) 21(4):1196–208. doi: 10.1093/bib/bbz062

7. Morris J, Singh JM, Eberwine JH. Transcriptome analysis of single cells. *J Visualized Exp: JoVE* (2011) 50:2634. doi: 10.3791/2634

8. Tang F, Barbacioru C, Wang Y, Nordman E, Lee C, Xu N, et al. Mrna-seq whole-transcriptome analysis of a single cell. *Nat Methods* (2009) 6(5):377–82. doi: 10.1038/nmeth.1315

9. Guo F, Li L, Li J, Wu X, Hu B, Zhu P, et al. Single-cell multi-omics sequencing of mouse early embryos and embryonic stem cells. *Cell Res* (2017) 27(8):967–88. doi: 10.1038/cr.2017.82

10. Gross A, Schoendube J, Zimmermann S, Steeb M, Zengerle R, Koltay P. Technologies for single-cell isolation. *Int J Mol Sci* (2015) 16(8):16897–919. doi: 10.3390/ijms160816897

11. Kamme F, Salunga R, Yu J, Tran DT, Zhu J, Luo L, et al. Single-cell microarray analysis in hippocampus Ca1: Demonstration and validation of cellular heterogeneity. *J Neurosci: Off J Soc Neurosci* (2003) 23(9):3607–15. doi: 10.1523/jneurosci.23-09-03607.2003

12. Chen J, Suo S, Tam PP, Han JJ, Peng G, Jing N. Spatial transcriptomic analysis of cryosectioned tissue samples with geo-seq. *Nat Protoc* (2017) 12(3):566–80. doi: 10.1038/nprot.2017.003

13. Keays KM, Owens GP, Ritchie AM, Gilden DH, Burgoon MP. Laser capture microdissection and single-cell rt-pcr without rna purification. *J Immunol Methods* (2005) 302(1-2):90–8. doi: 10.1016/j.jim.2005.04.018

14. Adan A, Alizada G, Kiraz Y, Baran Y, Nalbant A. Flow cytometry: Basic principles and applications. *Crit Rev Biotechnol* (2017) 37(2):163–76. doi: 10.3109/07388551.2015.1128876

15. García Alonso D, Yu M, Qu H, Ma L, Shen F. Advances in microfluidics-based technologies for single cell culture. *Adv Biosyst* (2019) 3(11):e1900003. doi: 10.1002/adbi.201900003

16. Macosko EZ, Basu A, Satija R, Nemesh J, Shekhar K, Goldman M, et al. Highly parallel genome-wide expression profiling of individual cells using nanoliter droplets. *Cell* (2015) 161(5):1202–14. doi: 10.1016/j.cell.2015.05.002

17. Valihrach L, Androvic P, Kubista M. Platforms for single-cell collection and analysis. *Int J Mol Sci* (2018) 19(3):807. doi: 10.3390/ijms19030807

18. Rosenberg AB, Roco CM, Muscat RA, Kuchina A, Sample P, Yao Z, et al. Single-cell profiling of the developing mouse brain and spinal cord with split-pool barcoding. *Sci (New York NY)* (2018) 360(6385):176–82. doi: 10.1126/science.aam8999

19. Liu Y, Shou Y, Zhu R, Qiu Z, Zhang Q, Xu J. Construction and validation of a ferroptosis-related prognostic signature for melanoma based on single-cell rna sequencing. *Front Cell Dev Biol* (2022) 10:818457. doi: 10.3389/fcell.2022.818457

20. Molodtsov AK, Khatwani N, Vella JL, Lewis KA, Zhao Y, Han J, et al. Resident memory Cd8(+) T cells in regional lymph nodes mediate immunity to metastatic melanoma. *Immunity* (2021) 54(9):2117–32 e7. doi: 10.1016/j.immuni.2021.08.019

21. Belote RL, Le D, Maynard A, Lang UE, Sinclair A, Lohman BK, et al. Human melanocyte development and melanoma dedifferentiation at single-cell resolution. *Nat Cell Biol* (2021) 23(9):1035–47. doi: 10.1038/s41556-021-00740-8

22. Gellatly KJ, Strassner JP, Essien K, Refat MA, Murphy RL, Coffin-Schmitt A, et al. Scrna-seq of human vitiligo reveals complex networks of subclinical immune activation and a role for Ccr5 in treg function. *Sci Trans Med* (2021) 13(610): eabd8995. doi: 10.1126/scitranslmed.abd8995

23. Gaydosik AM, Tabib T, Domsic R, Khanna D, Lafyatis R, Fuschiotti P. Single-cell transcriptome analysis identifies skin-specific T-cell responses in systemic sclerosis. *Ann Rheumatic Dis* (2021) 80(11):1453–60. doi: 10.1136/annrheumdis-2021-220209

24. Ständer S. Atopic dermatitis. *N Engl J Med* (2021) 384(12):1136–43. doi: 10.1056/NEJMra2023911

25. Agache I, Akdis C, Jutel M, Virchow JC. Untangling asthma phenotypes and endotypes. *Allergy* (2012) 67(7):835–46. doi: 10.1111/j.1398-9995.2012.02832.x

26. Lötvall J, Akdis CA, Bacharier LB, Bjermer L, Casale TB, Custovic A, et al. Asthma endotypes: A new approach to classification of disease entities within the asthma syndrome. *J Allergy Clin Immunol* (2011) 127(2):355–60. doi: 10.1016/j.jaci.2010.11.037

27. Brunner PM, Leung DYM, Guttman-Yassky E. Immunologic, microbial, and epithelial interactions in atopic dermatitis. *Ann Allergy Asthma Immunol* (2018) 120(1):34–41. doi: 10.1016/j.anai.2017.09.055

28. Czarnowicki T, He H, Krueger JG, Guttman-Yassky E. Atopic dermatitis endotypes and implications for targeted therapeutics. *J Allergy Clin Immunol* (2019) 143(1):1–11. doi: 10.1016/j.jaci.2018.10.032

29. Nomura I, Gao B, Boguniewicz M, Darst MA, Travers JB, Leung DY. Distinct patterns of gene expression in the skin lesions of atopic dermatitis and psoriasis: A gene microarray analysis. *J Allergy Clin Immunol* (2003) 112(6):1195–202. doi: 10.1016/j.jaci.2003.08.049

30. Suárez-Fariñas M, Ungar B, Correa da Rosa J, Ewald DA, Rozenblit M, Gonzalez J, et al. Rna sequencing atopic dermatitis transcriptome profiling provides insights into novel disease mechanisms with potential therapeutic implications. *J Allergy Clin Immunol* (2015) 135(5):1218–27. doi: 10.1016/j.jaci.2015.03.003

31. He H, Suryawanshi H, Morozov P, Gay-Mimbrera J, Del Duca E, Kim HJ, et al. Single-cell transcriptome analysis of human skin identifies novel fibroblast subpopulation and enrichment of immune subsets in atopic dermatitis. *J Allergy Clin Immunol* (2020) 145(6):1615–28. doi: 10.1016/j.jaci.2020.01.042

32. Ko KI, Merlet JJ, DerGarabedian BP, Zhen H, Suzuki-Horiuchi Y, Hedberg ML, et al. Nf-kappab perturbation reveals unique immunomodulatory functions in Prx1(+) fibroblasts that promote development of atopic dermatitis. *Sci Trans Med* (2022) 14(630):eabj0324. doi: 10.1126/scitranslmed.abj0324

33. Rojahn TB, Vorstandlechner V, Krausgruber T, Bauer WM, Alkon N, Bangert C, et al. Single-cell transcriptomics combined with interstitial fluid proteomics defines cell type-specific immune regulation in atopic dermatitis. *J Allergy Clin Immunol* (2020) 146(5):1056–69. doi: 10.1016/j.jaci.2020.03.041

34. Kim BS, Siracusa MC, Saenz SA, Noti M, Monticelli LA, Sonnenberg GF, et al. Tslp elicits il-33-Independent innate lymphoid cell responses to promote skin inflammation. *Sci Trans Med* (2013) 5(170):170ra16. doi: 10.1126/scitranslmed.3005374

35. Salimi M, Barlow JL, Saunders SP, Xue L, Gutowska-Owsiak D, Wang X, et al. A role for il-25 and il-33-Driven type-2 innate lymphoid cells in atopic dermatitis. *J Exp Med* (2013) 210(13):2939–50. doi: 10.1084/jem.20130351

36. Nakatani-Kusakabe M, Yasuda K, Tomura M, Nagai M, Yamanishi K, Kuroda E, et al. Monitoring cellular movement with photoconvertible fluorescent protein and single-cell rna sequencing reveals cutaneous group 2 innate lymphoid cell subtypes, circulating Ilc2 and skin-resident Ilc2. *JID Innov* (2021) 1(3):100035. doi: 10.1016/j.xjidi.2021.100035

37. Imai Y, Kusakabe M, Nagai M, Yasuda K, Yamanishi K. Dupilumab effects on innate lymphoid cell and helper T cell populations in patients with atopic dermatitis. *JID Innov* (2021) 1(1):100003. doi: 10.1016/j.xjidi.2021.100003

38. Alkon N, Bauer WM, Krausgruber T, Goh I, Griss J, Nguyen V, et al. Single-cell analysis reveals innate lymphoid cell lineage infidelity in atopic dermatitis. *J Allergy Clin Immunol* (2022) 149(2):624–39. doi: 10.1016/j.jaci.2021.07.025

39. Rindler K, Krausgruber T, Thaler FM, Alkon N, Bangert C, Kurz H, et al. Spontaneously resolved atopic dermatitis shows melanocyte and immune cell activation distinct from healthy control skin. *Front Immunol* (2021) 12:630892. doi: 10.3389/fimmu.2021.630892

40. Liu Y, Wang H, Taylor M, Cook C, Martínez-Berdeja A, North JP, et al. Classification of human chronic inflammatory skin disease based on single-cell immune profiling. *Sci Immunol* (2022) 7(70):eabl9165. doi: 10.1126/sciimmunol.abl9165

41. Michalek IM, Loring B, John SM. A systematic review of worldwide epidemiology of psoriasis. *J Eur Acad Dermatol Venereol: JEADV* (2017) 31 (2):205–12. doi: 10.1111/jdv.13854

42. Alwan W, Nestle FO. Pathogenesis and treatment of psoriasis: Exploiting pathophysiological pathways for precision medicine. *Clin Exp Rheumatol* (2015) 33 (5 Suppl 93):S2–6.

43. Haugh IM, Preston AK, Kivelevitch DN, Menter AM. Risankizumab: An anti-Il-23 antibody for the treatment of psoriasis. *Drug Design Dev Ther* (2018) 12:3879–83. doi: 10.2147/dddt.S167149

44. Leonardi C, Matheson R, Zachariae C, Cameron G, Li L, Edson-Heredia E, et al. Anti-Interleukin-17 monoclonal antibody ixekizumab in chronic plaque psoriasis. *N Engl J Med* (2012) 366(13):1190–9. doi: 10.1056/NEJMoa1109997

45. Kim J, Lee J, Kim HJ, Kameyama N, Nazarian R, Der E, et al. Single-cell transcriptomics applied to emigrating cells from psoriasis elucidate pathogenic versus regulatory immune cell subsets. *J Allergy Clin Immunol* (2021) 148(5):1281–92. doi: 10.1016/j.jaci.2021.04.021

46. Cheuk S, Wikén M, Blomqvist L, Nylén S, Talme T, Ståhle M, et al. Epidermal Th22 and Tc17 cells form a localized disease memory in clinically healed psoriasis. *J Immunol* (2014) 192(7):3111–20. doi: 10.4049/jimmunol.1302313

47. Hijnen D, Knol EF, Gent YY, Giovannone B, Beijn SJ, Kupper TS, et al. Cd8 (+) T cells in the lesional skin of atopic dermatitis and psoriasis patients are an important source of ifn-Γ, il-13, il-17, and il-22. *J Invest Dermatol* (2013) 133 (4):973–9. doi: 10.1038/jid.2012.456

48. Cheuk S, Schlums H, Gallais Sérézal I, Martini E, Chiang SC, Marquardt N, et al. Cd49a expression defines tissue-resident Cd8(+) T cells poised for cytotoxic function in human skin. *Immunity* (2017) 46(2):287–300. doi: 10.1016/j.immuni.2017.01.009

49. Liu J, Chang HW, Huang ZM, Nakamura M, Sekhon S, Ahn R, et al. Single-cell rna sequencing of psoriatic skin identifies pathogenic Tc17 cell subsets and reveals distinctions between Cd8(+) T cells in autoimmunity and cancer. *J Allergy Clin Immunol* (2021) 147(6):2370–80. doi: 10.1016/j.jaci.2020.11.028

50. FitzGerald O, Ogdie A, Chandran V, Coates LC, Kavanaugh A, Tillett W, et al. Psoriatic arthritis. *Nat Rev Dis Primers* (2021) 7(1):59. doi: 10.1038/s41572-021-00293-y

51. Costello PJ, Winchester RJ, Curran SA, Peterson KS, Kane DJ, Bresnihan B, et al. Psoriatic arthritis joint fluids are characterized by Cd8 and Cd4 T cell clonal expansions appear antigen driven. *J Immunol* (2001) 166(4):2878–86. doi: 10.4049/jimmunol.166.4.2878

52. Penkava F, Velasco-Herrera MDC, Young MD, Yager N, Nwosu LN, Pratt AG, et al. Single-cell sequencing reveals clonal expansions of pro-inflammatory synovial Cd8 T cells expressing tissue-homing receptors in psoriatic arthritis. *Nat Commun* (2020) 11(1):4767. doi: 10.1038/s41467-020-18513-6

53. Hughes TK, Wadsworth MH2nd, Gierahn TM, Do T, Weiss D, Andrade PR, et al. Second-strand synthesis-based massively parallel scrna-seq reveals cellular states and molecular features of human inflammatory skin pathologies. *Immunity* (2020) 53(4):878–94.e7. doi: 10.1016/j.immuni.2020.09.015

54. Kashem SW, Haniffa M, Kaplan DH. Antigen-presenting cells in the skin. *Annu Rev Immunol* (2017) 35:469–99. doi: 10.1146/annurev-immunol-051116-052215

55. Dutertre CA, Becht E, Irac SE, Khalilnezhad A, Narang V, Khalilnezhad S, et al. Single-cell analysis of human mononuclear phagocytes reveals subset-defining markers and identifies circulating inflammatory dendritic cells. *Immunity* (2019) 51(3):573–89.e8. doi: 10.1016/j.immuni.2019.08.008

56. Nakamizo S, Dutertre CA, Khalilnezhad A, Zhang XM, Lim S, Lum J, et al. Single-cell analysis of human skin identifies Cd14+ type 3 dendritic cells Co-producing Il1b and Il23a in psoriasis. *J Exp Med* (2021) 218(9):e20202345. doi: 10.1084/jem.20202345

57. Pantelyushin S, Haak S, Ingold B, Kulig P, Heppner FL, Navarini AA, et al. Rorγt+ innate lymphocytes and Γδ T cells initiate psoriasiform plaque formation in mice. *J Clin Invest* (2012) 122(6):2252–6. doi: 10.1172/jci61862

58. Teunissen MBM, Munneke JM, Bernink JH, Spuls PI, Res PCM, Te Velde A, et al. Composition of innate lymphoid cell subsets in the human skin: Enrichment of ncr(+) Ilc3 in lesional skin and blood of psoriasis patients. *J Invest Dermatol* (2014) 134(9):2351–60. doi: 10.1038/jid.2014.146

59. Villanova F, Flutter B, Tosi I, Grys K, Sreeneebus H, Perera GK, et al. Characterization of innate lymphoid cells in human skin and blood demonstrates increase of Nkp44+ Ilc3 in psoriasis. *J Invest Dermatol* (2014) 134(4):984–91. doi: 10.1038/jid.2013.477

60. Bielecki P, Riesenfeld SJ, Hütter JC, Torlai Triglia E, Kowalczyk MS, Ricardo-Gonzalez RR, et al. Skin-resident innate lymphoid cells converge on a pathogenic effector state. *Nature* (2021) 592(7852):128–32. doi: 10.1038/s41586-021-03188-w

61. Rupec RA, Boneberger S, Ruzicka T. What is really in control of skin immunity: Lymphocytes, dendritic cells, or keratinocytes? facts and controversies. *Clinics Dermatol* (2010) 28(1):62–6. doi: 10.1016/j.clindermatol.2009.04.004

62. Harirchian P, Lee J, Hilz S, Sedgewick AJ, Perez White BE, Kesling MJ, et al. A20 and Abin1 suppression of a keratinocyte inflammatory program with a shared single-cell expression signature in diverse human rashes. *J Invest Dermatol* (2019) 139(6):1264–73. doi: 10.1016/j.jid.2018.10.046

63. Kouwenhoven TA, Bronckers I, van de Kerkhof PCM, Kamsteeg M, Seyger MMB. Psoriasis dermatitis: An overlap condition of psoriasis and atopic dermatitis in children. *J Eur Acad Dermatol Venereol* (2019) 33(2):e74–e6. doi: 10.1111/jdv.15213

64. Bozek A, Zajac M, Krupka M. Atopic dermatitis and psoriasis as overlapping syndromes. *Mediators Inflammation* (2020) 2020:7527859. doi: 10.1155/2020/7527859

65. Napolitano M, Caiazzo G, Fabbrocini G, Balato A, Di Caprio R, Scala E, et al. Increased expression of interleukin-23a in lesional skin of patients with atopic dermatitis with psoriasiform reaction during dupilumab treatment. *Br J Dermatol* (2021) 184(2):341–3. doi: 10.1111/bjd.19459

66. Napolitano M, Gallo L, Patruno C, Fabbrocini G, Megna M. Eczematous reaction to ixekizumab successfully treated with dupilumab. *Dermatol Ther* (2020) 33(2):e13218. doi: 10.1111/dth.13218

67. Derrien T, Johnson R, Bussotti G, Tanzer A, Djebali S, Tilgner H, et al. The gencode V7 catalog of human long noncoding rnas: Analysis of their gene structure, evolution, and expression. *Genome Res* (2012) 22(9):1775–89. doi: 10.1101/gr.132159.111

68. Flynn RA, Chang HY. Long noncoding rnas in cell-fate programming and reprogramming. *Cell Stem Cell* (2014) 14(6):752–61. doi: 10.1016/j.stem.2014.05.014

69. Gil N, Ulitsky I. Regulation of gene expression by cis-acting long non-coding rnas. *Nat Rev Genet* (2020) 21(2):102–17. doi: 10.1038/s41576-019-0184-5

70. Isakova A, Neff N, Quake SR. Single-cell quantification of a broad rna spectrum reveals unique noncoding patterns associated with cell types and states. *Proc Natl Acad Sci U.S.A.* (2021) 118(51):e2113568118. doi: 10.1073/pnas.2113568118

71. Wang Y, Zhao Y, Bollas A, Wang Y, Au KF. Nanopore sequencing technology, bioinformatics and applications. *Nat Biotechnol* (2021) 39(11):1348–65. doi: 10.1038/s41587-021-01108-x

72. Chung KB, Oh J, Roh WS, Kim TG, Kim DY. Core gene signatures of atopic dermatitis using public rna-sequencing resources: Comparison of bulk approach with single-cell approach. *J Invest Dermatol* (2022) 142(3 Pt A):717–21.e5. doi: 10.1016/j.jid.2021.07.169

73. Kim D, Chung KB, Kim TG. Application of single-cell rna sequencing on human skin: Technical evolution and challenges. *J Dermatol Sci* (2020) 99(2):74–81. doi: 10.1016/j.jdermsci.2020.06.002

74. Bao S, Li K, Yan C, Zhang Z, Qu J, Zhou M. Deep learning-based advances and applications for single-cell rna-sequencing data analysis. *Brief Bioinform* (2022) 23(1):bbab473. doi: 10.1093/bib/bbab473

75. Shim J, Oh SJ, Yeo E, Park JH, Bae JH, Kim SH, et al. Integrated Analysis of Single-Cell and Spatial Transcriptomics in Keloids: Highlights on Fibrovascular Interactions in Keloid Pathogenesis. *J Invest Dermatol* (2022) 142(8):2128–2139.e11. doi: 10.1016/j.jid.2022.01.017.

frontiers | Frontiers in Immunology

TYPE Original Research
PUBLISHED 25 May 2023
DOI 10.3389/fimmu.2023.1094042

OPEN ACCESS

EDITED BY
Tina Sumpter,
University of Pittsburgh, United States

REVIEWED BY
Elham Majd,
University of Victoria, Canada
Cankun Wang,
The Ohio State University, United States

*CORRESPONDENCE
Shaomin Shi
dermatologist_shi@163.com
Delin Hu
hdl0522@163.com
Shengxiu Liu
liushengxiu@ahmu.edu.cn

†These authors have contributed equally to this work and share first authorship

RECEIVED 09 November 2022
ACCEPTED 15 May 2023
PUBLISHED 25 May 2023

CITATION
Liu Y, Zhang H, Mao Y, Shi Y, Wang X, Shi S, Hu D and Liu S (2023) Bulk and single-cell RNA-sequencing analyses along with abundant machine learning methods identify a novel monocyte signature in SKCM.
Front. Immunol. 14:1094042.
doi: 10.3389/fimmu.2023.1094042

Bulk and single-cell RNA-sequencing analyses along with abundant machine learning methods identify a novel monocyte signature in SKCM

Yuyao Liu[1†], Haoxue Zhang[2,3,4†], Yan Mao[5], Yangyang Shi[6], Xu Wang[7], Shaomin Shi[5*], Delin Hu[1*] and Shengxiu Liu[2,3,4*]

[1]Department of Burns, The First Affiliated Hospital of Anhui Medical University, Hefei, Anhui, China, [2]Department of Dermatovenerology, The First Affiliated Hospital of Anhui Medical University, Hefei, Anhui, China, [3]Key Laboratory of Dermatology, Ministry of Education, Hefei, Anhui, China, [4]Inflammation and Immune Mediated Diseases Laboratory of Anhui Province, Anhui Medical University, Hefei, Anhui, China, [5]Department of Dermatology, The Third Hospital of Hebei Medical University, Shijiazhuang, Hebei, China, [6]Department of Emergency Surgery, The First Affiliated Hospital of Anhui Medical University, Hefei, Anhui, China, [7]Department of General Surgery, The First Affiliated Hospital of Anhui Medical University, Hefei, Anhui, China

Background: Global patterns of immune cell communications in the immune microenvironment of skin cutaneous melanoma (SKCM) haven't been well understood. Here we recognized signaling roles of immune cell populations and main contributive signals. We explored how multiple immune cells and signal paths coordinate with each other and established a prognosis signature based on the key specific biomarkers with cellular communication.

Methods: The single-cell RNA sequencing (scRNA-seq) dataset was downloaded from the Gene Expression Omnibus (GEO) database, in which various immune cells were extracted and re-annotated according to cell markers defined in the original study to identify their specific signs. We computed immune-cell communication networks by calculating the linking number or summarizing the communication probability to visualize the cross-talk tendency in different immune cells. Combining abundant analyses of communication networks and identifications of communication modes, all networks were quantitatively characterized and compared. Based on the bulk RNA sequencing data, we trained specific markers of hub communication cells through integration programs of machine learning to develop new immune-related prognostic combinations.

Results: An eight-gene monocyte-related signature (MRS) has been built, confirmed as an independent risk factor for disease-specific survival (DSS). MRS has great predictive values in progression free survival (PFS) and possesses better accuracy than traditional clinical variables and molecular features. The low-risk group has better immune functions, infiltrated with more lymphocytes and M1 macrophages, with higher expressions of HLA, immune checkpoints, chemokines and costimulatory molecules. The pathway analysis based on seven databases confirms the biological uniqueness of the two

risk groups. Additionally, the regulon activity profiles of 18 transcription factors highlight possible differential regulatory patterns between the two risk groups, suggesting epigenetic event-driven transcriptional networks may be an important distinction. MRS has been identified as a powerful tool to benefit SKCM patients. Moreover, the IFITM3 gene has been identified as the key gene, validated to express highly at the protein level via the immunohistochemical assay in SKCM.

Conclusion: MRS is accurate and specific in evaluating SKCM patients' clinical outcomes. IFITM3 is a potential biomarker. Moreover, they are promising to improve the prognosis of SKCM patients.

KEYWORDS

skin cutaneous melanoma, single-cell, tumor immune microenvironment, monocyte, machine learning, IFITM3

Introduction

Skin cutaneous melanoma (SKCM) is the most aggressive type of all skin malignancies. Worldwide, an increase in the morbidity of SKCM has particularly raised alarm (1). For localized lesions, surgery is the most recommended treatment modality, perfectly able to assure wound healing, and is warranted in all stages of the disease (2, 3). Once the aggressive dissemination happens, other forms of therapies (chemotherapy, immunotherapy, targeted therapy and radiotherapy, or integrated combinations of them) must be provided simultaneously (4, 5). However, the overall prognosis of SKCM patients still stays poor (6) due to drug resistance, distant metastasis and high recurrence rate, etc. Therefore, more specific molecular biomarkers with prognostic and therapeutic significance are required.

In solid cancer, tumor microenvironment (TME) has been reckoned as an important structure. TME encompasses multiple cell types (stromal cells, fibroblasts, endothelial cells, innate and adaptive immune cells, etc.) and extracellular components (growth factors, cytokines, extracellular matrix, hormones, etc.) that surround cancerous cells (7). TME co-opts innate immune cells for tumor promotion (8). Abundant studies have given the importance of immune compositions in TME that can dynamically regulate cancer progression and influence therapeutic outcomes, which has made TME a promising therapeutic target (9–11). Tumor immune microenvironment (TIME) refers to the highly-heterogenous immune context in TME, and great attention has been drawn on understanding its potential role in tumorigenesis. Though ICI therapy has exhibited astonishing efficacy because of the high immunogenicity in SKCM (12), not all patients can be benefited. What's more, the available tumor staging system is inadequate for a qualified screening of patients who are suitable to accept ICI therapy. Thus, it is necessary to explore novel biomarkers and to understand their roles in the TIME of SKCM, which helps to uncover the potential biology background behind SKCM.

Single-cell RNA-sequencing (scRNA-seq) provides unprecedented opportunities to deconvolve immune system heterogeneity by uncovering novel distinct immune cell subsets, characterizing stochastic heterogeneity within a cell population and building developmental 'trajectories' for immune cells (13). This technique can overcome the limitations of traditional RNA-sequencing methods. Another classic population-based RNA-sequencing approach (bulk RNA-seq) is also important in deciphering genome-wide transcriptome variations (14, 15), and it may mask the transcriptional trends of distinct subpopulations with the most abundant cell types or states (16). The organic combination of scRNA-seq and bulk RNA-seq has been applied in studying onco-immunology (17). For example, Joanito I et al. (18) used it to identify two epithelial tumor cell states and refine the consensus molecular classification of colorectal cancer. Kang B et al. (19) revealed key features of the gastric tumor microenvironment through it. Gong L et al. (20) used it to reveal the stromal dynamics and tumor-specific characteristics in the microenvironment of nasopharyngeal carcinoma. Tumor heterogeneity and prognosis-related signatures have been explored with the integrative combination of the two approaches in uveal melanoma (21, 22). However, there is a lack of excavation of the TME in SKCM using scRNA-seq along with bulk RNA-seq. Besides, machine learning is an else indispensable tool, leveraging sophisticated algorithms in processing big, heterogeneous data automatically, professional at prediction problems by revealing useful patterns (23, 24). With the development of bioinformatics, machine learning has become a routine tool for assessing the risk and treatment needs of specific patients. At present, Lasso-Cox is the mainstream algorithm used for generating massive prognosis signatures (25, 26). However, limitations of relying on a single machine learning algorithm may hinder its ability to deliver optimal clinical care to patients, because of the uncertainty to ensure whether the data information of the current algorithm is sufficiently employed, let alone to compare whether the results have reached the population optimal solution. Such inadequate practices

can lead to potential overtreatment or undertreatment. Integrated approaches based on various algorithm combinations can fit a consensus model in predicting prognosis, which means the generated model could provide a more personalized evaluation methods to implement clinical decisions.

In the present study, we innovatively integrated aforementioned methods. A novel prognostic signature was described and validated to be a potential biomarker. Moreover, as scRNA-seq enables inference of cell-cell communication between tumor cells and their microenvironment (27), we also probed into the profiles of communication networks in SKCM and depicted the specific markers and the indispensable cell–monocyte. The results were confirmed to provide insights in deciphering TME and unveil biological mechanism in SKCM.

Materials and methods

Collection of SKCM sample data

The scRNA-seq dataset was obtained with accession number GSE115978 from the Gene Expression Omnibus (GEO) database. Immune cells in it were extracted according to cell markers defined in the original study and 2106 cells were included from 16 pre-immunotherapy patients (28). Raw mapped reads were normalized with counts per million (CPM) and analyzed with quality control using the "Seurat" R package from the normalized. The "FindVariableFeatures" function was performed on the scaled data to screen out the top 2000 genes with higher intercellular coefficient of variation for the downstream analysis (29, 30). The Bulk RNA-seq datasets (TCGA-SKCM, GSE65904 and GSE54467) were acquired from the TCGA and GEO databases respectively. The HTSeq-FPKM gene expression data and related clinical information of SKCM patients were downloaded from the TCGA database as the training group. We enrolled 446 samples whose follow-up time was greater than 0 days with full expression information. For further verification, we adopted the same inclusion criteria. The GSE65904 dataset included 210 SKCM patients, and the GSE54467 dataset included 71 SKCM patients. Via the "Combat" algorithm of the R package "sva", the possibility of batch effects caused by abiotic bias among the TCGA-SKCM, GSE65904 and GSE54467 datasets was correspondingly reduced (31). It should be noted that both TCGA and GEO databases are open to the public, free of charge. Therefore, this study strictly complies with the data extraction policy of the databases and does not require ethical review and approval from the ethics committee.

ScRNA sequencing and cell-cell interaction analysis

Principal components analysis (PCA) was conducted on the expression matrix of variable genes. The "FindClusters" function was used with a 0.8 resolution to identify clusters. Also, we performed the "RunTSNE" function to accomplish the dimensionality reduction and visualization processes of t-Distributed Stochastic Neighbor Embedding (t-SNE). The "singleR" package was applied and the cluster-specific markers (log2 |Fold Change| threshold of 1 and FDR threshold of 0.05) were recognized by "FindAllMarkers" function to automatically re-annotate all immune-cell clusters. Immune cells were annotated using the Monaco Immune Database in the Celldex package (1.3.0) (32). The "CellChat" R package (1.1.3) was utilized to infer the immune cell-immune cell communication in the tumor microenvironment (TME) of SKCM on the basis of receptor-ligand interactions (33). The linking numbers were calculated and the communication probability was collected to compute communication networks. The interacting times and total strength of interactions between two arbitrary cell groups were visually displayed. Scatter plots were drawn in order to visualize the dominant sender (signal source) and receiver cells (target) in 2D space, which could help identify the largest contributor signals to the efferent or afferent signals in immune cell sets. We adopted a pattern recognition approach, the global communication model, to discern the way how multiple immune cell types and signaling pathways work in coordination. The "select" function was applied to infer the quantity of patterns, which was comprehensively determined according to two indexes, Cophenetic and Silhouette based on the "non-negative matrix factorization (NMF)" R package (34).

Signature derived from machine learning-based integrative approaches

Considering the unquestioned importance of monocytes to cell communication, we exploited the monocyte-related signature (MRS). Warranting validations were conducted to make sure MRS has satisfying accuracy, stability and repeatability. We integrated up to 10 machine learning algorithms including random survival forest (RSF), elastic network (Enet), Lasso, Ridge, stepwise Cox, CoxBoost, partial least squares regression for Cox (plsRcox), supervised principal components (SuperPC), generalized boosted regression modeling (GBM), and survival support vector machine (survival-SVM). Upon these methods, a consensus model was produced. Altogether 101 algorithm combinations were performed to match prediction models based on the leave-one-out cross-validation (LOOCV) framework. The TCGA-SKCM dataset was set as a training dataset, the GSE65904 and GSE54467 datasets were set as external validation datasets. Further, the concordance index (C-index) in each pattern in all validation datasets was calculated (35). In total, eighty-seven genes with higher expression level in monocytes than in other immune cells based on scRNA were included in the analysis (log2| Fold Change| threshold of 2 and FDR threshold of 0.05). In line with included gene expression levels from different patterns, we used the linear combination function of each pattern to calculate risk scores. The combined pattern pair from the two external validation datasets with the highest average C-index value was ultimately considered as the most superior one.

Verifying the accuracy of the signature

After determining the best pattern pairs, we set the median value of the risk scores based on the training dataset as the cutoff to divide patients in both training and validation datasets into either high- or low-risk group. Kaplan-Meier (KM) survival analysis and log-rank test were used on the two groups via the "survival" and "survminer" R packages. Receiver operating characteristic (ROC) curves were depicted to evaluate the accuracy of this signature. What's more, we performed both the univariate and multivariate cox analysis to prove the independence of the signature. Time-dependent C-index was applied to compare the efficacy of this signature versus traditional clinical variables. In addition, decision curve analysis (DCA) was conducted to judge if the signature can benefit patients in clinical practice. The specific or preponderant cell type that the hub genes from MRS are expressed on were further verified in three independent single-cell datasets (GSE123139, GSE120575, GSE72056) using the "RunUMAP" function.

Immune microenvironment analysis

Seven different software were utilized to quantify the abundance of immune infiltration of SKCM patients, compare differences of the abundance between the high- and low-risk group, and calculate the Pearson correlations between analysis scores and immune cell contents (36–42). Furthermore, we employed the single sample gene set enrichment analysis (ssGSEA) enrichment scores to assess immune functions. Also, differences of the functions between the high- and low-risk group were then compared using the "wilcox" test (43). Additionally, Thorsson V et al. (44) rendered immunogenomics analyses of more than 10,000 cancers, identifying six immune subtypes that encompass multiple cancer types and are assumed to define immune response patterns influencing prognosis. Four types consist in the TCGA-SKCM, namely wound healing, IFN-gamma dominant, inflammatory and lymphocyte depleted. Subsequently, we focused on the distribution of each subtype in the high- and low-risk group.

Gene expression, pathway activity and transcriptional heterogeneity analyzes

On account of the training dataset, we compared expression differences of immune checkpoints, costimulatory molecules, chemokines and HLA related genes between the high- and low-risk group. The Molecular Signatures Database (MSigDB) is the most broadly used and comprehensive resource of >10,000 annotated gene sets for use with GSEA software, divided into Human and Mouse collections (45). Nine categories (H, C1-C9) are embodied in Human collections. We chose C2-C8 gene sets to conduct the gene set enrichment analysis (GSEA) for a thorough exposition in differential pathway activities between the high- and low-risk group. To expound on transcriptomics differences a bit further, we analyzed regulon activities of 18 kinds of transcription factors to speculate differential regulation modes in the high- and low-risk group (46).

Identifying hub genes in the signature

It's typically believed that if two gene products have similar functions, then terms annotated by them in the Gene Ontology (GO) tree would be close to each other and have high semantic similarity too. The "mgeneSim" function was used to gauge similarity by calculating geometric means of molecular functions and cellular components. Furthermore, we evaluated the importance of each gene by calculating its average similarity to other genes in the signature (47). In addition, we expounded hub gene expression in immune and nonimmune cells in ten SKCM single-cell datasets with the aid of tumor immune single-cell hub (TISCH) database (48, 49). On a final note, the Human Protein Atlas (HPA) database was used to verify whether the expression of hub genes in SKCM was different from that in normal skin at the protein level.

Statistical analysis

All data processing, statistical analysis, and plotting were performed in R 4.2.0 software. Correlations between two continuous variables were assessed by Pearson's correlation coefficients. Differential analysis was realized via the wilcox test. $P < 0.05$ was regarded as statistically significant.

Results

T cells and B cells are main cellular components in immune microenvironment of SKCM

We applied the scRNA-seq dataset (GSE115978) and selected 16 samples from untreated patients for further investigations. Strict quality control measures were taken to obtain 2106 immune cells from predetermined samples, which had 23686 different features. After that, we used the t-SNE algorithm on those 2186 cells to achieve dimension reduction and unsupervised clustering. To decide a desirable resolution parameter for cell clustering, we produced a cluster tree using various resolution values. It was noticed that along with the increase of the resolution, clusters weren't intertwined much. Therefore, we chose 0.8 as the best resolution because maximum fork clusters were observed (Figure 1A). From the t-SNE algorithm, 13 various cell clusters were revealed (Figure 1B). Using the "singleR" function, 7 kinds of immune cells were annotated, and the "plotScoreHeatmap" function showed the scores of all cells in all reference labels to check the confidence of the predictive labels throughout the dataset (Figure 1C). Among all immune cells, 5 types were annotated as main labels of the cluster. That is, the 0, 6, 8, 11 cell clusters were annotated as CD8+T cells, the 1, 4, 9 cell clusters were annotated as

10.3389/fimmu.2023.1094042

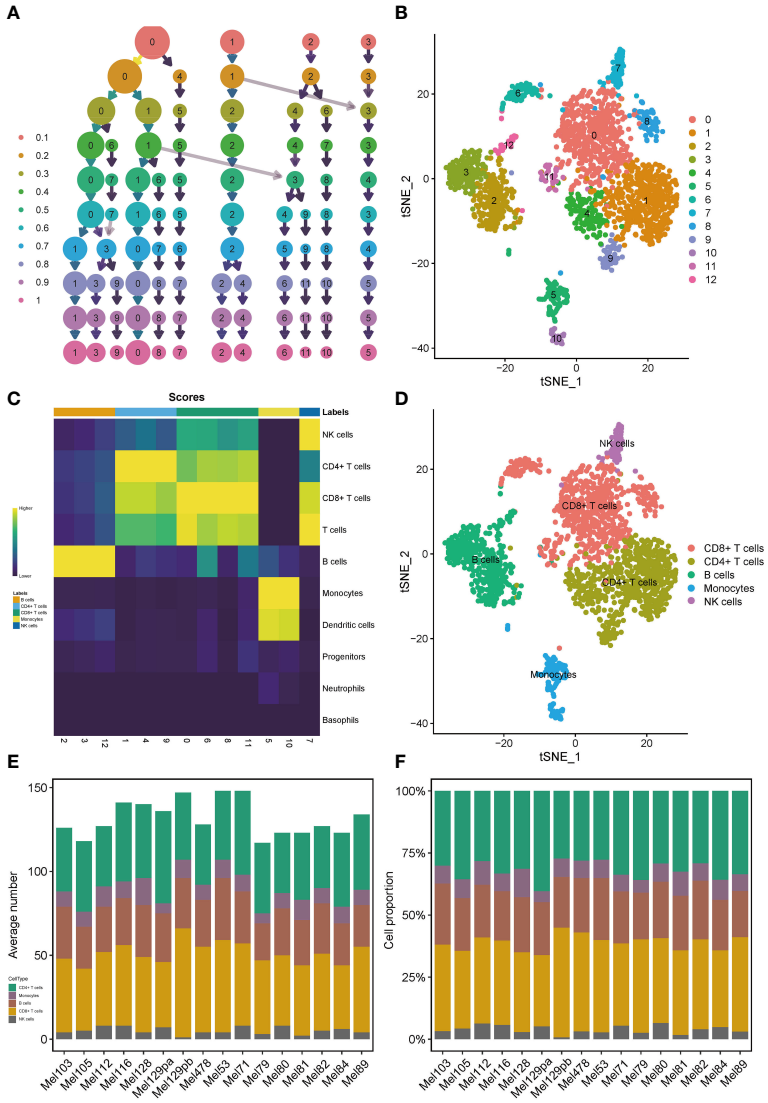

FIGURE 1
Profiles of immune cells in the TIME of SKCM on the scRNA transcriptome level. Clustering tree for the immune cells clustered using various resolution parameters and the best resolution was 0.8 **(A)**. The t-SNE algorithm helped visualize 13 various cell clusters **(B)**. 7 kinds of immune cells were annotated in the plotScoreHeatmap **(C)**. 5 types of immune cells were annotated as the main labels of the cluster **(D)**. T and B cells were the major compositions of the TIME in SKCM **(E, F)**.

CD4+T cells, the 2, 3 cell clusters were annotated as B cells, the 5, 10 cell clusters were annotated as monocytes and dendritic cells and the 7-cell cluster was annotated as NK cells (Figure 1D). It is interesting to note that, the number and proportion of the five main types of immune cells showed a high degree of similarity among 16 samples, suggesting that T and B cells were the major compositions of the SKCM immune microenvironment (Figures 1E, F).

Monocytes are major contributors to both incoming and outgoing signals in immune communication networks

We observed over-expressed ligands or receptors and their interactions in seven immune cell groups to identify interactions between immune cells (Figure 2A). Circle diagrams showed the interaction times and general strengths of interactions (proportion) between any two cell groups to visualize the integrated cell communication networks. Compared to other immune cells, monocytes were found to contribute the most to both incoming and outgoing signals in immune communication networks (Figures 2B–D). Different immune cell groups had obviously different contributive signals on the incoming and outgoing signals (Figure 2E). Then the cophenetic and silhouette indexes were combined to recognize 6 efferent and 5 afferent patterns (Figures 3A, D). Also, the incoming and outgoing signals were cell-specific. Notably, incoming signals of T cells, CD8+ T cells and NK cells bore similarity (Figures 3B, E). At last, Figures 3C, F displayed how much diverse signals in efferent and afferent patterns contributed to various cell groups.

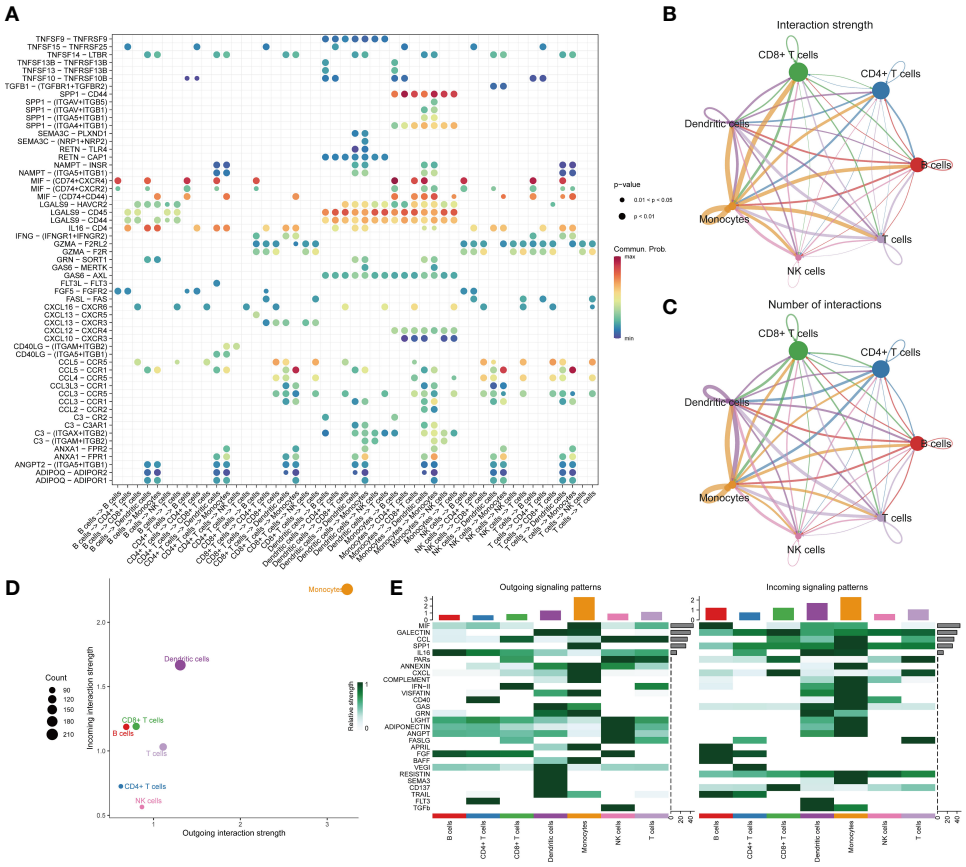

FIGURE 2
The landscape of immune cell-cell communication. The bubble chart shows overexpressed ligand–receptor interactions. Bubble size represents P value generated by the permutation test, and the color represents the possibility of interactions **(A)**. The circle diagrams show the interaction strength **(B)** and number **(C)** between immune cells. The dot plot shows dominant senders and receivers. The X and Y axes are the total outgoing or incoming communication probabilities associated with each cell group, respectively. The size of the dots is positively related to the number of inferred links (both outgoing and incoming) associated with each cell block. The colors of the dots represent different cell groups **(D)**. The heatmap shows the efferent or afferent contributions of contributions of all signals to different groups of immune cells **(E)**.

MRS exhibits robust and stable DSS predictive performances

In view of the dominant position of monocytes in cell communication, 87 biomarkers in the TCGA-SKCM that are specifically highly expressed in monocytes compared with other immune cells were fitted to 101 prediction models by the LOOCV framework. The C-index of each model was calculated in all validation datasets. An interesting fact was noticed that the best model combination was CoxBoost and stepCox (both) with the highest average C-index (0.638) (Figure 4A). Ultimately, an 8-gene monocyte-related signature (MRS) was accordingly established. In the training dataset TCGA-SKCM, we found that the low-risk group owned a relatively longer progression-free survival (PFS) (Figure 4B). The high-risk group had a significantly lower disease-specific survival (DSS) in the training dataset (Figure 4C), external validation datasets GSE65904 (Figure 4D) and GSE54467 (Figure 4E). Besides, the area under curve (AUC) values of the 1-, 3- and 5- year PFS (Figure 4F) and DSS (Figures 4G–I) identified by the MRS proved that MRS was a potent prediction tool with stability and strength. MRS had satisfactory specificity and sensitivity. Samples in GSE54467 with DSS within 1 year were too few, hence we chose to evaluate the AUC value of the 2-year DSS. Univariate Cox regression analysis showed that MRS, age, stage, T staging and N staging had close relation to DSS (Figure 4J). And the multivariate Cox regression analysis showed that MRS could be treated as an independent prognostic factor for SKCM patients (P< 0.001) (Figure 4K). This time-dependent C-index indicated that MRS outperformed conventional clinical variables (Figure 4L). Speaking of DCA, it explained that MRS could exactly benefit patients in contrast with conventional clinical variables (Figure 4M). All these indicators declared that MRS was stable and robust in the training queue. The classification of different risk groups could be repeated and verified in two independent validation datasets which manifested that MRS was hardly a spurious finding due to technique artifacts, chances or deviations of the sample eligibility criteria in TCGA. Moreover, the cell type that eight MRS-genes were expressed most intensively on was confirmed as monocyte in three single-cell external datasets (GSE123139 (Figure 5A), GSE120575 (Figure 5B),

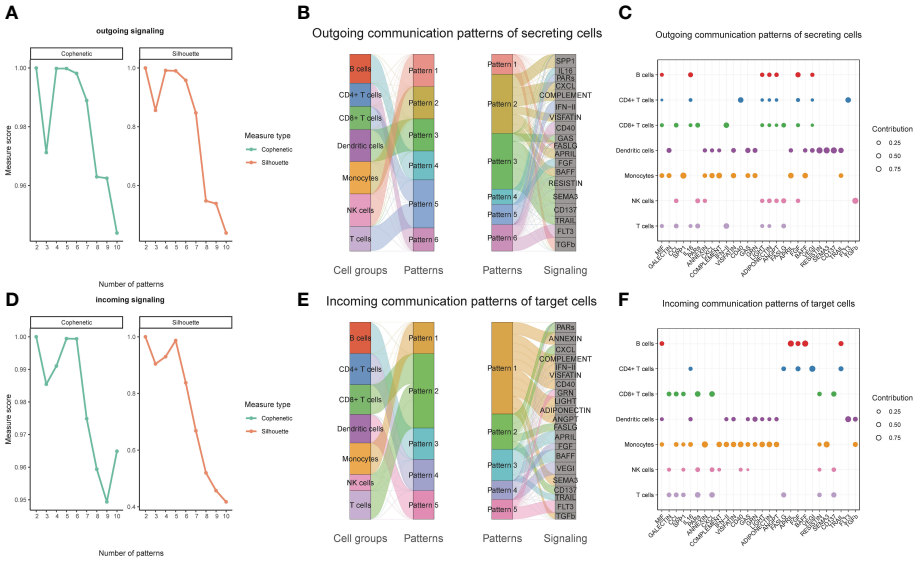

FIGURE 3
Identifying patterns of outgoing and incoming signals. Numbers of outgoing **(A)** and incoming **(D)** signals based on the Cophenetic and Silhouette indexes. The sankey diagram shows the relations between cell groups and outgoing communication patterns, outgoing communication patterns and signals **(B)**. And relations between cell groups and incoming communication patterns, incoming communication patterns and signals **(E)**. The dot plot shows the contributions of different signals to cell groups in the outgoing communication patterns **(C)**, and incoming communication patterns **(F)**.

GSE72056 (Figure 5C), which further proved that MRS was stable and repeatable.

Transcriptome-defined subclasses are biologically distinct and immune infiltration is statistically associated with a more favorable prognosis

Seven immune infiltration algorithms exerted consistence in which the high-risk group was always infiltrated with less immune cells (Figure 6A). Risk scores were significantly positively related to the cell contents of lymphocytes and M1 macrophages (Figure 6B). Among immune subtypes of SKCM, we observed that in the low-risk group, there were significantly more patients with IFN-gamma Dominant subtype, but less patients with Lymphocyte Depleted subtype (Figure 6C). Besides, ssGSEA results consistently showed that the low-risk group had better immune functions (Figure 6D). Immune filtration statistically correlated with better prognosis. The pathway analyzes on the seven datasets vigorously confirmed biological uniqueness of the high- and low-risk group. In the low-risk group, lymphocyte activation, antigen presentation and other related pathways were activated. While in the high-risk group, melanogenesis, keratinization and other related pathways were significantly enriched (Figure 7A). HLA, immune checkpoints, chemokines and costimulatory molecules were highly expressed in the low-risk group (Figure 7B). Moreover, the cell-regulon activity profiles encompassing 18 types of transcription factors highlighted the possible differential accommodative patterns between the high- and low-risk group (Figure 7C).

IFITM3 has been identified as the core gene in MRS with its high expression in SKCM

Using the "mgeneSim" function, we uncovered the key gene IFITM3 in MRS (Figure 8A). We employed the TISCH database to locate the expression situations of IFITM3 in immune and nonimmune cells in all ten SKCM single-cell datasets. It was found that IFITM3 not only was highly expressed in mononuclear macrophages, but also in those nonimmune and melanoma cells in the microenvironment (Figure 8B). Learning from the immunohistochemical data in the HPA database, we discovered that the expression of IFITM3 in SKCM at protein level was also higher than that in normal skin (Figures 8C, D). To sum up, all these results provided corroborative evidence for the exploration value of IFITM3 in the future study of SKCM.

Discussion

Due to the high rate of metastasis, invasiveness, and annually increasing morbidity, skin cutaneous melanoma (SKCM) is regarded as one of the most lethal skin malignancies globally (50). Conventional histopathology is the mainstay of the diagnosis of SKCM (51), immunohistochemistry and molecular testing have also been introduced to assist with diagnosis (52). Generally speaking, the present staging system for SKCM refers to the 8th edition of TNM classification issued by the American Joint Committee on Cancer (AJCC) in 2017 (53). After the diagnosis confirmed, timely and appropriate staging is of utmost significance, with which an accurate prognostic prediction along with an

10.3389/fimmu.2023.1094042

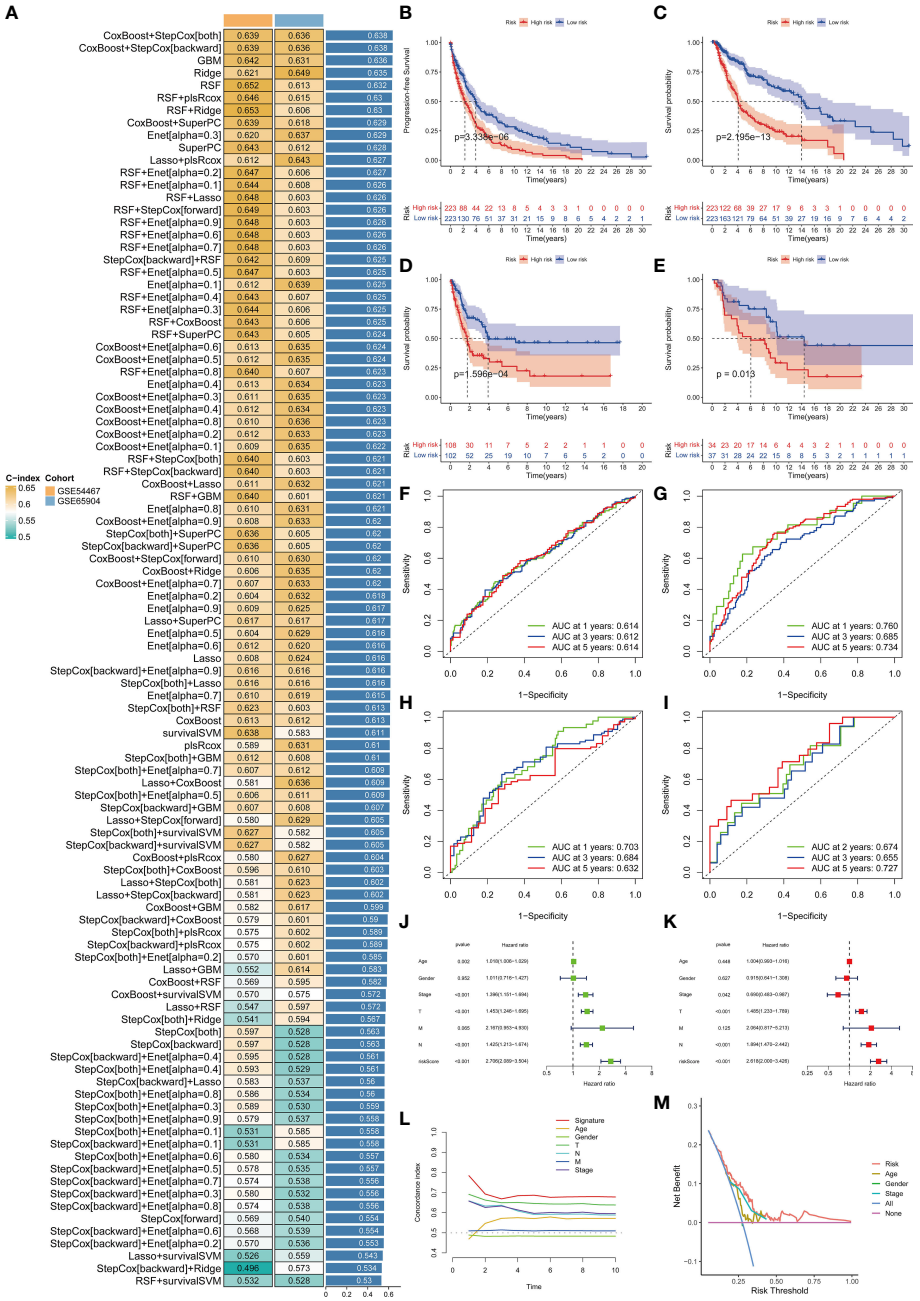

FIGURE 4
Establishment and validations of a consensus MRS via the machine learning-based integrative procedure. A total of 101 types of prediction models using the LOOCV framework and further calculated the C-index of each model in all validation datasets **(A)**. KM curves of PFS **(B)** and DSS **(C)** between the two risk groups in the training dataset TCGA-SKCM. KM curves of DSS in GSE65904 **(D)** and GSE54467 **(E)** datasets. ROC curves show the 1-, 3- and 5- year PFS in the TCGA-SKCM **(F)** and DSS in the TCGA-SKCM, GSE65904 and GSE54467 datasets **(G–I)**. Univariate **(J)** and multivariate Cox regression analysis **(K)** illustrated that the MRS could be used as an independent prognostic factor for SKCM patients (P< 0.001). Time dependent C-index curves **(L)**, DCA curves **(M)** show the MRS has the good potency in predicting prognosis of SKCM patients.

individualized treatment protocol shall be then provided (54). However, this traditional staging method uses a limited range of parameters equally for all patients, irrespective of clinical context (55) and person-specific heterogeneity. Therefore, sometimes there are limitations on proper treatments and the prognosis may be estimated imprecisely. The emergence of immune checkpoint inhibitors (ICIs) therapy, has made milestone advances in the treatment of SKCM in the last decade, benefiting thousands of SKCM patients and their survival has been prolonged (56, 57). However, only a subset of patients can benefit from ICI therapy. Further still, immune-related toxicities can be a more dangerous dilemma where up to 55% of the patients in the ipilimumab and nivolumab combination trail experienced grade 3 or 4 toxicities (58). As a result, development of a robust biomarker or gene signature to predict response and/or resistance and clinical outcomes is in dire need in SKCM patient management.

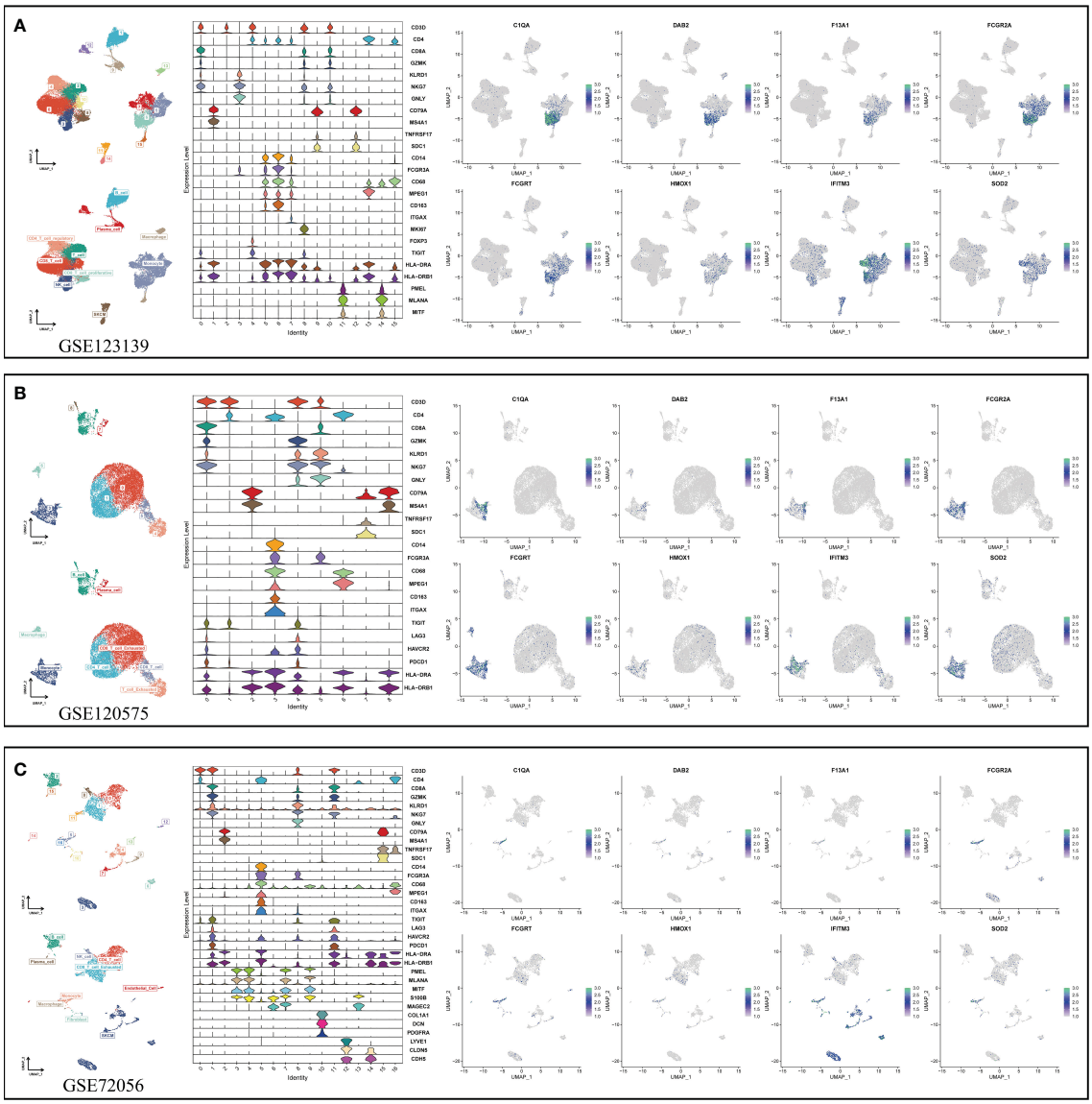

FIGURE 5
Using three single-cell datasets GSE123139 **(A)**, GSE120575 **(B)**, and GSE72056 **(C)** to verify eight MRS-gene expression location in different cell types. UMAP respectively displays dimension reduction clustering of the dataset. The violin map displays characteristic genes and cell annotation.

In this research, sophisticated, integrated multi-parameter analysis was conducted. We used PCA and t-SNE to cluster massive immune cells, utilizing the "singleR" to annotate them and eventually specific markers of each type of immune cell were identified. Significant specificity existed in the afferent and efferent signals of every immune cell. Monocytes, however, was discovered as a dominant contributor to immune cell-cell communications. Based on the LOOCV framework, we further screened out monocyte-specific markers, on which 101 combination patterns derived from 10 machine learning methods were fitted to ultimately establish a consensus monocyte-related signature (MRS). MRS was subsequently validated in two independent datasets, and the result showed that the best combination pattern consisted of CoxBoost and stepCox (both). MRS was then proved to have negative impact on DSS and PFS, namely the high-risk group identified by the MRS possessed relatively lower DSS and PFS. Our MRS had an excellent and stable performances in clinical use. It was an independent, superior index compared to other traditional clinical variables, and could be served as a good complement to them and their limitations shall be offset in a certain degree. The time-dependent C-index and DCA showed that MRS was a prominent prognosis prediction tool in contrast with those clinical variables, and can benefit patients in an actual way. What's more, its repeatability was also verified on two external independent queues.

Patients in the high- and low-risk group showed significant biological distinctness too. Hot and cold tumors, are an informal notion to reflect tumor immunogenicity, and the former is highly infiltrated (59). The very reverse, cold tumors is characterized by the lack or low presence of lymphocytes in the TME, resulting in non-responsiveness to ICI therapy (60). Therefore, recent studies have concentrated on the possibility and actuality to turn cold to hot tumors which shows the dynamic changes in the TIME (61), in

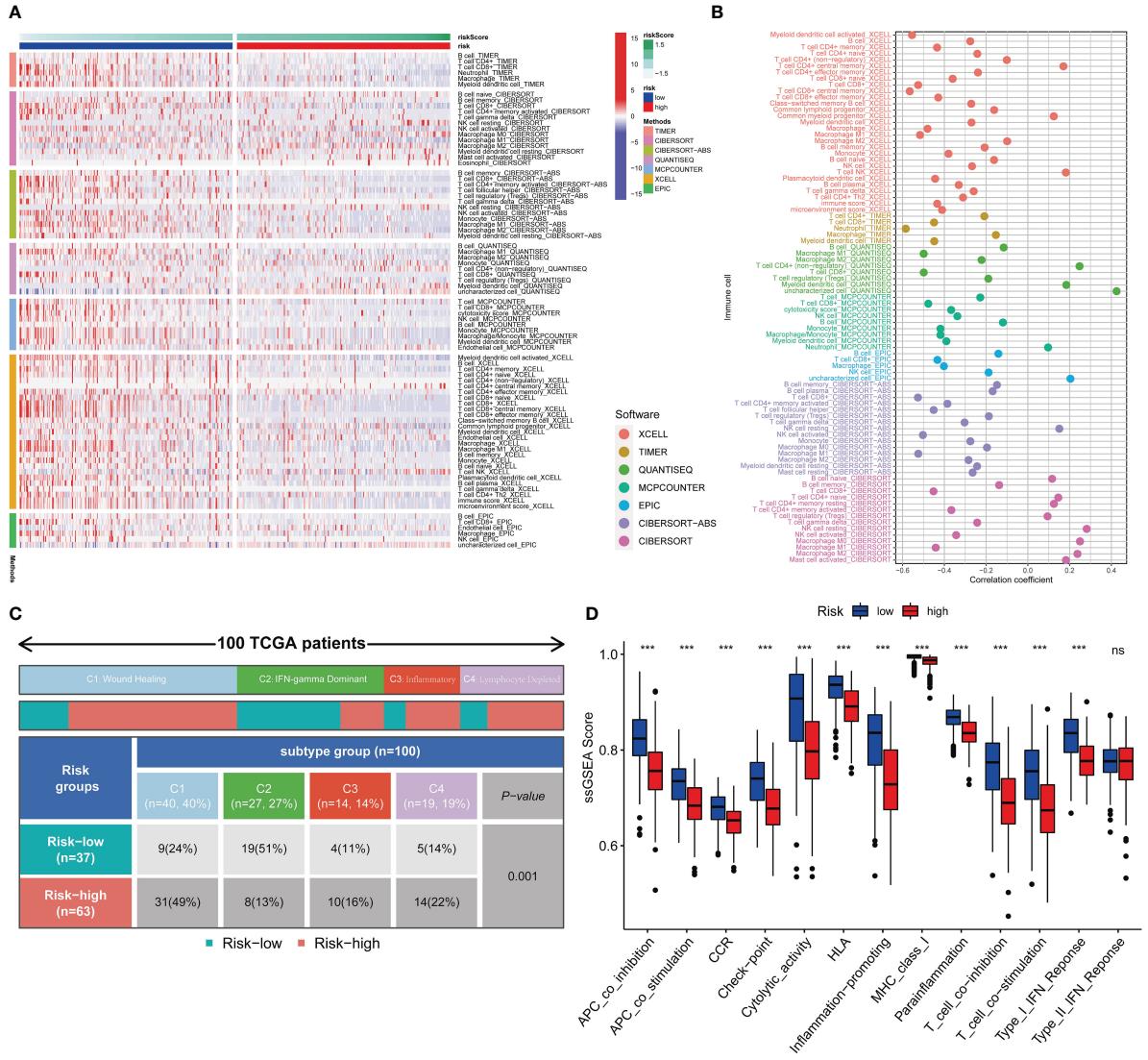

FIGURE 6
Immune infiltration profiles. Seven immune infiltration software exhibit different numbers of immune cells between the high- and low-risk group **(A)**. The bubble plot shows the correlation between different immune cells and risk scores **(B)**. The block diagram shows the proportion of the high- and low-risk samples in four TCGA-SKCM representative immune subtypes **(C)**. Comparisons of ssGSEA scores between the high- and low-risk group **(D)**. *** means P<0.001.

order to enhance the efficacy of ICI therapy. Notably, the low-risk samples demonstrated phenotypes of hot tumors, infiltrated with abundant lymphocytes and M1 macrophages, significantly enriched with immune-related pathways, and expressed highly of immune-related molecules. This consistently supported that the patients in the low-risk group may be more prone to respond to ICI therapy.

The MRS was composed of 8 genes (C1QA, DAB2, F13A1, FCGR2A, FCGRT, HMOX1, IFITM3, SOD2). Among the 8 hub genes, some have been demonstrated as prognostic biomarkers of cancers already. For example, FCGR2A has been experimentally validated as a positive factor for OS in SKCM (62). Heme Oxygenase 1 (HMOX1) is also regarded as a tumorigenesis-related regulator and is being explored also as a therapeutic target (63). After a comprehensive assessment of the relative importance of each gene, interferon induced transmembrane protein (IFITM3) was recognized as the one with a strong academic exploring value. IFITM3 belongs to the family of interferon induced antiviral proteins. IFITM3 is a well-studied gene in multiple diseases, and has close relation to cancers because it overexpresses in various types. Min J et al. once testified IFITM3's promotion influences on hepatocellular carcinoma (HCC) invasion and metastasis by regulating MMP9 through p38/MAPK signaling (64). Also in HCC, IFITM3 was demonstrated to facilitate proliferation by upregulating c-myc expression via the ERK1/2 signal pathway (65). Moreover, an investigation led by Chu PY et al. has revealed that the IFITM3 can expand malignant progression, promote cancer stemness and chemoresistance of gastric cancer by targeting MET/AKT/FOXO3/c-MYC axis (66). In addition, high expression of IFITM3 represents adverse prognosis in acute myeloid leukemia (67), and it can cause B-cell malignancies by

10.3389/fimmu.2023.1094042

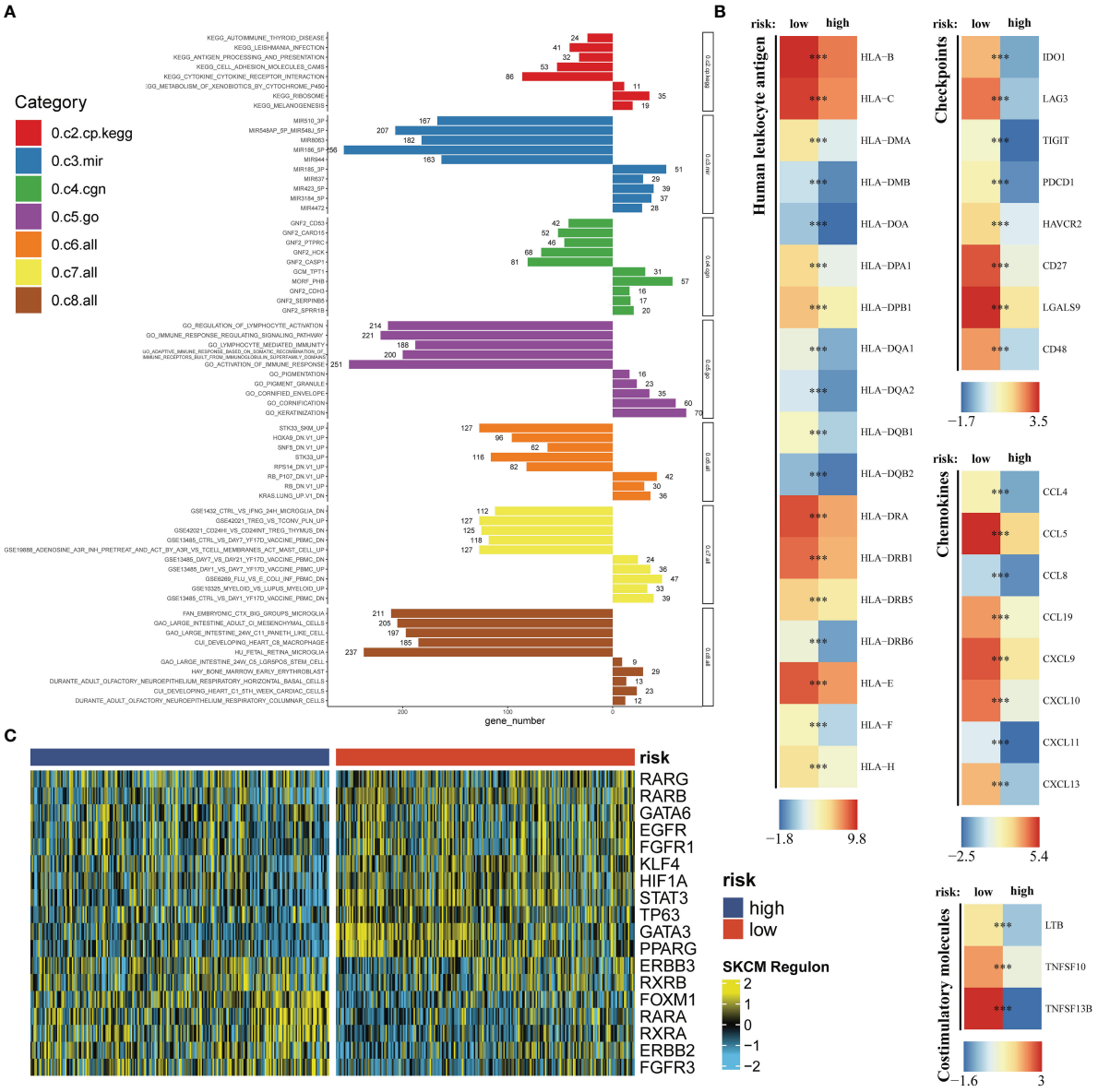

FIGURE 7
Exploration of the potential risk mechanism. The bar charts show GSEA results in seven gene sets **(A)**. Differential expressions of HLA, immune checkpoints, chemokines and costimulatory molecules between the high- and low-risk group **(B)**. The heatmap shows the cell-regulon activity profiles between the high- and low-risk group **(C)**. *** means P<0.001.

motivating PI3K pathway (68). Considering that IFITM3 participates in diverse signaling pathways that are likely to cause for oncogenesis and tumor development, it is deemed as a new therapeutic biomarker. Nevertheless, the potential role of IFITM3 in SKCM has not been fully understood yet. In the single-cell research, it is common to respectively study immune cells, nonimmune cells, and tumor cells, to avoid the situation where important information of life beings are mutually obscured by different types of cells. Our research aimed at the immune cell, hence we further evaluated the expression of IFITM3 in nonimmune and tumor cells based on the 10 single-cell datasets in the TISCH database. And the results showed that IFITM3 was highly expressed in the fibroblasts, myofibroblasts, endothelial cells and tumor cells. Via the HPA database, again IFITM3 was proved to express highly in SKCM at the protein level than in normal skins. The synthesis findings helped verify that IFITM3 is of great exploring values and more studies of it as a novel biomarker are needed.

The MRS can be duplicated via some basic PCR-based detection methods, making MRS an attractive tool for clinical transformation and implementation. But it is important to admit that our research has certain limitations as well. To begin with, this study was retrospective. The data and corresponding clinical information were obtained from public accessible TCGA and GEO databases, pretty limited sample size, absence of partial treatment and recurrence records and other artificial errors may potentially distort the findings. Secondly, since the role of IFITM3 in SKCM was not clear, more real-world studies enrolling more tumor

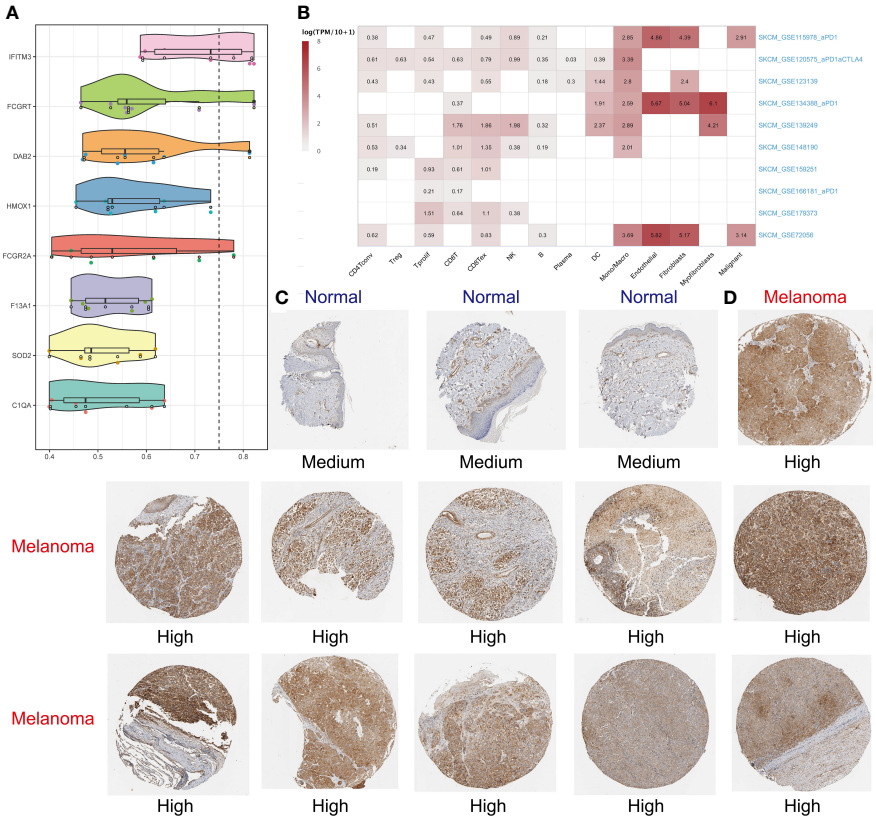

FIGURE 8
Identifying IFITM3 as the most important gene. The "mgeneSim" function revealing the key gene IFITM3 in the MRS **(A)**. Based on the TISCH database to locate the expression situations of IFITM3 in immune and nonimmune cells in all ten SKCM single-cell datasets **(B)**. The immunohistochemical staining shows IFITM3 expression at protein level in normal and melanoma tissues **(C, D)**.

specimens and more experiments *in vitro* or *in vivo* should be performed in the future to reveal its actual function. Finally, the current algorithm was based on transcriptome analysis. In the future, the exploration from a global perspective is needed on the law of organism's life activity. It's believed that multi-omics integration analysis can promote the deep understanding of life processes and physiological mechanisms, and improve the stability and accuracy of the algorithm to make it gradually perfect, because it provides more features for learning. Additionally, deep learning, as a special kind of machine learning, will automatically find the features that are important for classification, while in machine learning we have to provide these features manually. Therefore, developing new deep learning algorithms and combining multi-omics data can be a powerful and promising tool to help us improve clinical outcomes for individual SKCM patients.

Conclusions

Our study is the first to establish an 8-gene monocyte-related signature based on abundant machine learning methods. Through adequate validations, the signature has been proved to have stability and strength as a promising predictive biomarker and therapeutic target for SKCM patients. Also, the IFITM3 gene is identified from the signature, and its potential exploring values have been preliminarily confirmed, which may give new inspirations in future clinical use.

Data availability statement

The original contributions presented in the study are included in the article/Supplementary Material. Further inquiries can be directed to the corresponding authors.

Author contributions

YL and HZ designed the research plan, performed bioinformatics analysis, wrote the manuscript. YM, YS and XW finalized the manuscript. SL, DH and SS supervised the research progress and revised the manuscript. All authors contributed to the article and approved the submitted version.

Acknowledgments

The authors thank the reviewers for their valuable remarks.

Conflict of interest

The authors declare that the research was conducted in the absence of any commercial or financial relationships that could be construed as a potential conflict of interest.

Publisher's note

All claims expressed in this article are solely those of the authors and do not necessarily represent those of their affiliated organizations, or those of the publisher, the editors and the reviewers. Any product that may be evaluated in this article, or claim that may be made by its manufacturer, is not guaranteed or endorsed by the publisher.

Supplementary material

The Supplementary Material for this article can be found online at: https://www.frontiersin.org/articles/10.3389/fimmu.2023.1094042/full#supplementary-material

References

1. DE Gruijl FR, Armstrong BK. Cutaneous melanoma: sheep in wolves clothing? *Anticancer Res* (2022) 42(10):5021–5. doi: 10.21873/anticanres.16010

2. Orzan OA, Şandru A, Jecan CR. Controversies in the diagnosis and treatment of early cutaneous melanoma. *J Med Life* (2015) 8(2):132–41.

3. Zuluaga-Sepúlveda MA, Arellano-Mendoza I, Ocampo-Candiani J. Actualización en el tratamiento quirúrgico del melanoma cutáneo primario y metastásico [Update on surgical treatment of primary and metastatic cutaneous melanoma]. *Cir Cir* (2016) 84 (1):77–84. doi: 10.1016/j.circir.2015.06.020

4. Garbe C, Amaral T, Peris K, Hauschild A, Arenberger P, Bastholt L, et al. European Consensus-based interdisciplinary guideline for melanoma. part 2: treatment - update 2019. *Eur J Cancer* (2020) 126:159–77. doi: 10.1016/j.ejca.2019.11.015

5. Leonardi GC, Falzone L, Salemi R, Zanghì A, Spandidos DA, Mccubrey JA, et al. Cutaneous melanoma: from pathogenesis to therapy (Review). *Int J Oncol* (2018) 52 (4):1071–80. doi: 10.3892/ijo.2018.4287

6. Longvert C, Saiag P. Actualités dans le mélanome cutané [Melanoma update]. *Rev Med Interne* (2019) 40(3):178–83. doi: 10.1016/j.revmed.2018.11.005

7. Anderson NM, Simon MC. The tumor microenvironment. *Curr Biol* (2020) 30 (16):R921–5. doi: 10.1016/j.cub.2020.06.081

8. Hinshaw DC, Shevde LA. The tumor microenvironment innately modulates cancer progression. *Cancer Res* (2019) 79(18):4557–66. doi: 10.1158/0008-5472.CAN-18-3962

9. Xiao Y, Yu D. Tumor microenvironment as a therapeutic target in cancer. *Pharmacol Ther* (2021) 221:107753. doi: 10.1016/j.pharmthera.2020.107753

10. Bejarano L, Jordão MJC, Joyce JA. Therapeutic targeting of the tumor microenvironment. *Cancer Discov* (2021) 11(4):933–59. doi: 10.1158/2159-8290.CD-20-1808

11. Wu T, Dai Y. Tumor microenvironment and therapeutic response. *Cancer Lett* (2017) 387:61–8. doi: 10.1016/j.canlet.2016.01.043

12. Ralli M, Botticelli A, Visconti IC, Angeletti D, Fiore M, Marchetti P, et al. Immunotherapy in the treatment of metastatic melanoma: current knowledge and future directions. *J Immunol Res* (2020) 2020:9235638. doi: 10.1155/2020/9235638

13. Papalexi E, Satija R. Single-cell RNA sequencing to explore immune cell heterogeneity. *Nat Rev Immunol* (2018) 18(1):35–45. doi: 10.1038/nri.2017.76

14. Chen G, Ning B, Shi T. Single-cell RNA-seq technologies and related computational data analysis. *Front Genet* (2019) 10:317. doi: 10.3389/fgene.2019.00317

15. Ziegenhain C, Vieth B, Parekh S, Reinius B, Guillaumet-Adkins A, Smets M, et al. Comparative analysis of single-cell RNA sequencing methods. *Mol Cell* (2017) 65 (4):631–643.e4. doi: 10.1016/j.molcel.2017.01.023

16. Slovin S, Carissimo A, Panariello F, Grimaldi A, Bouché V, Gambardella G, et al. Single-cell RNA sequencing analysis: a step-by-Step overview. *Methods Mol Biol* (2021) 2284:343–65. doi: 10.1007/978-1-0716-1307-8_19

17. Kuksin M, Morel D, Aglave M, Danlos FX, Marabelle A, Zinovyev A, et al. Applications of single-cell and bulk RNA sequencing in onco-immunology. *Eur J Cancer* (2021) 149:193–210. doi: 10.1016/j.ejca.2021.03.005

18. Joanito I, Wirapati P, Zhao N, Nawaz Z, Yeo G, Lee F, et al. Single-cell and bulk transcriptome sequencing identifies two epithelial tumor cell states and refines the consensus molecular classification of colorectal cancer. *Nat Genet* (2022) 54(7):963–75. doi: 10.1038/s41588-022-01100-4

19. Kang B, Camps J, Fan B, Jiang H, Ibrahim MM, Hu X, et al. Parallel single-cell and bulk transcriptome analyses reveal key features of the gastric tumor microenvironment. *Genome Biol* (2022) 23(1):265. doi: 10.1186/s13059-022-02828-2

20. Gong L, Kwong DL, Dai W, Wu P, Li S, Yan Q, et al. Comprehensive single-cell sequencing reveals the stromal dynamics and tumor-specific characteristics in the microenvironment of nasopharyngeal carcinoma. *Nat Commun* (2021) 12(1):1540. doi: 10.1038/s41467-021-21795-z

21. Gao G, Deng A, Liang S, Liu S, Fu X, Zhao X, et al. Integration of bulk RNA sequencing and single-cell RNA sequencing to reveal uveal melanoma tumor heterogeneity and cells related to survival. *Front Immunol* (2022) 13:898925. doi: 10.3389/fimmu.2022.898925

22. Zhang X, Qiu J, Huang F, Han P, Shan K, Zhang C. Construction and verification of a hypoxia-related nine-gene prognostic model in uveal melanoma based on integrated single-cell and bulk RNA sequencing analyses. *Exp Eye Res* (2022) 223:109214. doi: 10.1016/j.exer.2022.109214

23. Cho YR, Kang M. Interpretable machine learning in bioinformatics. *Methods* (2020) 179:1–2. doi: 10.1016/j.ymeth.2020.05.024

24. Goecks J, Jalili V, Heiser LM, Gray JW. How machine learning will transform biomedicine. *Cell* (2020) 181(1):92–101. doi: 10.1016/j.cell.2020.03.022

25. Zhang G, Sun J, Zhang X. A novel cuproptosis-related LncRNA signature to predict prognosis in hepatocellular carcinoma. *Sci Rep* (2022) 12(1):11325. doi: 10.1038/s41598-022-15251-1

26. Feng ZH, Liang YP, Cen JJ, Yao HH, Lin HS, Li JY, et al. m6A-immune-related lncRNA prognostic signature for predicting immune landscape and prognosis of bladder cancer. *J Transl Med* (2022) 20(1):492. doi: 10.1186/s12967-022-03711-1

27. Bridges K, Miller-Jensen K. Mapping and validation of scRNA-Seq-Derived cell-cell communication networks in the tumor microenvironment. *Front Immunol* (2022) 13:885267. doi: 10.3389/fimmu.2022.885267

28. Jerby-Arnon L, Shah P, Cuoco MS, Rodman C, Su MJ, Melms JC, et al. A cancer cell program promotes T cell exclusion and resistance to checkpoint blockade. *Cell* (2018) 175(4):984–997.e24. doi: 10.1016/j.cell.2018.09.006

29. Satija R, Farrell JA, Gennert D, Schier AF, Regev A. Spatial reconstruction of single-cell gene expression data. *Nat Biotechnol* (2015) 33(5):495–502. doi: 10.1038/nbt.3192

30. Hao Y, Hao S, Andersen-Nissen E, Mauck WM 3rd, Zheng S, Butler A, et al. Integrated analysis of multimodal single-cell data. *Cell* (2021) 184(13):3573–3587.e29. doi: 10.1016/j.cell.2021.04.048

31. Johnson WE, Li C, Rabinovic A. Adjusting batch effects in microarray expression data using empirical bayes methods. *Biostatistics* (2007) 8(1):118–27. doi: 10.1093/biostatistics/kxj037

32. Aran D, Looney AP, Liu L, Wu E, Fong V, Hsu A, et al. Reference-based analysis of lung single-cell sequencing reveals a transitional profibrotic macrophage. *Nat Immunol* (2019) 20(2):163–72. doi: 10.1038/s41590-018-0276-y

33. Jin S, Guerrero-Juarez CF, Zhang L, Chang I, Ramos R, Kuan CH, et al. Inference and analysis of cell-cell communication using CellChat. *Nat Commun* (2021) 12(1):1088. doi: 10.1038/s41467-021-21246-9

34. Gaujoux R, Seoighe C. A flexible r package for nonnegative matrix factorization. *BMC Bioinf* (2010) 11:367. doi: 10.1186/1471-2105-11-367

35. Liu Z, Liu L, Weng S, Guo C, Dang Q, Xu H, et al. Machine learning-based integration develops an immune-derived lncRNA signature for improving outcomes in colorectal cancer. *Nat Commun* (2022) 13(1):816. doi: 10.1038/s41467-022-28421-6

36. Becht E, Giraldo NA, Lacroix L, Buttard B, Elarouci N, Petitprez F, et al. Estimating the population abundance of tissue-infiltrating immune and stromal cell populations using gene expression [published correction appears in genome biol. 2016 Dec 1;17 (1):249]. *Genome Biol* (2016) 17(1):218. doi: 10.1186/s13059-016-1070-5

37. Newman AM, Liu CL, Green MR, Gentles AJ, Feng W, Xu Y, et al. Robust enumeration of cell subsets from tissue expression profiles. *Nat Methods* (2015) 12 (5):453–7. doi: 10.1038/nmeth.3337

38. Aran D, Hu Z, Butte AJ. xCell: digitally portraying the tissue cellular heterogeneity landscape. *Genome Biol* (2017) 18(1):220. doi: 10.1186/s13059-017-1349-1

39. Li T, Fan J, Wang B, Traugh N, Chen Q, Liu JS, et al. TIMER: a web server for comprehensive analysis of tumor-infiltrating immune cells. *Cancer Res* (2017) 77(21): e108–10. doi: 10.1158/0008-5472.CAN-17-0307

40. van Veldhoven CM, Khan AE, Teucher B, Rohrmann S, Raaschou-Nielsen O, Tjønneland A, et al. Physical activity and lymphoid neoplasms in the European prospective investigation into cancer and nutrition (EPIC). *Eur J Cancer* (2011) 47 (5):748–60. doi: 10.1016/j.ejca.2010.11.010

41. Tamminga M, Hiltermann TJN, Schuuring E, Timens W, Fehrmann RS, Groen HJ. Immune microenvironment composition in non-small cell lung cancer and its association with survival. *Clin Transl Immunol* (2020) 9(6):e1142. doi: 10.1002/cti2.1142

42. Finotello F, Mayer C, Plattner C, Laschober G, Rieder D, Hackl H, et al. Molecular and pharmacological modulators of the tumor immune contexture revealed by deconvolution of RNA-seq data [published correction appears in genome med. 2019 jul 29;11(1):50]. *Genome Med* (2019) 11(1):34. doi: 10.1186/s13073-019-0638-6

43. Barbie DA, Tamayo P, Boehm JS, Kim SY, Moody SE, Dunn IF, et al. Systematic RNA interference reveals that oncogenic KRAS-driven cancers require TBK1. *Nature* (2009) 462(7269):108–12. doi: 10.1038/nature08460

44. Thorsson V, Gibbs DL, Brown SD, Wolf D, Bortone DS, Ou Yang TH, et al. The immune landscape of cancer [published correction appears in immunity. 2019 Aug 20;51(2):411-412]. *Immunity* (2018) 48(4):812–830.e14. doi: 10.1016/j.immuni.2018.03.023

45. Liberzon A, Birger C, Thorvaldsdóttir H, Ghandi M, Mesirov JP, Tamayo P. The molecular signatures database (MSigDB) hallmark gene set collection. *Cell Syst* (2015) 1 (6):417–25. doi: 10.1016/j.cels.2015.12.004

46. Lu X, Meng J, Su L, Jiang L, Wang H, Zhu J, et al. Multi-omics consensus ensemble refines the classification of muscle-invasive bladder cancer with stratified prognosis, tumour microenvironment and distinct sensitivity to frontline therapies. *Clin Transl Med* (2021) 11(12):e601. doi: 10.1002/ctm2.601

47. Han Y, Yu G, Sarioglu H, Caballero-Martinez A, Schlott F, Ueffing M, et al. Proteomic investigation of the interactome of FMNL1 in hematopoietic cells unveils a role in calcium-dependent membrane plasticity. *J Proteomics* (2013) 78:72–82. doi: 10.1016/j.jprot.2012.11.015

48. Szklarczyk D, Morris JH, Cook H, Kuhn M, Wyder S, Simonovic M, et al. The STRING database in 2017: quality-controlled protein-protein association networks, made broadly accessible. *Nucleic Acids Res* (2017) 45(D1):D362–8. doi: 10.1093/nar/gkw937

49. Sun D, Wang J, Han Y, Dong X, Ge J, Zheng R, et al. TISCH: a comprehensive web resource enabling interactive single-cell transcriptome visualization of tumor microenvironment. *Nucleic Acids Res* (2021) 49(D1):D1420–30. doi: 10.1093/nar/gkaa1020

50. Schadendorf D, van Akkooi ACJ, Berking C, Griewank KG, Gutzmer R, Hauschild A, et al. Melanoma [published correction appears in lancet. 2019 Feb 23;393(10173):746]. *Lancet* (2018) 392(10151):971–84. doi: 10.1016/S0140-6736(18) 31559-9

51. Bobos M. Histopathologic classification and prognostic factors of melanoma: a 2021 update. *Ital J Dermatol Venerol* (2021) 156(3):300–21. doi: 10.23736/S2784-8671.21.06958-3

52. Wilson ML. Histopathologic and molecular diagnosis of melanoma. *Clin Plast Surg* (2021) 48(4):587–98. doi: 10.1016/j.cps.2021.05.003

53. Gershenwald JE, Scolyer RA, Hess KR, Sondak VK, Long GV, Ross MI, et al. Melanoma staging: evidence-based changes in the American joint committee on cancer eighth edition cancer staging manual. *CA Cancer J Clin* (2017) 67(6):472–92. doi: 10.3322/caac.21409

54. Papageorgiou C, Apalla Z, Manoli SM, Lallas K, Vakirlis E, Lallas A. Melanoma: staging and follow-up. *Dermatol Pract Concept* (2021) 11(Suppl 1):e2021162S. doi: 10.5826/dpc.11S1a162S

55. Rashid S, Tsao H. Recognition, staging, and management of melanoma. *Med Clin North Am* (2021) 105(4):643–61. doi: 10.1016/j.mcna.2021.04.005

56. Achkar T, Tarhini AA. The use of immunotherapy in the treatment of melanoma. *J Hematol Oncol* (2017) 10(1):88. doi: 10.1186/s13045-017-0458-3

57. Cuevas LM, Daud AI. Immunotherapy for melanoma. *Semin Cutan Med Surg* (2018) 37(2):127–31. doi: 10.12788/j.sder.2018.028

58. Buchbinder EI, Flaherty KT. Biomarkers in melanoma: lessons from translational medicine. *Trends Cancer* (2016) 2(6):305–12. doi: 10.1016/j.trecan.2016.05.003

59. Galon J, Bruni D. Approaches to treat immune hot, altered and cold tumours with combination immunotherapies. *Nat Rev Drug Discov* (2019) 18(3):197–218. doi: 10.1038/s41573-018-0007-y

60. Ochoa de Olza M, Navarro Rodrigo B, Zimmermann S, Coukos G. Turning up the heat on non-immunoreactive tumours: opportunities for clinical development. *Lancet Oncol* (2020) 21(9):e419–30. doi: 10.1016/S1470-2045(20)30234-5

61. Hu R, Han Q, Zhang J. STAT3: a key signaling molecule for converting cold to hot tumors. *Cancer Lett* (2020) 489:29–40. doi: 10.1016/j.canlet.2020.05.035

62. Zhong F, Liu J, Gao C, Chen T, Li B. Downstream regulatory network of MYBL2 mediating its oncogenic role in melanoma. *Front Oncol* (2022) 12:816070. doi: 10.3389/fonc.2022.816070

63. Chau LY. Heme oxygenase-1: emerging target of cancer therapy. *J BioMed Sci* (2015) 22(1):22. doi: 10.1186/s12929-015-0128-0

64. Min J, Feng Q, Liao W, Liang Y, Gong C, Li E, et al. IFITM3 promotes hepatocellular carcinoma invasion and metastasis by regulating MMP9 through p38/MAPK signaling. *FEBS Open Bio* (2018) 8(8):1299–311. doi: 10.1002/2211-5463.12479

65. Min J, Hu J, Luo C, Zhu J, Zhao J, Zhu Z, et al. IFITM3 upregulates c-myc expression to promote hepatocellular carcinoma proliferation via the ERK1/2 signalling pathway. *Biosci Trends* (2020) 13(6):523–9. doi: 10.5582/bst.2019.01289

66. Chu PY, Huang WC, Tung SL, Tsai CY, Chen CJ, Liu YC, et al. IFITM3 promotes malignant progression, cancer stemness and chemoresistance of gastric cancer by targeting MET/AKT/FOXO3/c-MYC axis. *Cell Biosci* (2022) 12(1):124. doi: 10.1186/s13578-022-00858-8

67. Liu Y, Lu R, Cui W, Pang Y, Liu C, Cui L, et al. High IFITM3 expression predicts adverse prognosis in acute myeloid leukemia. *Cancer Gene Ther* (2020) 27(1-2):38–44. doi: 10.1038/s41417-019-0093-y

68. IFITM3 enhances PI3K pathway signaling to promote b-cell malignancies. *Cancer Discov* (2021) 11(1):12. doi: 10.1158/2159-8290.CD-RW2020-168

Glossary

SKCM	skin cutaneous melanoma
GEO	gene expression omnibus
MRS	monocyte-related signature
DSS	disease specific survival
PFS	progression free survival
HLA	human leukocyte antigen
ICIs	immune checkpoint inhibitors
TME	tumor microenvironment
TIME	tumor immune microenvironment
scRNA-seq	single-cell RNA sequencing
CPM	counts per million
TCGA	the cancer genome atlas
PCA	principal component analysis
t-SNE	t-Distributed Stochastic Neighbor Embedding
NMF	non-negative matrix factorization
RSF	random survival forest
Enet	elastic network
plsRcox	partial least squares regression for Cox
SuperPC	supervised principal components
GBM	generalized boosted regression modeling
survival-SVM	survival support vector machine
LOOCV	leave-one-out cross-validation
ROC	receiver operator characteristic curve
DCA	decision curve analysis
ssGSEA	single sample gene set enrichment analysis
MsigDB	Molecular Signatures Database
GSEA	gene set enrichment analysis
GO	Gene Ontology
TISCH	tumor immune single-cell hub
IFITM3	interferon induced transmembrane protein
AJCC	American Joint Committee on Cancer
HMOX1	Heme Oxygenase 1
HCC	hepatocellular carcinoma

Frontiers in Immunology

Explores novel approaches and diagnoses to treat immune disorders.

The official journal of the International Union of Immunological Societies (IUIS) and the most cited in its field, leading the way for research across basic, translational and clinical immunology.

Discover the latest Research Topics

See more →

Frontiers

Avenue du Tribunal-Fédéral 34
1005 Lausanne, Switzerland
frontiersin.org

Contact us

+41 (0)21 510 17 00
frontiersin.org/about/contact